I. *O*-ALKYL IMIDATE FORMATION VIA STAUDINGER LIGATION

II. DESIGN, SYNTHESIS AND BIOLIGICAL EVALUATION OF NOVEL REDUCTIVELY ACTIVATED HISTONE DEACETYLASE INHIBITORS

by

José A. Restituyo

A dissertation submitted in partial fulfillment of the

requirements for the degree of

Doctor of Philosophy

(Pharmaceutical Sciences)

at the

UNIVERSITY OF WISCONSIN-MADISON

2006

AWPP
R4360
2006

Committee's Page. This page is not to be hand-written except for the signatures

A dissertation entitled

I. O-alkyl Imidate Formation via Staudinger Ligation

II. Design, Synthesis and Biological Evaluation of Novel Reductively Activated Histone Deacetylase Inhibitors

submitted to the Graduate School of the
University of Wisconsin-Madison
in partial fulfillment of the requirements for the
degree of Doctor of Philosophy

by

Jose A. Restituyo

Date of Final Oral Examination: August 17, 2006

Month & Year Degree to be awarded: **December** **May** **August** 2006

****

Approval Signatures of Dissertation Committee

Signature, Dean of Graduate School

Committee's Page. This page is not to be hand-written except for the signatures

I. *O*-ALKYL IMIDATE FORMATION VIA STAUDINGER LIGATION

II. DESIGN, SYNTHESIS AND BIOLIGICAL EVALUATION OF NOVEL REDUCTIVELY ACTIVATED HISTONE DEACETYLASE INHIBITORS

José A. Restituyo

Under the direction of Professor Scott R. Rajski

At the University of Wisconsin-Madison

One of the objectives in the Rajski group is to develop tools by which to dissect DNA and protein methylation patterns. Accordingly, a wide variety of S-adenosyl-L-methionine (SAM) cofactor mimics have been synthesized by Rajski group members and evaluated in various biological systems. Nonetheless, a way by which these compounds could be identified once attached to their DNA target was needed. We reasoned that the well-studied Staudinger ligation could be applied to the identification of adenosine-linked materials bearing a C8 azide moiety. The data presented here show that aryl azides are very effective coupling partners in Staudinger ligation reactions of potential biological importance and that the principal product that results from these ligations bears a relatively stable imidate linkage. The studies detailed herein suggest the importance of simple esterification of commercially available triarylphosphines *en route* to a simplified and more broadly accessible Staudinger ligation scenario for use in chemical biology.

HDAC 1 is the critical lynchpin that interrelates hypoxia and angiogenesis. Significant evidence suggests that inhibition of HDAC 1 can have potent antiangiogenic, and thus antimetastasis effects. HDAC inhibitors TSA and FK-228 have been reported to

possess anti-angiogenic potential both *in vitro* and *in vivo*, showing that they inhibited hypoxia-induced production of the angiogenic mediator vascular endothelial cell growth factor (VEGF) by tumor cells and the migration as well as proliferation of the endothelial cells indirectly. FK-228's unique mode of activation highlights it as one of only two known HDAC inhibitor prodrugs.

We present here data that promote the notion that simple functional mimics of FK-228 can be readily generated. Our cyclic disulfide core structures induced H4 hyperacetylation in S2 *Drosophila* cells, thus supporting early assertions of cell permeability by these synthetic agents. These structures were coupled to a variety of cap groups to generate FK-228 mimics that have moderate HDAC inhibition profiles. We believe that the readily diversified FK-228 analogs presented here and the activities associated with them are likely to be useful in furthering the understanding of different HDAC's and have the potential to represent clinical candidates in the near future.

To my wife Monique and my daughter Alexandra for sometimes putting up with more than they had to…I LOVE YOU.

Acknowledgements

I would like to thank Professor Scott R. Rajski for all his guidance over the past years. The knowledge I have gained, and the lessons I have learned from him will stay with me for the remainder of my scientific career.

I find myself very fortunate as my graduate school experience has been nothing but positive. This is due, in large part, to the people that I have had the chance to work with over the years. To the Rajski group, this has been quite a rollercoaster ride...good thing I like rollercoasters and moreover, I had you all to share my experiences along the way. To Lindsay Comstock, Scott Petersen and Jared Mays thank you for your friendship, support and scientific insights over the years. I owe special thanks to Rachel Weller for without her I would have lost my mind during my years at UW. I could always count on you for anything, anytime, anywhere and for that I am eternally grateful. Thank you for being there for me when times were not so smooth.

I would like to extend my gratitude to Professor Wassarman as well as members on his lab. You guys made me feel very welcome while performing my experiments with you, thank you. I also thank Noel Peters over the SMSF for all her help, patience and guidance during the biological portion of this research.

I was fortunate enough to have very good friends among my graduate student peers. To Dr. Martin Hager, James Dowell and Oana Martin thank you for the many laughs and words of encouragements. I also thank members of the Lauhon, Mecozzi, and Rich groups. In particular, I thank the Rich group. During the beginnings of the Rajski group, we went to them for anything and they were always there for us. Me and my co-workers felt as if we were an extension of their lab. I always looked up to Nero Shah and

Matthias Brewer. They were key elements in my development as a scientist. Thank you for you friendship.

I would like to express my sincerest thanks to my family, for I have been blessed with a band of siblings like no other. To my brother Alejo, I could have not asked for a better role model. Thanks for believing in me. When I talk about you, people think you are God...and to me they are not too far from the truth. To my sisters, Angela, Aleika, Emily, Jannelly and Elizabeth I want to say thank you for your mental, physical and emotional support. I can not put into words all the feelings I have for you girls...it is largely because of you all that I became the man that I am now. I am proud of all of you. To the memory of my Mom, to my Dad and Adela for their unconditional love, their support and their inspiration, but more importantly for their genes! It is amazing how far one can get if you put your mind to it, and that I owed to you Dad. Thank you.

I want to thank my daughter, Alexandra. You have no idea how much joy your smiley face brings to my heart. You are my sunshine. Always remember, as long as one and one is two, there could never be a father who loves his daughter more than I love you.

Finally, with my deepest feelings, I would like to thank my lovely wife Monique, for the endless encouragement and love you have provided me with over the years. You have been an amazing source of strength when things were getting difficult and there is no doubt in my mind that none of this would have been possible without you. Because of you, I can now stand tall and be proud of who I am and where I am. *I Love You.*

Table of Contents

Abstract i

Acknowledgments iv

Table of Contents vi

Abbreviations ix

Chapter 1. O-Alkyl Imidates via Staudinger Ligation 1

1.1 Introduction 1

1.2 Staudinger Reaction 4

1.3 Staudinger Ligation 6

1.3.1 Non-traceless Staudinger Ligation 6

1.3.2 Traceless Staudinger Ligation 7

1.4 Ligation of Aryl Azides 9

1.5 O-Alkyl Imidate Formation 15

1.5.1 Coupling Expediency 15

1.5.2 Proposed Mechanism 20

1.6 Summary 24

1.7 References 25

Chapter 2. Histone Deacetylase Inhibitors 28

2.1 Background and Significance 28

2.1.1 Histone Deacetylse Biological Function 28

2.1.2 Classification of Histone Deacetylases 31

2.1.2.1 Class I Histone Deacetylases 31

2.1.2.2 Class II Histone Deacetylases 34

2.1.2.3. Class III Histone Deacetylases 37

2.2 Progress and Chemical Development of Histone Deacetylase Inhibitors 41
2.2.1 Histone Deacetylase Inhibitors 41
2.2.1.1 Hydroxamates 44
2.2.1.2 Short-Chain Fatty Acids 50
2.2.1.3 Benzamides 52
2.2.1.4 Cyclic Peptides 53
2.3 Project Goals 59
2.3.1 Target Selection and Specific Aims 59
2.4 Summary 61
2.5 References 63
Chapter 3. Synthetic Approaches to Core Cyclic Disulfides 76
3.1 Introduction 76
3.2 Synthetic Approaches 78
3.2.1 Retrosynthetic Approach 78
3.2.2 Attempted Synthesis of Cyclic Disulfides 78
3.2.3 Amended Retrosynthetic Approach of Cyclic Disulfides 81
3.2.4 Final Synthesis of Cyclic Disulfides 82
3.3 Synthetic Approaches to Diversified Cyclic Disulfides 83
3.3.1 Synthesis of Capped Disulfides 83
3.4 Summary 86
3.5 References 87
Chapter 4. Biological Evaluation of Novel Reductively Activated HDAC Inhibitors 90
4.1 *Drosophila* Melanogaster Experiments 90
4.2 Fluor-de-Lys Experiments 95

4.3 Cytotoxicity Experiments 98

4.4 Cytoblot Experiments 101

4.4.1 p53 and p21 Activation 102

4.4.2 Hyperacetylation of H3 and H4 105

4.4.3 Disruption of Keap1-Nrf2 Complex 107

4.4.4 AKT Activation 110

4.5 Summary 115

4.6 References 117

Chapter 5. Experimental Section 123

5.1 Chapter 1 Compounds 123

5.1.1 General Synthetic Procedures 123

5.1.2 General Synthetic Procedures for Staudinger Ligations 124

5.1.3 General Synthetic Procedures for Preparation of Esters **1.26** and **1.27** . 124

5.1.4 Compound Characterizations 125

5.2 Chapter 3 Compounds 141

5.2.1 General Synthetic Procedures 141

5.2.2 Synthetic Procedures for Disulfide Formation 142

5.2.3 General Synthetic Procedure for Cap Group Installation 152

5.3 Biological Experiments 161

5.3.1 General Procedure for SDS-PAGE and Western Blot Analysis 161

5.3.2 General Procedure for Fluor-de-Lys Assays 162

5.3.2 General Procedure for Cytotoxic Assays 162

5.3.3 General Procedure for Cytoblot Assays 164

5.4 References 165

Appendix 166

Abbreviations

Commonly used abbreviations are listed below.

Ac_2O	acetic anhydride
AcOH	acetic acid
ACN	acetonitrile
Boc	*tert*-butoxycarbonyl
Boc_2O	di-*tert*-butyl dicarbonate
Bu	butyl
t-Bu	*tert*-butyl
n-BuLi	*n*-butyl lithium
Bn	benzyl
°C	degrees Celsius
CDI	1,1'-carbonyldiimidazole
DCC	N,N'-dicyclohexylcarbodiimide
DEAD	diethyl azodicarboxylate
DIAD	diisopropyl azodicarboxylate
DIEA	N, N-diisopropylethylamine
DMAP	N,N-dimethylaminopyridine
DMF	N,N-dimethylformamide
DMSO	dimethylsulfoxide
DTT	dithiothreitol
ECL	enhanced chemiluminescence
EDCI	1-(3-dimethylaminopropyl)-3-ethylcarbodiimide hydrochloride
EI	electron impact mass spectrometry

ESI	electron spray ionization mass spectrometry
eq	equivalent
Et	ethyl
Et_2O	diethyl ether
EtOAc	ethyl acetate
EtOH	ethanol
g	gram
h	hour
HAT	histone acetyl transferase
HDAC	histone deacetylase
HOBt	1-hydroxybenzotriazole hydrate
HPLC	high performance liquid chromatography
HRMS	high resolution mass spectrometry
IC_{50}	concentration at 50% inhibition
J	coupling constant
L	liter
LDA	lithium diisopropylamide
LRMS	low resolution mass spectrometry
m	milli
M	molar
MALDI	matrix assisted laser desorption/ionization
μ	micro
Me	methyl
MeOH	methanol

mg	milligram
min	minute
mL	milliliter
mmol	millimoles
MS	mass spectrometry
n	nano
N	normal
NaH	sodium hydride
NMR	nuclear magnetic resonance
PAGE	polyacrylamide gel electrophoresis
PBS	phosphate saline buffer
pet ether	petroleum Ether
Ph	phenyl
Pr	propyl
PPh_3	triphenyl phosphine
PVDF	poly(vinylidene fluoride)
RP-HPLC	reverse phase high performance liquid chromatography
rt	room temperature
SAR	structure-activity relationship
SDS	sodium dodecyl sulfate
t	*tert*
TBS	*t*-butyl dimethyl silyl
TBSCl	*t*-butyl dimethyl silyl chloride
TBDPS	*t*-butyl diphenyl silyl
TBDPSCl	*t*-butyl diphenyl silyl chloride

TEA	triethylamine
TFA	trifluoroacetic acid
THF	tetrahydrofuran
TIPS	triispropyl silyl
TLC	thin layer chromatography
Trt	trityl

Chapter 1. O-Alkyl Imidates via Staudinger Ligation[†]

1.1 Introduction

In their studies of biological systems, molecular biologists and chemists are often faced with the need to link two molecular entities covalently, for example, to link a complex carbohydrate with a peptide or to attach a small molecular probe (such as a fluorescent dye, a radical probe, or an affinity tag) to a biopolymer. As biological systems are both rich in structural complexity and diverse in their functional reactivity, chemoselective ligation reactions have to be developed in which two mutually and uniquely reactive functional groups can be coupled, usually in an aqueous environment under physiological conditions. These uniquely reactive functional groups should be selective for one another and also tolerate a diverse array of other functionalities, thus rendering the use of protecting groups unnecessary and, in the ideal case, allowing its application in the complex environment of a living cell. Although several bioconjugation techniques are available for the *in vitro* preparation of bioconjugates substituted with a limited number of functional groups, truly chemoselective ligation reactions are rather limited.[1] Most ligation reactions rely on the reaction of an electrophile with a nucleophile. As biological systems are rich in diverse electrophilic and nucleophilic sites, only a few functional groups are available that exhibit orthogonal reactivity to the functional groups present.[2] In recent years, two reactions have been popularized in which an azide moiety serves as a reactive functional group, with the following three advantages: 1) the azide moiety is absent in almost all naturally occurring compounds ("bioorthogonal"); 2) despite

---

[†] The following publication largely contributed to this chapter: Restituyo, J.A.; Comstock, L.R.; Petersen, S.G.; Stringfellow, T.; Rajski, S.R. *Org. Lett.* **2003**, 5, 4357-4360.

their high intrinsic reactivity, azides undergo a selective ligation with a very limited number of reaction partners; 3) the azide group is small and can be introduced into biological samples without altering the molecular size significantly.

One of these bioorthogonal reactions is the Huisgen [3+2] cycloaddition. Initially developed in 1963, this reaction expoits the 1,3-dipolar nature of the azide to react with a terminal alkyne dipolarophile to form stable triazole adducts, thus avoiding the use of widely reactive electrophiles and nucleophiles.[3] Both azides and alkynes are abiotic or bioorthogonal, in that they are extremely rare and inert in biological systems, thereby becoming "lifeless" until they come into contact with each other. When brought together, their reaction is thermodynamically favorable by 30-35 kcal/mol.[4] This reaction requires activation of the alkyne species in order to be effective. Without alkyne activation the process requires elevated temperatures or pressures that are not compatible with biological systems. Sharpless and co-workers, in parallel with Meldal and co-workers, have demonstrated that the rate of cycloaddition between azides and alkynes can be accelerated approximately 10^6 fold using catalytic amounts of Cu(I).[5,6] This copper-catalyzed reaction, termed 'click' chemistry, proceeds readily at physiological temperatures and in the presence of biological materials to provide 1,4-disubstituted triazoles with nearly complete regioselectivity. The primary disadvantage of this copper-catalyzed cycloaddition is the cellular toxicity of the metal catalyst.[7]

Another recent and heavily exploited bioorthogonal reaction is the Staudinger ligation introduced by Saxon and Bertozzi. Bertozzi and co-workers modified the classic Staudinger reaction by introduction of an intramolecular electrophilic trap into the phosphine (Scheme 1.1);[8] this transformation ultimately produces a covalent link between one nitrogen atom of the azide and the triarylphosphine scaffold. The Staudinger ligation can be used to covalently attach probes to azide-bearing biomolecules. Like the azide,

phosphines do not react appreciably with biological functional groups and are therefore also bioorthogonal. Additionally, the reaction proceeds readily at pH 7 with no apparent toxic effects. A notable difference between the Staudinger ligation and the [3+2] Huisgen cycloaddition is that the Staudinger ligation does not require additives for rapid conjugation to proceed.

Scheme 1.1 Staudinger reaction and development of Bertozzi's phosphine

Staudinger Reduction

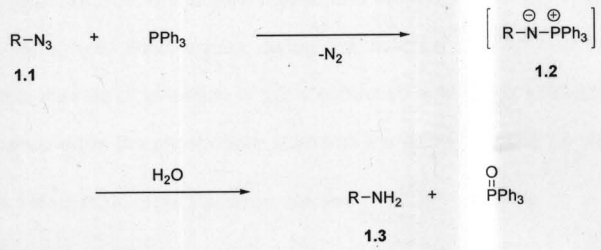

Staudinger Ligation

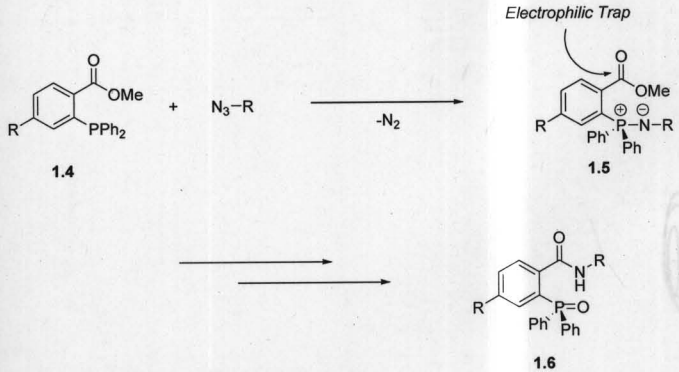

Top: Staudinger reaction between a triphenylphosphine and an azide to form an iminophosphorane (aza-ylide) with concomitant loss of nitrogen. In an aqueous solvent, the readily formed aza-ylide is hydrolyzed rapidly to generate the primary amine and triphenylphospine oxide. **Bottom**: Reaction of Bertozzi's phosphine with an electrophilic trap to capture the nucleophilic aza-ylide by intramolecular cyclization.

1.2 Staudinger Reaction

In 1919 Staudinger and Meyer reported that azides react smoothly with triaryl phosphanes to form iminophosphoranes (Scheme 1.1).[9] This imination reaction proceeds under mild conditions, almost quantitatively, and without noticeable formation of any side products. Over the last century detailed mechanistic studies have revealed that the mechanism of this reaction involves several intermediates (Scheme 1.2).[10] In a primary imination reaction, triphenylphosphine and azide **1.1** react to form a phosphazide **1.8**, which, as a rule, decomposes during the reaction with loss of nitrogen. It is interesting that the rate of formation of **1.8** is controlled only by the inductive properties of the groups attached to the phosphorus atom and the azide, and that no significant steric

Scheme 1.2 Mechanism of the Staudinger reaction

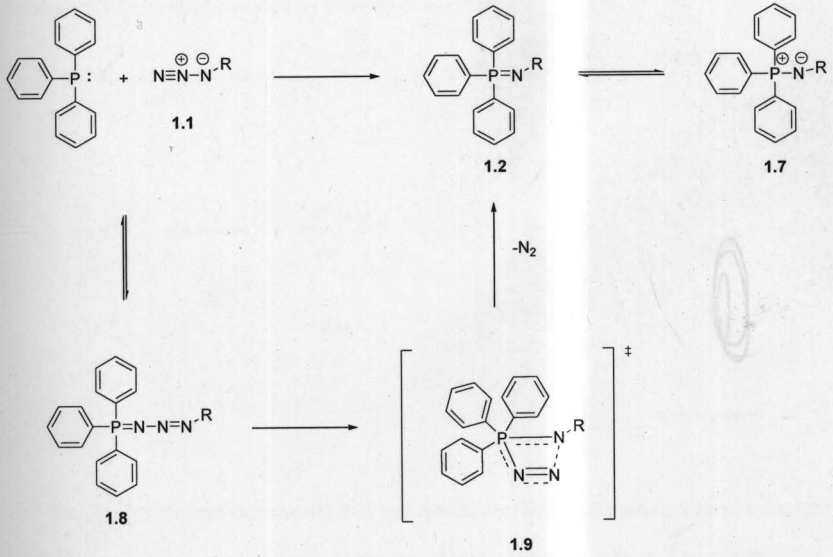

influence is observed. Phosphazides of the type **1.8** are stable at room temperature in organic solvents if substituents are present that delocalize the positive charge on the phosphorus atom and/or provide steric shielding of the phosphorus atom. The subsequent loss of nitrogen is thought to proceed via the 4-membered-ring transition state **1.9** with retention of the original configuration at phosphorus, without the participation of either free radicals or nitrenes.

The iminophosphorane (ylide) **1.2**, with its highly nucleophilic nitrogen atom, can react with almost any kind of electrophilic reagent, thus resulting in many reactions of significant synthetic importance (Scheme 1.3).[10,11] If the Staudinger reaction is carried out in an aqueous solvent, **1.2** is rapidly hydrolyzed to generate a primary amine and triphenylphosphine oxide. The so-called Staudinger reduction is a frequently used method for the smooth reduction of azides to amines.

Scheme 1.3 Trapping of aza-ylide by a variety of electrophiles

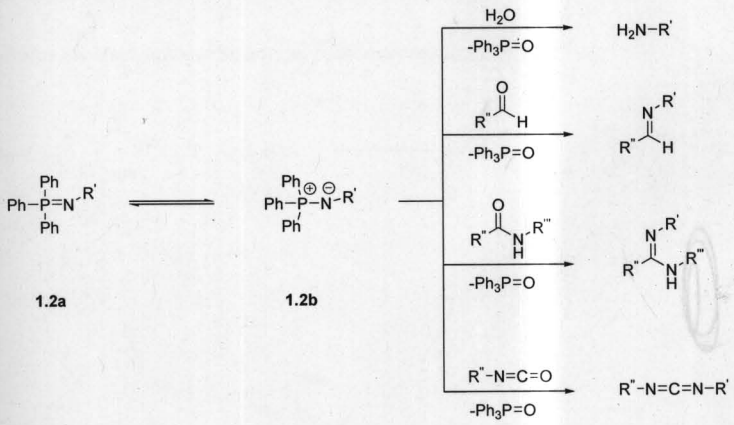

Staudinger himself discovered that aza-ylides can react with aldehydes or ketones to form imines.[9] The synthetic value of the aza-Wittig reaction is reflected by the fact that

it has found application in many total syntheses, for example, in syntheses of croomine, quinine, and dendrobine.[11] Less reactive carbonyl electrophiles, such as amides or esters, also undergo reaction with **1.2,** especially if the electrophilic attack proceeds in an intramolecular fashion. For example, the reaction of 2-azidobenzoyl chloride with a suitable amide is an excellent method for the construction of quinazolines (known to date as the Eguchi aza-Wittig protocol).[12]

1.3 Staudinger Ligation

1.3.1 Non-traceless Staudinger Ligation

In their pioneering studies on the metabolic engineering of cell surfaces, Bertozzi and co-workers recognized the limitation of the hydrazone ligation method, in which conjugates are formed between a hydrazide probe and a ketone-modified sample.[2] Their search for a milder reaction of two truly bioorthogonal functionalities led them to the highly efficient Staudinger reaction. As described above, reaction of an azide with a phosphine

Scheme 1.4 Mechanism of Staudinger ligation proposed by Bertozzi

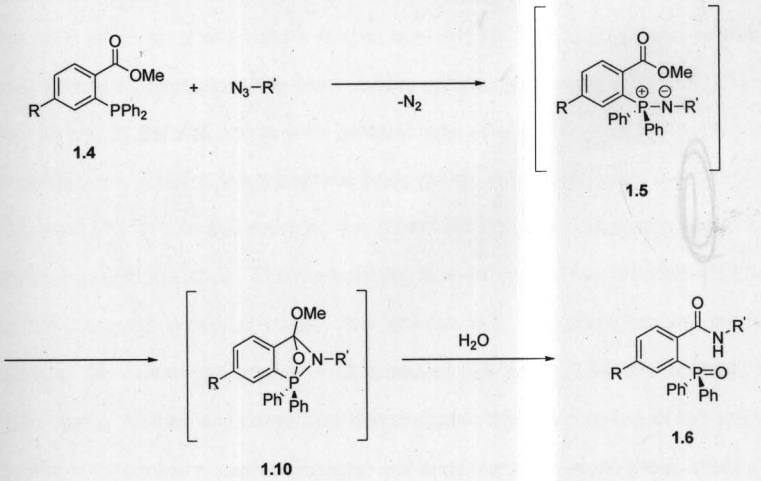

produces and aza-ylide that undergoes spontaneous hydrolysis to the amine and phosphine oxide in an aqueous environment. Saxon and Bertozzi designed the arylphosphine **1.4** based on the rationale that an appropriately located electrophilic trap, such as an ester moiety, within the structure of the phosphine, would capture the nucleophilic aza-ylide **1.5** by intramolecular cyclization (Scheme 1.4).[8] This process would ultimately produce a stable amide bond before the competing aza-ylide hydrolysis could take place. Phophine **1.4**, is not yet commercially available, but can be readily synthesized in moderate yields.[13,14] Mechanistic studies by ^{31}P NMR spectroscopy identified the aza-ylide **1.5** and the oxaphosphetane **1.10** as intermediates in the ligation reaction.[15] Moreover, crystal structure determination of **1.10** provided significant insight to a more accurate mechanism. In aqueous solvent, bicyclic intermediate **1.10** collapses resulting in the formation of the amide **1.6**.

1.3.2 Traceless Staudinger Ligation

Although the reaction described earlier works well in a biological environment, a modification in which an amide bond is formed between the two coupling partners to give a product without a triaryl phosphine oxide moiety appears even more attractive. Raines and co-workers, in parallel efforts with Bertozzi and co-workers, reported a traceless Staudinger ligation, in which the phosphine oxide moiety is cleaved during the hydrolysis step (Scheme 1.5).[16-19] In this reaction, the previously acylated phosphines of the type **1.11** are treated with the azide. The nucleophilic nitrogen atom of the aza-ylide **1.12** then attacks the carbonyl group to cleave the linkage with the phosphonium species. Hydrolysis of the rearranged product **1.13** produces the amide **1.14** and liberates the phosphine oxide. Raines and co-workers demonstrated that the coupling of two peptide units bearing a C-terminal phosphinothioester and an N-terminal α-azido group afford a

Scheme 1.5 Traceless Staudinger Ligation

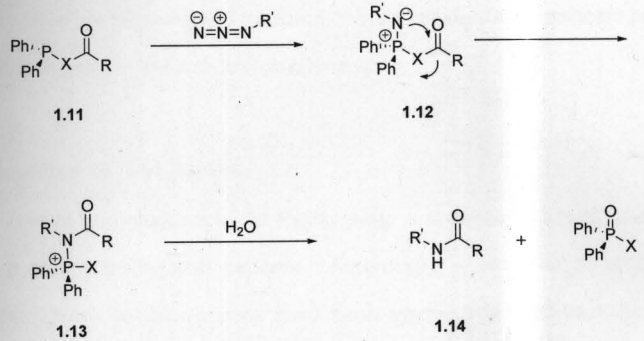

product without residual phosphine in the material (Scheme 1.6). In a proof-of-concept experiment they converted N-acetylglycine **1.15** into the thioester **1.16**, which reacted smoothly in aqueous THF with the protected azido amino acids **1.17a-c** to give the dipeptides **1.18a-c** in very good yields and without any detectable epimerization.[18]

Scheme 1.6 Peptide formation through traceless Staudinger ligation

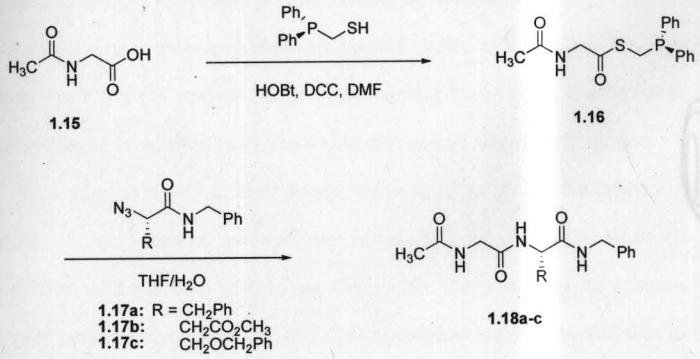

Although the full scope and limitations of the Staudinger ligation in peptide chemistry have not yet been fully explored, this approach holds significant promise in the future of basic protein research and drug discovery.

1.4 Ligation of Aryl Azides

One of the objectives in the Rajski group is to develop tools by which to dissect DNA and protein methylation patterns. Accordingly, a wide variety of S-adenosyl-L-methionine (SAM) cofactor mimics have been synthesized by Rajski group members (namely Lindsay Comstock, Scott Petersen and Rachel Weller) and evaluated in various biological systems.[20-22] Nonetheless, a way by which these compounds could be identified once attached to their DNA target was needed. Recognizing the potential of the Staudinger ligation, we sought to apply phosphines of class **1.4** toward the ligation of aryl azides. The ligation of alkyl azides to triarylphosphines of type **1.4** is well-known.[8,15,23] Bertozzi and co-workers have found that amides of type **1.6** are formed with yields and stabilities suitable for biochemical applications. [8,15,23] However, analogous couplings involving aryl azides, especially purinyl azides, were not apparent in the literature. We reasoned that similar chemistry could be applied to the identification of adenosine-linked materials bearing a C8 azide moiety. This invokes the utility of 8-azidoadenosine as a tetherable handle in addition to its more classical use as a photoaffinity label.[24,25]

To study the ability of 8-azidoadenosine to undergo the Staudinger ligation, the synthesis of two distinct phosphines containing the general structure **1.4** was accomplished with the help of Lindsay Comstock. As presented in scheme 1.7, facile coupling of pyrene butyric acid with 2,2'-(ethylenedioxy) bis(ethylamine) was achieved via standard peptide coupling conditions to produce amine **1.19** in 74% yield. Coupling of 1-

methyl-2-diphenylphosphinoterephthalate with either glycine ethyl ester hydrochloride or **1.19** afforded phosphines **1.20a** and **1.20b** in moderate yield (43%).

Scheme 1.7 Synthetic approach to triarylphosphines

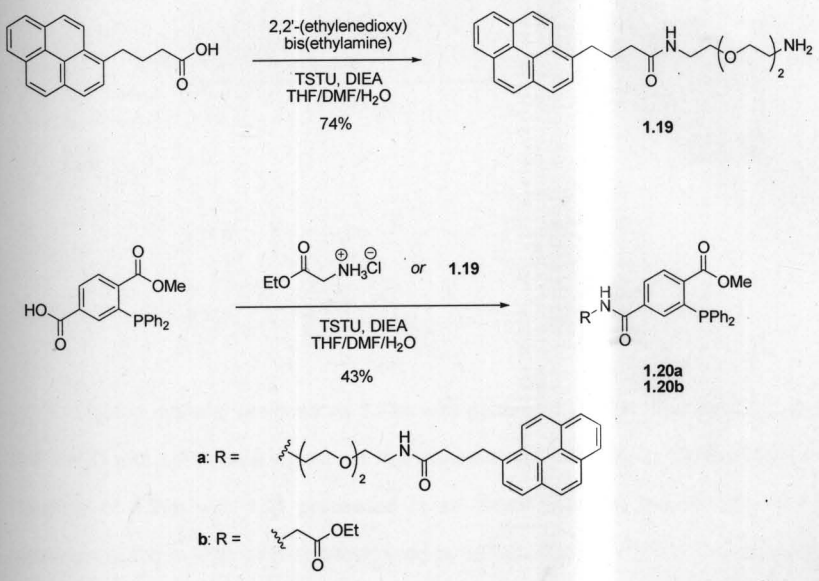

The proposed mechanism for triarylphosphine coupling to alkyl azides (Scheme 1.4) suggests that reaction of spectroscopically unique **1.19** with aryl azide 8-azidoadenosine (**1.21**) would afford the amide-linked adenylate **1.22a** (Scheme 1.8). Similarly, convergence of glycine-linked **1.20b** with **1.21** would afford the acylguanidine **1.22b**. The unique spectroscopic profile of **1.22a** would allow us to identify with a high degree of certainty the coupled material during HPLC reaction analyses.

Scheme 1.8 Expected Staudinger ligation products

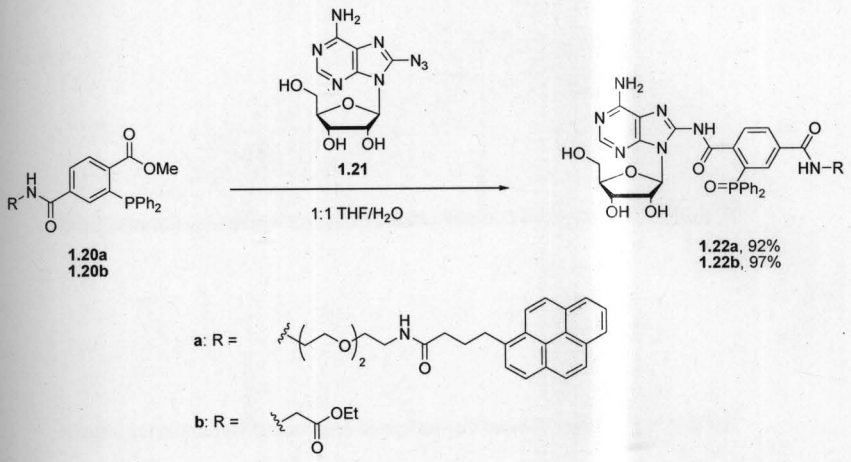

Ligated material assigned as **1.22a** was generated in 92% yield over 2 h in 1:1 THF / H_2O with both coupling partners in a concentration of 1 mM at 30 °C (Figure 1.1). Coupling of **1.20b** with **1.21** proceeded in an almost identical fashion, affording the presumed **1.22b** in 97% yield as ascertained by HPLC analysis. This is in stark contrast to the same coupling with alkyl azide **1.23**, where complete consumption of the alkyl azide required approximately 24 h to afford the ligated adduct **1.24** (Scheme 1.9). Results obtained from such ligation attempts are shown in Figure 1.2.

Figure 1.1 HPLC analysis of 8-azidoadenosine and pyrene containing phosphine **1.20a**

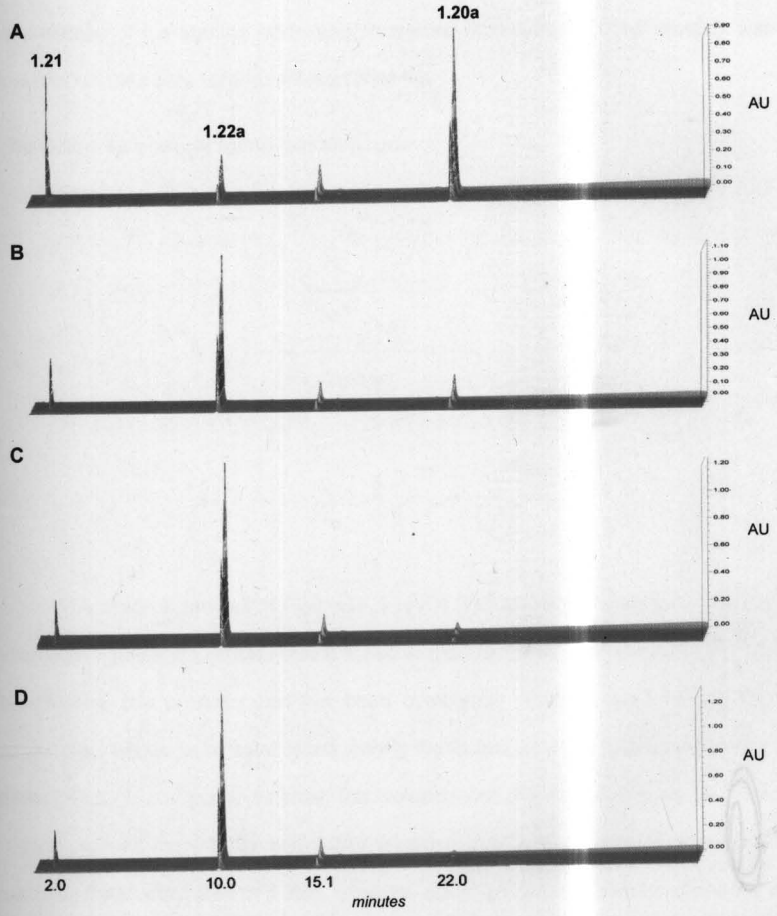

The reaction was performed in 1:1 THF/H_2O at 30 °C for the indicated times. Both **1.20a** and **1.21** were in 1mM concentrations. Column: Phenomenex Luna 5μ C8 column (150 x 4.60 mm). Flow rate: 1.5 mL/min (35-90% CH_3CN with 0.1% TFA over 30 minutes). Panel A: Reaction at 10 minutes. Panel B: Reaction at 50 minutes. Panel C: Reaction at 90 minutes. Panel D: Reaction at 130 minutes. Retention times: **1.21**, 2.0 minutes; **1.22a**, 10.0 minutes; phosphine oxide of **1.20a**, 15.1 minutes; **1.20a**, 22.0 minutes.

In comparing the reaction profile with that in Figure 1.1, an apparent and dramatic difference is the time profile for the ligation. Analysis within the first few minutes indicated the presence of the starting azide and phosphine material only. The reaction was very slow and reached only 50% completion after 8 h.

Scheme 1.9 Staudinger ligation with alkyl azide

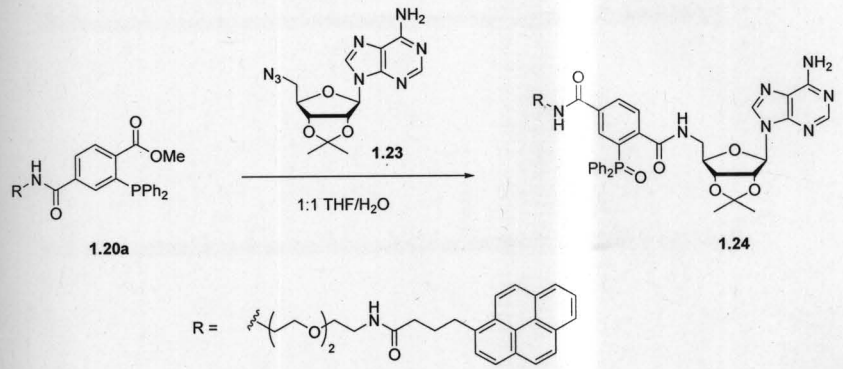

The reaction profiles of Figures 1.1 and 1.2 emphasize the profound impact upon Staudinger ligation efficiencies that is linked to the electronic nature of the azide involved. Nonetheless, the products had not been completely characterized. A key structural feature that needed to be established among the ligated products was the presence of the amide bond. Much to our surprise, the isolation and characterization of the Staudinger adducts derived from **1.20a** and **1.20b** revealed that neither material gave rise to the anticipated adducts **1.22a** or **1.22b**. Instead, the products consistently retained a methyl group, as revealed by ^{1}H NMR spectroscopy and mass spectrometry. Identification of the exact position of the methyl group was a challenge. After careful structure elucidation of purported **1.22b**, in the way of high resolution NMR experiments (gDQF-COSY, ROESY,

Figure 1.2 HPLC analysis of alkyl azide and pyrene containing phosphine **1.20a**

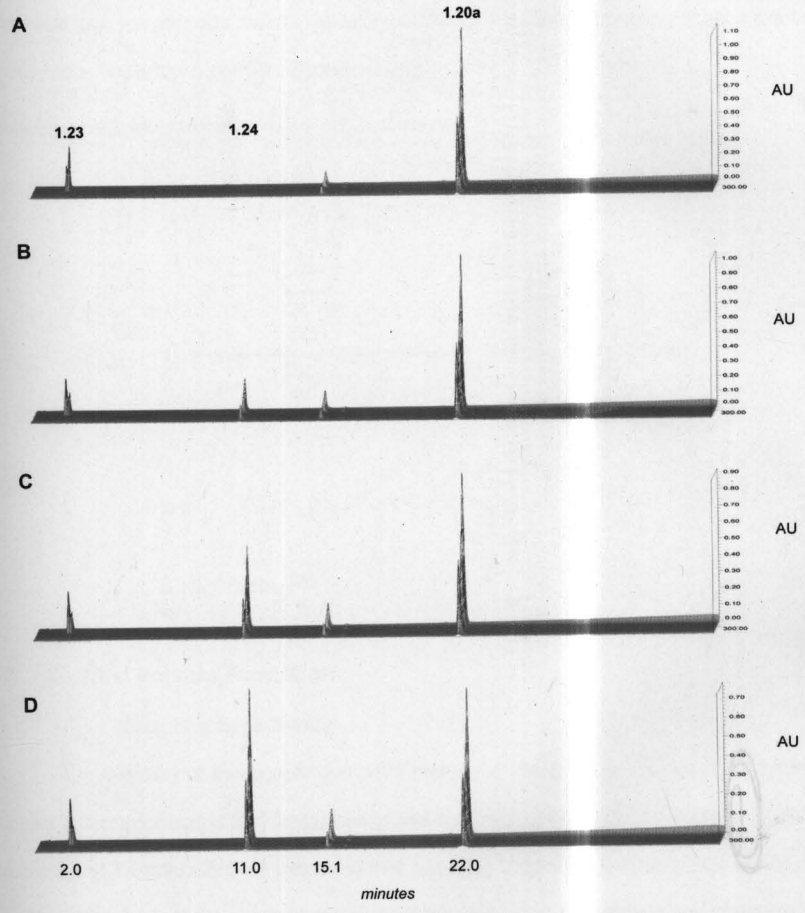

The reaction was performed in 1:1 THF/H_2O at 30 °C for the indicated times. Both **1.20a** and **1.23** were in 1mM concentrations. Column: Phenomenex Luna 5μ C8 column (150 x 4.60 mm). Flow rate: 1.5 mL/min (35-90% CH_3CN with 0.1% TFA over 30 minutes). Panel A: Reaction at 5 minutes. Panel B: Reaction at 145 minutes. Panel C: Reaction at 320 minutes. Panel D: Reaction at 495 minutes. Retention times: **1.23**, 2.0 minutes; **1.24**, 11.0 minutes; phosphine oxide of **1.20a**, 15.1 minutes; **1.20a**, 22.0 minutes.

gHMBC, and gHSQC) and with the aid of Dr. Thomas Stringfellow, it was determined that O-methylimidate **1.25b** was the Staudinger adduct resulting from reaction of **1.20b** and **1.21**. Notably, the alkoxide moiety typically lost during Staudinger coupling of alkyl azides is retained in the coupling of C8 azidoadenosine.

Scheme 1.10 Imidate formation with 8-azidoadenosine

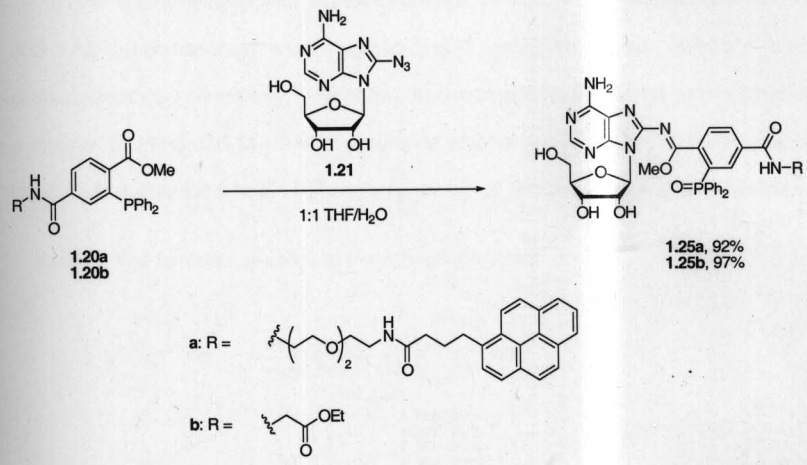

1.5 O-Alkyl Imidate Formation

1.5.1. Coupling Expediency

The feasibility of this coupling and the stability of the product promoted our further interest in terms of scope and limitations of the ligation reaction with aryl azides. During the course of investigation, we proposed that Staudinger ligations involving aryl azides do not require the use of the disubstituted phosphine developed by Bertozzi and co-workers. We envisioned that simple esterification of commercially available triarylphosphines with capped linkers of interest would allow a species still capable of coupling two abiotic substances, but whose ligation is more facile than the corresponding alkyl azide case and

for which phosphine construction is as simple as esterification. Widespread application of this precise coupling dictates, however, that azide and phosphine substitution patterns be examined with respect to coupling efficiency as well as imidate stability under aqueous conditions. As such, in collaboration with Lindsay Comstock a variety of electronically distinct azides and phosphines were constructed.

Using two commercially available phophino-acids, 2-(diphenylphosphino) benzoic acid and 2-diphenylphosphino-1-naphthoic acid, esterification was achieved via well studied Mitsunobu conditions.[26] As shown in Scheme 1.11, subjecting each phosphine to a mixture of PPh_3 and DIAD with a suitable alcohol produced the panel of phosphino esters **1.26a-e** and **1.27a-e**. Although synthesis of tert-butyl ester (**1.26f**) could not be

Scheme 1.11 Synthetic approach to triarylphosphine library

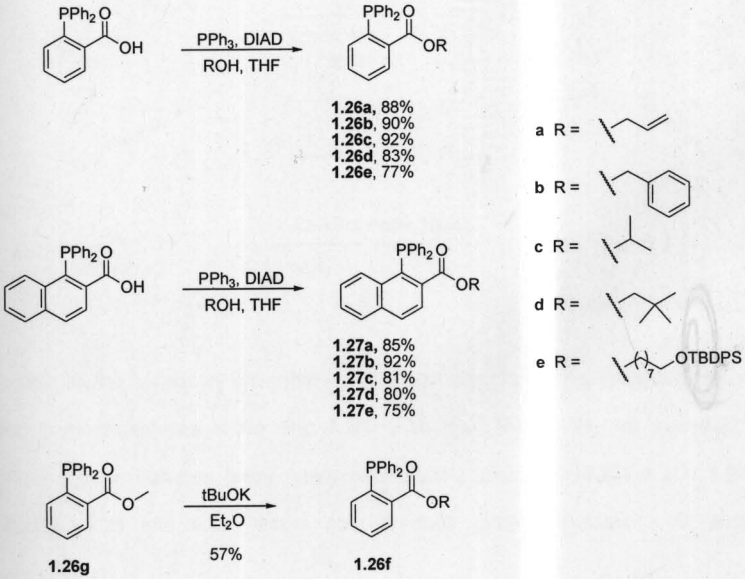

achieved via Mitsunobu conditions with tBuOH, its successful production was accomplished by subjecting 2-diphenylphosphanyl-benzoic acid methyl ester (**1.26g**) to potassium tert-butoxide in ether (57%).[27] Interestingly, all attempts to produce the tert-butyl ester analog of **1.27** were unsuccessful.

In order to evaluate the effects of the electronic nature of the azide on coupling effecincies, as well as, product stability, an electron rich and an electron poor azide were synthesized; our synthetic approach is shown in Scheme 1.12. Conversion of 4-azidophenacyl bromide and 4-butylaniline to the corresponding azides proceded smoothly and in good yields (85% and 81% respectively).[28]

Scheme 1.12 Synthetic approach to electronically distinct azides

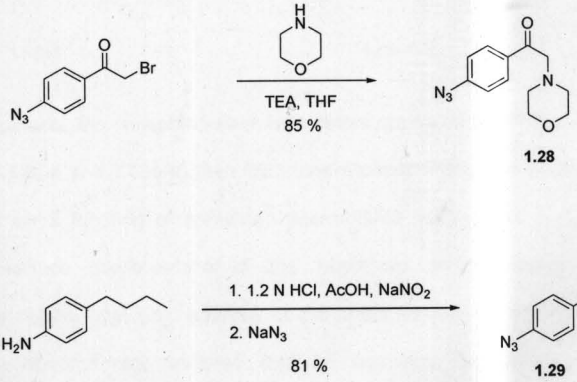

With all the necessary elements in hand and based upon the formation of O-alkyl imidates from phosphines **1.20a** and **1.20b** with aryl azide **1.21**, we expected that Staudinger ligation between these newly developed phosphines (**1.26a-e** and **1.27a-e**) and azides (**1.28** and **1.29**) would also produce O-alkyl imidates. All possible

combinations between the two azides and the ten phosphines synthesized were evaluated and the results obtained from ligations are summarized in Table 1.1.

Scheme 1.13 Anticipated ligation products with aryl azides

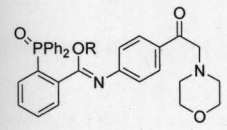

1.30a-f

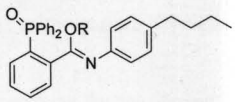

1.31a-e

a R =

b R =

c R =

d R =

e R = 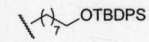

f R =

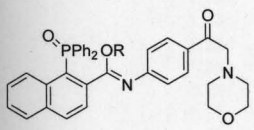

1.32a-f

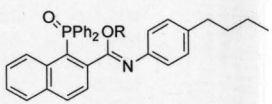

1.33a-f

In general, the phosphino-naphthoic esters appeared to afford more stable imidate adducts (**1.32a-e** and **1.33a-e**) than the triphenylphosphino esters (**1.30a-e** and **1.31a-e**). This could be a function of enhanced intermediate stabilization due to the expanded aromatic surface characteristic of the naphthoic esters relative to the simpler triphenylphosphino analogs. Analysis of the crude reaction products by TLC, ^{1}H NMR, and mass spectrometry revealed that all couplings proceeded with comparable efficiencies to the desired imidates. However, imidates resulting from condensation of butyl azide **1.29** and triphenylphosphino esters **1.26a-e** were not amenable to chromatographic purification. Following chromatography, low yields (< 20%) of unstable imidates were obtained contributing to already complicated mixtures of products. Only in the ligations of **1.26a** and **1.26b** with **1.29** could the initially anticipated amide product (**1.34**) be identified in significant quantities (37% yield for **1.31a** and 67% yield for **1.31b**).

This formation of an amide bond could be obtained upon production of a hydrolytically unstable imidate. The more electron rich allyl and benzyl moieties appeared to significantly contribute to the reduced stability of the corresponding imidates, in conjunction with the triphenylphosphine and n-butyl substituents, making these intermediates more prone to hydrolysis. In the majority of cases examined, imidates were

Table 1.1 O-Alkyl imidates yields for Staudinger ligation of ary azides

Phosphine	Azide	Product	Imidate (%)	Amide (%) [a]
1.26a	**1.28**	**1.30a**	64	-
1.26b	**1.28**	**1.30b**	53	-
1.26c	**1.28**	**1.30c**	66	-
1.26d	**1.28**	**1.30d**	67	-
1.26e	**1.28**	**1.30e**	66	-
1.26f	**1.28**	**1.30f**	89	-
1.27a	**1.28**	**1.32a**	64	-
1.27b	**1.28**	**1.32b**	62	-
1.27c	**1.28**	**1.32c**	40	-
1.27d	**1.28**	**1.32d**	38	-
1.27e	**1.28**	**1.32e**	55	-
1.26a	**1.29**	**1.31a**	11	37
1.26b	**1.29**	**1.31b**	7	67
1.26c	**1.29**	**1.31c**	15	<5
1.26d	**1.29**	**1.31d**	9	<5
1.26e	**1.29**	**1.31e**	18	<5
1.27a	**1.29**	**1.33a**	65	-
1.27b	**1.29**	**1.33b**	60	-
1.27c	**1.29**	**1.33c**	55	-
1.27d	**1.29**	**1.33d**	40	-
1.27e	**1.29**	**1.33e**	58	-

a. Structure of resulting amide **1.34**:

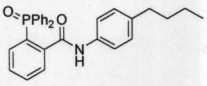

isolated in yields moderate by organic synthesis standards but certainly high enough to support the importance of this coupling in biologically oriented studies.

1.5.2 Proposed Mechanism

The substitution patterns of **1.20a**, **1.20b** and **1.27a-e**, coupled with the aromatic nature of the azides, suggest that there may be an alternative mechanistic foundation for O-alkyl imidate formation. In formulating a cogent answer to this finding, we considered the previously proposed mechanism by Bertozzi and co-workers, as well as the mechanism proposed for Staudinger reduction and intramolecular aza-Wittig (S-AW) processes used in the successful total syntheses of Apratoxin and (-)-Ephedradine A.[15,29,30]

The primary imination products from reaction of tertiary phosphines with azides are phosphazides, which break down to an aza-ylide following N_2 evolution (Scheme 1.4). These primary imination products are sometimes sufficiently stable to permit isolation. Phosphazides derived from aryl azides and triarylphosphines have been effectively trapped through formation of transition metal complexes and are well known to undergo intramolecular electrocyclic reactions affording access to extended heterocyclic systems.[30-33] Furthermore, isolable phosphazides have been formed from sterically hindered azides and phosphines or in cases where phosphorus electron density has been increased.[33] Substituent-dependent decreases in azide Nα electron density also correlate to phosphazide stability.[34] Steric bulk, in particular, is believed to play an important role in abrogating formation of the betaine necessary for N_2 liberation.

Seminal mechanistic work by Temple and Leffler supports the initial generation of the extended azaphosphonium ylide **1.35** (Scheme 1.14).[35] Model building revealed that the aryl amine of **1.35** is in close proximity to the carbonyl via a seven-membered transition state with the azide-derived triad in the thermodynamically more stable *cis* conformation.[36] The O-carboalkoxy moiety serves then to quench the negatively charged

Nα center, and the resulting tetrahedral intermediate immediately satisfies charge on the positively charged phosphorus, thus rendering bicyclic **1.36**. The phosphazido oxide **1.36** is proposed to decompose in short order via loss of nitrogen and concomitant installation of the phosphine oxide moiety. The resultant **1.37** is very often, in our hands, a stable material highly resistant to hydrolysis.

Scheme 1.14 Proposed mechanism of imidate formation

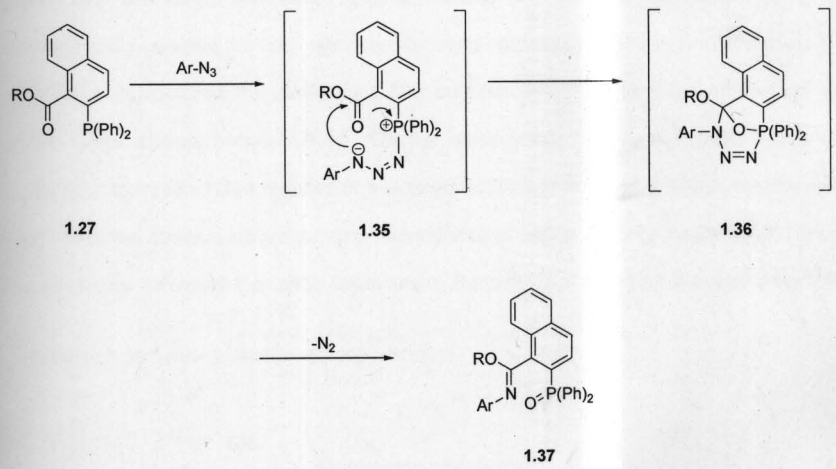

1.27 **1.35** **1.36**

1.37

This proposed mechanism with N_2 evolution as the final step sharply contrasts that shown in Scheme 1.4 (and most S-AW processes), where loss of N_2 precedes formation of aza-ylide. Attempts to visualize bicyclic **1.36** by ^{31}P NMR with 8-azidoadenosine were unsuccessful.[37] This could be explained by the mechanistic independence of a hydrolytic step in our experiments. This water independence was initially ascertained by HPLC-MS experiments, which showed that use of $^{18}OH_2$ during the ligation of **1.20a** to **1.21** did not lead to detectable ^{18}O incorporation into **1.25a**. This result was independently supported

by ^{31}P NMR experiments in which trace amounts of water (as a component of THF-*d*8) did not get consumed during the coupling of **1.20b** and **1.21**.

Recent work by Bertozzi and co-workers presents, in contrast to our findings, a series of aryl azides capable of amide formation as ligated products.[34] Scheme 1.15 shows the three aryl azides used in this study. In each scenario, the formation of the corresponding aza-ylide was rapid. What was noticeably different among these three aza-ylides was the large difference in time needed for effective conversion to their corresponding amides. The electron donating capability of the *p*-methoxyphenyl substituent destabilized the aza-ylide **1.39b** and resulted in more rapid conversion to amide **1.40b** in approximately 8 h. On the other hand, the electron withdrawing *p*-nitrophenyl aza-ylide **1.39c** resulted in a slow conversion to amide **1.40c** in approximately 48 h. With the observed dramatic time dependence in amide bond formation based upon the electronic nature of the azide substitution, Bertozzi and co-workers determined that

Scheme 1.15 Amide formation with aryl azides

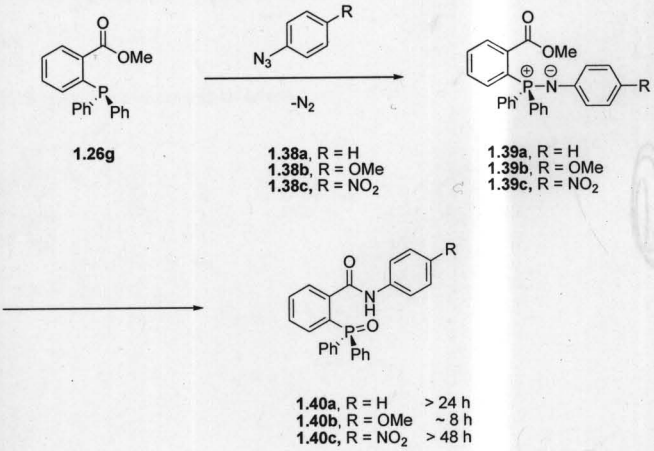

1.26g

1.38a, R = H
1.38b, R = OMe
1.38c, R = NO_2

1.39a, R = H
1.39b, R = OMe
1.39c, R = NO_2

1.40a, R = H > 24 h
1.40b, R = OMe ~ 8 h
1.40c, R = NO_2 > 48 h

the rate limiting step was the intramolecular cyclization of the aza-ylide onto the carbonyl.

Although the findings presented by Bertozzi and co-workers contradict those observed by us, a direct comparison can not be made. While the phosphines used were similar in nature, the azides tested by Bertozzi were both strongly electron donating and withdrawing. This is in sharp contrast to the morpholine-based (**1.28**) and butyl-based (**1.29**) azides, which are only slightly electron donating and withdrawing. Previous demonstrations firmly support the notion that slight variations in either the electronics of the phosphine or the azide can significantly alter the stability of the imidate product and result in either decomposition or amide bond formation. It is certainly possible that compounds **1.40a-c** form imidates as a transient intermediates, but the electronic nature of the azides may enhance the ability of such imidates to undergo hydrolysis to the corresponding amides, as observed by us with the allyl and benzyl imidates **1.31a** and **1.31b**. In the case of **1.31a** and **1.31b**, water may simply add to the imidate to eliminate the alkoxide and form the more stable amide **1.34**. Depending on the electron density of the phosphine, azide, and O-alkyl imidate substituents this hydrolysis step may proceed at different rates.

Scheme 1.16 Hydrolysis of imidate to amide

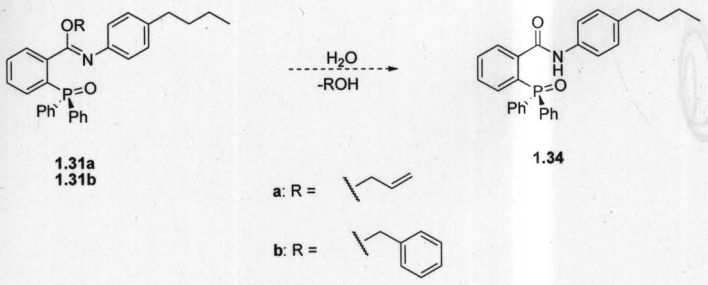

The mechanistic and functional differences of Staudinger ligations involving alkyl and aryl azides appear to be quite profound. At the heart of this difference are the significantly enhanced stability, attenuated nucleophilicity, and greater steric bulk of aryl-bearing ylides relative to their alkyl analogues. Our findings, as well as literature reports, support our proposed mechanism for O-alkyl imidate formation.

1.6 Summary

In summary, we have shown that aryl azides are very effective coupling partners in Staudinger ligation reactions of potential biological importance. The principal product that results from these ligations bears a relatively stable imidate linkage. The preference of aryl azides to give rise to imidate over amide Staudinger ligation products is likely a reflection of steric and electronic differences between the two types of azides but also seems susceptible to changes in phosphine structure as well. Modulation of these differences is expected to impact product profiles and must clearly be considered in the design of new abiotic coupling reagents. Moreover, studies detailed herein suggest the importance of simple esterification of commercially available triarylphosphines en route to a simplified and more broadly accessible Staudinger ligation scenario for use in chemical biology.

1.7 References

(1) Hermanson, G. T. *Bioconjugate Techniques*; Academic Press: San Diego, 1996; 785.

(2) Hang, H. C.; Bertozzi, C. R. Chemoselective Approaches to Glycoprotein Assembly. *Acc. Chem. Res.* **2001**, *34*, 727-736.

(3) Huisgen, R. 1,3-Dipolar Cycloadditions. *Angew. Chem. Int. Edn. Engl.* **1963**, *2*, 565-598.

(4) Prescher, J. A.; Bertozzi, C. R. Chemistry in Living Systems. *Nat. Chem. Biol.* **2005**, *1*, 13-21.

(5) Rostovtsev, V. V.; Green, L. G.; Fokin, V. V.; Sharpless, K. B. A Stepwise Huisgen Cycloaddition Process: Copper(I)-Catalyzed Regioselective "Ligation" of Azides and Terminal Alkynes. *Angew. Chem. Int. Edn. Engl.* **2002**, *41*, 2596-2599.

(6) Tornoe, C. W.; Christensen, C.; Meldal, M. Peptidotriazoles on Solid Phase: [1,2,3]-Triazoles by Regiospecific Copper(I)-Catalyzed 1,3-Dipolar Cycloadditions of Terminal Alkynes to Azides. *J. Org. Chem.* **2002**, *67*, 3057-3064.

(7) Link, A. J.; Tirrell, D. A. Cell Surface Labeling of Escherichia Coli via Copper(I)-Catalyzed [3+2] Cycloaddition. *J. Am. Chem. Soc.* **2003**, *125*, 11164-11165.

(8) Saxon, E.; Bertozzi, C. R. Cell Surface Engineering by a Modified Staudinger Reaction. *Science* **2000**, *287*, 2007-2010.

(9) Staudinger, H. M., J. Uber neue organische phosphoverbindungen III. Phosphinmethlenderivate und phosphinimine. *Helv. Chim. Acta* **1919**, *2*, 635-646.

(10) Gololobov, Y. G.; Kasukhin, L. F. Recent Advances in The Staudinger Reaction. *Tetrahedron* **1992**, *48*, 1353-1406.

(11) Fresneda, P.; Molina, P. Application of Iminophosphorane-Based Methodologies for the Synthesis of Natural Products. *Synlett* **2004**, 1-17.

(12) Eguchi, S.; Yamashita, K.; Matsushita, Y. Facile Synthesis of 1,4-Benzodiazepin-5-ones via Intramolecular Aza-Wittig Reaction. *Synlett* **1992**, 295-296.

(13) Saxon, E.; Bertozzi, C. R. Cell Surface Engineering by a Modified Staudinger Reaction. *Science* **2000**, *287*, 2007-2010.

(14) Luchansky, S. J.; Hang, H. C.; Saxon, E.; Grunwell, J. R.; Yu, C. et al. Constructing Azide-Labeled Cell Surfaces Using Polysaccharide Biosynthetic Pathways Methods in Enzymology. *Recognition of Carbohydrates in Biological Systems, Part A: General Procedures*; Academic Press, 2003; pp 249-272.

(15) Saxon, E.; Luchansky, S. J.; Hang, H. C.; Yu, C.; Lee, S. C. et al. Investigating Cellular Metabolism of Synthetic Azidosugars with the Staudinger Ligation. *J. Am. Chem. Soc.* **2002**, *124*, 14893-14902.

(16) Soellner, M. B.; Nilsson, B. L.; Raines, R. T. Staudinger Ligation of α-Azido Acids Retains Stereochemistry. *J. Org. Chem.* **2002**, *67*, 4993-4996.

(17) Nilsson, B. L.; Kiessling, L. L.; Raines, R. T. Staudinger Ligation: A Peptide from a Thioester and Azide. *Org. Lett.* **2000**, *2*, 1939-1941.

(18) Nilsson, B. L.; Kiessling, L. L.; Raines, R. T. High-Yielding Staudinger Ligation of a Phosphinothioester and Azide To Form a Peptide. *Org. Lett.* **2001**, *3*, 9-12.

(19) Saxon, E.; Armstrong, J. I.; Bertozzi, C. R. A "Traceless" Staudinger Ligation for the Chemoselective Synthesis of Amide Bonds. *Org. Lett.* **2000**, *2*, 2141-2143.

(20) Comstock, L. R.; Rajski, S. R. Methyltransferase-Directed DNA Strand Scission. *J. Am. Chem. Soc.* **2005**, *127*, 14136-14137.

(21) Petersen, S. G.; Rajski, S. R. o-Nitrobenzenesulfonamides in Nucleoside Synthesis: Efficient 5'-Aziridination of Adenosine. *J. Org. Chem.* **2005**, *70*, 5833-5839.

(22) Weller, R. L.; Rajski, S. R. Design, Synthesis, and Preliminary Biological Evaluation of a DNA Methyltransferase-Directed Alkylating Agent. *ChemBioChem* **2006**, *7*, 243-245.

(23) Kiick, K. L.; Saxon, E.; Tirrell, D. A.; Bertozzi, C. R. Incorporation of Azides Into Recombinant Proteins for Chemoselective Modification by the Staudinger Ligation. *Prod. Natl. Acad. Sci. U.S.A.* **2002**, *99*, 19-24.

(24) Lacapere, J. J.; Garin, J.; Trinnaman, B.; Green, N. M. Identification of Amino Acids Residues Photolabeled with 8-Azidoadenosine 5'-Diphosphate in the Catalytic Site of Sarcoplasmic Reticulum Ca-ATPase. *Biochem.* **1993**, *32*, 3414-3421.

(25) Pathak, T. Azidonucleosides: Synthesis, Reactions, and Biological Properties. *Chem. Rev.* **2002**, *102*, 1623-1668.

(26) Amos, R. A.; Emblidge, R. W.; Havens, N. Esterification Using a Polymer-Supported Phosphine Reagent. *J. Org. Chem.* **1983**, *48*, 3598-3600.

(27) Vasin, V. A.; Razin, V. V. Mild and Efficient Method for Preparation of tert-Butyl Esters. *Synlett* **2001**, 658-660.

(28) Broggini, G.; Molteni, G.; Zecchi, G. The Intramolecular Azide Cycloaddition Route to Triazolam Analogues. *Synthesis* **1995**, 647-648.

(29) Chen, J.; Forsyth, C. J. Synthesis of the Apratoxin 2,4-Disubstituted Thiazoline via an Intramolecular Aza-Wittig Reaction. *Org. Lett.* **2003**, *5*, 1281-1283.

(30) Cadierno, V.; Zablocka, M.; Donnadieu, B.; Igau, A.; Majoral, J.-P. et al. Unexpected Formal [1+3] Cycloadditions between Azides and α-Zirconated Phosphanes: A Route to Unprecedented Phosphazide and Iminophosphorane Complexes. *Chemistry - A European Journal* **2000**, *6*, 345-352.

(31) Molina, Pedro; Arques, A.; Victoria Vinader, M. Intramolecular Trapping of a Phosphazide by an Imine: Formation of 2,3-Diamino-2H-Indazole Derivatives from O-Azidobenzaldimines and Tertiary Phosphines. *Tetrahedron Lett.* **1989**, *30*, 6237-6240.

(32) Molina, P.; Lopez-Leonardo, C.; Llamas-Botia, J.; Foces-Foces, C.; Fernandez-Castano, C. Unexpected Staudinger Reaction of α-Azidoacetonitriles α-Phenyl Substituted with Triphenylphosphine. Preparation, X-ray Crystal and Molecular Structures of a Phosphazine, an Aminophosphonium Carbanion Salt and a Phosphazide, with (Z)-Configuration. *Tetrahedron* **1996**, *52*, 9629-9642.

(33) Desamparados Velasco, M.; Molina, P.; Fresneda, P. M.; Sanz, M. A. Isolation, Reactivity and Intramolecular Trapping of Phosphazide Intermediates in the Staudinger Reaction of Tertiary Phosphines with Azides. *Tetrahedron* **2000**, *56*, 4079-4084.

(34) Lin, F. L.; Hoyt, H. M.; vanHalbeek, H.; Bergman, R. G.; Bertozzi, C. R. Mechanistic Investigation of the Staudinger Ligation. *J. Am. Chem. Soc.* **2005**, *127*, 2686-2695.

(35) Leffler, J. E.; Temple, R. D. Staudinger Reaction Between Triarylphosphines and Azides. A Study of the Mechanism. *J. Am. Chem. Soc.* **1967**, *89*, 5235-5246.

(36) Widauer, C.; Grützmacher, H.; Shevchenko, I.; Gramlich, V. Insights into the Staudinger Reaction: Experimental and Theoretical Studies on the Stabilization of cis-Phosphazides. *European Journal of Inorganic Chemistry* **1999**, *1999*, 1659-1664.

(37) Restituyo, J. A.; Comstock, L. R.; Petersen, S. G.; Stringfellow, T.; Rajski, S. R. Conversion of Aryl Azides to O-Alkyl Imidates via Modified Staudinger Ligation. *Org. Lett.* **2003**, *5*, 4357-4360.

Chapter 2. Histone Deacetylase Inhibitors

2.1 Background and Significance

2.1.1 Histone Deacetylase Biological Function

The packing of DNA into the higher ordered and dynamic structure of chromatin provides a pivotal point of control for gene expression by regulating access of transcription factors to DNA. Chromatin is composed of multiple repeating units called nucleosomes; a single nucleosomal core particle comprises 146 base pairs of DNA wrapped around a histone octamer formed by four histone partners, an H3 - H4 tetramer and two H2A - H2B dimmers (Figure 2.1).[1] Histones are small basic proteins rich in amino-acids, lysine and arginine. The four nucleosomic histones involve two domains: the C-terminal domain, which is located inside the nucleosome core, and the N-terminal domain with lysine residues extending out of the nucleosome. The interaction of positively charged ε-amino groups of lysine residues of histone N-terminal tails with the negatively charged phosphate backbone of DNA results in chromatin condensation, which prohibits access to the transcription machinery, leading to transcriptional silencing.[1,2] Structural changes in chromatin are effected by chromatin remodeling complexes and enzymatic post-translational modifications. One of the well characterized post-translational modifications of histones that is known to impact transcriptional activity is the acetylation of the ε-amino group of lysine residues. Acetylation by histone acetyl transferase (HAT) proteins neutralizes the positive charges on histones and disrupts the electrostatic interactions between DNA and histone proteins, promoting chromatin unfolding which has been associated with gene expression. The opposite is also true; deacetylation orchestrated by histone deacetylase (HDAC) proteins restores the positive charge on histones thus

Figure 2.1 Crystal structure of the nucleosome core particle

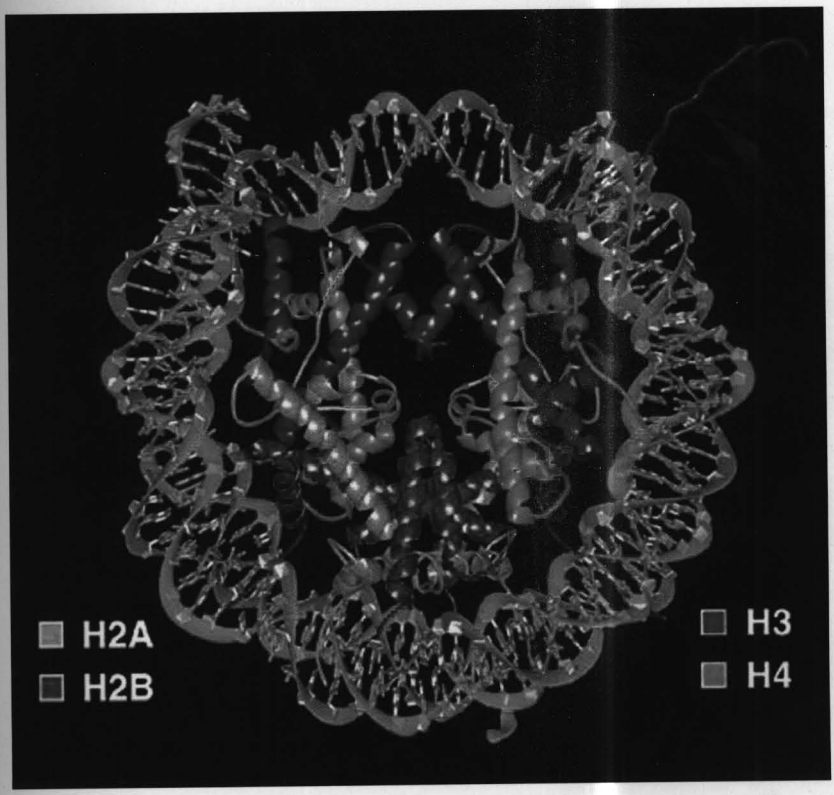

Nucleosome core particle: ribbon traces for the 146-bp DNA phosphodiester backbones (brown and turquoise) and eight histone protein main chains (blue: H 3; green: H 4; yellow: H 2A; red: H 2B. Adapted from Luger, K.; Mader, A. W.; Richmond, R. K.; Sargent, D. F.; Richmond, T. J. *Nature* **1997**, *389*, 251-260.

leading to chromatin condensation and gene suppression. Important positions for acetylation are Lys^{9} and Lys^{14} on histone H3, and Lys^{5}, Lys^{8}, Lys^{12} and Lys^{16} on histone H4. Other post-translational modifications of histones including methylation and

phosphorylation have also been associated with regulation of gene expression, and together with histone acetylation have provided the basis for the histone code. [3-6]

While the acetylation state of histone proteins is unquestionably very dynamic, it seems to depend on the net local balance between HAT and HDAC activities. Empirically observed is the fact that HDAC activity is invariably increased in cancer cells, resulting in altered gene transcription, impaired differentiation, increased cell survival, and dysregulated proliferation. Nonetheless, there is considerable evidence that these models are oversimplified. In cell culture studies, less than 10% of transcriptionally active genes appear to be altered in response to treatment with HDAC inhibitors, with a near equal proportion of these being induced as repressed.[7] This suggests that regulation of gene expression by acetylation is more highly selective than would be expected by a simple and unregulated physical disruption of histone-DNA structure, and that chromatin-associated non-histone proteins are likely involved in these processes. Alternatively, the histone code hypothesis dictates defined patterns of histone tail modifications, whereupon a particular modification in turn affects subsequent modifications. For instance, histone deacetylation has been shown to activate lysine (K) methylation, resulting in relatively stable transcriptional silencing.[2] In a series of experiments, Daujat et al. showed that upon estrogen stimulation H3 is initially acetylated at K18, then at K23, and finally methylated at arginine (R) 17.[8] A specific set of histone modifications was proposed to direct DNA methylation.[3] Of particular significance is the known affinity of bromodomain containing proteins such as TAFII250, p300/CBP and GCN5 for acetylated lysines, as well as the chromodomain of proteins such as HP 1 for methylated lysines, *not* the quaternary ammonium species resulting from deacetylation.[9,10] One last possibility to explain HDAC influence upon transcription involves the simple amalgamation of the two preceding theories. Additionally, these enzymes have been shown to regulate gene expression by

deacetylating transcription factors. For instance, the DNA binding activities of p53, E2F 1, GATA 1 and EKLF are negatively impacted by lysine deacetylation.[11-13]

2.1.2 Classification of Histone Deacetylases

Mammalian HDACs are divided into three major groups or classes based on their structural homologies to the three disctinct yeast HDACs: Rpd 3 (class I) ranging in size from 42 to 55 KDa, Had 1 (class II) ranging in size from 120 to 160 kDa, and the sirtuins [silent information regulators (SIRs)] Sir2/Hst (class III).

2.1.2.1 Class I Histone Deacetylases

The Rpd3 homologous class I HDACs include HDAC 1, HDAC 2, HDAC 3, and HDAC 8. They are widely expressed in a variety of tissues and are primarily localized in the nucleus. HDAC 1 and HDAC 2 are highly similar enzymes, with approximately 82% overall sequence similarity.[14-17] The catalytic domain on the N-terminus forms the major part of the protein.[15-17] HDAC 1 and HDAC 2 are inactive when produced by recombinant techniques, implying that cofactors are necessary for HDAC activity to occur. *In vivo*, HDAC 1 and HDAC 2 only display activity within a complex of proteins. These complexes consist of proteins necessary for modulating their deacetylase activity and for binding DNA, together with proteins that mediate the recruitment of HDACs to the promoters of genes.[18] Three protein complexes have been characterized that contain both HDAC 1 and HDAC 2: Sin3, NuRD (nucleosome remodelling and deacetylating) and Co-REST. Both the Sin3 complex (named after its characteristic element mSin3A) and the NuRD complex consist of a core complex containing HDAC 1, HDAC 2, retinoblastoma-associated protein 48 (RbAp48, which binds histone H4 directly) and RbAp46. The core complex alone does not possess maximal HDAC activity, and additional cofactors are needed.[18-20] HDAC 1 and HDAC 2 can also bind directly to DNA binding proteins such as

YY 1 (Yin and Yang 1, a cellular nuclear matrix regulatory protein), Rb binding protein-1 and Sp 1.[16,17,21-24]

In addition to the regulation of HDAC 1 and HDAC 2 activity by the availability of co-repressors, a second means of regulating activity is via post-translational modifications. Both activity and complex-formation are regulated by phosphorylation. HDAC 1 and HDAC 2 are phosphorylated at a low steady-state level in resting cells. Hyper-phosphorylation of HDAC 1 and HDAC 2 leads to a slight but significant increase in deacetylase activity, and at the same time to disruption of complex formation between HDAC 1 and HDAC 2 and between HDAC 1 and mSin3A/YY 1. When hypo-phosphorylation of HDAC 1 and HDAC 2 occurs, the activity of HDAC 1 and HDAC 2 decreases, but complex formation is increased. The apparently contradictory consequences of phosphorylation maintain HDAC activity at a certain optimal level. Mutational analysis of HDAC 1 shows that Ser^{421} and Ser^{423} are crucial phosphorylation sites; when they are mutated, complex formation is hampered and HDAC activity is decreased.[19,25]

HDAC 3 is evolutionarily most closely related to HDAC8, with 34% overall sequence identity, and HDAC 3 has the same domain structure as all class I HDACs. In HDAC 1 and HDAC 2, the regions that correspond to amino acids 181 - 333 of HDAC 3 are very similar to each other (93% similarity). However, the corresponding region in HDAC 3 has only 68% identity with HDAC 1 and HDAC 2. Surprisingly, the non-conserved C-terminal region of HDAC 3 is required for both deacetylase activity and transcriptional repression. In addition to the nuclear localization signal (NLS) that other class I HDACs have, a nuclear export signal (NES) is also present in HDAC 3 (amino acids 180 - 313). The balance between these two signals is probably dependent on cell type and on environmental conditions.[26] HDAC 3 shares structural and functional features with other

class I HDACs, but it exists in multi-subunit complexes that are different from other known HDAC complexes. This could imply that individual HDACs have distinct functions due to their complex specificity. SMRT (silencing mediator for retinoic acid and thyroid hormone receptors) and N-CoR (nuclear receptor co-repressor) are necessary factors for HDAC 3 activity. N-CoR and SMRT are two distinct, but highly related, proteins that share similar domain structure and function; both act as co-repressors. SMRT and N-CoR have a conserved deacetylase-activating domain for HDAC 3 activation.[27] HDAC 3 is able to form oligomers *in vitro* and *in vivo* with other HDACs.[26] Studies performed by Yang and co-workers, and Fischle and co-workers showed that HDAC 3 can co-precipitate with HDACs 4, 5, and 7 through complex-formation with SMRT and N-CoR.[26,28] Endogenous HDAC 3 mostly associates with itself, and only a small fraction of HDAC 3 interacts with HDAC 4. HDAC 3 can also be found in a complex with HDAC-related protein (HDRP).[17,29,30] Also, HDAC 3 shares the ability of HDAC 1 to mediate the Rb-RbAp48 interaction, suggesting a mediating role of these HDACs in the cell cycle process. HDAC 3, however, does not interfere with Rb-E2F activity, in contrast with HDAC 1 and HDAC 2.[31]

Of all the class I HDACs, HDAC 8 is most similar to HDAC 3 with 34% similarity. HDAC 8 consists largely of the catalytic domain with an NLS in the center.[22,32] Due to its recent discovery, it is not yet known whether HDAC 8 function is regulated by a co-repressor complex of proteins. Two different transcripts of 2.0 kb and 2.4 kb have been found. Northern blot analysis, after lengthy incubations, revealed a varying degree of HDAC 8 expression in several tissue types, suggesting a very low abundance of HDAC 8 mRNA.[33,34]

2.1.2.2 Class II Histone Deacetylases

The Had 1 homologous class II HDACs include HDAC 4, HDAC 5, HDAC 6, HDAC 7, HDAC 9, and HDAC 10 and are structurally much larger in size. Class II HDACs can shuttle between the nucleus and cytoplasm, suggesting different functions and cellular substrates from Class I HDACs. Class II HDACs also display a more limited tissue distribution. HDAC 4, HDAC 5 and HDAC 7 are found in the same region of the phylogenetic tree, and represent a subgroup within the class II HDACs. HDAC 4 and HDAC 5 are most similar to each other (overall similarity 70%), but HDAC 7 is also closely related (58 and 57% overall similarity, respectively). All three HDACs have their catalytic domain on the C-terminal half of the protein and the NLS is situated close to the N-terminus. Binding domains for C-terminal binding protein (CtBP), myocyte enhancer factor 2 (MEF2) and 14-3-3 protein are conserved in all three HDACs on the N-terminus.[14,35] Furthermore, HDAC 5 has a NES within the catalytic domain, suggesting nuclear-cytoplasmic trafficking. HDAC 4, HDAC 5 and HDAC 7 are able to interact with SMRT/N-CoR, and the co-repressors BCoR (Bcl-6-interacting co-repressor) and CtBP. The N-termini of HDAC 4, HDAC 5 and HDAC 7 interact specifically with and repress the myogenic transcription factor MEF2. MEF2 plays an essential role, as a DNA binding transcription factor, in muscle differentiation.[36] When MEF2 is associated with HDAC 4, 5 or 7, the function of MEF2 as a transcription factor is inhibited, thus blocking muscle cell differentiation. Calcium/calmodulin-dependent kinase (CaMK) activity overcomes this inhibition by dissociating the MEF2-HDAC complex due to phosphorylation of HDAC 4, 5, and 7. Subsequently, transport (along with the cellular export factor CRM1) of the HDAC out of the nucleus can occur, illustrating another type of regulation of HDAC activity.[27,37,38] Interestingly, HDAC 4, 5 and 7 associate with HDAC 3 *in vivo* via co-recruitment to the

SMRT/N-CoR factors in the nucleus, with an absence of HDAC 3 leading to inactivity. This suggests that HDAC 4, 5, and 7 function as a link between DNA-binding recruiters and the HDAC 3-containing HDAC complex.[26,28,29] The subcellular localization of HDAC 5 and HDAC 7 differs from that of HDAC 4 at the different stages of muscle cell differentiation. These HDACs might complement each other in order to control the differential regulation of gene expression during the various stages of differentiation in muscle cells. These three HDACs are able to 'fine tune' the repression of gene expression due to the need for co-repressors for their activity, and even more intriguingly via their ability to change localization in response to a specific signal, thus providing a carefully regulated sequence of changes in gene expression during differentiation.[16,22,28,29,32,35,36,39,40]

HDAC 6 is evolutionarily most closely related to HDAC 10. In general, the similarity of HDAC 6 with other human HDACs is low, with some resemblance to yeast HAD 1 (*Saccharomyces cerevisiae*) indicating an early separation from the other HDACs in evolution. HDAC 6 is a rather unique enzyme within the classical family of HDACs, because it contains two catalytic domains arranged in tandem.[22,32] Another unique feature of HDAC 6 is the presence of a HUB (HDAC 6, USP 3, and Brap 2-related zinc finger motif) domain on the C-terminus. This domain is a signal for ubiquitination, suggesting that this HDAC is particularly prone to degradation.[35] The catalytic domains of HDAC 6 are most similar to the catalytic domain of HDAC 9. HDAC 6 functions as a tubulin deacetylase, regulating microtubule-dependent cell motility.[41] Although it resides predominantly in the cytoplasm (having a NES) to exert its function, HDAC 6 is also found in the nucleus in a complex together with HDAC 11. The function of HDAC 6 has been little studied in comparison with other HDACs, but it seems to have many special and interesting features.[22,32,35,42]

HDAC 9 splice variants are clustered as a separate group related to HDACs 4, 5 and 7, within class II of the classical HDAC family. Like the class I HDACs, the HDAC 9 catalytic domain is located on the N-terminus. There are three known splice variants, HDAC 9a, HDAC 9b and HDAC-related protein (HDRP)/HDAC 9c, but more variants are suspected.[43] HDAC 9c/HDRP lacks the catalytic domain and is 50% similar to the N-terminus of HDAC 4 and HDAC 5. By analogy with HDAC 4, 5, and 7, HDRP is able to recruit HDAC 3, thus circumventing the lack of a catalytic domain. In addition, HDAC 9 is also able to interact with MEF2 (CaMK/14-3-3), indicating that HDAC 9 may have an important function in muscle differentiation. The alternative splicing might also represent another way of fine tuning HDAC activity. Certain cell types might express one isoform, while others express the other.[35,43]

HDAC 10 is the most recently discovered member of the class II HDACs. Two mRNA species, with a slight difference in length, have been found, suggesting the existence of two splice variants of HDAC 10.[44] Analysis of protein sequence identity shows that HDAC 10 is most closely related (37% overall similarity) to HDAC 6.[42] HDAC 10 has a catalytic domain on its N-terminus, as well as a NES and a putative second catalytic domain on the C-terminus. Also, two putative Rb binding domains have been found on HDAC 10, suggesting a role in regulation of the cell cycle. Furthermore, HDAC 10 is found to interact with HDACs 1, 2 and 3 (and/or SMRT) and HDACs 4, 5 and 7, but not with HDAC 6, although these results are under much scrutiny and debate. The fact that HDAC 10 is able to associate with many other HDACs presents the possibility that it might function as a recruiter rather than as a deacetylase. However, when expressed by recombination, HDAC 10 alone does show deacetylating activity.[16,42,44,45]

2.1.2.3 Class III Histone Deacetylases

Class III HDACs are evolutionary distinct, with a unique enzymatic mechanism dependent on the cofactor nicotinamide adenine dinucleotide (NAD^+). The sirtuins are virtually unaffected by all HDAC inhibitors in current development; instead, they are inhibited by nicotinamide (vitamine B_3). Nicotinamide inhibits a NAD-dependent p53 deacetylation induced by SIR2α and also enhances p53 acetylation levels *in vivo*.[46] Recent experiments by Motta and coworkers have shown that SIRT 1 is capable of decreasing apoptosis by restraining the mammalian forkhead protein foxo 3a.[47] Interestingly, the inhibition of forkhead activity by SIRT 1 parallels the effect of this deacetylase on the tumor suppressor p53. These results have significant implications regarding an important role for sirtuins in modulating the sensitivity of cells in p53-dependent apoptotic response and the possible effect in cancer therapy.[48,49]

2.1.3 Histone Deacetylases and Cancer

Abnormal activities of HATs and HDACs have been linked to the pathogenesis of cancer. Although inactivating mutations of HATs and overexpression of HDACs have been described, the best link between HDACs and cancer progression comes from models of acute promyelocytic leukemias, where chromosomal translocations result in chimeric proteins that alter transcriptional events and thereby interfere with normal cell growth, differentiation and apoptosis.[50] Chromosomal translocations between RARα (retinoic receptor α) and PLZF (promyelocytic leukemia zinc finger) or PML (promyelocytic leukemia protein) for example, lead to inappropriate recruitment of co-repressors and HDACs and abolish the ability of RARα to mediate myelocytic differentiation. Another well-documented example is AML1-ETO, where ETO recruits N-CoR and mSin3A

together with HDACs, which also interferes with retinoic acid functions and myeloid differentiation. In addition, a gene frequently dysregulated in lymphomas is BCL-6, which recruits a complex containing SMRT, mSin3A and HDAC. Together, these examples have in common the aberrant recruitment of HDACs to promoters mediating transcriptional repression, which strengthens the rationale for the development of HDAC inhibitors as cancer therapeutics.[51]

2.1.4 Cellular Activities of HDAC Inhibitors

The increased focus on HDAC inhibitors as targets for cancer treatment stems from their ability to alter several cellular functions known to be deregulated in cancer cells. HDAC inhibitors selectively induce cellular differentiation, growth arrest and apoptosis in a broad spectrum of tumor cells, without affecting normal cells, which contributes to their known low-level of toxicity compared to other anticancer agents.[32]

Angiogenesis is considered to be critical for neoplastic growth and progression. HDAC inhibitors phenyl butyrate (PB, **2.1**), TSA (**2.2**), trapoxin (TPX, **2.3**) and FK-228 (**2.4**) have been known to inhibit angiogenesis by the suppression of the production of vascular endothelial growth factor (VEGF), which is known to stimulate angiogenesis, from tumor cells and direct inhibition of endothelial cells migration and proliferation. Compounds **2.2** and **2.4** have been shown to inhibit the expression of VEGF and to induce the expression of angiogenic-inhibiting factors von Hippel-Lindau (VHL) and p53 under hypoxic conditions. These results demonstrate that HDACs are involved in oxygen-dependent gene expression and hypoxia-induced angiogenesis, and that the anti-angiogenic activity of HDAC inhibitors is derived from the regulation of gene expression.[52,53]

The anti-cancer properties of these drugs may be due to the accumulation of acetylated histones that leads to the activation (and/or repression) of gene transcription, and thereby inhibition of tumor cell growth. Expression profiling of cells cultured with HDAC inhibitors supports this model. Studies on genes regulated by HDAC inhibitors have revealed that a small number of genes (2 - 10%) are altered by HDAC inhibitors, most of which control cell growth and survival.[54,55] What remains unclear is whether gene repression is a direct or indirect effect of histone acetylation, or rather, the acetylation of non-histone proteins, such as transcription factors and other cellular proteins. Most likely, these acetylations occur in concert and are subject to some coordination. HDAC inhibitors rescue the differentiation of APL and acute myeloid leukemia (AML) cells, where the inability of RARα to signal differentiation resulted from chromosomal translocations (e.g. PLZF-RARα and AML1-ETO).[50]

HDAC inhibitors can also induce the differentiation of solid tumor cells, as demonstrated in the case of prostate and breast cancer cell lines by treatment with the suberoylanilide hydroxamic acid (SAHA, **2.5**) resulting in proliferative arrest and reversion of transformed morphology.[56,57] The differentiated phenotype induced by HDAC inhibitors has been correlated to the induction of gelsolin, an actin binding protein with an important role in maintaining the actin cytoskeleton.[58]

HDAC inhibitors are known to induce cell-cycle arrest both in G1 and G2 phase. The tumor suppressor protein $p21^{WAF/Cip1}$ is upregulated by HDAC inhibitors in a p53-independent fashion mediated through binding to one or more Sp 1 sites, and can also be regulated by phosphatidylinositol-3 kinase and protein kinase ε pathways.[59,60] $p21^{WAF/Cip1}$ acts as an inhibitor of cyclin E-Cdk 2 and cyclin A-Cdk 2 kinase complexes, leading to hypo-phosphorylation of Rb and the prevention of S phase progression.[61] Also, it has

been shown that HDAC inhibitors transcriptionally activate another regulator of G1 arrest, the *INK4d*. This is consistent with loss of anti-proliferative effects of HDAC inhibitors in $p19^{Ink4d}$-deficient cells.[62] Recently, in a non-transformed cell growth control model, HDAC inhibitors have been found to have anti-proliferative effects through stabilization of another cyclin-dependent kinase inhibitor, $p27^{KIP1}$, although $p21^{WA\ /Cip1}$ has been shown to be similarly stabilized.[63,64] HDAC inhibitors down regulate the expression of cell-cycle modifiers cyclin A and cyclin B1 in a variety of human cancer cell lines.[65] The molecular mechanisms by which HDAC inhibitors cause G2 arrest are unclear. However, the expression of Gadd45, which is involved in G2/M growth arrest upon DNA damage, is increased upon HDAC inhibition by the transcription factors Oct-1 and NF-Y.[66] Another mechanism by which HDAC inhibitors delay the G2/M transition involves the p38 MAPK checkpoint pathway.[67]

An important aspect of HDAC inhibition in tumor control is their ability to mediate cell death in cancer cells but not normal cells. Several mechanisms of cell death have been described and implicate caspases, both through intrinsic-mediated (mitochondria/cytochrome *c*) and death receptors pathways, depending on the cell type and class of HDAC inhibitor used.[68,69] In a myeloid leukemia cell line U937, the aniline-benzanilide HDAC inhibitor MS-275 (**2.6**) induced an early increase in reactive oxygen species (ROS), followed by loss of mitochondrial membrane potential and cytosolic release of cytochrome *c*, culminating in activation of the caspase cascade.[70,71] Intrinsic apoptosis was also triggered by **2.6** in chronic lymphocytic leukemia cells from patients. Caspases 3, 8 and 9 were activated and FLICE inhibitory protein (FLIP) was down regulated. In these circumstances, detectable ROS accumulation was delayed, suggesting that the accumulation of ROS may be an effect rather than an inducer of the apoptotic process.[72] More recently, Shao and co-workers demonstrated that HDAC

inhibitors induce caspase-independent autophagic cell death.[73] Interestingly, these events occur specifically in tumor cells and not in normal cells. Insight into the mechanistic basis of this difference was provided by the finding that HDAC inhibitors cause an increase of thioredoxin in normal cells but not in tumor cells. Thioredoxin is a scavenger of ROS that is essential for DNA synthesis, and has been linked to the resistance of cells to death induction by HDAC inhibitors.[70,71] Another line of evidence supporting the selective induction of cell death in tumor cells compared to normal cells is related to the ability of HDAC inhibitors to selectively increase the expression of TNF-related apoptosis inducing ligand (TRAIL) and its receptors DR 5, triggering a death signaling pathway. The knockdown of TRAIL blocked procaspase 8 activation, produced cleavage and immediate cytochrome *c* release, suggesting that the rapid **2.6**-induced apoptosis results from the activation of the extrinsic TRAIL-dependent pathway.[74] Therefore, different pathways of cell death operate upon HDAC inhibition and may depend on structural differences between HDAC inhibitors, and different cellular systems.

2.2 Progress and Chemical Development of Histone Deacetylase Inhibitors

2.2.1 Histone Deacetylase Inhibitors

A wide range of structures have been shown to inhibit the activity of class I and II HDAC enzymes. Class I and II histone deacetylase enzymes contain an active-site zinc as a critical component of their enzymatic pocket and are an emerging therapeutic target for the treatment of cancer as well as other diseases. HDAC inhibitors have been shown to bind directly to this active-site and thereby block substrate access, causing an accumulation of acetylated histones.

Design and understanding of the enzymatic inhibitory mechanisms for various HDAC inhibitors was aided by solving the crystal structure of an HDAC homologue that shares significant homology with class I and class II HDACs, including all critical active-site residues.[75] The active-site of class I and class II HDACs includes critical zinc and water molecules two charge-relay systems where aspartate residues act to increase the basicity of histidine residues by polarizing the epsilon nitrogen and an active-site tyrosine residue that coordinates to the acetyl oxygen during the transition state (Figure 2.2). In the case of TSA, the zinc ion acts by polarizing the acetyl carbonyl to make the carbonyl carbon a better electrophile for attack by the activated water molecule (Figure 2.2). It is important to note that substitution of other divalent cations, or chelation of the zinc cation by a small-molecular-weight chelator, abolishes enzymatic activity. A hydrophobic pocket high in aromatic and glycine residues leads to the active site, with the narrowest point having a distance of 7.5 Å marked by two opposing phenylalanine residues.

HDAC inhibitors possess diverse biological activities and can affect differentiation, growth arrest, and/or apoptosis in transformed cell cultures. *In vivo* xenograft studies have further demonstrated many of these agents to be effective in the inhibition of tumor growth. With few exceptions, these agents can be divided into structural classes including small-molecule hydroxamates, carboxylates (short-chain fatty acids), benzamides, and cyclic peptides. Despite the variety of structural characteristics, a tripartate structure exemplifies the overwhelming majority of effective HDAC inhibitors.[76] An HDAC recognition or affinity cap is invariably attached to an active site binding group via a linker devoid of elaborate functionality. It has been shown that the length and linearity of the linker are crucial for efficient HDAC inhibition. This is explained, in part, by a necessary resemblance to ε-N-acetyl lysine, the substrate for native HDAC action.[76-78]

Figure 2.2 Crystal structure of TSA on HDLP binding pocket

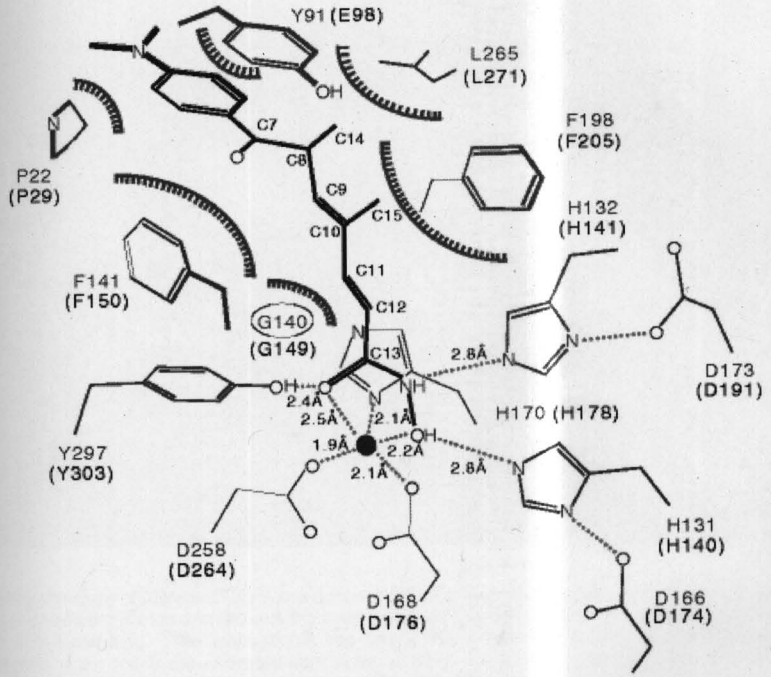

Schematic representation of HDLP-TSA interactions. TSA is in black and the protein is in red. HDLP residues are labeled in red with their counterparts in HDAC 1 indicated in black. Thatched semi-circles indicate van der Waals contacts between hydrophobic protein residues and TSA. Hydrogen bonds are shown as green dashed lines. Adapted from: Finnin, M. S.; Donigan, J. R.; Cohen, A.; Richon, V. M.; Rifkind, R. A. et al. *Nature* **1999**, *401*, 188-193.

Crystallographic studies of **2.2** and clinical candidate **2.5** bound to an HDAC homologue support this amino acid mimicry (Figure 2.3).[75] In addition to the availability of crystal structures, homology models have further aided in the identification and rational design of new HDAC inhibitors for use as chemical tools and potential therapeutics. The high level

Figure 2.3 Crystal Structure of TSA-HDLP and SAHA-HDLP complexes.

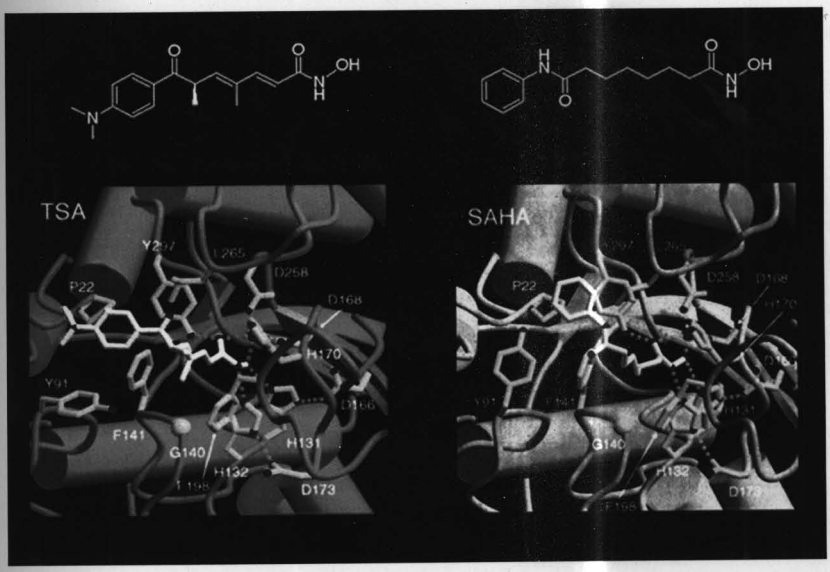

Crystal structure of TSA and SAHA bound to the HPLP protein. The linker spans the length of the hydrophobic pocket and delivers the hydroxamic acid pharmacophore which chelates with the active-site zinc. The hydrophobic cap sits at the gorge of the enzyme blocking the entrance to the active-site. Adapted from: Adapted from: Finnin, M. S.; Donigan, J. R.; Cohen, A.; Richon, V. M.; Rifkind, R. A. et al. *Nature* **1999**, *401*, 188-193.

of interest in developing efficacious HDAC inhibitors and the availability of design tools have led to an expansive group of agents that target class I and II HDACs.

2.2.1.1 Hydroxamates

This is the broadest class of inhibitors with high affinity for HDAC that has been shown to inhibit both class I and II HDACs. Inhibitors containing hydroxamic acid residues bind with high affinity to the HDAC catalytic site, blocking the access of the substrate to the zinc ion.[75] The general structure of these substances consists of three basic

components (Figure 2.4) *a*) a hydroxamic acid pharmacophore that chelates the active zinc in a bidentate manner, hydrogen bonds with residues composing the charge-relay systems, and displaces the nucleophilic water molecule present in the active site (*b*) a hydrophobic linker that has a length optimal for spanning the length of the hydrophobic pocket and dimensions capable of navigating the narrowest segment of the cavity and (*c*) a hydrophobic cap that blocks the entrance to the active site. Hydroxamates with five or six carbon spacers were found to be the most active inhibitors, and replacement of the hydroxamic acid with a carboxylate was found to eliminate inhibitory activity.[76,79] Most of the agents in this group are very potent (functioning at nanomolar to micromolar concentrations *in vitro*) and are reversible inhibitors of class I/II HDACs.

Figure 2.4 Tripartite motif as exemplified by TSA

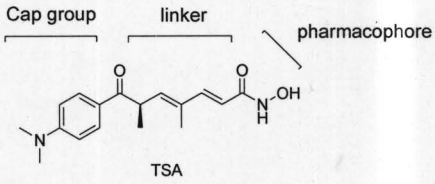

TSA

Trichostatin A was one of the first HDAC inhibitors to be described and is widely used as a reference in research in this field.[22,80] Isolated from *Streptomyces hygroscopicus*, it was initially developed as an antifungal agent until Yoshida and co-workers demonstrated the very potent activities of **2.2** as an HDAC inhibitor.[80] Its relative instability, toxicity to patients and lack of specificity for certain HDACs motivated the search for other substances.[81,82] The design of many synthetic drugs has been inspired by the structure of **2.2**; its aromatic "cap", hydroxamic acid functionality, and hydrophobic linker constitute the three integral structural features. Hydroxamate **2.2** blocks

proliferation and triggers apoptosis in hepatocellular carcinoma cells, blocks cell cycle progression in HeLa cells, and differentiation in ovarian cancer cells by changing p21 tumor suppressor gene and DNA-binding Id1 protein.[83,84] Park and co-workers have shown that **2.2** suppresses growth of pancreatic adenocarcinoma cells and ACHN renal cell carcinoma via cell cycle arrest in association with p27 or apoptosis.[85,86] Also, **2.2** is more sensitive in estrogen receptor α-positive breast cancer cells in inhibiting HDAC.[87]

Figure 2.5 Hydroxamic acids

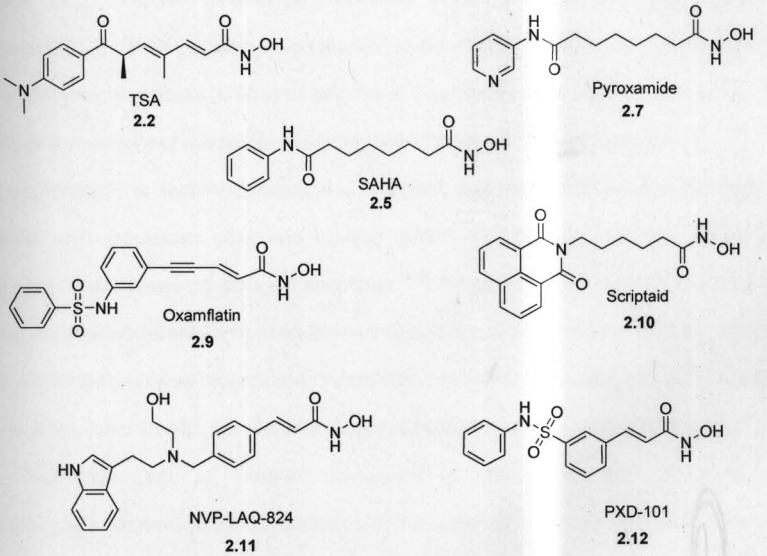

Simple hydroxamic acid derivatives such as **2.5** and pyroxamide (**2.7**) are active at submicromolar concentrations.[88-90] SAHA , developed by Aton Pharma/Merck, is a second-generation polar-planar compound that induces growth arrest, differentiation, and/or apoptosis and is under clinical investigation in both hematological and nonhematological malignancies.[57,89,91] In studies with breast cancer cells, **2.5** inhibited

clonogenic growth and induced apoptosis, whereas in malignant human hematopoietic cells, **2.5** induced marked toxicity but showed relatively minor maturation activity.[92,93] Also, **2.5** showed anti-proliferative and pro-apoptotic actions in several mouse xenografts and cancer cells, including prostate, bladder carcinoma, and myeloma. In addition, **2.5** induced the CDK inhibitor $p21^{WAF1/Cip1}$, and the inhibitory activity was independent of p53 status.[56,94,95] Hydroxamate **2.5** is currently being evaluated in phase I trial in patients with advanced multiple myeloma, AML, chronic myeloid leukemia (CML), acute lymphocytic leukemia (ALL), chronic lymphocytic leukemia (CLL), as well as myelodysplastic syndrome (MDS). SAHA is also being studied in two phase II trials, one in patients with cutaneous T-cell lymphoma (CTCL) or peripheral T-cell lymphoma (PTCL), and another in patients with recurrent or metastatic squamous cell cancer of the head and neck.

Pyroxamide is another compound in this class that induced terminal differentiation in murine erythroleukemic cells and caused growth inhibition in prostate carcinoma, bladder, and neuroblastoma cells via apoptosis.[96-98] In experiments with **2.5** and sodium butyrate (**2.8**), a model was proposed in which induction of apoptosis in Bcr/Abl+ cells by HDAC inhibitors involves coordinate inactivation of the cytoprotective Raf/MEK/ERK pathway in conjunction with the reactive oxygen species-dependent activation of JNK.[99]

Oxamflatin (**2.9**) is another compound in the same class that induces transcriptional activation of junD, causing cell cycle arrest and morphological changes similar to those caused by **2.2**.[100] Oxamflatin was originally identified as a compound inducing the morphological reversion of v-K-*ras*-transformed NIH 3T3 cells from a chemical library and it was shown that **2.9** induces a morphological change of HeLa cells similar to that induced by HDAC inhibitors like **2.2**.[101] Oxamflatin inhibits HDAC *in vitro* and *in vivo*, improving the expression of gelsolin, cyclin E and CDK inhibitors including $p21^{WAF1/Cip1}$.[100]

Using a high-throughput system based on a stably integrated transcriptional reporter to screen a library of 16,320 compounds (DIVERset, Chembridge, San Diego, CA), Su and co-workers identified a novel HDAC inhibitor, termed scriptaid, along with a closely related compound, nullscript. Scriptaid (**2.10**), the 6-(1,3-dioxo-*1H,3H*-benzo[*de*]isoquinolin-2-yl)- hexanoic acid hydroxyamide, conferred the greatest effect on augmentation of the signal transduction TGfb3 pathway including a number of human suppressor genes such as *SMAD4*. Using an immunoblotting assay of histone deacetylation, Su and co-workers demonstrated that **2.10** is a potent HDAC inhibitor with a >100-fold increase in histone acetylation, with a relatively low toxicity.[102] Nullscript, which possesses a shorter side-chain (3 methylene units) than **2.10** (5 methylene units) between the tricyclic core and the carbonyl group, was inactive in transcriptional facilitation. This confirms that a minimum linker chain length is required for HDAC inhibition.[102,103]

Novartis identified NVP-LAQ824 (**2.11**) as a hydroxamic acid based HDAC inhibitor and has demonstrated *in vitro* and *in vivo* anti-tumor activity. This potent HDAC inhibitor is a cinnamic hydroxamic acid derivative and has been shown to transcriptionally activate the $p21^{Cip1/WAF1}$ promoter, and to inhibit tumor cell growth at submicromolar concentrations, inducing cell cycle arrest in the G2/M phase, caspase-dependent apoptosis and inhibition of the proteasome. [104] In xenograft human tumor models in nude mice, **2.11** inhibited the growth of a variety of tumors such as colon HCT116 and lung A549 at doses ranging from 10 to 100 mg/Kg; the efficacy ranged from 32% to 7% T/C, showing low toxicity as determined by body weight change and having a maximum tolerated dose > 200 mg/Kg. [105] In dermal microvascular endothelial cells, **2.11** down-regulates the hypoxia inducible factor-1α (HIF-1α) and VEGF expression. Tumor growth

inhibition was also enhanced in mice with prostate and breast cancer xenografts, reaching approximately 85 and 80% inhibition, respectively.[105] Hydroxamate **2.11** entered phase I clinical trials for solid tumors, but little data concerning response or toxicity have been published.

PXD101 (**2.12**) is a novel hydroxamate HDAC inhibitor belonging to the class of sulfonates developed by TopoTarget Prolifix in UK. PXD101 was found to have inhibitory activity in the nanomolar ranges in leukemia cells. Studies performed by Plumb and co-workers showed that **2.12** delayed growth for xenografts of cisplatin-resistant ovarian tumor cells, had marked increase in acetylation of histones along with induction of $p21^{Cip1/WAF1}$ and apoptosis; and also showed anti-proliferative activity in a variety of tumor cell lines including non-small lung, breast and prostate.[106] Sulfonamide **2.12** is currently in phase II trial evaluation by CuraGen/TopoTarget/the National Cancer Institute, and is being administered as a single-agent, as well as, in combination with dexamethasone for the treatment of advanced multiple myeloma, in patients who have previously failed at least two treatment regimens; it is also undergoing phase I study in patients with solid tumors.

Newer compounds, such as cyclic hydroxamate peptides, structural combinations of a hydroxamates (e.g. TSA) and cyclic tetrapeptides (e.g. trapoxin), inhibit isoform selective HDACs at nanomolar concentrations. Work by Komatsy and co-workers showed that a cyclic hydroxamic acid-containing peptide derivative inhibited growth in four of five human tumor lines implanted into nude mice and showed great promise as a therapeutic agent with higher selective inhibition of HDAC, thus proving that the merger of structural features of various HDACs could be beneficial and provide useful leads.[107]

2.2.1.2 Short-Chain Fatty Acids

In 1971, Friend and co-workers made the remarkable discovery that DMSO differentiates murine virus-induced erythroleukemia cells into normal cells, as they attempted to determine the toxicity of DMSO to the leukemic cell lines.[108] It was found that cells grown in media containing 2% DMSO experienced only a slight decrease in the rate of growth within the first 48 hours, but after 5 days, Friend reported the surprising result that approximately 96% of the leukemia cells had either begun differentiation or had already differentiated into normal cells. Because of this, several compounds were synthesized and screened for activity in differentiation, growth arrest, and/or apoptosis.[32] Valproic acid (**2.13**), a well established anticonvulsant for seizures and bipolar disorders, has anti-growth activity on human endometrial cells, inhibits proliferation and induces apoptosis in acute myeloid leukemia cells expressing ABCB1 (P-glycoprotein) and the multidrug resistance protein ABCC1 (MRP1).[109-111] Acid **2.13** is effective *in vitro* as an HDAC inhibitor at relatively high (millimolar) concentrations and has much weaker affinity.

Figure 2.6 Small molecular weight carboxylates

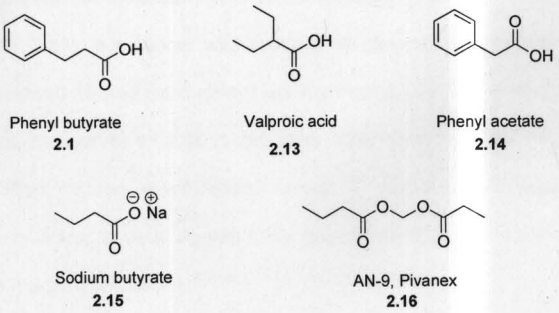

Several studies have shown that **2.13** selectively induces proteosomal degradation of HDAC 2. Researchers have also shown that **2.13** inhibits angiogenesis *in vitro*, as well

as, *in vivo,* and markedly affects genes relevant to proliferation and apoptosis.[112,113] Phenyl acetate (PA, **2.14**) is another carboxylate-derived inhibitor that can penetrate the central nervous system and, when tested in solid tumors, showed anti-tumor effects mediated by histone acetylation. PA is a metabolite of phenyl butyrate (PB, **2.1**) after β-oxidation in the liver and kidney.[114] PB, a well studied member of the short-chain fatty acids, can arrest cells in G1/G0 phase by inducing $p21^{WAF1}$ and other cdk-2 associated cell cycle proteins, alter levels of expression and activation of chemotaxis proteins, such as urokinase-plasminogen activator, induce apoptosis, inhibit telomerase, and increase major histocompatibility complex class I expression in various tumor models.[115] However, these short-chain fatty acids have a low potency due to their poor Zn^{2+} binding capabilities and their short side chains, thus limiting their contact with the catalytic pocket of HDACs.[68]

In human CCRF-CEM cells, acute T-lymphoblastic leukemia cells, sodium butyrate (**2.15**) caused G2/M cell cycle arrest and apoptotic cell death.[116] Butyrate induced histone acetylation and granulocyte maturation in acute myeloid leukemia and selectively inhibited growth in human prostate cancer and cervical carcinoma cells.[117-119] Sodium Butyrate is under extensive clinical evaluation in both hematological malignancies and solid tumors. AN-9 (Pivanex, **2.16**), a butanoic acid prodrug, is currently undergoing phase II clinical trials after it showed 10-fold more potent activity than **2.15** in leukemia tumor cell lines.[120] The anti-neoplastic activity of **2.16** stems from rapid hydrolysis and release of butyrate, permitting efficient delivery to subcellular targets.[121] Despite the overall weak activity of short-chain fatty acids, several agents have been studied clinically because of their use for alternative medical conditions.[122-124]

2.2.1.3 Benzamides

The synthetic benzamide derivatives include a structurally diverse group of compounds such as MS-275 (**2.6**) and CI-994 (**2.17**). N-acetyldinaline **2.17** has shown efficacy in solid tumors in murine models but did not inhibit HDACs directly.

Figure 2.7 Benzamides

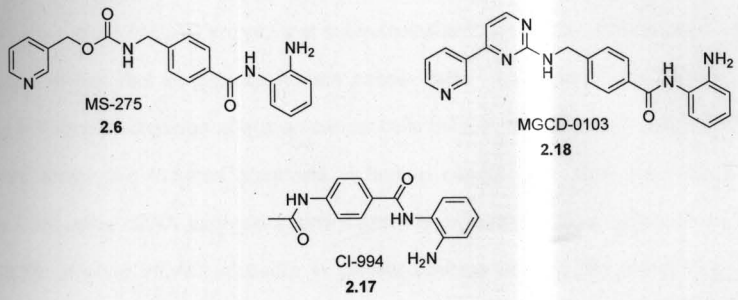

The mechanism of its action is unknown, but it seems to inhibit both histone deacetylation and cellular proliferation at the G1 - S phase transition.[125,126] CI-994 has entered Phase I trials for patients with refractory solid tumors. Benzaminde **2.6**, developed by Schering AG, inhibits HDACs *in vitro* at micromolar concentrations, but the mechanism is also not clearly understood. It is believed that the diaminophenyl group is very important for the inhibitory behavior; possibly, both amino functionalities chelate the metallic ion in the catalytic site. MS-275-associated HDAC inhibitory activity is accompanied by an increase in expression of cyclin-dependent kinase inhibitor $p21^{WAF1/Cip1}$ and accumulation in G1 phase.[127,128] MS-275 displays anti-proliferative activity in several human cancer cell lines, including breast, colorectum, leukemia, lung, ovary, and pancreas. Also, **2.6** suppressed growth of several pediatric cancer cell lines in a dose-dependent manner, as well as tumors transplanted in nude mice.[129] In collaboration with the National Cancer Institute,

2.6 and **2.17** are undergoing clinical trials. Of particular note is **2.6** which is currently in phase I/II clinical evaluation in patients with lung or colorectal cancer. There are reports of novel non-hydroxamate sulfonamide anilides similar in structure to **2.6** being synthesized that have shown lower toxicity and comparable anti-proliferative activity.[65,103]

Currently under development by MethylGene Inc./Taiho Pharmaceuticals, MGCD-0103 (**2.18**) is a non-hydroxamate small molecule HDAC inhibitor, which selectively targets certain class I HDAC enzymes at submicromolar IC_{50}'s *in vitro* and induces hyper-acetylation of histones in cultured human cancer cells. MGCD-0103, selectively and potently inhibited proliferation of human cancer cells but not normal cells. It caused G2/M cell cycle arrest and induced apoptosis in human cancer cells in a dose-dependent manner. By using cDNA expression array analysis of human cancer cells treated with either **2.18** or other HDAC inhibitors in clinical development, it was found that **2.18** regulated the transcription of a small subset of downstream genes, reflecting its inhibitory specificity. *In vivo*, **2.18** significantly inhibited growth of human tumors in various xenograft models in nude mice in a dose-dependent manner with minimal toxicity after oral administration. In conjunction with its antitumor activities, **2.18** induced hyperacetylation of both white blood cells and tumors in tested animals. MGCD0103 appears to have a favorable therapeutic index *in vivo* and is now in Phase I clinical trials.[130]

2.2.1.4 Cyclic Peptides

Cyclic peptides bearing epoxy-ketones may act by chemically modifying an active-site nucleophile with the epoxy group and forming H-bonds with the ketone. These agents are intended to trap HDACs through the reaction of the epoxide moiety with an amino acid, thus forming a covalent attachment in the binding pocket. However, the lability of the epoxide functionality prevents significant *in vivo* activity, which makes them of little

pharmacologic interest. The only HDAC inhibitors in this set of compounds are a number of natural products with significant *in vitro* activity, such as trapoxin (TPX, **2.3**), HC-toxin, (**2.19**) both containing a 2-amino-8-oxodecanoic acid (Aoe) moiety, and apicidin (**2.20**) which contains the 2-amino-8-oxodecanoic acid, but without the epoxide moiety.

Figure 2.8 Cyclic peptides

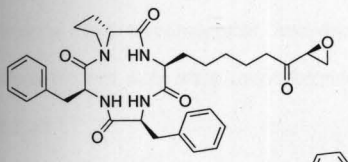

Trapoxin
2.3

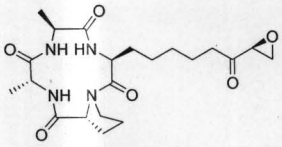

HC-Toxin
2.19

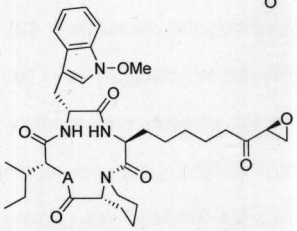

Apicidin
2.20

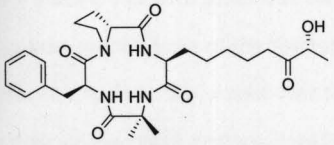

Chlamydocin
2.21

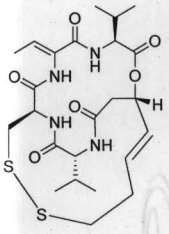

FK-228
2.4

TPX was the first cyclic tetrapeptide to be identified with potent activity as an HDAC inhibitor *in vitro*.[131] TPX was originally isolated from the culture broth of *Helicoma ambiens* RF-1023 exhibiting detransformation activities against v-sis oncogene-transformed NIH3T3 cells (sis/NIH3T3) as antitumor agent.[132] The structure was found to

be cyclo (L-phenylalanyl-L-phenylalanyl-D-pipecolinyl-L-Aoe). TPX inhibited mammalian HDAC at nanomolar concentrations and, interestingly, the inhibition of **2.3** was found to be irreversible, in contrast to other inhibitors. Therefore, it is believed that **2.3** binds covalently to HDAC, leading to its deviating property. In addition, studies by Komatsu and co-workers showed that **2.3** causes the accumulation of highly acetylated histones in a variety of mammalian cells, and a specific G1 and G2 phase cell cycle arrest of rat fibroblasts and morphological and biochemical changes in the phenotypes of F9 teratocarcinoma cells were demonstrated, effects that had also been observed with **2.2** and **2.15**.[107]

In a further approach, **2.3** was shown to specifically alter the expression and activity of proteins involved in cell cycle regulation of different human tumor cell lines.[133] For example, **2.3** induced transcription and elevated protein levels of the cdk inhibitor $p21^{waf1}$ without altering the protein levels of cdk2, cdk4 or cyclin B, resulting in G1 and G2 cell cycle arrest in H1299 human lung and MDA-MB-435 breast carcinoma cells, as well as induction of apoptosis in A549 lung carcinoma cells. Thus, inhibition of HDAC is able to activate a specific subset of genes that control cell cycle arrest and apoptosis.

The host-specific toxin of the filamentous fungus *C. carbonum*, is another cyclic tetrapeptide with specific and potent inhibitory effects on HDACs. *C. carbonum* (also known as *Helminthosporium carbonum*, HC-toxin) causes leaf spot and ear rot of maize plants that are homozygous recessive at the Hm locus, whereas maize that is heterozygous or homozygous dominant at Hm is 100-fold less sensitive to **2.19** and develops only small, nonexpanding lesions when infected with Tox2+ isolates.[134] The production of **2.19** [structure cyclo-(D-proline-L-alanine-D-alanine-L-Aoe)] is under the control of TOX2, a complex genetic locus that consists of at least three different duplicated genes that are unique to Tox2+ isolates, encoding a 570-kDa tetrapartite

cyclic peptide synthetase, a putative membrane antibiotic efflux pump encoded by TOXA and a gene called TOXC that encodes a putative Aoe synthase.[134,135] The demonstration that HC toxin inhibits partially purified HD1-A, HD1-B and HD2 of maize, but also HDACs of chicken and the myxomycete *P. polycephalum* led to the hypothesis that HDAC is the biologically significant site of action of HC toxin.[136] Furthermore, treatment of maize plants with HC toxin demonstrated that HDACs are also inhibited *in vivo*, resulting in the accumulation of highly acetylated histone H3 and H4 subspecies in both maize embryos and tissue cultures.[136,137] Although, it is not clear how **2.19** allows colonization of susceptible maize, it is speculated that inhibition of maize HDACs by **2.19** promotes infection of maize by *C. carbonum* and thereby causes the accumulation of hyperacetylated core histones and the development of a compatible disease interaction, e. g. by interfering with the induction of defense genes in maize. A strong inhibitory effect on HDACs was also demonstrated for chlamydocin (**2.21**), a cyclic tetrapeptide containing the Aoe side chain with the structure cyclo (L-Aoe-*a*-aminobutyric acid-L-phenylalanyl-D-proline- L-Aoe). It is produced by the soil inhabiting fungus *Diheterospora chlamydosporia* and was originally isolated as a cytostatic agent against mammalian cells.[138]

Another naturally ocurring cyclic tetrapeptide which is structurally related to trapoxin is the fungal metabolite apicidin. Apicidin (**2.20**) with the structure cyclo(*N*-*O*-methyl-L-tryptophanyl-L-isoleucinyl-D-piecolinyl-L-2-amino-8-oxodecanoyl) was isolated from fermentations of *Fusarium* spp. as an antiprotozoal agent against Apicomplexan parasites such as *Plasmodium berghei* and *Cryptosporidium parvum*, which represent significant threats to human and animal health via malaria and cryptosporidiosis, respectively.[139,140] Park and co-workers have shown that the antiparasitic activity of **2.20** might be due to nanomolar inhibition of apicomplexan HDAC, causing hyper-acetylation of histones.[141] In addition to the biological and toxic effects, Kim and co-workers described a

possible involvement of HDAC in the ras-signaling pathway via inhibition by **2.20**.[142] In that case, **2.20** inhibited H-ras-induced malignant phenotypes in MCF10A human breast epithelial cells. Furthermore, they showed morphological reversal and growth inhibition of H-ras MCF10A cells induced by **2.20**, similar to that observed with **2.9**.[101] These results present **2.20** as an attractive tool for the development of antimalarial agents, but the detransforming activities of **2.20** and other inhibitors of HDACs support a potential use in the treatment of cancer. In an effort to identify parasite-selective HDAC inhibitors, Merck researchers generated indole-modified apidicin analogues possessing picomolar enzyme activity, as well as tryptophan-replacement analogues displaying 20- to 100-fold parasite selectivity.[143] This approach highlighted the importance of the cap group in terms of cell specificity and paved the way for other researchers for the synthesis of selective HDAC inhibitors.

FK228 (**2.4**), formerly FR901228, was discovered from a fermentation broth of the soil bacterium *Chromobacterium violaceum*, and differs structurally from other constituents of the cyclic peptide class.[144,145] FK-228, discovered and developed by Fujisawa/Gloucester Pharmaceutical, contains a unique bicyclic structure with four amino acids and a β-hydroxyamide moiety, which collectively form a 16-membered lactone with a disulfide bridge. Depsipeptide **2.4** is currently the only member of the cyclic peptide class under clinical investigation and of the HDAC inhibitors known to date, only **2.4** appears to have any cell selectivity.[146,147] This is due, in part, to its unique mode of activation. Research by Furumai and co-workers addressed the long standing question of FK-228's mode of action.[148] It has been postulated that the disulfide bond is reduced in the cellular environment, releasing the free thiol analogue as the active species. To address this issue, **2.4** was converted to its reduced form, redFK, in the presence of DTT

and evaluated for its inhibitory activity against various HDACs prepared from 293T cells (Figure 2.9). This reduction was shown to occur in the cellular environment via participation of glutathione. HDAC activity is significantly lowered after capping of the two sulfhydryl groups via methylation, lending further support to the active species of **2.4** being redFK. RedFK is more active against HDAC 1 and HDAC 2 compared to HDAC 4 and HDAC 6. HDAC 1 is reversibly inhibited by redFK, and a cysteine to serine HDAC1 mutant is still sensitive to redFK, suggesting that redFK is not covalently bound to the conserved Cys-151 in the active site. Computer modeling suggests that the thiol of the four-carbon side chain passes down the HDAC tube-like channel toward the active site residues and interacts with the zinc via a water molecule. FK-228 represents the only HDAC inhibitor prodrug by entering the cell and then being reduced in the cellular environment to redFK, generating the sulfhydryl groups responsible for inhibiting HDAC activity.

Figure 2.9 Formation of RedFK-228 and DimethylFK-228

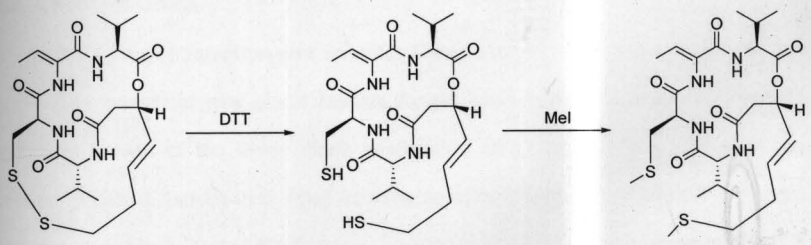

FK-228
2.4

RedFK-228

DimethylFK-228

The antitumor activity of **2.4** has been studied extensively in tumor-bearing animals. Early studies on **2.4** reported a prolonged life span in mice bearing murine leukemia and melanoma, and had potent antitumor activities against human lung

carcinoma and gastric adenocarcinoma that had been implanted in mice, in addition to syngeneic murine solid tumors including colon carcinoma, reticulum cell sarcoma and fibrosarcoma.[145] In another study the effects of **2.4** on the growth of tumor xenografts and the expression of p21 *in vivo* have been examined, demonstrating that the sensitivity to **2.4** was very different among tumor xenografts (PC-3 prostate cancer > DU-145 prostate cancer > ACHN renal cancer), and that the inhibitory degree could be predicted through assessment of p21 gene induction.[149] Such a differential sensitivity of tumor xenografts could be related to the effect of **2.4** on the expression of angiogenesis factors, such as VEGF and basic fibroblast growth factor (bFGF).[150] Similarly, mice treated with **2.4** survived longer than controls in a SCID mouse lymphoma model.[151] Furthermore, **2.4** significantly prevented leukemia death of NOD SCID mice that were injected with human APL cell line expressing the PML-RAR· fusion protein by synergistically enhancing the sensitivity of human APL cells to ATRA *in vivo*.[152,153]

2.3 Project Goals

2.3.1 Target Selection and Specific Aims

The growth of new blood vessels (angiogenesis) into a cancer is required for continued growth of the tumor mass beyond 1-2 mm. Increased numbers of blood vessels in breast cancer, and other cancers as well, correlates closely with metastasis and poor prognosis. Tumor hypoxia is a major inducer of VEGF gene expression. VEGF expression is under the control of the hypoxia-inducible factor (HIF-1), a heterodimeric transcription factor recognized as the key regulator of the hypoxia response in a variety of cell types. HIF-1 activates the transcription of genes encoding angiogenic growth factors

and vasomotor regulators. Importantly, HIF expression levels are characteristically increased in many cancerous tumor types, particularly prostate carcinomas.

Hypoxia, HIF-1α and angiogenesis are all coupled by the actions of HDAC 1. Hypoxia-dependent upregulation of HDAC 1 negatively regulates VHL levels, which in turn enhances HIF-1α. This connection became evident after studies performed by Fumari and co-workers on TSA and FK-228. These studies revealed that TSA and FK-228, both inhibitors of HDAC 1, have very potent anti-angiogenic properties and were able to upregulate tumor suppressor protein p53 as well as VHL protein. Despite their potency, TSA and FK-228 do not inhibit HDAC 1 exclusively. Remarkably, FK-228 is the only known HDAC inhibitor that requires intracellular reductive activation, endowing it with selectivity towards hypoxic cells, while other HDAC inhibitors, including TSA, are promiscuous. Specific HDAC inhibitors would be extremely valuable, both as tools for probing the biological function of these enzymes and also for therapeutic purposes.

Using the cue of reductive activation presented by FK-228, we have developed simple analogs that share its novel mechanism of action while presenting a significantly reduced synthetic barrier and allowing for facile structural diversification. Evaluation of the capacity of these agents for redox-triggered HDAC inhibition is also investigated.

With this in mind, the specific aims for this research are as follows:

1) Develop an efficient synthesis for core cyclic disulfides of various sizes. This was anticipated to aid in the linker optimization of our coumpounds. We expected that different linker lengths would correlate to altered efficiencies of HDAC inhibition.
2) Assay these cyclic disulfides for their ability to inhibit HDACs using *Drosophila melanogaster* Schneider 2 cells.

3) Devise and execute an efficient method by which ancillary amine-bearing cap groups could be affixed to the core cyclic disulfides.

4) Assay these capped cyclic disulfides for their ability to inhibit HDACs in HeLa cell extract as well as in A549 lung cancer cells.

5) Determine the cytotoxicity of the agents constructed on nine human cancer cell lines representing a broad range of carcinomas and calculate the IC_{50} values.

2.4 Summary

Acetylation and deacetylation of nucleosomal histones play important roles in the modulation of chromatin structure, chromatin function and in the regulation of gene expression. Histone acetyltransferases and histone deacetylases are two opposing classes of enzymes, which tightly control histone acetylation status. An imbalance in the equilibrium of histone acetylation has been associated with carcinogenesis and cancer progression. So far, a number of structurally distinct classes of compounds have been identified as HDAC inhibitors including the shortchain fatty acids, hydroxamates, cyclic tetrapeptides and benzamides. These compounds lead to an accumulation of acetylated histone proteins both in tumor cells and in normal tissues.

HDAC inhibitors are able to activate differentiation, to arrest the cell cycle in Gb1 and/or G2, and to induce apoptosis in transformed or cancer cells. Attention is currently being drawn to molecular mechanisms involving histone deacetylases. An induction of $p21^{WAF/CIP1}$ and a suppression of angiogenic stimulating factors have been observed in tumor cells following exposure to HDAC inhibitors. In xenograft models, several HDAC inhibitors have demonstrated antitumor activity with few side effects. Several clinical trials showed that HDAC inhibitors in well-tolerated doses have significant antitumoral activities.

A combination of HDAC inhibitors with differentiation-inducing agents and cytotoxic drugs is an innovative therapeutic strategy.

Some evidence promoting the notion that certain HDACs inhibitors display different degrees of HDAC specificity exists, however significant research must still be performed to delineate differences in HDAC function, their roles in cancer and their sensitivities to drugs. The unearthing of specific roles for these HDAC isozymes during human tumorigenesis will provide scientists with a key element for the development of more specific HDAC inhibitors. This may enhance their clinical activity by reducing their non-specific toxicities, and optimizing potential interactions with other rationally designed therapeutic agents.

The histone code is just beginning to be deciphered and as a result, its complexity and its role in carcinogenesis are far from understood. It is obvious that a wide variety of posttranscriptional protein modifications are responsible for regulating transcription of any given gene and, as such, can play important roles in human cancer cell behaviors. The fact that many HDACs appear to be multifunctional complicates attempts to dissect their function *via* genetic means alone. These considerations, in combination with the known deregulation of HDAC activity/function implicated in a wide array of malignant diseases suggest that cell selective HDAC inhibitors might represent powerful biochemical and therapeutic tools.

2.5 References

(1) Luger, K.; Mader, A. W.; Richmond, R. K.; Sargent, D. F.; Richmond, T. J. Crystal Structure of The Nucleosome Core Particle at 2.8 Å Resolution. *Nature* **1997**, *389*, 251-260.

(2) Roth, S. Y.; Denu, J. M.; Allis, C. D. Histone Acetyl Transferases. *Annu. Rev. Biochem.* **2001**, *70*, 81-120.

(3) Jenuwein, T.; Allis, C. D. Translating the Histone Code. *Science* **2001**, *293*, 1074-1080.

(4) Bannister, A. J.; Schneider, R.; Kouzarides, T. Histone Methylation: Dynamic or Static? *Cell* **2002**, *109*, 801-806.

(5) Carmena, M.; Earnshaw, W. C. The Cellular Geography of Aurora Kinases. *Nat Rev Mol Cell Biol* **2003**, *4*, 842-854.

(6) Goto, H.; Yasui, Y.; Nigg, E.; Inagaki, M. Aurora-B Phosphorylates Histone H3 at Serine28 with Regard to The Mitotic Chromosome Condensation. *Genes Cells* **2002**, *7*, 11-17.

(7) Glaser, K. B.; Staver, M. J.; Waring, J. F.; Stender, J.; Ulrich, R. G. et al. Gene Expression Profiling of Multiple Histone Deacetylase (HDAC) Inhibitors: Defining a Common Gene Set Produced by HDAC Inhibition in T24 and MDA Carcinoma Cell Lines. *Mol. Cancer Ther.* **2003**, *2*, 151-163.

(8) Daujat, S.; Bauer, U.-M.; Shah, V.; Turner, B.; Berger, S. et al. Crosstalk Between CARM1 Methylation and CBP Acetylation on Histone H3. *Curr Biol* **2002**, *12*, 2090-2097.

(9) Hassan, A. H.; Prochasson, P.; Neely, K. E.; Galasinski, S. C.; Chandy, M. et al. Function and Selectivity of Bromodomains in Anchoring Chromatin-Modifying Complexes to Promoter Nucleosomes. *Cell* **2002**, *111*, 369-379.

(10) Agalioti, T.; Chen, G.; Thanos, D. Deciphering the Transcriptional Histone Acetylation Code for a Human Gene. *Cell* **2002**, *111*, 381-392.

(11) Juan, L.-J.; Shia, W.-J.; Chen, M.-H.; Yang, W.-M.; Seto, E. et al. Histone Deacetylases Specifically Down-regulate p53-dependent Gene Activation. *J. Biol. Chem.* **2000**, *275*, 20436-20443.

(12) Gu, W.; Roeder, R. G. Activation of p53 Sequence-Specific DNA Binding by Acetylation of the p53 C-Terminal Domain. *Cell* **1997**, *90*, 595-606.

(13) Sakaguchi, K.; Herrera, J. E.; Saito, S. i.; Miki, T.; Bustin, M. et al. DNA Damage Activates p53 Through a Phosphorylation-Acetylation Cascade. *Genes Dev.* **1998**, *12*, 2831-2841.

(14) Wade, P. A. Transcriptional Control at Regulatory Checkpoints by Histone Deacetylases: Molecular Connections Between Cancer and Chromatin. *Hum. Mol. Genet.* **2001**, *10*, 693-698.

(15) Cress, W. D.; Seto, E. Histone Deacetylases, Transcriptional Control, and Cancer. *J Cell Physiol* **2000**, *184*, 1-16.

(16) Kao, H.-Y.; Downes, M.; Ordentlich, P.; Evans, R. M. Isolation of a Novel Histone Deacetylase Reveals that Class I and Class II Deacetylases Promote SMRT-Mediated Repression. *Genes Dev.* **2000**, *14*, 55-66.

(17) Li, J.; Lin, Q.; Wang, W.; Wade, P.; Wong, J. Specific Targeting and Constitutive Association of Histone Deacetylase Complexes During Transcriptional Repression. *Genes Dev.* **2002**, *16*, 687-692.

(18) Zhang, Y.; Ng, H.-H.; Erdjument-Bromage, H.; Tempst, P.; Bird, A. et al. Analysis of The NuRD Subunits Reveals a Histone Deacetylase Core Complex and a Connection with DNA Methylation. *Genes Dev.* **1999**, *13*, 1924-1935.

(19) Galasinski, S. C.; Resing, K. A.; Goodrich, J. A.; Ahn, N. G. Phosphatase Inhibition Leads to Histone Deacetylases 1 and 2 Phosphorylation and Disruption of Corepressor Interactions. *J. Biol. Chem.* **2002**, *277*, 19618-19626.

(20) Ashburner, B. P.; Westerheide, S. D.; Baldwin, A. S., Jr. The p65 (RelA) Subunit of NF-{kappa}B Interacts with the Histone Deacetylase (HDAC) Corepressors HDAC1 and HDAC2 To Negatively Regulate Gene Expression. *Mol. Cell. Biol.* **2001**, *21*, 7065-7077.

(21) Ito, K.; Barnes, P. J.; Adcock, I. M. Glucocorticoid Receptor Recruitment of Histone Deacetylase 2 Inhibits Interleukin-1beta -Induced Histone H4 Acetylation on Lysines 8 and 12. *Mol. Cell. Biol.* **2000**, *20*, 6891-6903.

(22) Yoshida, M.; Furumai, R.; Nishiyama, M.; Komatsu, Y.; Nishino, N. et al. Histone Deacetylase as a New Target for Cancer Chemotherapy. *Cancer Chemother Pharmacol* **2001**, *48*, S20-S26.

(23) Taplick, J.; Kurtev, V.; Kroboth, K.; Posch, M.; Lechner, T. et al. Homo-Oligomerization and Nuclear Localization of Mouse Histone Deacetylase 1. *J Molec Biol* **2001**, *308*, 27-38.

(24) Nair, A. R.; Boersma, L. J.; Schiltz, L.; Chaudry, A.; Muschel, R. J. Paradoxical Effects of Trichostatin A: Inhibition of NF-Kappa-Associated Histone Acetyltransferase Activity, Phosphorylation of hGCN5 and Downregulation of Cyclin A and B1 mRNA. *Cancer Lett.* **2001**, *166*, 55-64.

(25) Pflum, M. K. H.; Tong, J. K.; Lane, W. S.; Schreiber, S. L. Histone Deacetylase 1 Phosphorylation Promotes Enzymatic Activity and Complex Formation. *J. Biol. Chem.* **2001**, *276*, 47733-47741.

(26) Yang, W.-M.; Tsai, S.-C.; Wen, Y.-D.; Fejer, G.; Seto, E. Functional Domains of Histone Deacetylase-3. *J. Biol. Chem.* **2002**, *277*, 9447-9454.

(27) Guenther, M. G.; Barak, O.; Lazar, M. A. The SMRT and N-CoR Corepressors Are Activating Cofactors for Histone Deacetylase 3. *Mol. Cell. Biol.* **2001**, *21*, 6091-6101.

(28) Fischle, W.; Dequiedt, F.; Fillion, M.; Hendzel, M. J.; Voelter, W. et al. Human HDAC7 Histone Deacetylase Activity Is Associated with HDAC3 in Vivo. *J. Biol. Chem.* **2001**, *276*, 35826-35835.

(29) Fischle, W.; Dequiedt, F.; Hendzel, M. J.; Guenther, M. G.; Lazar, M. A. et al. Enzymatic Activity Associated with Class II HDACs Is Dependent on a Multiprotein Complex Containing HDAC3 and SMRT/N-CoR. *Mol. Cell* **2002**, *9*, 45-57.

(30) Ozawa, Y.; Towatari, M.; Tsuzuki, S.; Hayakawa, F.; Maeda, T. et al. Histone Deacetylase 3 Associates with and Represses The Transcription Factor GATA-2. *Blood* **2001**, *98*, 2116-2123.

(31) Heinzel, T.; Lavinsky, R. M.; Mullen, T.-M.; Söderström, M.; Laherty, C. D. et al. A Complex Containing N-CoR, mSin3 and Histone Deacetylase Mediates Transcriptional Repression. *Nature* **1997**, *387*, 43-48.

(32) Marks, P. A.; Rifkind, R. A.; Richon, V. M.; Breslow, R.; Miller, T. et al. Histone Deacetylases and Cancer: Causes and Therapies. *Nat Rev Cancer* **2001**, *1*, 194-202.

(33) Hu, E.; Chen, Z.; Fredrickson, T.; Zhu, Y.; Kirkpatrick, R. et al. Cloning and Characterization of a Novel Human Class I Histone Deacetylase that Functions as a Transcription Repressor. *J. Biol. Chem.* **2000**, *275*.

(34) Buggy, J. J.; Sideris, M. L.; Mak, P.; Lorimer, D. D.; McIntosh, B. et al. Cloning and Characterization of a Novel Human Histone Deacetylase, HDAC8. *Biochem. J.* **2000**, *350*, 199-205.

(35) Bertos, N. R.; Wang, A. H.; Yang, X. J. Class II Histone Deacetylases : Structure, Function, and Regulation. *Biochem. Cell Biol.* **2001**, *79*, 243-252.

(36) McKinsey, T. A.; Zhang, C. L.; Olson, E. N. Control of Muscle Development by Dueling HATs and HDACs. *Current Opinion in Genetics & Development* **2001**, *11*, 497-504.

(37) Andreucci, J. J.; Grant, D.; Cox, D. M.; Tomc, L. K.; Prywes, R. et al. Composition and Function of AP-1 Transcription Complexes During Muscle Cell Differentiation. *J. Biol. Chem.* **2002**, *277*, 16426-16432.

(38) McKinsey, T. A.; Zhang, C. L.; Lu, J.; Olson, E. N. Signal-Dependent Nuclear Export of a Histone Deacetylase Regulates Muscle Differentiation. *Nature* **2000**, *408*.

(39) Dressel, U.; Bailey, P. J.; Wang, S. C.; Downes, M.; Evans, R. M. et al. A Dynamic Role for HDAC7 in MEF2-Mediated Muscle Differentiation. *J. Biol. Chem.* **2001**, *276*.

(40) Wu, X.; Li, H.; Park, E. J.; Chen, J. D. SMRTE inhibits MEF2C Transcriptional Activation by Targeting HDAC4 and 5 to Nuclear Domains. *J. Biol. Chem.* **2001**, *276*, 24177-24185.

(41) Hubbert, C.; Guardiola, A.; Shao, R.; Kawaguchi, Y.; Ito, A. et al. HDAC6 is a Microtubule-Associated Deacetylase. *Nature* **2002**, *417*, 455-458.

(42) Guardiola, A. R.; Yao, T.-P. Molecular Cloning and Characterization of a Novel Histone Deacetylase HDAC10. *J. Biol. Chem.* **2002**, *277*, 3350-3356.

(43) Zhou, X.; Marks, P. A.; Rifkind, R. A.; Richon, V. M. Cloning and Characterization of a Histone Deacetylase, HDAC9. *Prod. Natl. Acad. Sci. U.S.A.* **2001**, *98*.

(44) Fischer, D. D.; Cai, R.; Bhatia, U.; Asselbergs, F. A.; Song, C. et al. Isolation and Characterization of a Novel Class II Histone Deacetylase, HDAC10. *J. Biol. Chem.* **2002**, *277*, 6656-6666.

(45) Tong, J. K. Dissecting Histone Deacetylase Function. *Chem. Biol.* **2002**, *9*, 668-670.

(46) Luo, J.; Nikolaev, A. Y.; Imai, S.-i.; Chen, D.; Su, F. et al. Negative Control of p53 by Sir2α Promotes Cell Survival under Stress. *Cell* **2001**, *107*, 137-148.

(47) Motta, M. C.; Divecha, N.; Lemieux, M.; Kamel, C.; Chen, D. et al. Mammalian SIRT1 Represses Forkhead Transcription Factors. *Cell* **2004**, *116*, 551-563.

(48) Schwer, B.; North, B. J.; Frye, R. A.; Ott, M.; Verdin, E. The Human Silent Information Regulator (Sir)2 Homologue hSIRT3 is a Mitochondrial Nicotinamide Adenine Dinucleotide-Dependent Deacetylase. *J. Cell Biol.* **2002**, *158*, 647-657.

(49) North, B. J.; Marshall, B. L.; Borra, M. T.; Denu, J. M.; Verdin, E. The Human Sir2 Ortholog, SIRT2, Is an NAD+-Dependent Tubulin Deacetylase. *Molecular Cell* **2003**, *11*, 437-444.

(50) Gayther, S. A.; Batley, S. J.; Linger, L.; Bannister, A.; Thorpe, K. et al. Mutations Truncating the EP300 Acetylase in Human Cancers. **2000**, *24*, 300-303.

(51) Amann, J. M.; Nip, J.; Strom, D. K.; Lutterbach, B.; Harada, H. et al. ETO, A Target of t(8;21) in Acute Leukemia, Makes Distinct Contacts with Multiple Histone Deacetylases and Binds mSin3A through Its Oligomerization Domain. *Mol. Cell. Biol.* **2001**, *21*, 6470-6483.

(52) Qian, D. Z.; Wang, X.; Kachhap, S. K.; Kato, Y.; Wei, Y. et al. The Histone Deacetylase Inhibitor NVP-LAQ824 Inhibits Angiogenesis and Has a Greater Antitumor Effect in Combination with the Vascular Endothelial Growth Factor

Receptor Tyrosine Kinase Inhibitor PTK787/ZK222584. *Cancer Res* **2004**, *64*, 6626-6634.

(53) Kwon, H. J.; Kim, M. S.; Kim, M. J.; Nakajima, H.; Kim, K.-W. Histone Deacetylase Inhibitor FK228 Inhibits Tumor Angiogenesis. *Int. J. Cancer* **2002**, *97*, 290-296.

(54) Mariadason, J. M.; Corner, G. A.; Augenlicht, L. H. Genetic Reprogramming in Pathways of Colonic Cell Maturation Induced by Short Chain Fatty Acids: Comparison with Trichostatin A, Sulindac, and Curcumin and Implications for Chemoprevention of Colon Cancer. *Cancer Res* **2000**, *60*, 4561-4572.

(55) Joseph, J.; Mudduluru, G.; Antony, S.; Vashistha, S.; Ajitkumar, P. et al. Expression Profiling of Sodium Butyrate (NaB)-Treated Cells: Identification of Regulation of Genes Related to Cytokine Signaling and Cancer Metastasis by NaB. *Oncogene* **2004**, *23*, 6304-6315.

(56) Butler, L. M.; Agus, D. B.; Scher, H. I.; Higgins, B.; Rose, A. et al. Suberoylanilide Hydroxamic Acid, An Inhibitor of Histone Deacetylase, Suppresses the Growth of Prostate Cancer Cells In Vitro and In Vivo. *Cancer Res* **2000**, *60*, 5165-5170.

(57) Munster, P. N.; Troso-Sandoval, T.; Rosen, N.; Rifkind, R.; Marks, P. A. et al. The Histone Deacetylase Inhibitor Suberoylanilide Hydroxamic Acid Induces Differentiation of Human Breast Cancer Cells. *Cancer Res* **2001**, *61*, 8492-8497.

(58) Vigushin, D. M.; Coombes, R. C. Histone Deacetylase Inhibitors in Cancer Treatment. *Anti-Cancer Drugs* **2002**, *13*, 1-13.

(59) Han, J.-W.; Ahn, S. H.; Kim, Y. K.; Bae, G.-U.; Yoon, J. W. et al. Activation of p21WAF1/Cip1 Transcription through Sp1 Sites by Histone Deacetylase Inhibitor Apicidin. Involvement of Protein Kinase C. *J. Biol. Chem.* **2001**, *276*, 42084-42090.

(60) Kim, Y. K.; Han, J.-W.; Woo1, Y. N.; Chun, J. K.; Yoo, J. Y. et al. Expression of p21WAF1/Cip1 Through Sp1 Sites by Histone Deacetylase Inhibitor Apicidin Requires PI 3-Kinase-PKC Signaling Pathway. *Oncogene* **2003**, *22*, 6023-6031.

(61) Sandor, V.; Senderowicz, A.; Mertins, S.; Sackett, D.; Sausville, E. et al. p21-Dependent G1Arrest with Downregulation of Cyclin D1 and Upregulation of Cyclin E by The Histone Deacetylase Inhibitor FR901228. *Br J. Cancer* **2000**, *83*, 817-825.

(62) Yokota, T.; Matsuzaki, Y.; Miyazawa, K.; Zindy, F.; Roussel, M. F. et al. Histone Deacetylase Inhibitors Activate INK4d Gene Through Sp1 Site in its Promoter. *Oncogene* **2004**, *23*, 5340-5349.

(63) Chen, J. S.; Faller, D. V. Histone Deacetylase Inhibition-Mediated Post-Translational Elevation of $P27^{Kip1}$ Protein Levels is Required for G_1 Arrest in Fibroblasts. *J Cell. Phys.* **2005**, *202*, 87-99.

(64) Hirsch, C. L.; Bonham, K. Histone Deacetylase Inhibitors Regulate p21WAF1 Gene Expression at the Post-Transcriptional Level in HepG2 Cells. *FEBS Letters* **2004**, *570*, 37-40.

(65) Fournel, M.; Trachy-Bourget, M.-C.; Yan, P. T.; Kalita, A.; Bonfils, C. et al. Sulfonamide Anilides, a Novel Class of Histone Deacetylase Inhibitors, Are Antiproliferative against Human Tumors. *Cancer Res* **2002**, *62*, 4325-4330.

(66) Hirose, T.; Sowa, Y.; Takahashi, S.; Saito, S.; Yasuda, C. et al. p53-Independent Induction of Gadd45 by Histone Deacetylase Inhibitor: Coordinate Regulation by Transcription Factors Oct-1 and NF-Y. *Oncogene* **2003**, *22*, 7762-7773.

(67) Mikhailov, A.; Shinohara, M.; Rieder, C. L. Topoisomerase II and Histone Deacetylase Inhibitors Delay the G2/M Transition by Triggering the p38 MAPK Checkpoint Pathway. *J. Cell Biol.* **2004**, *166*, 517-526.

(68) Johnstone, R. W. Histone Deacetylase Inhibitors: Novel Drugsfor the Treatment of Cancer. *Nat Rev Drug Discov* **2002**, *1*, 287-299.

(69) Glick, R. D.; Swendeman, S. L.; Coffey, D. C.; Rifkind, R. A.; Marks, P. A. et al. Hybrid Polar Histone Deacetylase Inhibitor Induces Apoptosis and CD95/CD95 Ligand Expression in Human Neuroblastoma. *Cancer Res* **1999**, *59*, 4392-4399.

(70) Ungerstedt, J. S.; Sowa, Y.; Xu, W. S.; Shao, Y.; Dokmanovic, M. et al. Role of Thioredoxin in The Response of Normal and Transformed Cells to Histone Deacetylase Inhibitors. *Prod. Natl. Acad. Sci. U.S.A.* **2005**, *102*, 673-678.

(71) Rosato, R. R.; Almenara, J. A.; Grant, S. The Histone Deacetylase Inhibitor MS-275 Promotes Differentiation or Apoptosis in Human Leukemia Cells through a Process Regulated by Generation of Reactive Oxygen Species and Induction of p21CIP1/WAF1 1. *Cancer Res* **2003**, *63*, 3637-3645.

(72) Lucas, D. M.; Davis, M. E.; Parthun, M. R.; Mone, A. P.; Kitada, S. et al. The Histone Deacetylase Inhibitor MS-275 Induces Caspase-Dependent Apoptosis in B-Cell Chronic Lymphocytic Leukemia Cells. *Leukemia* **2004**, *18*, 1207-1214.

(73) Shao, Y.; Gao, Z.; Marks, P. A.; Jiang, X. Apoptotic and Autophagic Cell Death Induced by Histone Deacetylase Inhibitors. *Prod. Natl. Acad. Sci. U.S.A.* **2004**, *101*, 18030-18035.

(74) Nebbioso, A.; Clarke, N.; Voltz, E.; Germain, E.; Ambrosino, C. et al. Tumor-Selective Action of HDAC Inhibitors Involves TRAIL Induction in Acute Myeloid Leukemia Cells. **2005**, *11*, 77-84.

(75) Finnin, M. S.; Donigan, J. R.; Cohen, A.; Richon, V. M.; Rifkind, R. A. et al. Structures of Histone Deacetylase Homologue Bound to the TSA and SAHA Inhibitors. *Nature* **1999**, *401*, 188-193.

(76) Breslow, R.; Belvedere, S.; Gershell, L. Development of Cytodifferentiating Agents for Cancer Chemotherapy. *Helv. Chim. Acta* **2000**, *83*, 1685-1692.

(77) Marks, P. A.; Richon, V. M.; Breslow, R.; Rifkind, R. A. Histone Deacetylase Inhibitors as New Cancer Drugs. *Curr. Opin. Oncol.* **2001**, *13*, 477-483.

(78) Taunton, J.; Collins, J. L.; Schreiber, S. L. Synthesis of Natural and Modified Trapoxins, Useful Reagents for Exploring Histone Deacetylase Function. *J. Am. Chem. Soc.* **1996**, *118*, 10412-10422

(79) Woo, S.; Frechette, S.; Abou Khalil, E.; Bouchain, G.; Vaisburg, A. et al. Structurally Simple Trichostatin A-like Straight Chain Hydroxamates as Potent Histone Deacetylase Inhibitors. *J. Med. Chem.* **2002**, *45*.

(80) Yoshida, M.; Nomura, S.; Beppu, T. Effects of Trichostatins on Differentiation of Murine Erythroleukemia Cells. *Cancer Res.* **1987**, *47*, 3688-3691.

(81) Jung, M.; Brosch, G.; Kolle, D.; Scherf, H.; Gerhauser, C. et al. Amide Analogues of Trichostatin A as Inhibitors of Histone Deacetylase and Inducers of Terminal Cell Differentiation. *J. Med. Chem.* **1999**, *42*, 4669-4679.

(82) Jung, M. Inhibitors of Histone Deacetylase as New Anticancer Agents. *Curr. Med. Chem.* **2001**, *8*, 1505-1511.

(83) Strait, K. A.; Dabbas, B.; Hammond, E. H.; Warnick, C.; Terry, I. et al. Cell Cycle Blockade and Differentiation of Ovarian Cancer Cells by the Histone Deacetylase Inhibitor Trichostatin A Are Associated with Changes in p21, Rb, and Id Proteins. *Mol Cancer Ther* **2002**, *1*, 1181-1190.

(84) Hoshikawa, Y.; Kwon, H. J.; Yoshida, M.; Horinouchi, S.; Beppu, T. Trichostatin A Induces Morphological Changes and Gelsolin Expression by Inhibiting Histone Deacetylase in Human Carcinoma Cell Lines. *Experimental Cell Research* **1994**, *214*, 189-197.

(85) Donadelli, M.; Costanzo, C.; Faggioli, L.; Scupoli, M. T.; Moore, P. S. et al. Trichostatin A, An Inhibitor of Histone Deacetylases, Strongly Suppresses Growth of Pancreatic Adenocarcinoma Cells. *Molecular Carcinogenesis* **2003**, *38*, 59-69.

(86) Park, W. H.; Jung, C. W.; Park, J. O.; Kim, K.; Kim, W. S. et al. Trichostatin Inhibits the Growth of ACHN Renal Cell Carcinoma Cells via Cell Cycle Arrest in Association with p27, or Apoptosis. *Int. J. Oncol.* **2003**, *22*, 1129-1134.

(87) Margueron, R.; Licznar, A.; Lazennec, G.; Vignon, F.; Cavailles, V. Oestrogen Receptor Alpha Increases $p21^{(WAF1/CIP1)}$ Gene Expression and the Antiproliferative Activity of Histone Deacetylase Inhibitors in Human Breast Cancer Cells. *J. Endocrinol.* **2003**, *179*, 41-53.

(88) Richon, V. M.; Zhou, X.; Rifkind, R. A.; Marks, P. A. Histone Deacetylase Inhibitors: Development of Suberoylanilide Hydroxamic Acid (SAHA) for the Treatment of Cancers. *Blood Cells Mol Dis* **2001**, *27*, 260-264.

(89) Richon, V. M.; Emiliani, S.; Verdin, E.; Webb, Y.; Breslow, R. et al. A Class of Hybrid Polar Inducers of Transformed Cell Differentiation Inhibits Histone Deacetylases. *Prod. Natl. Acad. Sci. U.S.A.* **1998**, *95*, 3003-3007.

(90) Marks, P. A.; Richon, V. M.; Miller, T.; Kelly, W. K. Histone Deacetylase Inhibitors. *Adv Cancer Res* **2004**, *91*, 137-168.

(91) Richon, V. M.; Webb, Y.; Merger, R.; Sheppard, T.; Jursic, B. et al. Second Generation Hybrid Polar Compounds are Potent Inducers of Transformed Cell Differentiation. *Prod. Natl. Acad. Sci. U.S.A.* **1996**, *93*, 5705-5708.

(92) Vrana, J. A.; Decker, R. H.; Johnson, C. R.; Wang, Z.; Jarvis, W. D. et al. Induction of Apoptosis in U937 Human Leukemia Cells by Suberoylanilide Hydroxamic Acid (SAHA) Proceeds Through Pathways that are Regulated by Bcl-2/Bcl-XL, c-Jun and p21CIP1, but Independent of p53. *Oncogene* **1999**, *18*, 7016-7025.

(93) Huang, L.; Pardee, A. B. Suberoylanilide Hydroxamic Acid as a Potential Therapeutic Agent for Human Breast Cancer Treatment. *Mol Med* **2000**, *6*, 849-866.

(94) Richon, V. M.; Sandhoff, T. W.; Rifkind, R. A.; Marks, P. A. Histone Deacetylase Inhibitor Selectively Induces p21WAF1 Expression and Gene-Associated Histone Acetylation. *Prod. Natl. Acad. Sci. U.S.A.* **2000**, *97*, 10014-10019.

(95) Gui, C. Y.; Ngo, L.; Xu, W. S.; Richon, V. M.; Marks, P. A. Histone Deacetylase (HDAC) Inhibitor Activation of p21WAF1 Involves Changes in Promoter-Associated Proteins, Including HDAC1. *Prod. Natl. Acad. Sci. U.S.A.* **2004**, *101*, 1241-1246.

(96) Butler, L. M.; Webb, Y.; Agus, D. B.; Higgins, B.; Tolentino, T. R. et al. Inhibition of Transformed Cell Growth and Induction of Cellular Differentiation by Pyroxamide, an Inhibitor of Histone Deacetylase. *Clin Cancer Res* **2001**, *7*, 962-970.

(97) Kouraklis, G.; Theocharis, S. Histone Deacetylase Inhibitors and Anticancer Therapy. *Curr Med Chem Anti-Cancer Agents* **2002**, *2*, 477-484.

(98) Kutko, M. C.; Glick, R. D.; Butler, L. M.; Coffey, D. C.; Rifkind, R. A. et al. Histone Deacetylase Inhibitors Induce Growth Suppression and Cell Death in Human Rhabdomyosarcoma in vitro. *Clin Cancer Res* **2003**, *9*, 5749-5755.

(99) Yu, C.; Subler, M.; Rahmani, M.; Reese, E.; Krystal, G. et al. Induction of Apoptosis in BCR/ABL+ cells by Histone Deacetylase Inhibitors Involves Reciprocal Effects on the RAF/MEK/ERK and JNK Pathways. *Cancer Biol Ther* **2003**, *2*, 544-551.

(100) Kim, Y. B.; Lee, K. H.; Sugita, K.; Yoshida, M.; Horinouchi, S. Oxamflatin is a Novel Antitumor Compound that Inhibits Mammalian Histone Deacetylase. *Oncogene* **1999**, *18*, 2461-2470.

(101) Sonoda, H.; Nishida, K.; Yoshioka, T.; Ohtani, M.; K, S. Oxamflatin: A Novel Compound which Reverses Malignant Phenotype to Normal One via Induction of JunD. *Oncogene* **1996**, *13*, 143-149.

(102) Su, G. H.; Sohn, T. A.; Ryu, B.; Kern, S. E. A Novel Histone Deacetylase Inhibitor Identified by High-Throughput Transcriptional Screening of a Compound Library. *Cancer Res* **2000**, *60*, 3137-3142.

(103) Bouchain, G.; Delorme, D. Novel Hydroxamate and Anilide Derivatives as Potent Histone Deacetylase Inhibitors: Synthesis and Antiproliferative Evaluation. *Curr Med Chem* **2003**, *10*, 2359-2372.

(104) Catley, L.; Weisberg, E.; Tai, Y. T.; Atadja, P.; Remiszewski, S. et al. NVP-LAQ824 is a Potent Novel Histone Deacetylase Inhibitor with Significant Activity Against Multiple Myeloma. *Blood* **2003**, *102*, 2615-2622.

(105) Atadja, P.; Gao, L.; Kwon, P.; Trogani, N.; Walker, H. et al. Selective Growth Inhibition of Tumor Cells by a Novel Histone Deacetylase Inhibitor, NVP-LAQ824. *Cancer Res* **2004**, *64*, 689-695.

(106) Plumb, J. A.; Finn, P. W.; Williams, R. J.; Bandara, M. J.; Romero, M. R. et al. Pharmacodynamic Response and Inhibition of Growth of Human Tumor Xenografts by the Novel Histone Deacetylase Inhibitor PXD101. *Mol Cancer Ther* **2003**, *2*, 721-728.

(107) Komatsu, Y.; Tomizaki, K.-y.; Tsukamoto, M.; Kato, T.; Nishino, N. et al. Cyclic Hydroxamic-Acid-Containing Peptide 31, a Potent Synthetic Histone Deacetylase Inhibitor with Antitumor Activity. *Cancer Res* **2001**, *61*, 4459-4466.

(108) Friend, C.; Scher, W.; Holland, J. G.; Sato, T. Hemoglobin Synthesis in Murine Virus-Induced Leukemic Cells In Vitro: Stimulation of Erythroid Differentiation by Dimethyl Sulfoxide. *Prod. Natl. Acad. Sci. U.S.A.* **1971**, *68*, 378-382.

(109) Tang, R.; Faussat, A. M.; Majdak, P.; Perrot, J. Y.; Chaoui, D. et al. Valproic Acid Inhibits Proliferation and Induces Apoptosis in Acute Myeloid Leukemia Cells Expressing P-gp and MRP1. *Leukemia* **2004**, *18*, 1246-1251.

(110) Takai, N.; Desmond, J. C.; Kumagai, T.; Gui, D.; Said, J. W. et al. Histone Deacetylase Inhibitors Have a Profound Antigrowth Activity in Endometrial Cancer Cells. *Clin. Cancer Res.* **2004**, *10*, 1141-1149.

(111) Gurvich, N.; Tsygankova, O. M.; Meinkoth, J. L.; Klein, P. S. Histone Deacetylase is a Target of Valproic Acid-Mediated Cellular Differentiation. *Cancer Res.* **2004**, *64*, 1079-1086.

(112) Michaelis, M.; Michaelis, U. R.; Fleming, I.; Suhan, T.; Cinatl, J. et al. Valproic Acid Inhibits Angiogenesis In Vitro and In Vivo. *Mol. Pharmacol.* **2004**, *65*, 520-527.

(113) Thelen, P.; Schweyer, S.; Hemmerlein, B.; Wuttke, W.; Seseke, F. et al. Expressional Changes After Histone Deacetylase Inhibition by Valproic Acid in LNCaP Human Prostate Cancer Cells. *Int. J. Oncol.* **2004**, *24*, 25-31.

(114) Piscitelli, S. C.; Thibault, A.; Figg, W. D.; Tompkins, A.; Headlee, D. et al. Disposition of Phenylbutyrate and its Metabolites, Phenylacetate and Phenylacetylglutamine. *J. Clin. Pharmacol.* **1995**, *35*, 368-373.

(115) Carducci, M. A.; Nelson, J. B.; Chan-Tack, K. M.; Ayyagari, S. R.; Sweatt, W. H. et al. Phenylbutyrate Induces Apoptosis in Human Prostate Cancer and Is More Potent than Phenylacetate. *Clin. Cancer Res.* **1996**, *2*, 379-387.

(116) Bernhard, D.; Ausserlechner, M. J.; Tonko, M.; Loffler, M.; Hartmann, B. L. et al. Apoptosis Induced by the Histone Deacetylase Inhibitor Sodium Butyrate in Human Leukemic Lymphoblasts. *FASEB J.* **1999**, *13*, 1991-2001.

(117) Kuefer, R.; Hofer, M.; Altug, V.; Zorn, C.; Genze, F. et al. Sodium Butyrate and Tributyrin Induce In Vivo Growth Inhibition and Apoptosis in Human Prostate Cancer. *Br. J. Cancer* **2004**, *90*, 535-541.

(118) Gozzini, A.; Rovida, E.; Dello Sbarba, P.; Galimberti, S.; Santini, V. et al. Butyrates, as a Single Drug, Induce Histone Acetylation and Granulocytic Maturation: Possible Selectivity on Core Binding Factor-Acute Myeloid Leukemia Blasts. *Cancer Res.* **2003**, *63*, 8955-8961.

(119) Finzer, P.; Stohr, M.; Seibert, N.; Rosl, F. Phenylbutyrate Inhibits Growth of Cervical Carcinoma Cells Independent of HPV Type and Copy Number. *J. Cancer Res. Clin. Oncol.* **2003**, *129*, 107-113.

(120) Batova, A.; Shao, L.; Diccianni, M.; Yu, A.; Tanaka, T. et al. The Histone Deacetylase Inhibitor AN-9 has Selective Toxicity to Acute Leukemia and Drug-Resistant Primary Leukemia and Cancer Cell Lines. *Blood* **2002**, *100*, 3319-3324.

(121) Zimra, Y.; Nudelman, A.; Zhuk, R.; Rabizadeh, E.; Shaklai, M. et al. Uptake of Pivaloyloxymethyl Butyrate Into Leukemic Cells and its Intracellular Esterase-Catalyzed Hydrolysis. *J. Cancer Res. Clin. Oncol.* **2000**, *126*, 693-698.

(122) Melchior, S.; Brown, L.; Figg, W.; Quinn, J.; Santucci, R. et al. Effects of Phenylbutyrate on Proliferation and Apoptosis in Human Prostate Cancer Cells In Vitro and In Vivo. *Int. J. Oncol.* **1999**, *14*, 501-508.

(123) Gore, S.; Weng, L.; Figg, W.; Zhai, S.; Donehower, R. et al. Impact of Prolonged Infusions of The Putative Differentiating Agent Sodium Phenylbutyrate on Myelodysplastic Syndromes and Acute Myeloid Leukemia. *Clin Cancer Res.* **2002**, *8*, 963-970.

(124) Gore, S.; Weng, L.; Zhai, S.; Figg, W.; Donehower, R. et al. Impact of The Putative Differentiating Agent Sodium Phenylbutyrate on Myelodysplastic Syndromes and Acute Myeloid Leukemia. *Clin. Cancer Res.* **2001**, *7*, 2330-2339.

(125) Prakash, S.; Foster, B.; Meyer, M.; Wozniak, A.; Heilbrun, L. et al. Chronic Oral Administration of CI-994: a Phase 1 Study. *Investig. New Drugs* **2001**, *19*, 1-11.

(126) LoRusso, P.; Demchik, L.; Foster, B.; Knight, J.; Bissery, M. et al. Preclinical Antitumor Activity of CI-994. *Investig. New Drugs* **1996**, *14*, 349-356.

(127) Suzuki, T.; Ando, T.; Tsuchiya, K.; Fukazawa, N.; Saito, A. et al. Synthesis and Histone Deacetylase Inhibitory Activity of New Benzamide Derivatives. *J. Med Chem.* **1999**, *42*, 3001-3003.

(128) Saito, A.; Yamashita, T.; Mariko, Y.; Nosaka, Y.; Tsuchiya, K. et al. A Synthetic Inhibitor of Histone Deacetylase, MS-27-275, with Marked In Vivo Antitumor Activity Against Human Tumors. *Proc Natl Acad Sci USA* **1999**, *96*, 4592-4597.

(129) Jaboin, J.; Wild, J.; Hamidi, H.; Khanna, C.; Kim, C. et al. MS-27–275, An Inhibitor of Histone Deacetylase, has Marked In Vitro and In Vivo Antitumor Activity Against Pediatric Solid Tumors. *Cancer Res.* **2002**, *62*, 6108-6115.

(130) Gelmon, K.; Tolcher, A.; Carducci, M.; Reid, G. K.; Li, Z. et al. Phase I Trials of the Oral Histone Deacetylase (HDAC) Inhibitor MGCD0103 Given Either Daily or 3x Weekly for 14 Days Every 3 Weeks in Patients (pts) with Advanced Solid Tumors. *J Clin Oncol* **2005**, *23*, 3147.

(131) Kijima, M.; Yoshida, M.; Sugita, K.; Horinouchi, S.; Beppu, T. Trapoxin, An Antitumor Cyclic Tetrapeptide, Is an Irreversible Inhibitor of Mammalian Histone Deacetylase. *J. Biol. Chem.* **1993**, *268*, 22429-22435.

(132) Itazaki, H.; Nagashima, K.; Sugita, K.; Yoshida, H.; Kawamura, Y. et al. Isolation and Structural Elucidation of New Cyclotetrapeptides, Trapoxins A and B, Having Detransformation Activities as Antitumor Agents. *J. Antibiot.* **1990**, *43*, 1524-1532.

(133) Sambucetti, L. C.; Fischer, D. D.; Zabludoff, S.; Kwon, P. O.; Chamberlin, H. et al. Histone Deacetylase Inhibition Selectively Alters the Activity and Expression of Cell Cycle Proteins Leading to Specific Chromatin Acetylation and Anti-Proliferative Effects. *J. Biol. Chem.* **1999**, *274*, 34940-34947.

(134) Walton, J. D.; Ransom, R.; Pitkin, J. W. Northern Corn Leaf Spot of Maize: Chemistry, Enzymology, and Molecular Genetics of a Host-Selective Phytotoxin. In *Plant-Microbe Interactions*; Stacey, G., Keen, N. T. Eds.; Chapman and Hall: New York, 1997; pp 94-123.

(135) Scott-Craig, J. S.; Panaccione, D. G.; Pocard, J. A.; Walton, J. D. The Cyclic Peptide Synthetase Catalyzing HC-toxin Production in the Filamentous Fungus Cochliobolus Carbonum is Encoded by a 15.7-Kilobase Open Reading Frame. *J. Biol. Chem.* **1992**, *267*, 26044-26049.

(136) Brosch, G.; Ransom, R.; Lechner, T.; Walton, J. D.; Loidl, P. Inhibition of Maize Histone Deacetylases by HC toxin, The Host-Selective Toxin of Cochliobolus Carbonum. *Plant Cell* **1995**, *7*, 1941-1950.

(137) Ransom, R. F. a. W., J. D. Histone Hyperacetylation in Maize in Response to treatment with HC Toxin or Infection by the Filamentous Fungus Cochliobolus Carbonum. *Plant Physiol.* **(1997**, *115*, 1021-1102.

(138) Closse, A.; Huguenin, R. Isolation and Structural Clarification of Chlamydocin. *Helv. Chim. Acta* **1974**, *57*, 533-545.

(139) Darkin-Rattray, S. J.; Gurnett, A. M.; Myers, R. W.; Dulski, P. M.; Crumley, T. M. et al. Apicidin: A Novel Antiprotozoal Agent that Inhibits Parasite Histone Deacetylase. *Proc. Natl. Acad. Sci. U.S.A.* **1996**, *93*, 13143-13147.

(140) Andrews, K. T.; Walduck, A.; Kelso, M. J.; Fairlie, D. P.; Saul, A. et al. Anti-Malarial Effect of Histone Deacetylation Inhibitors and Mammalian Tumour Cytodifferentiating Agents. *Int. J. Parasitol.* **2000**, *30*, 761-768.

(141) Park, J. S.; Lee, K. R.; Kim, J. C.; Lim, S. H.; Seo, J. A. et al. A Hemorrhagic Factor (Apicidin) Produced by Toxic Fusarium Isolates from Soybean Seeds. *Appl. Environ. Microbiol.* **1999**, *65*, 126-130.

(142) Kim, M.; Son, M.; Kim, W.; In Park, Y.; Moon, A. Apicidin, An Inhibitor of Histone Deacetylase, Prevents H-ras-Induced Invasive Phenotype. *Cancer Lett.* **2000**, *157*, 23-30.

(143) Colletti, S. L.; Li, C.; Fisher, M. H.; Wyvratt, M. J.; Meinke, P. T. Tryptophan-Replacement and Indole-Modified Apicidins: Synthesis of Potent and Selective Antiprotozoal Agents. *Tetrahedron Lett.* **2000**, *41*, 7825-7829.

(144) Shigematsu, N.; Ueda, H.; Takase, S.; Tanaka, H. FR9011228, A Novel Antitumor Bicyclic Depsipeptide Produced by Chromobacterium Violaceum. *J. Antibiot.* **1994**, *47*, 311-314.

(145) Ueda, H.; Nakajima, H.; Hori, Y.; Fujita, T.; Nishimura, M. et al. FR901228, A Novel Antitumor Bicyclic Depsipeptide Produced by Chromobacterium Violaceum. *J. Antibiot.* **1994**, *47*, 301-310.

(146) Sandor, V.; Bakke, S.; Robey, R. W.; Kang, M. H.; Blagosklonny, M. V. et al. Phase I Trial of The Histone Deacetylase Inhibitor, Depsipeptide (FR901228, NSC 630176), in Patients with Refractory Neoplasms. *Clin. Cancer Res.* **2002**, *8*, 718-728.

(147) Marshall, J. L.; Rizvi, N.; Kauh, J.; Dahut, W.; Figuera, M. et al. A Phase I Trial of Depsipeptide (FR901228) in Patients with Advanced Cancer. *J. Exp. Ther. Oncol.* **2002**, *2*, 325-332.

(148) Furumai, R.; Matsuyama, A.; Kobashi, N.; Lee, K.-H.; Nishiyama, M. et al. FK228 (Depsipeptide) as a Natural Prodrug That Inhibits Class I Histone Deacetylases. *Cancer Res.* **2002**, *62*, 4916-4921.

(149) Sasakawa, Y.; Naoe, Y.; Inoue, T.; Sasakawa, T.; Matsuo, M. et al. Effects of FK228, A Novel Histone Deacetylase Inhibitor, on Tumor Growth and Expression of p21 and c-myc Genes In Vivo. *Cancer Lett* **2003**, *195*, 161-168.

(150) Sasakawa, Y.; Naoe, Y., Noto, T; Inoue, T.; Sasakawa, T.; Matsuo, M. et al. Antitumor Efficacy of FK228, a Novel Histone Deacetylase Inhibitor, Depends on the Effect on Expression of Angiogenesis Factors. *Biochem Pharmacol* **2003**, *66*, 897-906.

(151) Sasakawa, Y.; Naoe, Y.; Inoue, T.; Sasakawa, T.; Matsuo, M. et al. Effects of FK228, A Novel Histone Deacetylase Inhibitor, on Human Lymphoma U-937 Cells In Vitro and In Vivo. *Biochem Pharmacol* **2002**, *64*, 1079-1090.

(152) Imai, T.; Adachi, S.; Nishijo, K.; Ohgushi, M.; Okada, M. et al. FR901228 Induces Tumor Regression Associated with Induction of Fas Ligand and Activation of Fas Signaling in Human Osteosarcoma Cells. *Oncogene* **2003**, *22*, 9231-9242.

(153) Kosugi, H.; Ito, M.; Yamamoto, Y.; Towatari, M.; Ueda, R. et al. In Vivo Effects of a Histone Deacetylase Inhibitor, FK228, on Human Acute Promyelocytic Leukemia in NOD/Shi-scid/scid Mice. *Jpn J. Cancer Res.* **2001**, *92*, 529-536.

Chapter 3. Synthetic Approaches to Core Cyclic Disulfides

3.1 Introduction

HDAC 1 is the critical lynchpin that interrelates hypoxia and angiogenesis. Significant evidence suggests that inhibition of HDAC 1 can have potent antiangiogenic, and thus antimetastasis effects. TSA (**2.2**) and FK-228 (**2.4**) have been reported to possess anti-angiogenic potential both *in vitro* and *in vivo*, showing that they inhibited hypoxia-induced production of the angiogenic mediator vascular endothelial cell growth factor (VEGF) by tumor cells and the migration as well as proliferation of the endothelial cells indirectly. However, HDAC 1 inhibition by **2.2** is not specific to hypoxic cells. This is consistent with the notion that, like all effective HDAC inhibitors, **2.2** does not require an activating event *en route* to expression of bioactivity.[1-9] FK228 is one of two exceptions to this rule; intracellular cleavage of FK-228's disulfide bond precedes HDAC active site metal binding by the thiol capped butene moiety and highlights **2.4** as one of only two known HDAC inhibitor prodrugs.

Thioredoxin (Trx) is found in high levels in many human cancers and increases both aerobic and hypoxia-induced HIF-1α concentrations promoting the notion that Trx-activated agents might display beneficial tumor cell selectivity.[10-15] The likelihood that **2.4** undergoes Trx-mediated activation has been proposed as a critical element behind the potent antitumor activity of this HDAC inhibitor.[16,17] Glutathione (GSH) has also been implicated in **2.4** activation and presents another possible manifold by which tumor cell selectivity arises.[16,17] FK228 is currently in Phase I clinical trials for thyroid and other advanced malignancies, combination therapy for lung cancer, and also for leukemias. The agent is in Phase II clinical trials for T cell lymphomas and other phase II projections

involve Non-Hodgkins lymphoma and acute myelogenous leukemia, and pancreatic cancer. Alarmingly, the advancement of **2.4** through clinical trials has been hindered due to a shortage of the natural product.[18] The scarcity of **2.4** from natural sources and its very promising future promoted our interest in developing HDAC inhibitors that share FK-228's novel mechanism of action but differed significantly in their level of synthetic demand. The very novel structure of **2.4** presents a significant synthetic challenge which has hampered efforts to understand how this and related compounds might be used as tumor cell selective antiangiogenic agents. The primary objective of my research was to synthesize and evaluate cell permeable reductively activated HDAC inhibitors using the natural product antitumor agent **2.4** as a functional ancestor. We hypothesized that very simple, easily synthesized analogs of **2.4** could retain FK-228's mechanism of cellular activation, i.e. redox enzymes overexpressed by hypoxic tumor cells will relieve the otherwise conformationally restricted pharmacophore via cleavage of a labile bond, thus affording an active HDAC inhibitor.

Our efforts related to **2.4** do not extend to close structural congeners but rather, mechanistically related ones, therefore all congeners of **2.4** contained the same pharmacophore but differed extensively in the identity of their recognition unit (or cap group). Towards this end, we synthesized a small library of cyclic disulfides to which an assortment of cap groups was easily appended. We anticipate that issues such as cell permeability and HDAC enzyme selectivity may readily be addressed in the long term by cap selection.

3.2 Synthetic Approaches to Cyclic Disulfides

3.2.1 Retrosynthetic Approach

Scheme 3.1 depicts the initial retrosynthesis proposed for the generation of simple cyclic disulfides. We envisioned that TBS protected acid **3.4** could be coupled to S-benzyl

Scheme 3.1 Retrosynthetic approach for cyclic disulfides

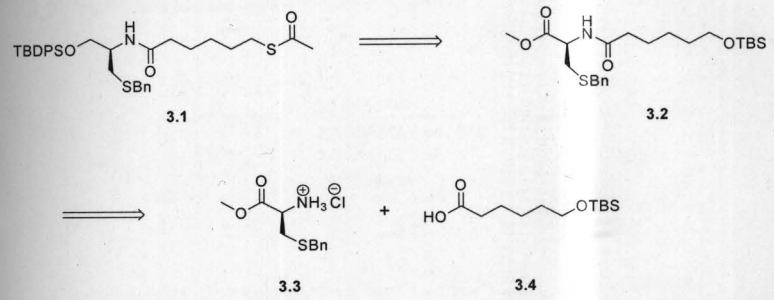

cysteine methyl ester **3.3** through one of various well-established peptide coupling procedures, to produce methyl ester **3.2**. Reduction of methyl ester **3.2** followed by subsequent protection of the resulting alcohol and displacement of the existing TBS protected alcohol with thioacetic acid would then generate the desired key intermediate **3.1**. Finally, removal of the benzyl and acetyl protecting groups on intermediate **3.1** followed by intramolecular cyclization would produce our desired cyclic disulfides.

3.2.2 Attempted Synthesis of Cyclic Disulfides

Our synthetic approach began with the hydrolysis of the commercially available ε-caprolactone **3.5** followed by TBS protection to yield **3.4** (68%) (Scheme 3.2).[19] Facile coupling of **3.4** to **3.3** was achieved using DCC and NMM in CH_2Cl_2 to produce **3.2** in 89% yield. We then reduced methyl ester **3.2** via $LiBH_4$ and protected the resulting alcohol by

means of TBDPSCl in DMF. The resulting intermediate was deprotected using TFA:H_2O to afford **3.6** in 80% yield over three steps.[20]

Scheme 3.2 Initial synthetic approach to cyclic disulfides

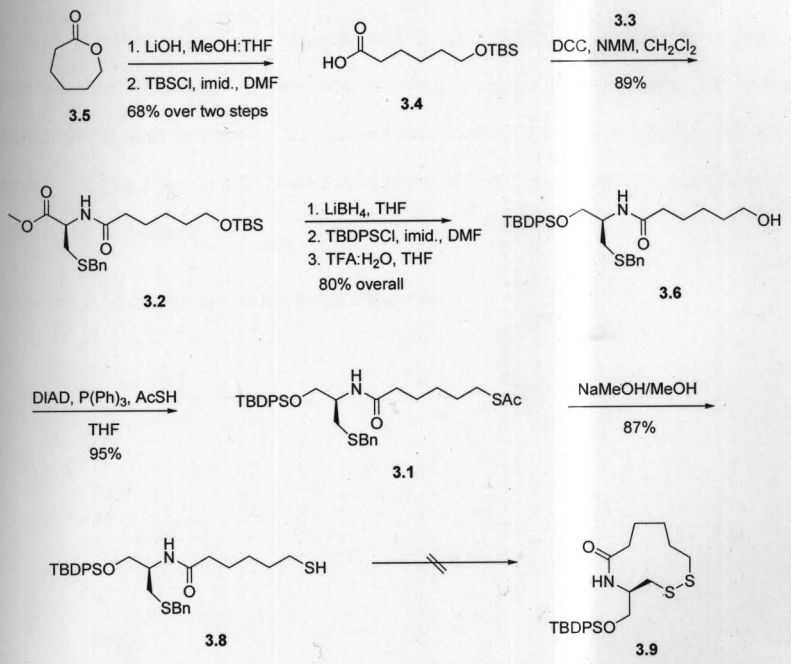

Next, **3.6** was converted to its thioacetyl analog via Mitsunobu conditions in the presence of thioacetic acid to afford **3.1** in 95% yield.[21,22] Deacetylation of intermediate **3.1** was achieved without any complications using sodium methoxide in methanol thus producing **3.7** in 87% yield. As shown in Scheme 3.2, the next step in our synthesis involved the removal of the benzyl protecting group on intermediate **3.8** followed by intramolecular cyclization to produce our desired compound **3.9**. With key intermediate **3.8** in hand,

methods for the removal of the S-benzyl protecting group were investigated and a survey of the literature revealed that using dissolving metal reduction conditions (sodium over liquid ammonia) was the most viable and efficient method.[22,23] Unfortunately, these conditions proved to be problematic. Debenzylation of **3.8** occurred under dissolving metal reduction conditions but was accompanied by production of a complex mixture of unwanted side reactions. These side reactions included polymerization, as well as, decomposition upon removal of the solvent due to the instability of the resulting dithiol species. At this point it was clear that a more efficient route was needed in order to circumvent these issues.

Scheme 3.3 1,8-Naphthalimide cap group installation

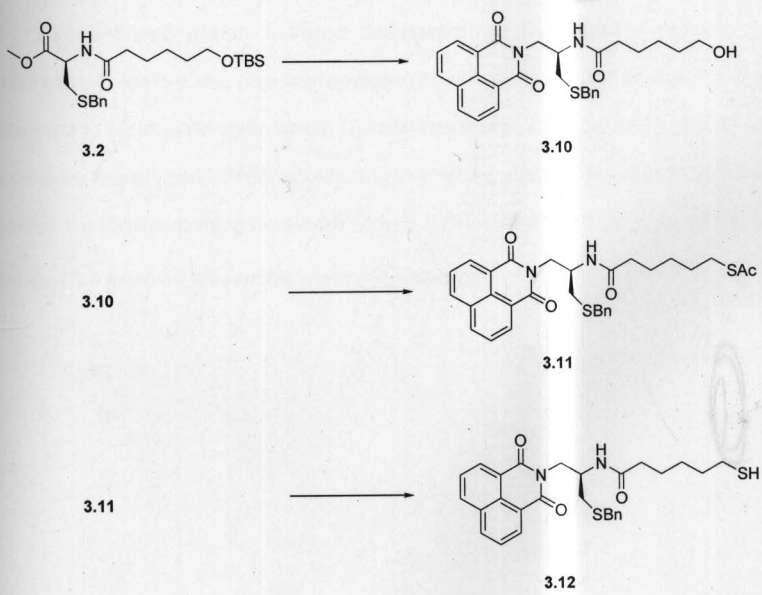

3.2 **3.10** **3.11** **3.12**

Although this initial approach failed to yield our desired disulfides, it provided us with useful intermediates (compounds **3.1** and **3.6**) that were later bioassayed and provided evidence supporting our hypothesis that simple, sulfur containing alkyl chains are capable of HDAC inhibition. In addition, compound **3.2** was further manipulated and a 1, 8-naphthalimide cap group installed via Mitsunobu conditions, to afford analogs **3.10, 3.11** and **3.12** (Scheme 3.3). Selection of this cap group was inspired by Scriptaid (**2.10**), a commercially available HDAC inhibitor displaying 1/3 the potency of TSA. We expected installation of this group to provide information regarding the impact of the cap group region of our molecules.

3.2.3 Amended Retrosynthetic Approach of Cyclic Disulfides

As mentioned earlier, S-benzyl deprotection of compound **3.1** proved to be problematic. Therefore, the originally envisioned synthetic route (Scheme 3.2) was not a viable route to our desired compounds. To alleviate these problems, other thiol protecting groups were investigated. While researching the literature, we came across the synthesis of several disulfide containing molecules bearing triphenylmethane (trityl) as the preferred

Scheme 3.4 Amended retrosynthesis for cyclic disulfides

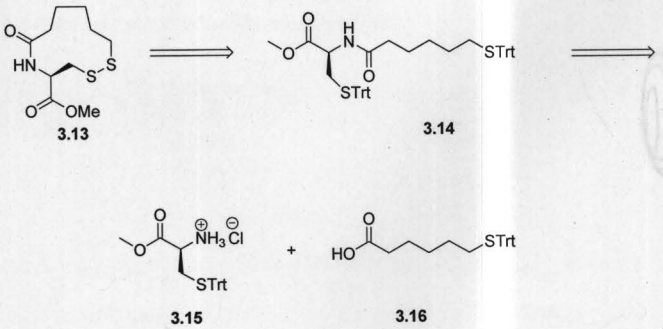

method for thiol protection.[18,24-26] Moreover, removal of this protecting group was facile and resulted in concomitant disulfide bond formation. With this in mind, a new synthetic sequence was devised wherein di-*S*-trityl protected amides such as **3.14** could be generated by standard carbonyldiimidazole (CDI) coupling of *S*-trityl cysteine methyl ester **3.15** and the suitably functionalized acid **3.16**. Cyclization of **3.14** was then envisioned to be accomplished by using well-established thiol deprotection/oxidation conditions (Scheme 3.4). It is worth noting that reduction of the methyl ester **3.2** followed by silyl protection is not necessary via this procedure therefore this route provides us with a useful handle by which our compounds could later be diversified.

3.2.4 Final Synthesis of Cyclic Disulfides

Synthesis of our core cyclic disulfides started with the conversion of commercially available bromo acid **3.17** to the corresponding S-trityl analog **3.16** (Scheme 3.5).[27] This intermediate was easily coupled, via CDI peptide coupling conditions, to S-trityl cysteine methyl ester **3.15** to afford the ditrityl species **3.14** in 65% yield. It is important to note that compound **3.15** was not commercially available. However, we were able to easily synthesize **3.15** in excellent yields using methods previously reported by Rudolph et al.[28]

Scheme 3.5 Final synthetic approach to cyclic disulfides

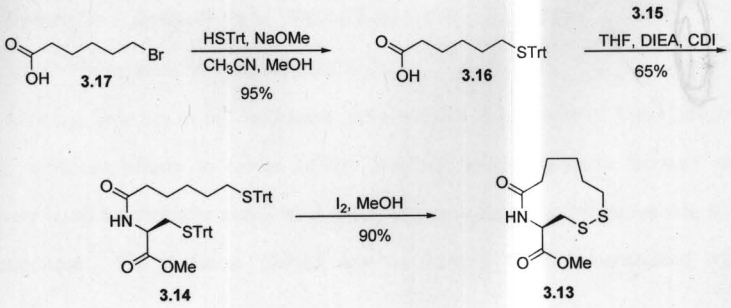

Di-S-trityl compound **3.14** was added to a solution of iodine in methanol and removal of the trityl protecting groups as well as *in situ* macrocyclization was completed in one step affording the desired methyl ester **3.13** in high yield (90%).

Elegant SAR studies performed by Furumai and co-workers showed that the length and linearity of the linker portion of the molecule is crucial for efficient HDAC inhibition.[29] This could be explained, in part, by a necessary resemblance to ε-N-acetyl lysine, the substrate for native HDAC action.[5] Crystallographic studies of **2.2** and suberoylanilide hydroxamic acid (SAHA, **2.5**) bound to an HDAC homologue support this amino acid mimicry.[30] Deviation from linearity shortens the distance between the recognition cap and active site binding groups thus rendering biologically inactive molecules. This is exemplified by **2.10** and its 2 carbon shorter analog Nullscript, where the latter, although containing all other essential parts, has no activity towards HDAC inhibition. Taking this into account, Jared Mays and I synthesized cyclic disulfide core structures bearing 4, 5, and 6 methylene unit linkers between the resulting Zn^{2+} binding thiol and the rest of the framework with the expectation that different linker lengths would correlate to altered efficiencies of HDAC inhibition. Methyl ester **3.13** and related congeners were later tested and the results of these assays are discussed in chapter 4.

3.3 Synthetic Approaches to Diversified Cyclic Disulfides

3.3.1 Synthesis of Capped Disulfides

Although workers in the field have identified the importance of linker length and linearity, synthetic efforts to derive HDAC and cell specificity have focused almost exclusively upon functionality composing either the cap region or the active site binding pharmacophore. For instance, Colletti and co-workers have demonstrated that N-

alkylated indole analogs of apicidin (**2.20**) show a greater than 20-fold preference for targeting malarial HDACs over human HDAC1.[31] Based on this result, we identified core disulfide methyl ester **3.13** and related congeners as important intermediates *en route* to an array of more elaborate cyclic disulfides. These analogs provided us with a methyl ester handle which could be easily manipulated, and an array of lipophilic cap groups could be installed to this end.

Our specific interest in lipophilic cap groups was motivated in large part by the vast experience of other groups in the field.[7,32] In particular, crystal structures of the histone deacetylase like protein (HDLP), a histone protein isolated from the hyperthermophilic bacterium Aquifex aeolicus, bound to known HDAC inhibitors TSA and SAHA highlight the importance of inhibitor interactions with a number of phenylalanine resides lining the enzyme channel leading to a deeply buried active site.[30] Moreover, we envisioned that amides derived from **3.13** would permit delineation of the impact of slightly different linker lengths between the presumed Zn^{2+} binding thiol and the remainder of these simple agents. At this point, it was determined that hydrolysis of **3.13** and related congeners with LiOH would produce structures such as **3.18**, and in turn these could be coupled to various amine-bearing cap groups to produce an assortment of derivatives.

Scheme 3.6 Hydrolysis of methyl ester **3.13**

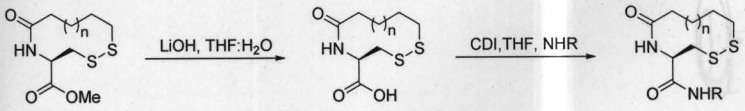

3.13a, n = 1
3.13b, n = 2
3.13c, n = 3

3.18a, 72%
3.18b, 55%
3.18c, 37%

3.19a-c

Indeed, carboxylic acid **3.18** and related structures were successfully coupled to a variety of amine-bearing cap groups therefore producing a library of cyclic disulfides in moderate to high yields (Scheme 3.7). Interestingly, we found that, while core structures containing 4 and 5 methylene units (**3.13a** and **3.13b**) could be readily hydrolyzed and further manipulated, the larger cyclic structure with 6 methylene units (**3.13c**) was not

Scheme 3.7 Small panel of diversified cyclic disulfides

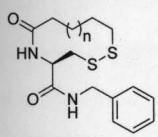

3.20a, 29%
3.20b, 26%
3.20c, N/A

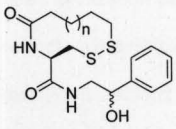

3.21a, 76%
3.21b, 75%
3.21c, 100%

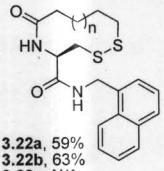

3.22a, 59%
3.22b, 63%
3.22c, N/A

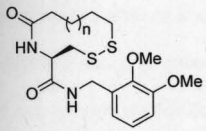

3.23a, 94%
3.23b, 73%
3.23c, N/A

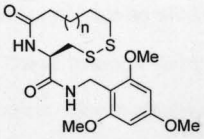

3.24a, 74%
3.24b, 75%
3.24c, N/A

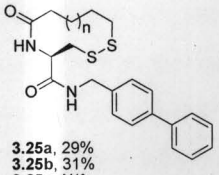

3.25a, 29%
3.25b, 31%
3.25c, N/A

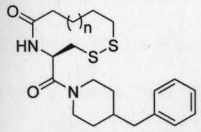

3.26a, 97%
3.26b, 95%
3.26c, N/A

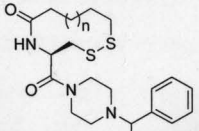

3.27a, 79%
3.27b, 80%
3.27c, N/A

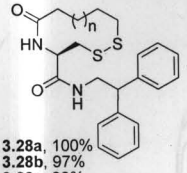

3.28a, 100%
3.28b, 97%
3.28c, 93%

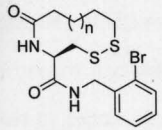

3.29a, 41%
3.29b, N/A
3.29c, N/A

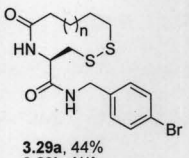

3.29a, 44%
3.29b, N/A
3.29c, N/A

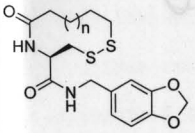

3.31a, 51%
3.31b, N/A
3.31c, N/A

amenable to clean saponification and attempts to produce amides from this substance were complicated by significant decomposition.

3.4 Summary

Two routes for the synthesis of our cyclic disulfides were investigated. The first originally proposed synthetic approach failed to yield any desired product. The key debenzylation step and synchronized cyclization proved to be more difficult than expected and an array of undesired side products were obtained instead. Although unsuccessful, in terms of obtaining our desired disulfides, various intermediates produced via this route were used to assert that simple, sulfur containing alkyl chains are capable of HDAC inhibition (discussed in chapter 4). Also, motivated by **2.10** potency and structural features, a small panel of linear, sulfur containing alkyl chains was designed containing a 1, 8-naphthalimide cap group. These analogs were designed to study the effects of different cap groups on our compounds. These results are discussed in chapter 4.

The redesigned synthetic approach explored the use of a different sulfur protecting group: the triphenylmethane or trityl group. Inspired by the total synthesis of molecules such as Spiruchostatin A and FR-901375, where a disulfide bond is the highlight of their molecular structure, we decided to use a similar approach and utilize a di-S-trityl intermediate that could be easily constructed and readily cyclized using iodine/methanol. This route allowed us to successfully construct a variety of cyclic scaffolds/core structures containing 4, 5 and 6 methylene units between the pharmacophore and the rest of the molecular framework. These structures were later diversified by simple peptide couplings, thus producing a library of capped disulfides. To our dismay, we found that the cyclic core structure with 6 methylene units was not easily

hydrolyzed, therefore only a limited number of amides from this core were generated. These analogs were tested for their potency and effectiveness as HDAC inhibitors in various cell lines and their results are also discussed in chapter 4.

3.5 References

(1) Hassig, C. A.; Schreiber, S. L. Nuclear Histone Acetylases and Deacetylases and Transcriptional Regulation: HATs off to HDACs. *Curr. Opin. Chem. Biol.* **1997**, *1*, 300-308.

(2) Hung, D. T.; Jamison, T. F.; Schreiber, S. L. Understanding and Controlling the Cell Cycle with Natural Products. *Chem. Biol.* **1996**, *3*, 623-639.

(3) Pazin, M. J.; Kadonaga, J. T. What's Up and Down with Histone Deacetylation and Transcription? *Cell* **1997**, *89*, 325-328.

(4) Roth, S. Y.; Denu, J. M.; Allis, C. D. Histone Acetyl Transferases. *Annu. Rev. Biochem.* **2001**, *70*, 81-120.

(5) Breslow, R.; Belvedere, S.; Gershell, L. Development of Cytodifferentiating Agents for Cancer Chemotherapy. *Helv. Chim. Acta* **2000**, *83*, 1685-1692.

(6) Marks, P. A.; Richon, V. M.; Breslow, R.; Rifkind, R. A. Histone Deacetylase Inhibitors as New Cancer Drugs. *Curr. Opin. Oncol.* **2001**, *13*, 477-483.

(7) Taunton, J.; Collins, J. L.; Schreiber, S. L. Synthesis of Natural and Modified Trapoxins, Useful Reagents for Exploring Histone Deacetylase Function. *J. Am. Chem. Soc.* **1996**, *118*, 10412-10422.

(8) Kijima, M.; Yoshida, M.; Sugita, K.; Horinouchi, S.; Beppu, T. Trapoxin, An Antitumor Cyclic Tetrapeptide, Is an Irreversible Inhibitor of Mammalian Histone Deacetylase. *J. Biol. Chem.* **1993**, *268*, 22429-22435.

(9) Sternson, S. M.; Wong, J. C.; Grozinger, C. M.; Schreiber, S. L. Synthesis of 7200 Small Molecules Based on a Substructural Analysis of the Histone Deacetylase Inhibitors Trichostatin and Trapoxin. *Org. Lett.* **2001**, *3*, 4239-4242.

(10) Welsh, S. J.; Williams, R.; Birmingham, A.; Newman, D. J.; Kirkpatrick, D. L. et al. The Thioredoxin Redox Inhibitors 1-methylpropyl 2-imidazolyl disulfide and Pleurotin Inhibit Hypoxia-induced Factor 1 and Vascular Endotheliel Growth Factor Formation. *Mol. Cancer. Ther.* **2003**, *2*, 235-243.

(11) Verdoucq, L.; Vignols, F.; Jacquot, J.-P.; Chartier, Y.; Meyer, Y. In Vivo Characterization of a Thioredoxin h Target Protein Defines a New Peroxiredoxin Family. *J. Biol. Chem.* **1999**, *274*, 19714-19722.

(12) Shao, L.-e.; Diccianni, M. B.; Tanaka, T.; Gribi, R.; Yu, A. L. et al. Thioredoxin Expression in Primary T-Cell Acute Lymphoblastic Leukemia and Its Therapeutic Implication. *Cancer Res.* **2001**, *61*, 7333-7338.

(13) Kahlos, K.; Soini, Y.; Saily, M.; Koistinen, P.; Kakko, S. et al. Up-Regulation of Thioredoxin and Thioredoxin Reductase in Human Malignant Pleural Mesothelioma. *Int. J. Cancer* **2001**, *95*, 198-204.

(14) Becker, K.; Gromer, S.; Schirmer, R. H.; Muller, S. Thioredoxin Reductase as a Pathophysiological Factor and Drug Target. *Eur. J. Biochem.* **2000**, *267*, 6118-6125.

(15) Arner, E. S. J.; Holmgren, A. Physiological Functions of Thioredoxin and Thioredoxin Reductase. *Eur. J. Biochem.* **2000**, *267*, 6102-6109.

(16) Furumai, R.; Matsuyama, A.; Kobashi, N.; Lee, K.-H.; Nishiyama, M. et al. FK228 (Depsipeptide) as a Natural Prodrug That Inhibits Class I Histone Deacetylases. *Cancer Res.* **2002**, *62*, 4916-4921.

(17) Kwon, H. J.; Kim, M. S.; Kim, M. J.; Nakajima, H.; Kim, K.-W. Histone Deacetylase Inhibitor FK228 Inhibits Tumor Angiogenesis. *Int. J. Cancer* **2002**, *97*, 290-296.

(18) Li, K. W.; Wu, J.; Xing, W.; Simon, J. A. Total Synthesis of the Antitumor Depsipeptide FR- 901,228. *J. Am. Chem. Soc.* **1996**, *118*, 7237-7238.

(19) Nicolau, K. C.; Hwang, C.-K.; Marron, B. E.; DeFrees, S. A.; Couladouros, E. A. et al. Bridging of Macrodithiono-lactones to Bicyclic Systems. Synthesis and Modeling of Oxapolycyclic Frameworks. *J. Am. Chem. Soc.* **1990**, *112*, 3040-3055.

(20) Zhu, X. F.; Williams, H. J.; Scott, A. I. Facile and Highly Selective 5'-Desilylation of Multisilylated Nucleosides. *J. Chem. Soc. Perkin I* **2000**, *15*, 2305-2306.

(21) Volante, R. P. A New Highly Efficient Method for the Conversion of Alcohols to Thiolesters and Thiols. *Tetrahedron Lett.* **1981**, *22*, 3119-3122.

(22) Koreeda, M.; Yang, W. The Chemistry of 1,2-Dithiins: Synthesis of 1,2-Dithiin and 3,6-Disubstituted 1,2-Dithiins. *Synlett* **1994**, 201-203.

(23) Corrie, J. E. T.; Hlubucek, J. R.; Lowe, G. Synthesis of a Cephalosporin Analogue. *J. Chem. Soc. Perkin Trans. 1* **1977**, 1421-1425.

(24) Chen, Y.; Gambs, C.; Abe, Y.; Wentworth, P. J.; Janda, K. D. Total Synthesis of the Depsipeptide FR-901375. *J. Org. Chem.* **2003**, *68*, 8902-8905.

(25) Yurek-George, A.; Habens, F.; Brimmell, M.; Packham, G.; Ganesan, A. Total Synthesis of Spiruchostatin A, A Potent Histone Deacetylase Inhibitor. *J. Am. Chem. Soc.* **2004**, *126*, 1030-1031.

(26) Doi, T.; Iijima, Y.; Shin-ya, K.; Ganesan, A.; Takahashi, T. A Total Synthesis of Spiruchostatin A. *Tetrahedron Lett.* **2006**, *47*, 1177-1180.

(27) Majer, P.; Jackson, P. F.; Delahanty, G.; Grella, B. S.; Ko, Y. S. et al. Synthesis and Biological Evaluation of Thiol-Based Inhibitors of Glutamate Carboxypeptidase II: Discovery of an Orally Active GCP II Inhibitor. *J. Med. Chem.* **2003**, *46*, 1989-1996.

(28) Rudolph, J.; Theis, H.; Hanke, R.; Endermann, R.; Johannsen, L. et al. seco-Cyclothialidines: New Concise Synthesis, Inhibitory Activity toward Bacterial and Human DNA Topoisomerases, and Antibacterial Properties. *J. Med. Chem.* **2001**, *44*, 619-626.

(29) Furumai, R.; Komatsu, Y.; Nishino, N.; Khochbin, S.; Yoshida, M. et al. Potent Histone Deacetylase Inhibitors Built from Trichostatin A and Cyclic Tetrapeptide Antibiotics Including Trapoxin. *Proc. Natl. Acad. Sci. U.S.A.* **2001**, *98*, 87-92.

(30) Finnin, M. S.; Donigan, J. R.; Cohen, A.; Richon, V. M.; Rifkind, R. A. et al. Structures of Histone Deacetylase Homologue Bound to the TSA and SAHA Inhibitors. *Nature* **1999**, *401*, 188-193.

(31) Colletti, S. L.; Myers, R. W.; Darkin-Rattray, S. J.; Schmatz, D. M.; Fisher, M. H. et al. Design and Synthesis of Histone Deacetylase Inhibitors: The Development of Apicidin Transition State Analogs. *Tetrahedron Lett.* **2000**, *41*, 7837-7841.

(32) Miller, T. A.; Witter, D. J.; Belvedere, S. Histone Deacetylase Inhibitors. *J. Med. Chem.* **2003**, *46*, 5097-5116.

Chapter 4. Biological Evaluation of Novel Reductively Activated HDAC Inhibitors

4.1 *Drosophila Melanogaster* Experiments

Simple animal model systems that mimic some of the steps of mammalian tumorigenesis can provide a rapid means to uncover novel pathways of cancer. One such model organism that has been widely studied is *Drosophila melanogaster.* Indeed, the virtues of *D. melanogaster* as a genetically tractable model organism, relevant to human disease has been well documented.[1,2] *D. melanogaster* represents a simpler system than the mouse for modeling cancer. For instance, four of the hallmarks of cancer: self-sufficiency in growth / proliferation signals, insensitivity to anti-proliferative signals, evading apoptosis and invasion / metastasis are relevant to *D. melanogaster.*[3] Because of these traits, *Drosophila* makes an excellent eukaryotic model in which HDAC inhibitors can be studied. In addition, the ability to ablate expression of specific genes using RNA interference provides significant motivation for selecting *Drosophila* as a primary long-term model in which to examine reductively activated HDAC inhibitors.[4]

To validate our hypothesis that simple, sulfur containing alkyl chains are capable of HDAC inhibition, we assessed the bioactivity of compounds **3.1** and **3.6** using *Drosophila* Schneider 2 (S2) cells in collaboration with Professor David Wassarman (UW-Department of Pharmacology). Briefly, 2 x 10^6 cells in 10 mL medium were brought to 2 x 10^{-6} M solutions and incubated with our synthetic compounds at room temperature for specified times. The cells were then isolated by centrifugation and dounced in lysis buffer thus affording intact *Drosophila* nuclei. The nuclei were isolated by centrifugation, dissolved in SDS-PAGE loading dye and processed via standard Western blotting

methodology using goat anti-H4 acetyl-Lys or anti acetyl-Lys H3 as primary antibodies and horseradish peroxidase-based detection (HRP-ECL method). Anti-H2B antibody was used to ensure equal protein loading per well.

It is important to note that several other groups have reported on the viability of simple alkyl thiols as HDAC inhibiting pharmacophores.[5-7] For instance, Nishino and co-workers reported a number of thiol-containing trapoxin-like cyclic tetrapeptides with marked HDAC inhibitory activities.[7] Simple non-cyclic disulfide analogs of these agents displayed significantly enhanced HDAC inhibition upon reduction. In addition, Suzuki and co-workers have reported a series of thiol containing analogs of SAHA which also display very potent HDAC inhibition.[5]

The data obtained from these experiments indicated that linear and simplified versions of FK-228 can act as HDAC inhibitors in cells and may potentially be good leads into the design of more active and viable compounds (Figure 4.1). Indeed, compounds **3.1** and **3.7** proved to be potent cellular HDAC inhibitors at 48 and 72 h incubations. Lanes 1 and 4 correspond to histone isolated from cells treated with **3.6**. Importantly, **3.6** serves as a control agent lacking a Zn^{2+} chelating / binding pharmacophore moiety but retaining the synthetically useful TBDPS moiety which, from the biological perspective, serves as a highly lipophilic "cap" group. Cells treated with **3.6** rendered little acetylated H4 as reflected by little or no peroxidase-dependent signal. Conversely, cells subjected to both **3.1** and **3.7** rendered, after lysis and processing, a significant amount of acetylated H4, consistent with HDAC inhibition. Although **3.7** is "activated" in the sense that its thiol terminus is capable of zinc binding once in the HDAC active-site, **3.1** clearly is not. Studies by Colletti and co-workers showed that thio-acetyl analogs of apicidin and trapoxin are efficiently deactylated by HDACs.[8] Based on Colletti's work, we proposed that enzymatic deacetylation of **3.1** is likely to be operative in these studies thereby

Figure 4.1 Western blot analysis of histones isolated from *Drosophila* S2 cells

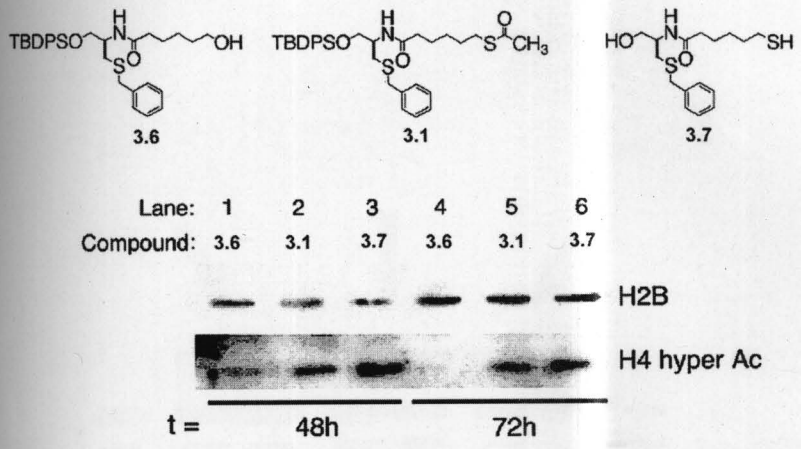

Drosophila S2 cells were treated with **3.1**, **3.6** and **3.7** and incubated for 48 or 72 h at room temperature. H2B detection used to ensure equivalent protein loading to each well. Dark, bottom bands in lanes 2, 3, 5 and 6 correspond to hyperacetylated H4.

allowing for two mechanisms of HDAC inhibition by **3.1**; competition with acetyl-Lys for HDAC binding and simple metal binding following enzymatic processing.

Similar analysis of cells treated with acyclic thiol-based agents **3.11** and **3.12** also revealed that both induce H4 hyperacetylation (Figure. 4.2). Notably, the same phenomenon is observed where the acetylthiol agent **3.11** appears to be much more potent than free thiol counterpart **3.12**. Again, this enhanced activity may be due either to enhanced stability of **3.11** over **3.12** or to the bimodal mechanism of action supported by the work of Colletti and co-workers.[8] These data support the notion that simple aliphatic thiols are likely to mimic the biological activity and usefulness of activated FK228.

Figure 4.2 Western blot analysis of cells treated with Scriptaid analogs.

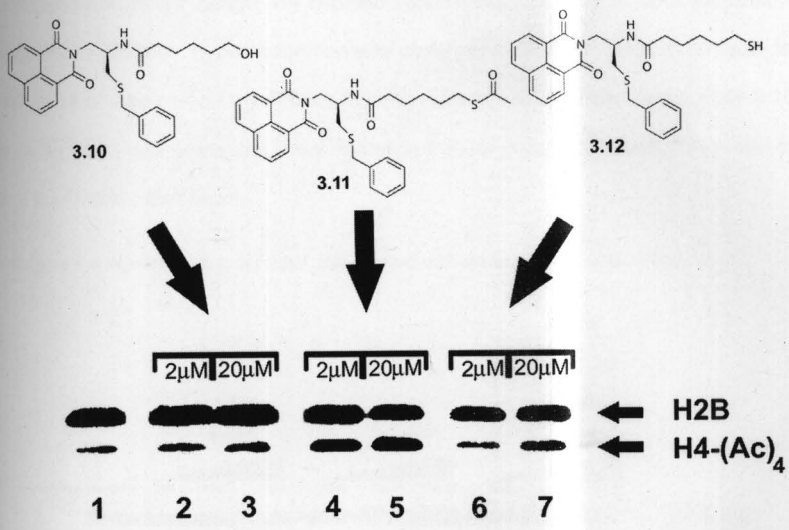

Western blot analysis of histones isolated from *Drosophila* S2 cells treated with Scriptaid analogs **3.10**, **3.11**, and **3.12**. H2B detection was used to ensure equivalent protein loading to each well. Dark bottom bands most prominent in lanes 4, 5 and 7 indicate the enhanced abundance of tetra-Ac-Lys H4, consistent with HDAC inhibition by acyclic thiol-based Scriptaid analogs **3.11** and **3.12**. Lane 1 is a dioxane solvent control. Compound concentrations in cell medium are indicated above each lane. All cells were treated for a period of 48 hours at ambient temperature prior to nuclei isolation and processing.

Encouraged by these results, we evaluated the bioactivities of methyl esters **3.13a**, **3.13b**, and **3.13c.** We hypothesized that methyl esters **3.13a-c** would have reasonable cell permeability traits therefore compounds **3.13a-c** were tested for their ability to induce histone hyperacetylation in *Drosophila* S2 cells. In this round of experiments, S2 cells were subjected to varying concentrations of the three methyl esters for a period of 48 h at ambient temperature after which time nuclei were isolated and histones analyzed.

Histone H4 lysine-acetylation status was assessed using Western blots with anti-$(Ac)_4$-H4 antibody. Much to our delight, H4 hyperacetylation was observed in cells subjected to methyl esters **3.13a-c**. Hyperacetylation was observed at disulfide concentrations as low as 20 μM and was particularly striking in cells subjected to disulfide methyl ester **3.13b** containing the 5 methylene-unit linker spanning the purported Zn^{2+} binding thiol and the rest of the peptidic framework.

Figure 4.3 Western blot analysis of cells treated with cyclic disulfide core structures.

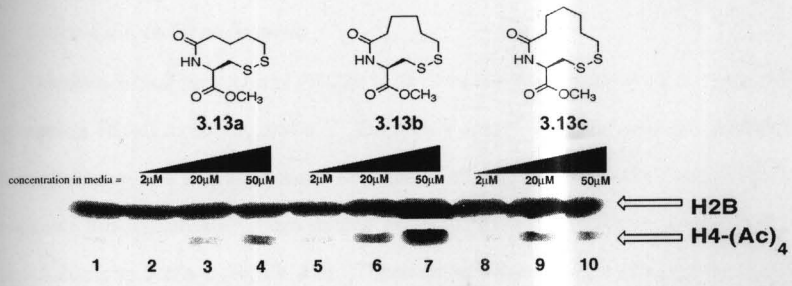

Western blot analysis of histones isolated from *Drosophila* S2 cells treated with cyclic disulfides core structures **3.13a**, **3.13b**, and **3.13c**. H2B detection was used to ensure equivalent protein loading to each well. Dark bottom bands most prominent in lanes 6 and 7 indicate the enhanced abundance of tetra-Ac-Lys H4, consistent with HDAC inhibition by cyclic core structure **3.13b**. Lane 1 is a dioxane solvent control. Compound concentrations of in cell medium are indicated above each lane. All cells were treated for a period of 48 hours at ambient temperature prior to nuclei isolation and processing.

Significantly, the use of anti-H2B antibody revealed that alterations in $(Ac)_4$-H4 signal are, in fact, due to altered acetylation status and not simple alterations in absolute protein loadings. Although not a quantitative method, it is clear from examination of H2B-derived signals in all lanes that comparable amounts of protein were added to each well of the SDS-PAGE gel. Hence, differences in H4 signal are small molecule-dependent and not a result of uneven protein loading. These results confirmed that simple cyclic

disulfides devoid of relatively large and lipophilic cap groups, characteristic of both natural and synthetic effective HDAC inhibitors, can induce significant histone hyperacetylation in cells. Additionally, this suggested that, once diversified, amides strategically derived from compounds **3.13a-c** could serve as good leads for new types of HDAC inhibitors inspired by FK-228's structure. As such, a small library of "capped" disulfides were successfully produced (Chapter 3) and their capacity for HDAC inhibition assayed using HeLa cell extracts and the commercially available Fluor-de-Lys detection kit.[9]

4.2 Fluor-de-Lys Experiments

The intracellular reduction of FK-228 to its corresponding dithiol plays a crucial role in the agent's HDAC inhibition profile.[10] Even very small molecules, we hypothesized, might capitalize on this activating event *en route* to HDAC inhibition. The data of Figure 4.4 supports this hypothesis. From methyl esters **3.13a-c** we produced amide-bearing analogs **3.20a-c** to **3.28a-c** (Figure 4.4). These compounds were all assayed for HDAC inhibition using the Fluor-de-Lys fluorescence-based assay with the help of Noël Peters at the UW Small Molecule Screening Facility / UW Comprehensive Cancer Center. This assay uses HeLa cell extracts as the source of HDAC activity and an acetylated substrate.[9] Deacetylation of the substrate sensitizes it to the developer which then generates a fluorophore.[11-13] The fluorophore is excited with 360 nm light and the emitted light is detected at 460 nm on a plate reader. To emulate the reducing environment prominent within many tumor cells because of high glutathione (GSH), Thioredoxin (Trx) and Thioredoxin Reductase (TrxR) levels, Fluor-de-Lys assays were performed with synthetic agents **3.13a-c** and **3.20a-c** to **3.28a-c** in the presence of dithiothreitol (DTT).

Figure 4.4 Dependence of redox-triggered alterations in HDAC activity on linker length and cap group.[26]

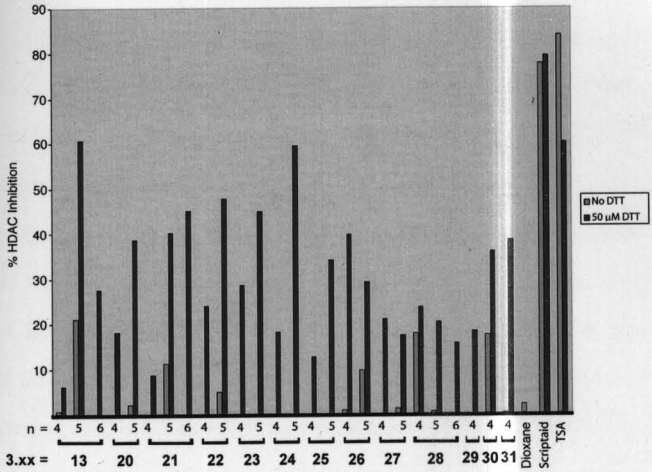

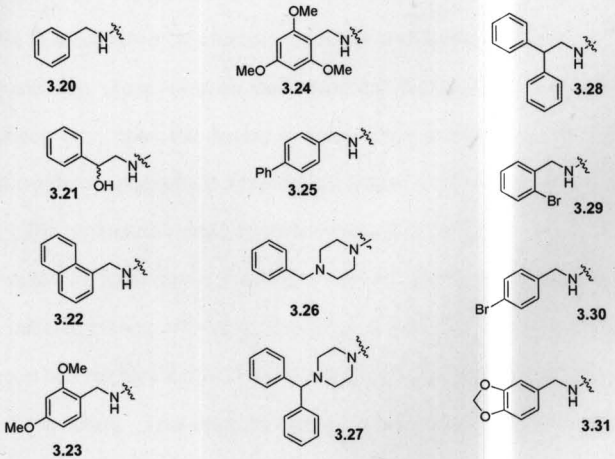

Control reactions lacking DTT, as well as those including DTT in dioxane, were performed in parallel.[14-16] Due to the limited availability of FK-228, we selected the highly potent, commercially available and well-studied HDAC inhibitors Scriptaid (>100-fold increase acetylation in PANC-1 cells) and TSA (IC_{50} value of 1.44nM against partially purified mouse HDAC) to serve as positive inhibitor controls. While activities of HDAC inhibitors may vary based on many factors (e.g., assay method, cell line, etc.) these activities clearly reflect the potency of both control agents.

The data presented in Figure 4.4 reveals a clear dependence upon DTT of most members of the disulfide library to effect HDAC inhibition. For instance, disulfide **3.24b** bearing the trimethoxybenzylamine cap group is completely devoid of activity in the absence of DTT. However, the presence of DTT converts **3.24b** into an agent whose HDAC inhibition (at 20 μM concentration) is comparable to Scriptaid and TSA. Evaluation of the dioxane + DTT control reveals DTT itself to be completely devoid of anti-HDAC activity. It is noteworthy that, as predicted, HDAC inhibition is integrally tied to linker length. This is exemplified by compounds **3.25a** and **3.25b** where, despite bearing the same aliphatic cap group (4-phenylbenzylamine), **3.25b** induces significantly greater HDAC inhibition than does the analog containing the shorter 4 methylene linker. The same linker length dependence is apparent for almost all members of the disulfide library examined. The majority of cyclic disulfides examined follow this trend, thus confirming the hypothesis that small cyclic disulfides may serve as more-easily constructed and readily-diversifiable mimics of FK-228. Importantly, clear dependencies upon linker length and cap group identity play a role in the moderate HDAC inhibition activities displayed by members of the library. That such alterations in activity are observed with even subtle

structural alteration from one compound to the next is supported by the well-established impact that both linker and cap identities have upon HDAC inhibitor effectiveness.[17,18]

4.3 Cytotoxicity Experiments

In collaboration with Noël Peters, we chose the fifteen most active compounds from our library, based on the Fluor-de-Lys experiments, and tested them for antitumor cell activities. The activity of each new agent was assessed by using a high-throughput cytotoxicity assay on nine human cancer cell lines representing a broad range of carcinomas, including breast (MCF-7), colon (DU145), CNS (SF-268), liver (Hep3B), lung (A549), and ovary (SK-OV-3) and a mouse mammary normal epithelial (Nmumg) control line. The data presented within Figure 4.5 reveal agents with promising IC_{50} values. The top two hits in our library were compounds **3.25b** and **3.26b**. Compound **3.25b** exhibited promising cytotoxicity against seven cancer cell lines (4.8 μM ± 2.0 μM in the case of A549) and also showed some selectivity because two of the nine cell lines tested were resistant to the cytotoxic effects of the agent. In contrast, compound **3.26b** was a less potent cytotoxin than **3.25b**, but exhibited significant selectivity towards three of the nine cell lines (Hep3B, SF-268 and SK-OV-3) with an average IC_{50} value of 14μM ± 3 μM. In addition, various agents from our library showed promising and selective inhibition. For instance, compound **3.13b** showed exquisite selectivity because it was 5 times more cytotoxic towards SF-268 cells (IC_{50} = 20 μM ± 3 μM) than any other cell line. This result is particularly interesting since **3.13b** is devoid of any lipophilic cap group thus highlighting once more the importance of cap group identity and the role it plays in the attenuation of cytotoxicity; we believe this to be attributable to HDAC inhibition. Other members of our library, although not as potent as **3.25b**, also were significantly active and selective.

Figure 4.5 Summary of IC_{50} data from high-throughput cytotoxicity assay

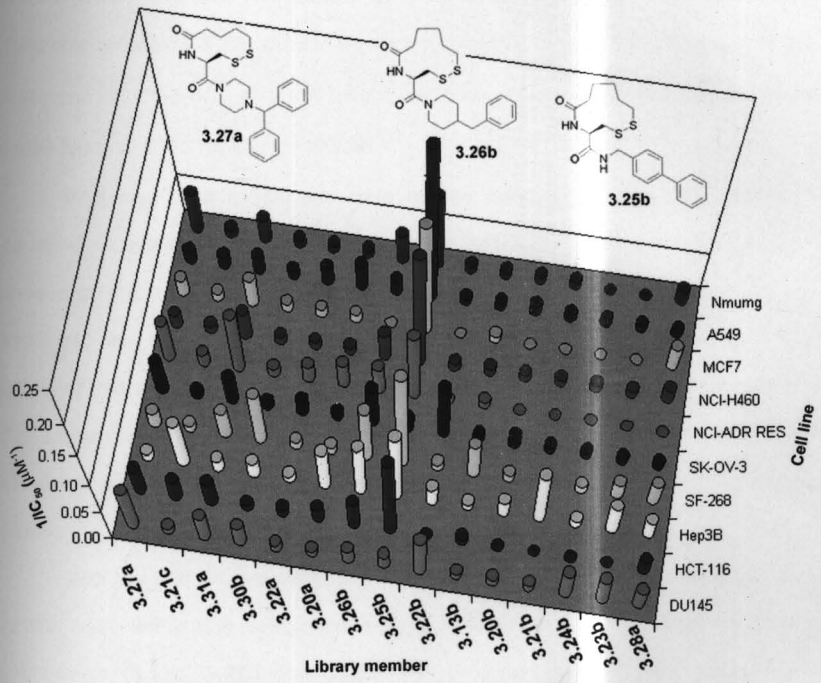

Reciprocal of IC_{50} values are displayed for clarity, with the current illustration representing and IC_{50} range of 4.8 μM (**3.25b**, A549) to > 45 μM (**3.22a**, all cell lines). In the assay, live cells were distinguished by the presence of a ubiquitous intracellular enzymatic activity that converts the non-fluorescent cell-permeable molecule calcein AM to the intensively fluorescent molecule calcein, which is retained within live cells. The IC_{50} value of each library member represents at least three replicates of dose-response experiments conducted over five concentrations of 2-fold dilutions. Structures of the three compounds selected for the cytoblot experiments are shown. DU145, human colon carcinoma; HCT-116, human colon carcinoma; Hep3B, human liver carcinoma; SF-268, human CNS glioblastoma; SK-OV-3, human ovary adenocarcinoma; NCI/ADR-RES, human breast carcinoma; NCI-H460, human lung carcinoma; MCF7, human breast carcinoma; A549, human lung adenocarcinoma; Nmumg, mouse mammary normal epithelial cells.

For example, **3.21b** exhibited dramatic selectivity towards only Hep3B cells (IC_{50} = 13 μM ± 2 μM), displaying almost 9 times more cytotoxicity than against any other cell line. Another library member with notable cell selectivity was **3.22b.** This naphthalene-containing substance **3.22b** showed significant selectivity against DU145 (IC_{50} = 17 μM ± 3 μM) and SK-OV-3 (IC_{50} = 13 μM ± 3 μM) cell lines, relative to the other seven cell lines (in the case of HCT-116, IC_{50} = >100μM).

In general, our compounds were not as cytotoxic as the highly potent and commercially available HDAC inhibitors Scriptaid and TSA. However, these compounds showed promising IC_{50} values (low micromolar range) thus further strengthening our hypothesis that simple functional mimics of FK-228 can be readily generated. We are confident that after further modifications and manipulation, these readily diversified FK-228 analogs are likely to be useful in further understanding the role of different HDAC's. Moreover, such agents have the potential to represent clinical candidates in the near future.

With this in mind, we identified the three most cytotoxic compounds in our library (**3.25b, 3.26b** and **3.27a**) along with the three most active compounds from the Fluor-de-Lys assays (**3.13b, 3.22b** and **3.24b**) and assessed their cellular impacts on an assortment of cancer-related proteins using "in-cell" Western blots (cytoblots)(Figure 4.6). Importantly, our choice of cancer-related proteins (biomarkers) to be evaluated was influenced heavily by the FK-228 literature.[19]

Figure 4.6 Selected library members for cytoblot experiments

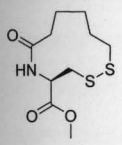

3.13b

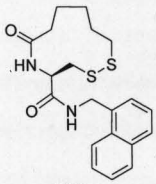

3.22b

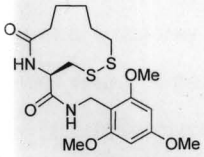

3.24b

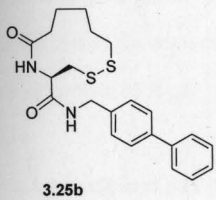

3.25b

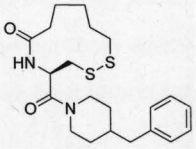

3.26b

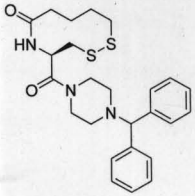

3.27a

4.4 Cytoblot Experiments

In 1999, Schreiber and co-workers reported the development of a miniaturized cell-based assay format that enables a genetic-like approach to understanding cellular pathways in mammalian systems using small molecules, rather than mutations, as the source of gene product alterations.[20] This whole-cell immunodetection assay can sensitively detect changes in specific cellular macromolecules in high-density arrays of mammalian cells. Furthermore, this assay is compatible with screening large numbers of small molecules in nanoliter to microliter culture volumes. They referred to this assay format as a cytoblot, and have demonstrated the use of cytoblotting to monitor biosynthetic processes such as DNA synthesis, and post-translational processes such as acetylation and phosphorylation.[20] The cytoblot assay does not require the generation of

stably transfected cell lines, the use of radioactivity or the use of sensitive optical imaging systems, but simply uses a specific primary antibody directed against the endogenous cellular molecule of interest (biomarker). The real advantage of cytoblots is that they can be used for high-throughput screening of small molecules in cell-based assays. Together with small molecule libraries, the cytoblot assay has been used to perform chemical genetic screens analogous to those used in classical genetics and thus has helped in the understanding of a wide variety of cellular processes, especially those involving post-translational modifications. Based on this, using the human lung adenocarcinoma A549 cell line we tested six compounds from our library against nine antibodies including tumor suppressor protein p53, p21, hyperacetylated H3 and hyperacetylated H4.

4.4.1 p53 and p21 protein levels

p53 is a short-lived protein and is sustained at low levels in normal physiological conditions.[21,22] In unstressed mammalian cells p53 is continually ubiquitinated by interacting with MDM2, COP1, Pirh2, and ARF-BP1.[23-28] Subsequently p53 protein is degraded by the 26S proteosome.[27,29] However, p53 is maintained at a relative high level by posttranslational modifications in response to various stresses. The principal posttranslational modifications of p53 in response to DNA damage include phosphorylation and acetylation, through which p53 exerts its biochemical functions.[30-34] Transcriptional coactivators p300/CREB-binding protein (CBP) and p300 / CBP-associated factor (PCAF) were reported to acetylate p53 at K373, K382 and K320, respectively.[35-37] Lysine acetylation at these sites is linked to p53 ability to regulate cell cycle arrest and apoptosis.[38-40] As mentioned earlier, phosphorylation also regulates the activity of p53. The level of p53 is low after mitosis but increases during G_1. During S phase, the protein becomes phosphorylated by the M-phase cyclin-CDK complex of the

cell cycle and also by casein kinase II (CKII). Sequences at the N-terminus of the p53 protein function as a transcription activator indicating the role of p53 in the transcription of genes involved in suppression of cell growth.

One major cell cycle regulating gene that is a target for p53 is the CDK inhibitory protein (CIP), $p21^{CIP}$. Work by Gartel and co-workers, and by Nakano and co-workers demonstrated that activation of p53 resulted in increased expression of $p21^{CIP}$ with a resultant arrest in the G_1 and G_2 phase of the cell cycle.[41,42]

Although activity levels are not extremely high, there is clear correlation between the levels of p53 and p21 in our assays. Most of our compounds showed a substantial increase in activation of p53 protein relative to our positive control HDAC inhibitor TSA (Figure 4.7). Particularly, compounds **3.26b** and **3.27a** showed a 2-fold increase over TSA followed by compound **3.13b, 3.24b, 3.22b** and **3.25b** which showed equal or slightly higher activities than TSA, respectively. This is in contrast to reports by Yu and co-workers where they show that FK-228 does not modulate p53 levels in A549 cells.[43] Moreover, our results correlate with increases in p21 activation. That is to say that compounds capable of effecting significant p53 overexpression also enhanced levels of p21 protein; **3.26b** and **3.27a** being the most active. Interestingly, Zhao and co-workers found that p21 activation on non-small cell lung cancer (NSCLC) cells by TSA was p53-independent whereas FK-228-induced p21 expression relied on p53 activation.[44] These results support our findings, where the activation of p53 is more pronounced on our synthetic FK-228 analogs than that of TSA, but p21 activation by TSA is comparable to that of our compounds.

Figure 4.7 p53 and p21 activation

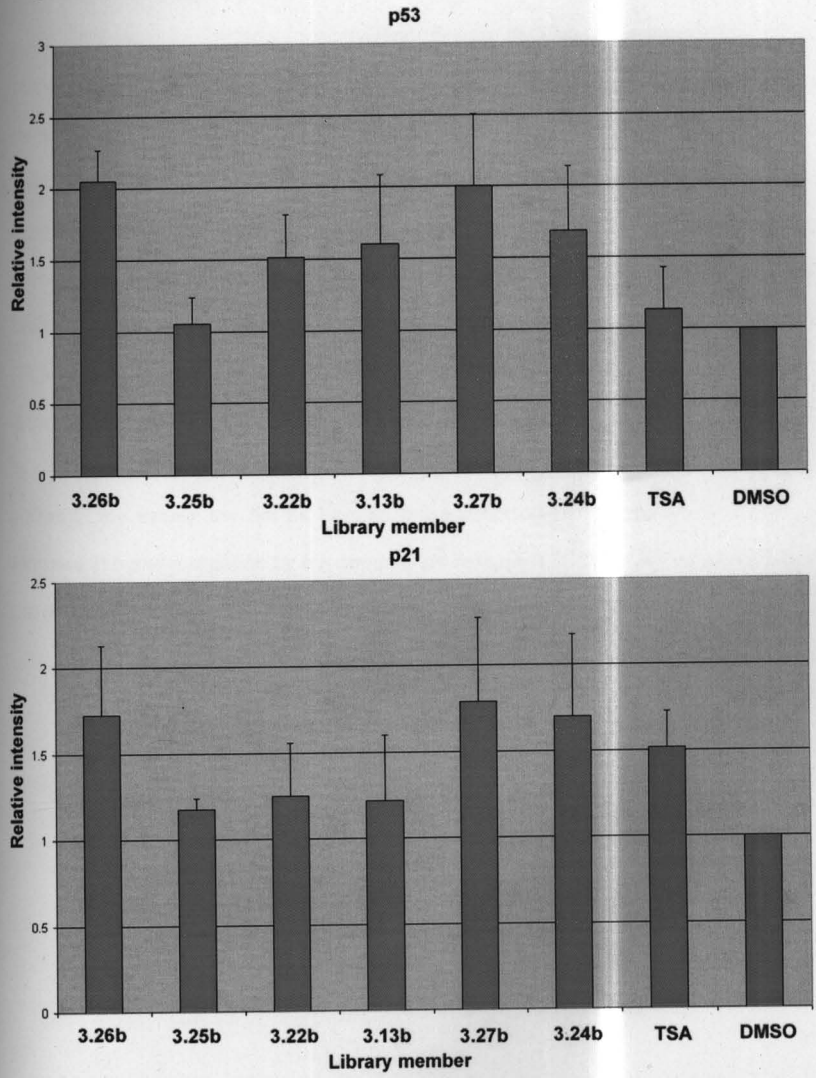

A549 cells were incubated with library members (1 μM) and TSA (0.5 μM) for 24 hours prior to fixation. Fixed cells were permeabilized and cytoblots performed using specific primary antibodies directed against biomarkers of interest.

4.4.2 Hyperacetylation of H3 and H4

Inhibition of histone deacetylation results in the hyperacetylation of core nucleosomal histones, primarily H3 and H4. The results obtained from this assay demonstrate that all six of our compounds increased H3 and H4 acetylation levels in A549 cells. In our experiments, all of our compounds showed a marked increase in H4 hyperacetylation. Notably, compound **3.26b** showed a 4-fold increase in H4 hyperacetylation when compared to TSA (Figure 4.8). Also, compound **3.27a** exhibited a dramatic increase in H4 acetylation with an almost 4-fold increase when compared to TSA (Figure 4.8). This complements our earlier results in *Drosophila* cells where H4 hyperacetylation was very pronounced with our compounds. Somewhat surprisingly, H3 hyperacetylation was not as evident and pronounced in these cytoblot experiments. Although the values are not as high as those obtained for H4, the trend of a marked increase in hyperacetylation by our compounds compared to TSA still true suggesting that the activity of our compounds could be related to their distinct mechanism of action.

Figure 4.8 H4 and H3 hyperacetylation

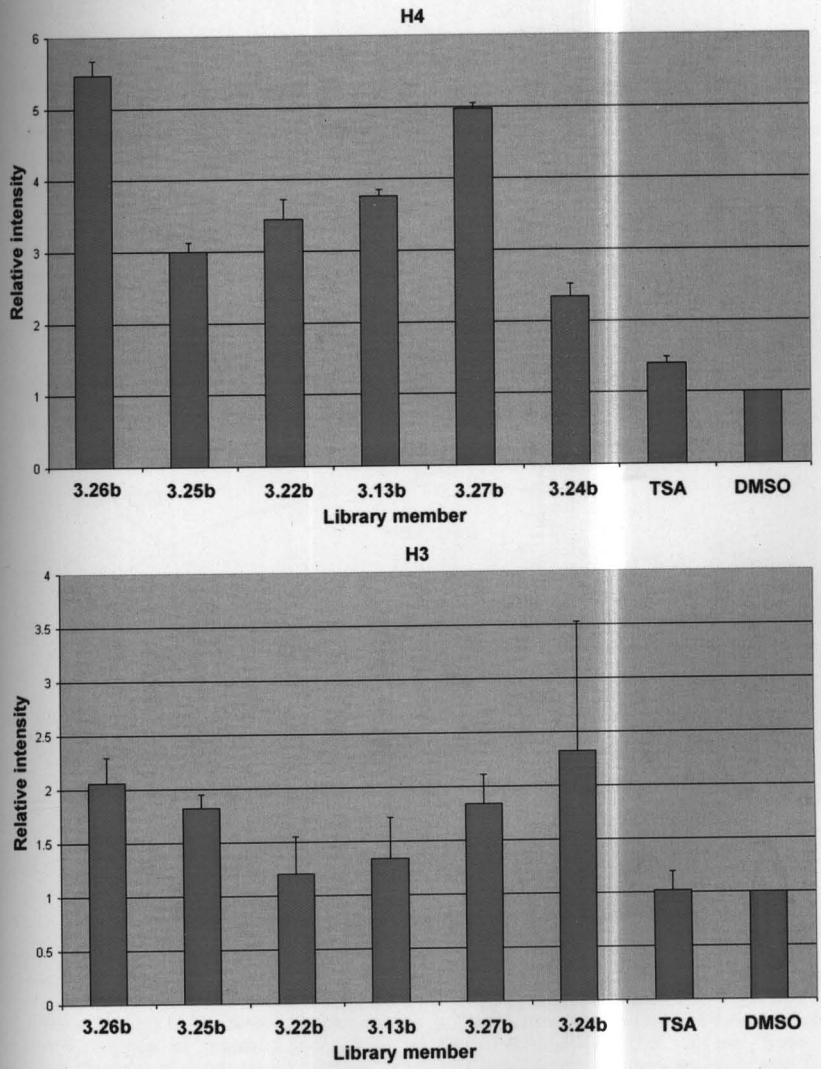

A549 cells were incubated with library members (1 μM) and TSA (0.5 μM) for 24 hours prior to fixation. Fixed cells were permeabilized and cytoblots performed using specific primary antibodies directed against biomarkers of interest.

4.4.3 Disruption of Keap1-Nrf2 Complex

Although FK-228 is equipotent to TSA regarding inhibition of HDAC activity in cultured cells, the mechanisms regulating FK-228 mediated cytotoxicity have not been fully elucidated. Indeed, several studies have indicated that histone acetylation alone is not sufficient to account for the anti-proliferative effects of HDAC inhibitors.[45-47]

Transcription factor Nrf2 regulates basal and inducible expression of phase 2 proteins that protect cells against the toxic effects of electrophiles and oxidants. Under basal conditions, Nrf2 is sequestered in the cytoplasm by Keap1, a multidomain, cysteine

Figure 4.9 Keap1 mechanism of phase 2 response regulation.

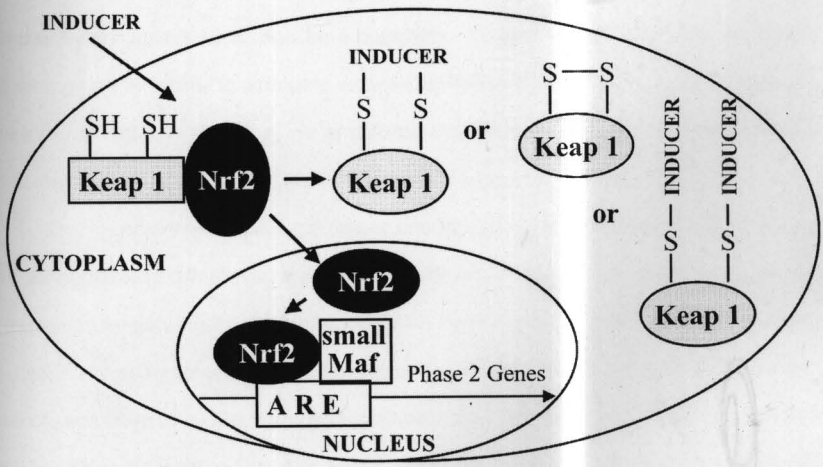

Nrf2 is anchored in the cytoplasm by binding to Keap1, which is attached to the actin cytoskeleton. Inducers disrupt the Keap1-Nrf2 complex, and Nrf2 migrates to the nucleus where it forms heterodimers with other transcription factors such as small Maf that bind to the ARE regions of phase 2 genes and accelerate their transcription. Several types of modifications of Keap1 by inducers are shown. Adapted from Dinkova-Kostova, Albena T. et al. Proc. Natl. Acad. Sci. USA **2002**, 99, 11908-11913

rich protein that is bound to the actin cytoskeleton. Keap1 acts both as a repressor of the Nrf2 transactivation and as a sensor of phase 2 inducers. Phase 2 inducers (namely, electrophiles and oxidants) react with sulfhydryl groups of Keap1, resulting in the disruption of the Keap1-Nrf2 complex (Figure 4.9).[48] Disruption of this complex liberates Nrf2 allowing it to translocate to the nucleus and transactivate cyto-protective genes via a common upstream regulatory element, the antioxidant response element (ARE). Also, AKT-dependent phosphorylation of Nrf2 releases it from this complex. Could this be a component of the mechanism by which FK-228 induces growth arrest and apoptosis in lung cancer cells? Keap1 is known to have twenty five cysteine thiol residues therefore Keap1-mediated activation of FK-228 by disulfide bond reduction seems plausible. Given that our compounds are FK-228 functional mimetics, disruption of the Keap1-Nrf2 complex by our agents could also be a possibility. To explore this possibility, we tested our analogs for the ability to attenuate intracellular Keap1 and Nrf2 levels. The results are presented in Figure 4.10. Also, we envisioned that evaluation of our compounds would aid in the understanding of FK-228's role in regards to Keap1-Nrf2 complex.

Our experiments indicate that all but one compound activate Keap1 more so than TSA although these differences are slight. It is important to note that there are no reports in the literature showing Keap1-Nrf2 modulation by the HDAC inhibitors TSA or FK-228. To date, only sulforaphane, an isothiocyanate-containing HDAC inhibitor isolated from broccoli, has been shown to display this bimodal mechanism of activation that calls into play both Keap1 modification and HDAC inhibition.[49] These results are particularly significant because they suggest that disulfide-containing molecules, such as FK-228, may disrupt the Keap1-Nrf2 complex thus resulting in Nrf2 activation.

Figure 4.10 Activation of Keap1 and Nrf2

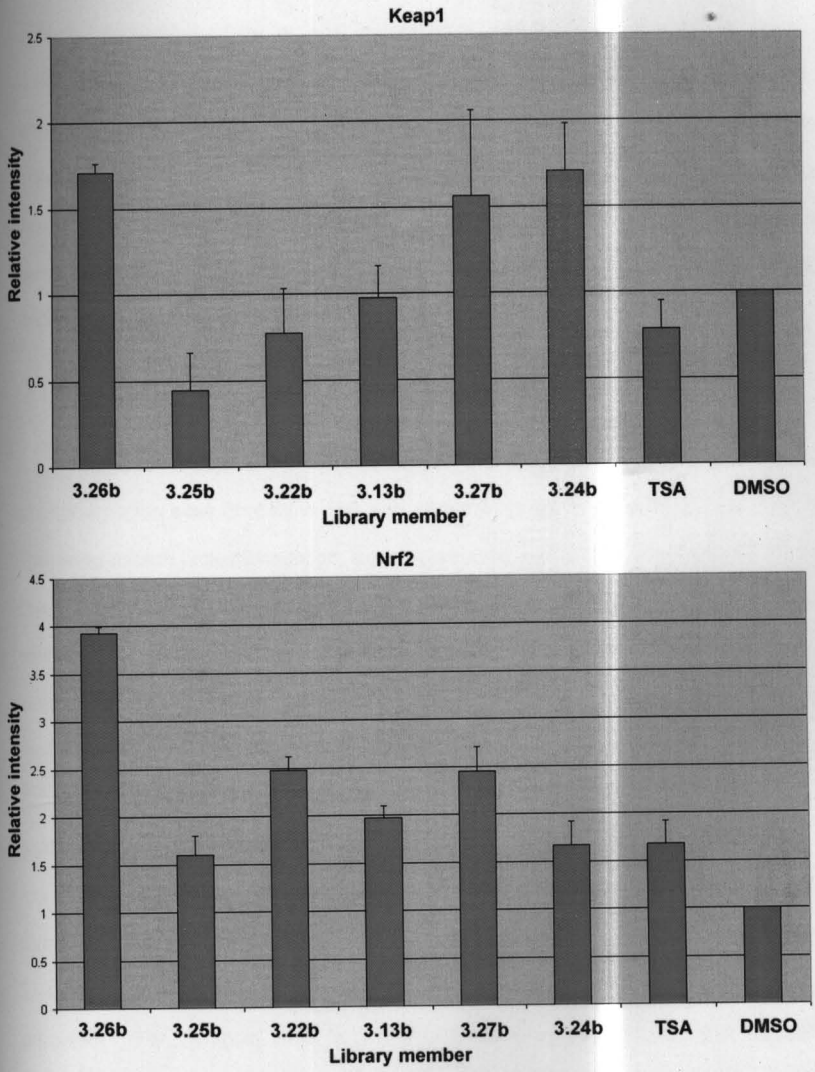

A549 cells were incubated with library members (1 μM) and TSA (0.5 μM) for 24 hours prior to fixation. Fixed cells were permeabilized and cytoblots performed using specific primary antibodies directed against biomarkers of interest.

In addition, we observed that enhanced levels of Nrf2 by all our compounds occurred regardless of the agents' impact on Keap1 levels. For instance, compound **3.26b** induced high level of overexpression of both Keap1 and Nrf2. However, **3.25b** suppressed Keap1 (relative to TSA), but enhanced Nrf2 levels. This suggests that Keap1-independent enhancement of Nrf2 can also be achieved. One possible explanation for this is that our compounds activate the phosphoinositide-3-kinase (PI3K)/AKT signaling pathway thus phosphorylating Nrf2. and leading to its destruction via proteolytic processing within the cell.

4.4.4 AKT Activation

In unstimulated cells, AKT exists in the cytoplasm and the two regulatory phosphorylation sites (threonine 308 and serine 473) are in an unphosphorylated state. Following growth factor stimulation, the pleckstrin homology (PH) domain of AKT binds to the lipid products of phosphatidylinositol-3 kinase (PI3K), and AKT is recruited to plasma membrane. AKT is then sequentially phosphorylated at T308 and S473 by upstream kinases referred to as 3-phosphoinositide-dependent protein kinase 1 (PDK1) and PDK2, respectively, to yield a fully activated kinase.[50,51]

AKT is a critical regulator of PI3K-mediated cell survival.[52,53] A large number of studies have demonstrated in various cell types that constitutive activation of AKT signaling is sufficient to block cell death induced by a variety of apoptotic stimuli and that transduction of dominant-negative AKT inhibits growth factor-induced cell survival.[54-56] The pro-survival function of AKT has also been demonstrated in the context of the intact organism. For instance, work by Staveley and co-workers showed that mutation of *Drosophila* AKT leads to embryonic lethality due to massive apoptosis during embryogenesis.[57]

Figure 4.11 Mechanism of Akt activation and partial list of downstream molecules

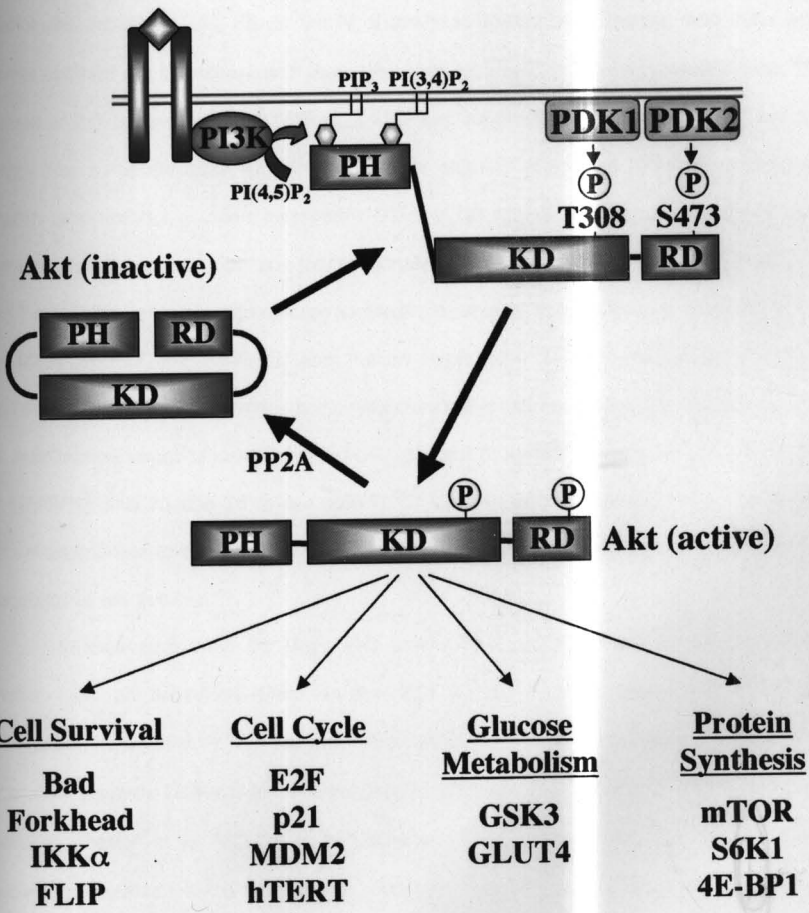

Akt is activated by growth factors or cytokines in a PI3K-dependent manner and phosphorylation of two residues by PDK1 (T308) and PDK2 (S473) is required for its full activation. Downstream target molecules are grouped according to their function. These downstream molecules include both direct Akt substrates and indirect downstream effectors. Adapted from Shiojima, I. et al. *Circ Res* **2002**, *90*, 1243-1250.

Several downstream targets of AKT are recognized to be apoptosis-regulatory molecules including Bad, FKHR family of forkhead transcription factors, and IKKα and these findings are consistent with the notion that AKT functions as a survival kinase.[58-64] However, other downstream effectors of AKT are involved in different aspects of cellular regulation. For example, (1) AKT enhances glucose uptake by inducing membrane translocation of the glucose transporter GLUT4, (2) AKT promotes glycogen synthesis through the phosphorylation and inactivation of glycogen synthase kinase-3 (GSK-3), (3) AKT regulates cell cycle and cellular senescence, at least in part, through modulating the activities of E2F, p21, MDM2, and human telomerase reverse transcriptase subunit (hTERT), and (4) AKT enhances protein synthesis through increasing the phosphorylation of mammalian target of rapamycin (mTOR), eukaryotic initiation factor 4E-binding protein 1 (4E-BP1), and 70-kDa S6 kinase (S6K1).[65-71] Taking all these events into account, it is more appropriate to classify AKT as a multifunctional protein kinase rather than a simple regulator of cell survival.

Studies performed by Mayo and co-workers suggest that inhibition of HDAC activity has an activation effect on the AKT pathway, rather than inhibition of the aforementioned pathway.[72] Their work suggested that the pro-apoptotic action of HDAC inhibitors (namely TSA and sodium butyrate) is blunted by their ability to stimulate NF-κB gene expression in an AKT-dependent manner. They proposed that inhibition of HDAC activity modulates NF-κB transcription through mechanisms involving AKT-dependent phosphorylation of p300, recruitment of p300 to chromatin, and modulation of transactivation potential of this co-activator complex. Moreover, in their studies, inhibition of NF-κB nuclear translocation or transcriptional activity significantly increased apoptosis in NSCLC cells following the addition of HDAC inhibitors. These findings promote the

notion that NF-κB provides a significant protective role against HDAC inhibitor-mediated apoptosis. In addition, this suggests that a combined molecular targeting that inhibits both NF-κB and HDAC activities may provide a significant anti-neoplastic therapy for patients with NSCLC.

Our results showed a marked increase in phosphorylation of both T308 and S473 AKT residues for all our compounds (Figure 4.12). Particularly, compound **3.26b** showed a 3-fold increase in pThrAKT activation as compared to TSA (Figure 4.12). This result is especially significant because compound **3.26b** showed the strongest activity on our Nrf2 experiments thus supporting our early assertions that activation the PI3K/AKT signaling pathway would likely result in Keap1-independent Nrf2 activation. Notably, the same trend is displayed by all our compounds.

Figure 4.12 Activation of PI3K/AKT signaling pathway

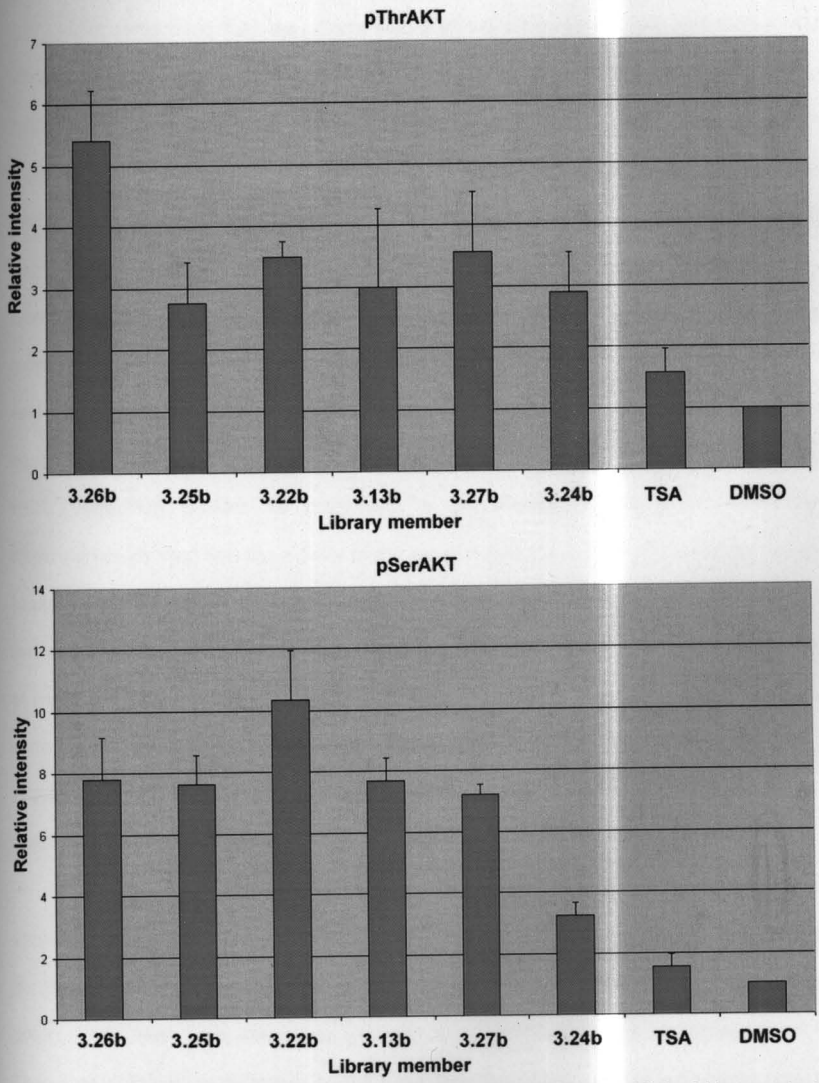

A549 cells were incubated with library members (1 μM) and TSA (0.5 μM) for 24 hours prior to fixation. Fixed cells were permeabilized and cytoblots performed using specific primary antibodies directed against biomarkers of interest.

4.5 Summary

We anticipated that our efforts would afford a number of cell permeable HDAC inhibitors whose activity is significantly enhanced by the cellular disulfide reductants glutathione, thioredoxin and thioredoxin reductase. Indeed, we have shown that *Drosophila* S2 cells subjected to compounds **3.10**, **3.11** and **3.12** rendered a significant amount of hyperacetylated histone H4 as determined by Western blot analyses of nuclear lysates. This supports early assertions of cell permeability by these synthetic agents. Compound **3.11** showed the most pronounced bands at concentrations as low as 2 μM. Increasing concentrations of our cyclic disulfide core structures (compounds **3.13a**, **3.13b** and **3.13c**) were active at concentrations as low as 20 μM. These core structures were coupled to a variety of cap groups and resulted in FK-228 mimics that have moderate HDAC inhibition profiles as presented in our Fluor-de-Lys experiments. These experiments showed that the activity of our capped cyclic disulfides is dependent upon the presence of reductants. This is consistent with FK-228's mode of action, where a pre-reduction step is needed for the compound to be active. Moreover, we observed a range of moderate HDAC inhibition (20-58%) by our compounds. In addition, we observed that even subtle structural changes have a profound impact upon HDAC inhibition. These results support our hypothesis that structurally simpler functional mimics of FK-228 can be made retaining HDAC activity.

The top fifteen compounds from our library were selected and evaluated for their antitumor properties. This was done using a high-throughput cytotoxicity assay on nine human cancer cell lines representing a broad range of carcinomas, including breast, colon, CNS, liver, lung, and ovary and a mouse mammary normal epithelial control line The data obtained from these experiments revealed some agents with promising IC_{50}

values. Although not as cytotoxic as TSA or other published HDAC inhibitors, our compounds showed values representative of good leads thus, further optimization and development of these agents into more active HDAC inhibitors is warranted.

Based on the results of the Fluor-de-Lys assay and the cytotoxicity assays, we chose a total of six compounds and assessed their ability to activate an assortment of cancer-related proteins including p53, p21, hyperacetylated H3 and H4, Keap1, Nrf2 and AKT. In general, our compounds enhanced the activity/expression of all the aforementioned proteins. TSA was used as a positive control and showed a similar trend but to a lesser degree of intensity. Altered expression of p53 was observed by almost all our compounds. Compounds **3.26b** and **3.27a** showed the highest activity, a 2-fold increase over TSA. These results are in contrast to data obtained by Yu and co-workers on depsipeptide FK-228. In their studies, FK-228 showed no increase in p53 activity on human adenocarcinoma A549 cells. Unfortunately, difficulties encountered in attempts to acquire authentic FK-228 prohibit direct comparison with our new class of cyclic disulfides.

Hyperacetylation of histone H4 was very prominently induced by our library of compounds when compared to TSA with an average 2-fold increase in hyperacetylation. These data substantiate those obtained by application of the methyl ester core structures **3.13a-c** in *Drosophila* cells. Perhaps the most noteworthy result of our studies was presented by compound **3.26b**, which showed a 3-fold increase in pThrAKT activation of the apoptosis regulatory protein kinase AKT. This result is especially significant because compound **3.26b** also showed the strongest activity on our Nrf2 experiments. This provides support to our hypothesis that activation of the PI3K/AKT signaling pathway would result in Keap1-independent Nrf2 activation. Activation of AKT will result in Nrf2 phosphorylation with concomitant release from the Keap1-Nrf2 complex thus making Nrf2 available for nuclear exportation and activation of other proteins.

We believe that the readily diversified FK-228 analogs presented here and the activities associated with them are likely to be useful in further understanding different HDAC's. Moreover, these agents have the potential to represent clinical candidates in the near future.

4.6 References

(1) Bier, E. Drosophila, The Golden Bug, Emerges As a Tool for Human Genetics. *Nature Rev. Genet.* **2005**, *6*, 9-23.

(2) Brumby, A. M.; Richardson, H. E. Using Drosophila Melanogaster to Map Human Cancer Pathways. *Nature Cancer Rev* **2005**, *5*, 626-639.

(3) Hanahan, D.; Weinberg, R. A. The Hallmarks of Cancer. *Cell* **2000**, *100*, 57-70.

(4) Ballestar, E.; Pile, L. A.; Wassarman, D. A.; Wolffe, A. P.; Wade, P. A. A Drosophila MBD Family Member is a Transcriptional Corepressor Associated with Specific Genes. *Eur. J. Biochem.* **2001**, *268*, 5397-5406.

(5) Suzuki, T.; Kouketsu, A.; Matsuura, A.; Kohara, A.; Ninomiya, S.-I. et al. Thiol-based SAHA Analogues as Potent Histone Deacetylase Inhibitors. *Bioorg. Med. Chem. Lett.* **2004**, *14*, 3313-3317.

(6) Suzuki, T.; Kouketsu, A.; Itoh, Y.; Hisakawa, S.; Maeda, S. et al. Highly Potent and Selective Histone Deacetylase 6 Inhibitors Designed Based on a Small-Molecular Substrate. *J. Med. Chem.* **2006**, *49*, 4809-4812.

(7) Nishino, N.; Jose, B.; Okamura, S.; Ebisusaki, S.; Kato, T. et al. Cyclic Tetrapeptides Bearing a Sulfhydryl Group Potently Inhibit Histone Deacetylases. *Org. Lett.* **2003**, *5*, 5072-5082.

(8) Colletti, S. L.; Myers, R. W.; Darkin-Rattray, S. J.; Schmatz, D. M.; Fisher, M. H. et al. Design and Synthesis of Histone Deacetylase Inhibitors: The Development of Apicidin Transition State Analogs. *Tetrahedron Lett.* **2000**, *41*, 7837-7841.

(9) Hoffman, K.; Brosch, G.; Loidl, P.; Jung, M. A Non-Isotopic Assay for Histone Deacetylase Activity. *Nucleic Acids Res.* **1999**, *27*, 2057-2058.

(10) Furumai, R.; Matsuyama, A.; Kobashi, N.; Lee, K.-H.; Nishiyama, M. et al. FK228 (Depsipeptide) as a Natural Prodrug That Inhibits Class I Histone Deacetylases. *Cancer Res.* **2002**, *62*, 4916-4921.

(11) Gurvich, N.; Tsygankova, O. M.; Meinkoth, J. L.; Klein, P. S. Histone Deacetylase Is a Target of Valproic Acid-Mediated Cellular Differentiation. *Cancer Res* **2004**, *64*, 1079-1086.

(12) Kapustin, G. V.; Fejer, G.; Gronlund, J. L.; McCafferty, D. G.; Seto, E. et al. Phosphorus-Based SAHA Analogues as Histone Deacetylase Inhibitors. *Org. Lett.* **2003**, *5*, 3053-3056.

(13) Zhou, X.; Marks, P. A.; Rifkind, R. A.; Richon, V. M. Cloning and Characterization of a Histone Deacetylase, HDAC9. *Prod. Natl. Acad. Sci. U.S.A.* **2001**, *98*.

(14) Sartorelli, A. C. Therapeutic Attack of Hypoxic Cells of Solid Tumors: Presidential Address. *Cancer Res.* **1988**, *48*, 775-778.

(15) Moore, H. W. Bioactivation as a Model for Drug Design Bioreductive Alkylation. *Science* **1977**, *197*, 527-532.

(16) Wipf, P.; Lynch, S. M.; Birmingham, A.; Giselle, T.; Jimenez, A. et al. Natural Product Based Inhibitors of the Thioredoxin-Thioredoxin Reductase System. *Organic & Biomolecular Chemistry* **2004**, *2*, 1651-1658.

(17) Furumai, R.; Komatsu, Y.; Nishino, N.; Khochbin, S.; Yoshida, M. et al. Potent Histone Deacetylase Inhibitors Built from Trichostatin A and Cyclic Tetrapeptide Antibiotics Including Trapoxin. *Proc. Natl. Acad. Sci. U.S.A.* **2001**, *98*, 87-92.

(18) Miller, T. A.; Witter, D. J.; Belvedere, S. Histone Deacetylase Inhibitors. *J. Med. Chem.* **2003**, *46*, 5097-5116.

(19) Sasakawa, Y.; Naoe, Y.; Sogo, N.; Inoue, T.; Sasakawa, T. et al. Marker Genes to Predict Sensitivity to FK228, a Histone Deacetylase Inhibitor. *Biochem. Pharmacol.* **2005**, *69*, 603-616.

(20) Stockwell, B. R.; Haggarty, S. J.; Schreiber, S. L. High-throughput Screening of Small Molecules in Miniaturized Mammalian Cell-Based Assays Involving Post-Translational Modifications. *Chem. Biol.* **1999**, *6*, 71-83.

(21) Levine, A. J. p53, The Cellular Gatekeeper for Growth and Division. *Cell* **1997**, *88*, 323-331.

(22) Ko, L. J.; Prives, C. p53: Puzzle and Paradigm. *Genes Dev.* **1996**, *10*, 1054-1072.

(23) Leng, R. P.; Lin, Y.; Ma, W.; Wu, H.; Lemmers, B. et al. Pirh2, A p53-Induced Ubiquitinprotein Ligase, Promotes p53 Degradation. *Cell* **2003**, *112*, 779-791.

(24) Oliner, J. D.; Kinzler, K. W.; Meltzer, P. S.; George, D. L.; Vogelstein, B. Amplification of a Gene Encoding a p53-Associated Protein in Human Sarcomas. *Nature* **1992**, *358*, 80-83.

(25) Momand, J.; Zambetti, G. P.; Olson, D. C.; George, D.; Levine, A. J. The Mdm-2 Oncogene Product Forms a Complex with The p53 Protein and Inhibits p53-Mediated Transactivation. *Cell* **1992**, *69*, 1237-1245.

(26) Gottifredi, V.; Prives, C. Molecular Biology. Getting p53 Out of The Nucleus. *Science* **2001**, *292*, 1851-1852.

(27) Dornan, D.; Wertz, I.; Shimizu, H.; Arnott, D.; Frantz, G. D. et al. The Ubiquitin Ligase COP1 is a Critical Negative Regulator of p53. *Nature* **2004**, *429*, 86-92.

(28) Chen, D., N. ; Kon, M. L.; Zhang, W.; Qin, J.; Gu, W. ARF-BP1/Mule is a Critical Mediator of the ARF Tumor Suppressor. *Cell* **2005**, *121*, 1071-1083.

(29) Honda, R.; Tanaka, H.; Yasuda, H. Oncoprotein MDM2 is a Ubiquitin Ligase E3 for Tumor Suppressor p53. *FEBS Lett.* **1997**, *420*, 25-27.

(30) Shieh, S. Y.; Ahn, J.; Tamai, K.; Taya, Y.; Prives, C. The Human Homologs of Checkpoint Kinases Chk1 and Cds1 (Chk2) Phosphorylate p53 at Multiple DNA Damage-Inducible Sites. *Genes Dev.* **2000**, *14*, 289-300.

(31) Lambert, P. F.; Kashanchi, F.; Radonovich, M. F.; Shiekhattar, R.; Brady, J. N. Phosphorylation of p53 Serine 15 Increases Interaction with CBP. *J. Biol. Chem.* **1998**, *273*, 33048-33053.

(32) Hupp, T. R.; Lane, D. P. Allosteric Activation of Latent p53 Tetramers. *Curr. Biol.* **1994**, *4*, 865-875.

(33) Giaccia, A. J.; Kastan, M. The Complexity of p53 Modulation: Emerging Patterns from Divergent Signals. *Genes Dev.* **1998**, *12*, 2973-2983.

(34) Gu, W.; Roeder, R. Activation of p53 Sequence-Specific DNA Binding by Acetylation of The p53 C-Terminal Domain. *Cell* **1997**, *90*, 595-606.

(35) Liu, L.; Scolnick, D.; Trievel, R. C.; Zhang, H. B.; Marmorstein, R. et al. p53 Sites Acetylated In Vitro by PCAF and p300 are Acetylated In Vivo in Response to DNA Damage. *Mol. Cell. Biol.* **1999**, *19*, 1202-1209.

(36) Lill, N. L.; Grossman, S.; Ginsberg, D.; DeCaprio, J.; Livingston, D. M. Binding and Modulation of p53 by p300/CBP Coactivators. *Nature* **1997**, *387*, 823-827.

(37) Gu, W.; Roeder, R. G. Activation of p53 Sequence-Specific DNA Binding by Acetylation of the p53 C-Terminal Domain. *Cell* **1997**, *90*, 595-606.

(38) Ito, A.; Lai, C. H.; Zhao, X.; Saito, S.; Hamilton, M. H. et al. p300/CBP-Mediated p53 Acetylation is Commonly Induced by p53-Activating Agents and Inhibited by MDM2. *EMBO J.* **2001**, *20*, 1331-1340.

(39) Guo, A.; Salomoni, P.; Luo, J.; Shih, A.; Zhong, S. et al. The Function of PML in p53-Dependent Apoptosis. *Nat. Cell Biol.* **2000**, *2*, 730-736.

(40) Luo, J.; Su, F.; Chen, D.; Shiloh, A.; Gu, W. Deacetylation of p53 Modulates its Effect on Cell Growth and Apoptosis. *Nature* **2000**, *408*, 377-381.

(41) Nakano, K.; Mizi, T.; Sowa, Y.; Orita, T.; Yoshino, T. et al. Butyrate activates the WAF1/Cip1 Gene Promoter Through Sp1 Sites in a p53-Negative Human Colon Cancer Cell Line. *J. Biol. Chem.* **1997**, *272*, 22199-22206.

(42) Gartel, A. L.; Tyner, A. L. Transcriptional Regulation of the p21(WAF1/CIP1) Gene. *Exp. Cell Res.* **1999**, *246*, 280-289.

(43) Yu, X.; Guo, Z. S.; Marcu, M. G.; Neckers, L.; Nguyen, D. M. Modulation of p53, ErB1, ErB2, and Raf-1 Expression in Lung Cancer Cells by Depsipeptide FR901228. *J. Natl. Cancer Institute* **2002**, *94*, 504-513.

(44) Zhao, Y.; Lu, S.; Wu, L.; Chai, G.; Wang, H. et al. Acetylation of p53 at Lysine 373/382 byt the Histone Deacetylase Inhibitor Depsipeptide Inducess Expression of p21Waf1/Cip1. *Mol. Cell. Biol.* **2006**, *26*, 2782-2790.

(45) Brinkmann, H.; Dahler, A.; Popa, C.; Serewko, M. M.; Parsond, P. G. et al. Histone Hyperacetylation Induced by Histone Deacetylase Inhibitors is not Sufficient to Cause Growth Inhibition in Human Dermal Fibroblasts. *J. Biol. Chem.* **2001**, *276*, 22491-22499.

(46) Richon, V. M.; Emiliani, S.; Verdin, E.; Webb, Y.; Breslow, R. et al. A Class of Hybrid Polar Inducers of Transformed Cell Differentiation Inhibits Histone Deacetylases. *Prod. Natl. Acad. Sci. U.S.A.* **1998**, *95*, 3003-3007.

(47) Saunders, N.; Dicker, A.; Popa, C.; Jones, S.; Dahler, A. Histone Deacetylase Inhibitors as Potential Anti-Skin Cancer Agents. *Cancer Res.* **1999**, *59*, 399-404.

(48) Guengerich, F. Enzymatic Oxidation of Xenobiotic Chemicals. *Crit Rev Biochem Mol Biol* **1990**, *25*, 97-153.

(49) Myzaka, M. C.; Dashwood, R. H. Chemoprotection by Sulforaphane: Keep one Eye Beyond Keap1. *Cancer Lett.* **2006**, *233*, 208-218.

(50) Downward, J. Mechanisms and Consequences of Activation of Protein Kinase B/Akt. *Curr Opin Cell Biol.* **1998**, *10*, 262-267.

(51) Hemmings, B. A. Akt signaling: Linking Membrane Events to Life and Death Decisions. *Science* **1997**, *275*, 628-630.

(52) Franke, T. F.; Yang, S.; Chan, T. O.; Datta, K.; Kazlauskas, A. et al. The Protein Kinase Encoded by The Akt Protooncogene is a Target of The PDGF-Activated Phosphatidylinositol 3-kinase. *Cell* **1995**, *81*, 727-736.

(53) Yao, R.; Cooper, G. Requirement for Phosphatidylinositol-3 Kinase in The Prevention of Apoptosis by Nerve Growth Factor. *Science* **1995**, *267*, 2003-2006.

(54) Dudek, H.; Datta, S. R.; Franke, T. F.; Birnbaum, M. J.; Yao, R. et al. Regulation of Neuronal Survival by The Serine-Threonine Protein Kinase Akt. *Science* **1997**, *275*, 661-665.

(55) Fujio, Y.; Guo, K.; Mano, T.; Mitsuuchi, Y.; Testa, J. R. et al. Cell Cycle Withdrawal Promotes Myogenic Induction of Akt, a Positive Modulator of Myocyte Survival. *Mol Cell Biol.* **1999**, *19*, 5073-5082.

(56) Fujio, Y.; Nguyen, T.; Wencker, D.; Kitsis, R. N.; Walsh, K. Akt Promotes Survival of Cardiomyocytes In Vitro and Protects Against Ischemia-Reperfusion Injury in Mouse. *Heart. Circulation.* **2000**, *101*, 660-667.

(57) Staveley, B. E.; Ruel, L.; Jin, J.; Stambolic, V.; Mastronardi, F. G. et al. Genetic Analysis of Protein Kinase B (AKT) in Drosophila. *Curr Biol.* **1998**, *8*, 599-602.

(58) Romashkova, J. A.; Makarov, S. S. NF- B is a Target of AKT in Anti-Apoptotic PDGF Signalling. *Nature.* **1999**, *401*, 86-90.

(59) Ozes, O. N.; Mayo, L. D.; Gustin, J. A.; Pfeffer, S. R.; Pfeffer, L. M. et al. NF- B Activation by Tumour Necrosis Factor Requires The Akt Serine/Threonine Kinase. *Nature* **1999**, *401*, 82-85.

(60) Tang, E. D.; Nunez, G.; Barr, F. G.; Guan, K. L. Negative Regulation of The Forkhead Transcription Factor FKHR by Akt. *J Biol Chem.* **1999**, *274*, 16741-16746.

(61) Kops, G. J.; de Ruiter, N. D.; De Vries-Smits, A. M.; Powel, I. D. R.; Bos, J. L. et al. Direct Control of The Forkhead Transcription Factor AFX by Protein Kinase B. *Nature.* **1999**, *398*, 630-634.

(62) del Peso, L.; Gonzalez-Garcia, M.; Page, C.; Herrera, R.; Nunez, G. Interleukin-3-Induced Phosphorylation of BAD Through The Protein Kinase Akt. *Science.* **1997**, *278*, 687-689.

(63) Datta, S. R.; Dudek, H.; Tao, X.; Masters, S.; Fu, H. et al. Akt Phosphorylation of BAD Couples Survival Signals to The Cellintrinsic Death Machinery. *Cell.* **1999**, *91*, 231-241.

(64) Brunet, A.; Bonni, A.; Zigmond, M. J.; Lin, M. Z.; Juo, P. et al. Akt Promotes Cell Survival by Phosphorylating and Inhibiting a Forkhead Transcription Factor. *Cell* **1997**, *96*, 857-868.

(65) Shah, O. J.; Anthony, J. C.; Kimball, S. R.; Jefferson, L. S. 4E-BP1 and S6K1: Translational Integration Sites for Nutritional and Hormonal Information in Muscle. *Am J Physiol.* **2000**, *279*, E715-E729.

(66) Rossig, L.; Badorff, C.; Holzmann, Y.; Zeiher, A. M.; Dimmeler, S. Glycogen Synthase Kinase-3 Couples Akt-Dependent Signaling to The Regulation of p21Cip1 Degradation. *J Biol Chem.* **2001**, *277*, 9684-9689.

(67) Rossig, L.; Jadidi, A. S.; Urbich, C.; Badorff, C.; Zeiher, A. M. et al. Akt-Dependent Phosphorylation of p21(Cip1) Regulates PCNA Binding and Proliferation of Endothelial Cells. *Mol Cell Biol.* **2001**, *21*, 5644-5657.

(68) Breitschopf, K.; Zeiher, A. M.; Dimmeler, S. Pro-Atherogenic Factors Induce Telomerase Inactivation in Endothelial Cells Through an Akt-Dependent Mechanism. *FEBS Lett.* **2001**, *493*, 21-25.

(69) Mayo, L. D.; Donner, D. B. A Phosphatidylinositol 3-Kinase/Akt Pathway Promotes Translocation of Mdm2 From the Cytoplasm to The Nucleus. *Proc Natl Acad Sci U S A.* **2001**, *98*, 11598-11603.

(70) Zhou, B. P.; Liao, Y.; Xia, W.; Spohn, B.; Lee, M. H. et al. Cytoplasmic Localization of p21Cip1/WAF1 by Akt-Induced Phosphorylation in HER-2/Neu-Overexpressing Cells. *Nat Cell Biol.* **2001**, *3*, 245-252.

(71) Kang, S. S.; Kwon, T.; Kwon, D. Y.; Do, S. I. Akt Protein Kinase Enhances Human Telomerase Activity Through Phosphorylation of Telomerase Reverse Transcriptase Subunit. *J Biol Chem.* **1999**, *274*, 13085-13090.

(72) Mayo, M. W.; Denlinger, C. E.; Broad, R. M.; Yeung, F.; Reilly, E. T. et al. Ineffectiveness of Histone Deacetylase Inhibitors to Induce Apoptosis Involves the Transcriptional Activation of NF-{kappa}B through the Akt Pathway. *J. Biol. Chem.* **2003**, *278*, 18980-18989.

Chapter 5. Experimental Section

5.1 Chapter 1 Compounds

5.1.1 General Synthetic Procedures

All reactions were carried out under an atmosphere of argon using flame-dried glassware. A Büchi rotary evaporator equipped with a water condenser, and a water aspirator was used to concentrate *in vacuo*. Samples were further dried under reduced pressure on a high vacuum line.

Tetrahydrofuran (THF) was distilled from sodium metal and benzophenone. Dichloromethane (CH_2Cl_2), and toluene were distilled from calcium hydride. Diisopropylamine was dried over CaH_2 and subsequently distilled under argon and stored in a septum sealed serum bottle over solid KOH. All other solvents were purchased from Aldrich Chemical Company and used without further purification. All amino acids were purchased from Chem-Impex. All commercial reagents were purchased from Aldrich Chemical Co., or Acros Organics. Reactions were cooled to 0 °C via ice baths.

Flash column chromatography was performed using Merck grade 60 silica gel (230-400 mesh) and TLC analysis was carried out using Merck 60F-254 pre-coated silica sheets. Visualization of TLC plates was achieved using ultraviolet light, polyphosphomolybdic acid and cerium sulfate in EtOH with H_2SO_4, ninhydrin in EtOH with H_2SO_4 or iodine.

^1H NMR spectra were taken on a Varian Unity Inova 400, or a Varian Unity Inova 500 spectrometer in $CDCl_3$ at ambient temperature unless otherwise noted. ^1H chemical shifts in $CDCl_3$ were reported in ppm (δ units) downfield from tetramethylsilane. Solvent

peaks were used as internal references for all ^{13}C NMR. The triphenylphosphine peak at –0.6 was used as an internal reference for all ^{31}P spectra.

Mass spectroscopy was obtained at the University of Wisconsin-Madison School of Pharmacy. Electrospray ionization time of flight mass spectra (ESI-MS) was performed on a Micromass LCT Mass Spectrometer (Beverly, MA). Electron impact mass spectra (EI-MS) and fast atom bombardment spectra (FAB-MS) were performed on a Micromass AutoSpec Mass Spectrometer-magnetic sector (Beverly, MA).

Analytical HPLC was performed on a Waters 600 Controller system equipped with a Waters 717plus autosampler, a degasser, a Waters 996 photodiode array detector, and a Luna Phenomenex (C18, 4.6 mm x 150 mm, 5 micron) or Varian Microsorb column (C18, 4.6 mm x 150 mm) at 30 °C unless otherwise stated. All solvent were HPLC grade and contained 0.1% TFA unless otherwise stated.

5.1.2 General Synthetic Procedures for Staudinger Ligations

To the aryl azide (0.0124 g, 0.0505 mmol) in 252.5 µL 1:1 THF:H_2O was added the phosphine (0.0200 g, 0.0505 mmol) in 252.5 µL 1:1 THF:H_2O. The reaction was stirred at ambient temperature for 1.5 h. The product was extracted into ethyl acetate, washed with brine, and dried over Na_2SO_4. The solvent was removed *in vacuo* and the resulting material was chromatographed [9:1 Pet Ether: (4:2:1 EtOAc:CH_2Cl_2:MeOH] to yield the desired conjugate as a light yellow oil.

5.1.3 General Procedure for preparation of Esters (1.26 and 1.27)

To PPh_3 (0.490 mmo) in 2.3 mL of THF at 0 °C was added DIAD (0.490 mmol). The reaction was stirred for 15 minutes, followed by the addition of the desired alcohol

(0.327 mmol) in 1 mL of THF. After stirring for an additional 5 minutes, the carboxylic acid (0.327 mmol) was added to the mixture. The slurry was stirred for an additional 5 minutes at 0 °C, allowed to reach ambient temperature and stirred until the precipitated disappeared. The solvent was removed *in vacuo* and the resulting material chromatographed [9:1 Pet Ether: (4:2:1 EtOAc:CH_2Cl_2:MeOH] to yield the desired ester.

5.1.4 Compound Characterizations

N-(2-(2-Aminoethoxy)ethoxy)ethyl)-4-(pyren-4-yl)butanamide. (**1.19**) To 1-Pyrenebutyric acid (1.03 g, 3.56 mmol) in 18 mL of a 2:1:1 THF:DMF:H_2O mixture, DIEA (3.09 mL, 17.79 mmol) was added. Reaction stirred at ambient temperature for 10 minutes, followed by addition of TSTU (1.29 g, 4.27 mmol) and stirred for 30 minutes. Solution diluted with 14 mL of THF and added to a solution of THF (18 mL) containing 2,2'-(ethylenedioxy)bis(ethylamine) (5.27 g, 35.58 mmol). The reaction was stirred for an additional 2 h. The reaction was washed with $NaHCO_3$ and extracted several times with CH_2Cl_2. The organic layer was dried over Na_2SO_4, and solvent removed *in vacuo*. The resulting material was column chromatographed (column was pre-treated with TEA) (2:1:1 CH_2Cl_2:EtOAc:MeOH with 1.5% TEA) to afford 1.09 g (74%) of the desired amine. ^{1}H NMR ($CDCl_3$) δ 8.23 (d, J = 9.2 Hz, 1H), 8.09 (dd, J = 7.2 Hz, 1.6 Hz, 2H), 8.03 (d, J = 9.2 Hz, 2H), 7.95-7.90 (m, 3H), 7.78 (d, J = 8Hz, 1H), 6.50 (bt, 1H), 3.46-3.39 (m, 8H), 3.33-3.27 (m, 4H), 2.63 (bm, 2H), 2.23-2.14 (m, 4H), 1.60 (s, 2H); ^{13}C NMR ($CDCl_3$) δ 173.0, 136.2, 131.6, 131.1, 128.9, 127.7, 127.5, 126.9, 126.0, 125.2, 125.1,125.0, 124.9, 123.6, 73.2, 70.3, 70.1, 70.0, 41.6, 39.3, 36.1, 32.9, 27.7.

2-Diphenylphosphanyl-N-(2-{2-[2-(4-pyren-1-yl-butyrylamine)-ethoxy]-ethoxy}ethyl)-terephthalamic acid methyl ester. (**1.20a**) To 1-methyl-2-diphenylphosphinoterephthalate (0.250 g, 0.687 mmol) was added 3.4 mL of a 2:1:1 THF:DMF:H_2O mixture along with DIEA (350 μL, 2.00 mmol). The solution was stirred at room temperature for 5 minutes followed by addition of TSTU (0.260 g, 0.860 mmol). The reaction was stirred for 1 h at room temperature followed by dilution with 2.5 mL of THF and transferred to a stirring solution of 2,2'-(ethylenedioxy)bis(ethylamine) (1.50 g, 6.80 mmol) in 3 mL of THF. The reaction was stirred for 2 h and later partitioned between saturated NaH_2CO_3 and $CHCl_3$. The aqueous fraction was extracted several times with $CHCl_3$ and organic layers combined. 0.30 mmol of this crude material was coupled to the activated NHS ester of pyrenebutyric acid in the following manner: To pyrenebutyric acid (0.087 g, 0.300 mmol) in 1.5 mL of the THF:DMF:H_2O mixture note above along with DIEA (151 μL, 0.870 mmol). The solution of acid was stirred for 5 minutes followed by addition of TSTU (0.113 g, 0.370 mmol). The NHS ester was formed over the course of 1 h and the diluted with 1 mL of THF. To the NHS ester was then added the phosphanyl amine (0.148 g, 0.300 mmol) diluted into 1.2 mL of anhydrous THF. The coupling was performed over the course of 2 h; the reaction was then partitioned between $CHCl_3$ and saturated $NaHCO_3$. The organic layers was then washed with $NaHCO_3$, 0.5N HCl, H_2O and brine. Finally the solutionwas dried over Na_2SO_4, solvent removed *in vacuo* and the resulting residue subjected to 2 rounds of PTLC purification (5:5:3:1 Hex:CH_2Cl_2:EtOAc:MeOH) to afford 0.096 g (43% yield) of desired product. ^{1}H NMR ($CDCl_3$) δ 8.30 (d, J = 9.2 Hz, 1H), 8.16 (d, J = 7.6 Hz, 2H), 8.10 (d, J = 9.2 Hz, 2H), 8.05-7.96 (m, 4H), 7.85 (d, J = 7.6 Hz, 1H), 7.71 (dd, J = 8.0, 1.6 Hz, 1H), 7.39-7.25 (m, 10H), 6.34-6.26 (m, 1H), 5.96-5.88 (m, 1H), 3.77 (s, 3H), 3.60-3.32 (m, 14H), 2.32-2.12 (m, 4H); ^{13}C NMR ($CDCl_3$) δ 173.0, 166.9, 166.7, 141.9,

141.6, 137.5, 137.4, 136.8, 136.1, 134.2, 134.0, 133.0, 131.6, 131.1, 130.1, 129.2, 129.0, 128.8, 127.7, 127.6, 127.0, 126.8, 126.1, 125.2, 125.1, 123.6, 73.2, 70.4, 70.3, 70.1, 69.7, 68.2, 52.4, 50.9, 40.0, 39.4, 36.2, 33.0, 27.6, 25.8. HRMS-MALDI: calcd for $C_{47}H_{45}N_2O_6P$ (M+Na) 787.2910, measured 787.2887.

2-Diphenylphoaphanyl-N-ethoxycarbonylmethyl-terephthalamic acid methyl ester. (**1.20b**) To 1-methyl-2-diphenylphosphinoterephthalate (0.150 g, 0.420 mmol) was added 2 mL of a 2:1:1: THF:DMF:H_2O mixture along with DIEA (206 μL, 1.200 mmol). The solution was stirred for 5 minutes followed by addition of TSTU (0.260 g, 0.516 mmol). The reaction was stirred for 30 minutes followed by addition of DIEA (433 μL, 2.520 mmol) and glycine ethyl ester hydrochloride (0.173 g, 1.260 mmol). The reaction was stirred for 4 h at room temperature and then partitioned between 20 mL cold 1N HCl and $CHCl_3$ (30 mL). Organic layer was washed several times with cold 1N HCl, saturated $NaHCO_3$ and brine. Organic layer was dried over Na_2SO_4 and solvent removed *in vacuo*. Resulting material was column purified (10:10:6:2:1 Hex.:CH_2Cl_2:EtOAc:MeOH:Pet. Ether) to afford 0.0794 g (43% yield) of the desired product. ^{1}H NMR ($CDCl_3$) δ 8.09 (dd, J = 8.1, 3.5 Hz, 1H), 7.81 (dd, J = 8.1, 1.5 Hz, 1H), 7.38-7.22 (m, 11H), 6.45-6.38 (m, 1H), 4.21 (q, J = 7.2 Hz, 2H), 4.08 (d, J = 5.2 Hz, 2H), 3.74 (s, 3H), 1.27 (t, J = 7.2 Hz, 3H); ^{13}C NMR ($CDCl_3$) δ 169.8, 166.8, 166.4, 142.1, 141.8, 137.2, 136.6, 134.2, 133.9, 132.7, 131.2, 129.3, 129.0, 128.9, 127.1, 61.9, 52.5, 42.1, 14.1. HRMS-MALDI: calcd for $C_{25}H_{24}NO_6P$ (M+Na) 472.1294, measured 472.1296.

[4-[6-Amino-9-(3,4-dihydroxy-5-hydroxymehtyl-tetrahydro-furan-2-yl)-9H-purin-8-ylcarbamoyl]-3-(diphenyl-phosphinoyl)-benzoylamino-acetic acid methyl ester. (**1.25a**) To 8-azidoadenosine (0.0123 g, 0.0400 mmol) in 1 mL of a 1:1THF:H_2O mixture was added 2-diphenylphosphanyl-N-ethoxycarbonylmethyl-terephthalamic acid methyl ester (0.0174 g, 0.0400 mmol) in 1 mL of a 1:1 THF:H_2O mixture and the reaction stirred at 30 °C for 2 h. The reaction mixture was then extrcted with EtOAc, washed with brine and dried over Na_2SO_4. The solvent was removed and the resulting material was column purified (3:2 Hex.:EtOAc) to yield 0.034 g (92% yield) of the desired product. ^{1}H NMR ($CDCl_3$) δ 8.28 (d, J = 14.4 Hz, 1H), 8.04 (d, J = 8.0 Hz, 1H), 7.87-7.77 (m, 5H), 7.73 (s, 1H), 7.52-7.39 (m, 7H), 6.43 (d, J = 7.6 Hz, 1H), 5.36 (s, 2H), 4.99-4.90 (m, 1H), 4.33 (d, J = 4.8 Hz, 1H), 4.21 (s, 1H), 4.14 (q, J = 7.2 Hz, 2H), 4.06 (d, J = 5.6 Hz, 1H), 3.86 (d, J = 11.6 Hz, 1H), 3.65 (d, J = 11.6 Hz, 1H), 3.32 (s, 3H), 1.22 (t, J = 7.2 Hz, 3H); ^{31}P NMR ($CDCl_3$) δ 19.8; ^{13}C NMR ($CDCl_3$) δ 171.4, 170.2, 167.8, 166.3, 154.8, 151.5, 148.7, 147.8, 139.2, 136.4, 134.7, 131.5, 130.8, 129.4, 128.9, 128.4, 128.3, 118.6, 88.7, 88.3, 73.4, 72.9, 68.2, 63.6, 61.7, 60.6, 52.8, 42.0, 25.8, 21.2, 14.4. HRMS-MALDI: calcd for $C_{35}H_{36}N_7O_9P$ (M+H) 730.2391, measured 730.1780.

(Z)-Mehtyl-N-6-amino-9-((2R,5S)-3,4-dihydroxy-5-(hydroxymethyl)-tetrahydro-furan-2-yl)-9H-purin-8-yl-2-(diphenylphosphoryl)-4-((2-(2-(2-(4-pyren-1-yl) butanamido)ethoxy)ethoxy)ethyl)carbamoyl)benzimidate. (**1.25b**) To 8-azidoadenosine (0.0123 g, 0.0400 mmol) in 1 mL of 1:1 THF:H_2O was added pyrene phosphine 2-diphenylphosphanyl-N-(2-{2-[2-(4-pyren-1-yl-butyrylamino)-ethoxy]-ethoxy}-ethyl)-terephthalamic acid methyl ester (0.0306 g, 0.0400 mmol) in 1 mL of 1:1 THF:H_2O. The reaction was incubated at 30 °C for 2 h. The reaction mixture was then extrcted with

EtOAc, washed with brine and dried over Na_2SO_4. The solvent was removed and the resulting material was column purified (3:2 Hex.:EtOAc) to yield 0.034 g (97% yield) of the desired product. ^{1}H NMR ($CDCl_3$) δ 8.37 (d, J = 14.4 Hz, 1H), 8.24 (d, J = 9.6 Hz, 1H), 8.14-7.94 (m, 9H), 7.87-7.80 (m, 5H), 7.53-7.42 (m, 5H), 6.56 (d, J = 7.2 Hz, 1H), 5.01 (dd, J = 6.8, 5.2 Hz, 1H), 4.48 (d, J = 5.2 Hz, 1H), 4.30 (s, 1H), 3.96 (d, J = 12.8 Hz, 1H), 3.73-3.25 (m, 27H) 2.27-2.01 (m, 4H); ^{31}P NMR ($CDCl_3$) δ 22.6; ^{13}C NMR ($CDCl_3$) δ 173.0, 167.8, 154.8, 151.6, 148.7, 135.7, 135.6, 132.7, 130.8, 131.8, 130.7, 129.0, 128.5, 126.7, 125.7, 125.1, 124.6, 124.2, 120.6, 70.4, 70.3, 70.2, 69.8, 68.2, 52.4, 51.0, 40.1, 39.4, 36.2, 33.1, 27.8, 25.9. HRMS-MALDI: calcd for $C_{35}H_{57}N_8O_{10}P$ (M+Na) 1067.3830, measured 1067.3420.

2-Diphenylphosphanyl-benzoic acid allyl ester. (**1.26a**,88 %) ^{1}H NMR ($CDCl_3$) δ 8.07 (m, 1H), 7.30 (m, 12H), 6.93 (m, 1H), 5.84 (ddt, J= 17.2, 10.4, 5.6 Hz, 1H), 5.28 (dd, J= 17.2, 1.2 Hz, 1H), 5.17 (dd, J= 10.4, 1.2 Hz, 1H), 4.64 (d, J= 5.6 Hz, 1H); ^{31}P NMR ($CDCl_3$) δ -3.35; ^{13}C NMR ($CDCl_3$) δ 166.5, 140.8, 140.5, 138.1, 138.0, 134.5, 134.4, 134.3, 134.2, 133.9, 132.1, 130.8, 130.8, 128.7, 128.6, 128.5, 128.3, 118.5, 65.9. HRMS-MALDI: calcd for $C_{22}H_{19}O_2P$ ($M + H^+$) 347.11, measured 347.123.

2-Diphenylphosphanyl-benzoic acid benzyl ester. (**1.26b**, 90%) ^{1}H NMR ($CDCl_3$) δ 8.07 (m, 1H), 7.29 (m, 17H), 6.94 (m, 1H), 5.19 (s, 2H); ^{31}P NMR ($CDCl_3$) δ -3.44; ^{13}C NMR ($CDCl_3$) δ 166.7, 140.9, 140.7, 138.4, 138.1, 138.0, 135.9, 135.3, 134.5, 134.4, 134.2, 134.2, 134.0, 132.2, 131.0, 130.9, 128.8, 128.7, 128.6, 128.6, 128.5, 128.4, 128.3, 67.0. HRMS-MALDI: calcd for $C_{26}H_{21}O_2P$ ($M + H^+$) 397.13, measured 397.140.

2-Diphenylphosphanyl-benzoic acid isopropyl ester. (**1.26c**, 92 %) ^{1}H NMR ($CDCl_3$) δ 8.03 (m, 1H), 7.30 (m, 12H), 6.90 (m, 1H), 5.11 (sept, J= 6.4 Hz, 1H), 1.17 (s, 6H); ^{31}P NMR ($CDCl_3$) δ -3.69; ^{13}C NMR ($CDCl_3$) δ 166.6, 140.2, 139.9, 138.4, 138.3, 135.4, 135.3, 134.4, 134.2, 133.9, 133.8, 131.8, 130.7, 130.6, 128.9, 128.7, 128.6, 128.5, 128.3, 69.1, 21,9. HRMS-MALDI: calcd for $C_{22}H_{21}O_2P$ ($M + H^+$) 349.13, measured 349.139.

2-Diphenylphosphanyl-benzoic acid 2,2-dimethyl-propyl ester. (**1.26d**, 83.0%) ^{1}H NMR ($CDCl_3$) δ 8.08 (m, 1H), 7.30 (m, 12H), 6.95 (m, 1H), 3.89 (s, 2H), 0.94 (s, 9H); ^{31}P NMR ($CDCl_3$) δ -3.73; ^{13}C NMR ($CDCl_3$) δ 166.8, 141.0, 140.8, 138.2, 138.1, 134.7, 134.5, 134.1, 133.9,133.8, 132.0, 130.5, 130.5, 128.8, 128.7, 128.6, 128.6, 128.5, 128.3, 74.6, 31.6, 26.7. HRMS-MALDI: calcd for $C_{24}H_{25}O_2P$ ($M + H^+$) 377.16, measured 377.170.

2-Diphenylphosphanyl-benzoic acid 8-(tert-butyl-diphenyl-silanyloxy)-octyl ester. (**1.26e**, 77%) ^{1}H NMR ($CDCl_3$) δ 8.04 (m, 1H), 7.67 (m, 4H), 7.32 (m, 18H), 6.92 (m, 1H), 4.14 (t, J= 6.8 Hz, 2H), 3.65 (t, J= 6.8 Hz, 2H), 1.55 (m, 4H), 1.30 (m, 8H), 1.05 (s, 9H); ^{31}P NMR ($CDCl_3$) δ -3.63; ^{13}C NMR ($CDCl_3$) δ 167.2, 140.5, 140.2, 138.3, 138.2, 135.7, 135.4, 135.1, 134.9, 134.5, 134.4, 134.3, 134.2, 134.0, 133.9, 133.8, 132.1, 132.0, 130.7, 129.7, 128.8, 128.7, 128.7, 128.6, 128.6, 128.6, 128.4, 127.8, 65.6, 64.1, 32.7, 29.4, 28.6, 27.1, 26.1, 25.9, 19.4. HRMS-MALDI: calcd for $C_{43}H_{49}O_3PSi$ ($M + H^+$) 673.32, measured 673.336.

2-Diphenylphosphanyl-benzoic acid methyl ester. (**1.26g**, 83%) ^{1}H NMR ($CDCl_3$) δ 8.10 (m, 1H), 7.35 (m, 12H), 6.99 (m, 1H), 3.77 (s, 3H); ^{31}P NMR ($CDCl_3$) δ -3.23; ^{13}C NMR ($CDCl_3$) δ 167.3, 140.7, 140.4, 138.0, 137.9, 134.4, 134.2, 134.1, 133.9, 132.0, 130.7,

130.7, 128.7, 128.6, 128.5, 128.3, 52.1. HRMS-MALDI: calcd for $C_{20}H_{17}O_2P$ ($M + H^+$) 321.10, measured .

2-Diphenylphosphanyl-benzoic acid tert-butyl ester. (**1.26f**) To 2-Diphenylphosphanyl-benzoic acid methyl ester (0.13 g, 0.40 mmol) in 40.3 mL anhydrous ether was added 1M tBuOK (580 µL, 0.58 mmol). After stirring for 1 h, the resulting precipitate was filtered through Al_2O_3 and washed with ether. The organic solvent was evaporated and the resulting residue was chromatographed [9:1 Pet Ether/ (4:2:1 EtOAc/CH_2Cl_2/MeOH] to yield product (0.083 g, 57%). ^1H NMR ($CDCl_3$) δ 7.98 (m, 1H), 7.35 (m, 12H), 6.88 (m, 1H), 1.39 (s, 9H); ^{31}P NMR ($CDCl_3$) δ -3.33; ^{13}C NMR ($CDCl_3$) δ 166.7, 139.6, 139.1, 138.5, 138.3, 136.8, 136.6, 134.3, 134.1, 134.0, 131.4, 130.5, 130.4, 128.7, 128.6, 128.5, 128.2, 82.2, 28.0.

3-Diphenylphosphanyl-naphthalene-2-carboxylic acid allyl ester. (**1.27a**, 85% yield) ^1H NMR ($CDCl_3$) δ 7.93-7.91 (m, 1H), 7.77-7.772 (m, 2H), 7.51-7.47 (m, 2H), 7.32-7.26 (m, 10H), 7.15(dd, J= 8.4, 3.2, 1H), 5.84 (ddt, J = 17.0, 10.4, 6.0 Hz, 1H), 5.26 (dd, J = 2.8., 1.6 Hz, 1H), 5.22 (dd, J = 2.8, 1.6 Hz, 1H), 4.82 (dt, J = 6.0, 1.2 Hz, 2H); ^{31}P NMR ($CDCl_3$) δ -8.14; ^{13}C NMR ($CDCl_3$) δ 169.0, 139.2, 138.9, 137.1, 136.9,134.1, 133.9, 133.7, 133.6, 133.4, 133.2, 131.9,130.1, 130.0, 129.8, 129.0, 128.9, 128.8, 128.7, 128.4, 127.7, 127.5, 125.5, 119.2, 70.2. HRMS-MALDI: calcd for $C_{26}H_{21}O_2P$ ($M + H^+$): 397.135, measured: 397.120.

3-Diphenylphosphanyl-naphthalene-2-carboxylic acid benzyl ester. (**1.27b**, 92% yield) ^1H NMR ($CDCl_3$) δ 7.90-7.85 (m, 1H), 7.80-7.72 (m, 2H), 7.52-7.47 (m, 2H), 7.32-7.26 (m,

10H), 7.21-7.25(m, 5H), 7.20 (dd, J = 8.4, 3.2, 1H), 5.40 (s, 2H); ^{31}P NMR ($CDCl_3$) δ -8.31; ^{13}C NMR ($CDCl_3$) δ 169.3, 139.5, 139.2, 137.1, 137.0, 135.5,134.1, 133.9, 133.7, 133.6, 133.2, 133.0, 130.1, 130.0, 129.9, 129.0, 128.9, 128.4, 127.7, 127.6, 125.5, 70.3. HRMS-MALDI: calcd for $C_{26}H_{21}O_2P$ (M + H^+): 447.151, measured: 447.148.

3-Diphenylphosphanyl-naphthalene-2-carboxylic acid isopropyl ester. (**1.27c**, 81% yield) ^1H NMR ($CDCl_3$) δ 8.00 (dd, J = 8.8, 1.2 Hz, 1H), 7.85-7.80 (m, 2H), 7.62-7.54 (m, 2H), 7.35-7.38 (m, 10H), 7.20 (dd, J = 8.4, 3.2, 1H), 5.45 (sept, J = 6.0 Hz, 1H), 1.33 (d, J = 6.4Hz, 6H); ^{31}P NMR ($CDCl_3$) δ -9.39; ^{13}C NMR ($CDCl_3$) δ 168.9, 137.2, 137.1, 134.1, 133.9, 133.7, 133.6, 132.4, 132.2, 130.0, 129.9, 129.8, 128.8, 128.7, 128.4, 127.6, 127.4, 125.5, 70.01, 21.9. HRMS-MALDI: calcd for $C_{26}H_{23}O_2P$ (M + H^+): 399.151, measured: 399.145

3-Diphenylphosphanyl-naphthalene-2-carboxylic acid 2,2-dimethyl-propyl ester. (**1.27d**, 80% yield) ^1H NMR ($CDCl_3$) δ 7.98-7.90 (m, 1H), 7.83-776(m, 2H), 7.57-7.49 (m, 2H), 7.37-7.29 (m, 10H), 7.23-7.15 (m, 1H), 4.18 (s, 2H) 0.90 (s, 9H); ^{31}P NMR ($CDCl_3$) δ -8.71; ^{13}C NMR ($CDCl_3$) δ 169.8, 137.9, 137.1, 137.0, 133.9, 133.8, 133.7, 133.6, 132.7, 132.5, 130.1, 129.9, 129.8, 129.0, 128.8, 128.7, 128.3, 127.9, 127.6, 127.5, 125.6, 75.1, 31.4, 26.7. HRMS-MALDI: calcd for $C_{28}H_{27}O_2P$ (M + H^+): 427.182, measured: 427.165

3-Diphenylphosphanyl-naphthalene-2-carboxylic acid 8-(tert-butryl-diphenyl-silanyloxy)-octyl ester. (**1.27e**, 75% yield) ^1H NMR ($CDCl_3$) δ 7.97-7.94 (m, 1H), 7.80-7.34 (m, 2H), 7.68-765 (m, 4H), 7.55-7.48 (m, 2H), 7.39-7.28 (m, 16H), 7.18-7.15 (m, 1H), 4.36 (t, J = 6.4 Hz, 2H), 3.64 (t, J = 6.4 Hz, 2H), 1.57-1.49(m, 4H), 1.32-1.18 (m, 8H),1.04 (s, 9H); ^{31}P

NMR ($CDCl_3$) δ -8.35; ^{13}C NMR ($CDCl_3$) δ 169.5, 142.2, 140.0, 139.6, 137.3, 137.2,135.9, 134.4, 133.8, 133.7, 133.6, 133.0, 132.9, 130.1, 130.0, 129.9, 129.8, 129.0, 128.9, 128.8, 128.7, 128.4, 127.9, 127.7, 127.5, 125.6, 66.0, 64.2, 32.8, 29.4, 28.7, 27.2, 26.2, 19.5, 14.5. HRMS-MALDI: calcd for $C_{47}H_{51}O_4PSi$ ($M + H^+$): 739.337, measured: 739.330.

1-(4-Azide-phenyl)-2-morpholin-4-yl-ethanone. (**1.28**) To tetrahydro-1,4-oxazine (0.038 g, 0.43 mmol) was added 2 mL of THF along with TEA (62.4 μL, 0.45 mmol). The solution was chilled to 0 °C for 15 minutes, followed by the addition of 4-azidophenacyl bromide (0.052 g, 0.22 mmol). The solution was stirred and protected from light at 0 °C for 2 h. The TEA-HCl salts were filtered from the solution and the THF removed *in vacuo*. PTLC (7:3:2:0.5 Hex:EtOAc:CH_2Cl_2:MeOH) afforded product (0.05 g, 85% yield). ^1H NMR ($CDCl_3$) δ 8.05-8.04 (m, 1H), 8.03-8.02 (m, 1H), 7.10-7.09 (m, 1H), 7.08-7.07 (m, 1H), 3.78-3.75 (m, 6H), 2.61-2.59 (m, 4H); ^{13}C NMR ($CDCl_3$) δ 194.9, 145.4, 132.8, 130.4, 119.2, 67.0, 64.9, 54.0. ESI: calcd for $C_{12}H_{14}N_4O_2$ ($M + H^+$): 247.12, measured: 247.0.

1-Azido-4-butyl-benzene. (**1.29**) To 4-butyl aniline (4.5 g, 30.60 mmol) in 150 mL 1.2N HCl and 300 mL glacial acetic acid at 0 °C was added $NaNO_2$ (4.22 g, 61.20 mmol) in portions. The solution was stirred at 0 °C for 30 minutes followed by addition of cold Et_2O (250mL). NaN_3 (9.7 g, 149.0 mmol) was added in portions over 15 minutes and allowed to stirr an additional 30 minutes. The aqueous layer was removed and the organic was washed ($NaHCO_3$, brine,), dried over $NaSO_4$ and solvent removed *in vacuo*. The resulting material was chromatographed (Pet Ether) to afford the desired product (4.32 g, 81% yield). ^1H NMR ($CDCl_3$) δ 7.19 (d, J = 8.4Hz, 2H), 7.97 (d, J = 8.4 Hz, 2H), 2.62 (t, J = 7.6 Hz, 2H), 1.67-1.57 (m, 2H), 1.412-1.35 (m, 2H), 0.965 (t, J = 7.6 Hz, 3H); ^{13}C NMR

($CDCl_3$) δ 140.0, 137.5, 130.0, 119.1, 35.2, 33.9, 22.5, 14.2. ESI: calcd for $C_{10}H_{13}N_3$ (M + H^+): 176.11, measured: 176.10.

2-(Diphenyl-phosphinoyl)-N-[4-(2-morpholin-4-yl-acetyl)-phenyl]-benzimidic acid allyl ester. (**1.30a**, 64%)) ^1H NMR ($CDCl_3$) δ 7.88-7.85 (m, 1H), 7.70-7.61 (m, 7H), 7.57-7.52 (m, 4H), 7.47 (td, J= 7.6, 2.8 Hz, 4H), 6.63 (d, J = 8.8 Hz, 2H), 5.51 (ddt, J = 17.2, 10.4, 6.4 Hz, 1H), 5.04 (dd, J= 17.6, 1.2 Hz, 1H), 5.02 (dd, J = 10.4, 1.2 Hz, 1H), 4.35 (d, J= 6.0 Hz, 2H), 3.77-3.75 (m, 4H), 3.69 (s, 2H), 2.57-2.54 (m, 4H); ^{31}P NMR ($CDCl_3$) δ 9.13; ^{13}C NMR ($CDCl_3$) δ 194.2, 167.4, 137.1, 137.1, 134.7, 134.6, 132.5, 132.4, 132.3, 132.2, 132.1, 132.1, 131.6, 131.3, 131.1, 131.0, 130.7, 130.7, 138.4, 130.3, 129.8, 129.0, 128.9, 125.4, 122.6, 122.4, 118.7, 67.1, 66.5, 64.2, 54.2. HRMS-MALDI: calcd for $C_{34}H_{33}N_2O_4P$ (M + H^+) 565.22, measured 565.216.

2-(Diphenyl-phosphinoyl)-N-[4-(2-morpholin-4-yl-acetyl)-phenyl]-benzimidic acid benzyl ester. (**1.30b**, 53%) ^1H NMR ($CDCl_3$) δ 7.86 (dd, J= 7.2, 3.6 Hz, 1H), 7.69-7.63 (m, 7H), 7.54-7.51 (m, 4H), 7.42 (td, J = 7.6, 2.8 Hz, 4H), 7.26-7.17 (m, 3H), 6.98 (d, J = 8.8 Hz, 2H), 6.66 (d, J = 8.8 Hz, 2H), 4.91 (s, 2H), 3.77-3.75 (m, 4H), 3.68 (s, 2H), 2.57-2.54 (m, 4H); ^{31}P NMR ($CDCl_3$) δ 9.05; ^{13}C NMR ($CDCl_3$) δ 194.2, 167.6, 137.1, 137.1, 135.3, 134.7, 134.6, 132.5, 132.4, 132.3, 132.2, 132.1, 132.1, 131.2, 131,1, 130.9, 130.8, 130.7, 130.2, 129.8, 129.8, 128.9, 128.8, 128.5, 128.4, 128.2, 125.5, 122.6, 122.4, 67.4, 67.0, 64.2, 54.2. HRMS-MALDI: calcd for $C_{38}H_{35}N_2O_4P$ (M + H^+) 615.23, measured 615.231.

2-(Diphenyl-phosphinoyl)-N-[4-(2-morpholin-4-yl-acetyl)-phenyl]-benzimidic acid isopropyl ester. (**1.30c**, 66%) ^{1}H NMR ($CDCl_3$) δ 7.90-7.85 (m, 1H), 7.71-7.61 (m, 8H), 7.56-7.52 (m, 3H), 7.46 (td, J = 7.6, 3.2 Hz, 4H), 6.62 (d, J= 8.8 Hz, 2H), 4.78 (sept, J= 6.4 Hz, 1H), 3.77-3.75 (m, 4H), 3.68 (s, 2H), 2.57-2.54 (m, 4H), 0.97 (d, J = 6.4 Hz, 6H); ^{31}P NMR ($CDCl_3$) δ 9.73; ^{13}C NMR ($CDCl_3$) δ 194.2, 166.7, 137.3, 137.3, 135.2, 135.1, 132.6, 132.5, 132.3, 132.0, 132.0, 131.2, 131.1, 131.0, 130.9, 129.8, 128.9, 128.8, 125.4, 122.6, 122.4, 67.1, 66.1, 64.2, 54.2, 21.5. HRMS-MALDI: calcd for $C_{34}H_{35}N_2O_4P$ ($M + H^+$) 567.23, measured 567.228.

2-(Diphenyl-phosphinoyl)-N-[4-(2-morpholin-4-yl-acetyl)-phenyl]-benzimidic acid (2,2-dimethyl-propyl) ester. (**1.30d**, 67%) ^{1}H NMR ($CDCl_3$) δ 7.90-7.85 (m, 1H), 7.71-7.61 (m, 8H), 7.59-7.52 (m, 3H), 7.47-7.43 (m, 4H), 6.63 (d, J = 8.8 Hz, 2H), 3.77-3.75 (m, 4H), 3.68 (s, 2H), 3.58 (s, 2H), 2.57-2.254 (m, 4H), 0.77 (s, 9H); ^{31}P NMR ($CDCl_3$) δ 9.38; ^{13}C NMR ($CDCl_3$) δ 194.1, 167.3, 137.1, 137.0, 135.2, 135.1, 132.5, 132.4, 132.3, 132.0, 132.0, 131.2, 131.1, 130.5, 130.4, 129.8, 129.7, 128.9, 128.8, 125.4, 122.6, 122.4, 74.8, 67.1, 64.2, 54.2, 31.4, 26.5. HRMS-MALDI: calcd for $C_{36}H_{39}N_2O_4P$ ($M + H^+$) 595.26, measured 595.244.

2-(Diphenyl-phosphinoyl)-N-[4-(2-morpholin-4-yl-acetyl)-phenyl]-benzimidic acid [8-(tert-Butyl-diphenyl-silanyloxy)-octyl] ester. (**1.30e**, 66%) ^{1}H NMR ($CDCl_3$) δ 7.87-7.84 (m, 1H), 7.70-7.64 (m, 11H), 7.55-7.51 (m, 4H), 7.40-7.34 (m, 10H), 6.63 (d, J = 8.8 Hz, 2H), 3.82 (t, J = 6.8 Hz, 2H), 3.77-3.75 (m, 4H), 3.68 (s, 2H), 3.64 (t, J = 6.8 Hz, 2H), 2.57-2.52 (m, 4H), 1.59-1.49 (m, 2H), 1.35-1.20 (m, 4H), 1.17-1.09 (m, 6H), 1.04 (s, 9H); ^{31}P NMR ($CDCl_3$) δ 9.18; ^{13}C NMR ($CDCl_3$) δ 194.1, 167.7, 137.4, 137.3, 135.7, 134.9, 134.8, 134.3,

132.5, 132.4, 132.3, 132.2, 132.1, 132.0, 131.0, 130.9, 130.7, 130.7, 130.4, 129.8, 129.7, 129.7, 129.1, 128.9, 128.8, 128.5, 128.4, 127.7, 125.4, 122.5, 122.4, 119.1, 67.0, 66.0, 64.1, 54.2, 32.7, 29.3, 29.3, 28.1, 27.0, 25.9, 25.8, 19.4. HRMS-MALDI: calcd for $C_{55}H_{63}N_2O_5PSi$ (M + H^+) 891.42, measured 891.331.

2-(Diphenyl-phosphinoyl)-N-[4-(2-morpholin-4-yl-acetyl)-phenyl]-benzimidic acid (tert-butyl ester. (**1.30f**, 89%) ^{1}H NMR ($CDCl_3$) δ 7.88-7.86 (m, 1H), 7.70-7.60 (m, 8H), 7.54-7.50 (m, 3H), 7.46-7.41 (m, 4H), 6.62 (d, J = 8.4 Hz, 2H), 3.76 (t, J = 4.4 Hz, 4H), 3.69 (s, 2H), 2.56 (bt, 4H), 1.17 (s, 9H); ^{31}P NMR ($CDCl_3$) δ 10.2; ^{13}C NMR ($CDCl_3$) δ 194.1, 166.1, 138.4, 135.2, 135.1, 132.5, 132.4, 132.3, 131.9, 131.0, 130.9, 130.7, 129.6, 128.7, 128.6, 125.2, 122.7, 122.5, 82.6, 67.0, 64.1, 54.2, 27.7. HRMS-MALDI: calcd for $C_{35}H_{37}N_2O_4PSi$ (M + H^+) 581.249, measured 581.250.

3-(Diphenyl-phosphinoyl)-N-[4-(2-morpholin-4-yl-acetyl)-phenyl]-naphthalene-2-carboximidic acid allyl ester. (**1.32a**, 64%) ^{1}H NMR ($CDCl_3$) δ 9.17 (s, 1H), 8.31 (d, J = 8.0 Hz, 1H), 7.87-784 (m, 2H), 7.77-7.69 (m, 4H), 7.64-7.35 (m, 6H), 7.31 (d, J = 8.4 Hz, 2H), 7.24 (dd, J = 12.0, 8.0 Hz, 2H), 7.05 (d, J = 8.4 Hz, 2H), 5.78 (ddt, J = 17.0, 10.4, 6.0 Hz, 1H), 5.21 (dd, J = 17.2, 1.2 Hz, 1H), 5.12 (dd, J = 10.4, 1.2 Hz, 1H), 4.73 (d, J = 6.4 Hz, 2H), 3.77-3.75 (m, 4H), 3.69 (s, 2H), 2.57-2.52 (m, 4H); ^{31}P NMR ($CDCl_3$) δ 33.32; ^{13}C NMR ($CDCl_3$) δ 195.0, 166.9, 151.2, 137.9, 137.5, 136.7, 135.0,134.2, 133.0, 131.8, 131.5, 130.4, 129.6, 128.7, 128.0, 127.1, 125.9, 121.8, 115.1, 67.1, 66.5, 64.2, 54.2. HRMS-MALDI: calcd for $C_{38}H_{35}N_2O_4P$ (M + H^+): 615.241, measured: 615.225

3-(Diphenyl-phophinoyl-N-[4-2-morpholin-4-yl-acetyl)-phenyl]-naphthalene-2-carboximidic acid benzyl ester. (**1.32b**, 62%) ^{1}H NMR ($CDCl_3$) δ 9.20 (s, 1H), 8.30 (d, J = 8.0 Hz, 1H), 7.87-783 (m, 2H), 7.75-7.70 (m, 4H), 7.63-7.22 (m, 15H), 7.04 (d, J = 8.8 Hz, 2H), 4.65 (s, 2H), 3.77-3.75 (m, 4H), 3.68 (s, 2H), 2.57-2.52 (m, 4H); ^{31}P NMR ($CDCl_3$) δ 33.26; ^{13}C NMR ($CDCl_3$) δ 195.0, 166.2, 150.4, 140.6, 137.9, 136.6, 135.1, 134.2, 132.9, 131.5, 130.4, 129.6, 128.7, 128.6, 128.0, 127.3, 127.1, 125.9, 121.8, 67.9, 67.0, 64.2, 54.2. HRMS-MALDI: calcd for $C_{42}H_{37}N_2O_4P$ ($M + H^+$): 665.256, measured: 665.241

3-(Diphenyl-phosphinoyl)-N-[4-(2-morpholin-4-yl-acetyl)-phenyl]-naphthalene-2-carboximidic acid isopropyl ester. (**1.32c**, 40%) ^{1}H NMR ($CDCl_3$) δ 9.20 (s, 1H), 8.29 (d, J = 8.0 Hz, 1H), 7.86-784 (m, 2H), 7.75-7.71 (m, 4H), 7.64-7.33 (m, 6H), 7.30 (d, J = 8.4 Hz, 2H), 7.25 (dd, J = 12.0, 8.0 Hz, 2H), 7.05 (d, J = 8.4 Hz, 2H), 5.05 (sept, J = 6.4 Hz, 1H), 3.77-3.75 (m, 4H), 3.68 (s, 2H), 2.57-2.54 (m, 4H), 1.16 (d, J = 6.4 Hz, 6H); ^{31}P NMR ($CDCl_3$) δ 33.26; ^{13}C NMR ($CDCl_3$) δ 195.0, 166.7, 150.2, 137.9, 136.7, 136.0, 135.2, 133.0, 131.8, 129.7, 128.5, 127.9, 127.1, 126.0, 122.0, 66.9, 66.1, 64.2, 54.2, 21.5. HRMS-MALDI: calcd for $C_{38}H_{37}N_2O_4P$ ($M + H^+$): 617.256, measured: 617.252.

3-(Diphenyl-phosphinoyl)-N-[4-(2-morpholin-4-yl-acetyl)-phenyl]-naphthalene-2-carboximidic acid 2,2-dimethyl-propyl ester. (**1.32d**, 38%) ^{1}H NMR ($CDCl_3$) δ 9.21 (s, 1H), 8.30 (d, J = 8.0 Hz, 1H), 7.86-784 (m, 2H), 7.76-7.70 (m, 4H), 7.64-7.32 (m, 6H), 7.31 (d, J = 8.4 Hz, 2H), 7.24 (dd, J = 12.0, 8.0 Hz, 2H), 7.05 (d, J = 8.4 Hz, 2H), 3.77-3.75 (m, 4H), 3.60 (s, 2H), 3.58 (s, 2H), 2.57-2.52 (m, 4H), 0.79 (s, 9H); ^{31}P NMR ($CDCl_3$) δ 33.18; ^{13}C NMR ($CDCl_3$) δ 195.0,166.5, 150.3, 137.9, 136.7, 136.0, 135.0, 132.9, 131.5, 129.6,

128.6, 128.0, 125.6, 121.8, 75.0, 67.1, 64.2, 54.2, 31.4, 26.5. HRMS-MALDI: calcd for $C_{40}H_{41}N_2O_4P$ ($M + H^+$): 645.288, measured: 645.281.

3-(Diphenyl-phosphinoyl)-N-[4-(2-morpholin-4-yl-acetyl)-phenyl]-naphthalene-2-carboximidic acid 8-(tert-butyl-diphenyl-silanyoxy)-octyl ester. (**1.32e**, 55%) ^1H NMR ($CDCl_3$) δ 9.20 (s, 1H), 8.30 (d, J = 8Hz, 1H), 7.86-784 (m, 2H), 7.76-7.70 (m, 4H), 7.64-7.32 (m, 16H), 7.31 (d, J = 8.4 Hz, 2H), 7.24 (dd, J = 12.0, 8.0 Hz, 2H), 7.05 (d, J = 8.4 Hz, 2H), 3.80 (t, J = 6.8 Hz, 2H), 3.77-3.75 (m, 4H), 3.68 (s, 2H), 3.62 (t, J = 6.8 Hz, 2H), 2.57-2.54 (m, 4H), 1.59-1.49 (m, 2H), 1.35-1.20 (m, 4H), 1.17-1.09 (m,6H), 1.02 (s, 9H); ^{31}P NMR ($CDCl_3$) δ 33.23; ^{13}C NMR ($CDCl_3$) δ 166.5, 150.3, 137.9, 136.7, 136.0, 135.0, 132.9, 131.5, 129.6, 128.6, 128.0, 125.6, 121.8, 75.0, 35.5, 31.5, 34.6, 26.5, 22.7, 14.0. HRMS-MALDI: calcd for $C_{59}H_{65}N_2O_5PSi$ ($M + H^+$): 941.447, measured: 941.432

N-(4-Butyl-phenyl)-2-(diphenyl-phosphinoyl)-naphthalene-1-carboximidic acid allyl ester. (**1.33a**, 65%) ^1H NMR ($CDCl_3$) δ 9.17 (s, 1H), 8.31 (d, J = 8.0 Hz, 1H), 7.87-784 (m, 2H), 7.77-7.69 (m, 4H), 7.64-7.35 (m, 6H), 7.31 (d, J= 8.4 Hz, 2H), 7.24 (dd, J = 12.0, 8.0 Hz, 2H), 7.05 (d, J = 8.4 Hz, 2H), 5.78 (ddt, J= 17.0, 10.4, 6.0 Hz, 1H), 5.21 (dd, J = 17.2, 1.2 Hz, 1H), 5.12 (dd, J= 10.4, 1.2 Hz, 1H), 4.73 (d, J= 6.4 Hz, 2H), 2.55 (t, J = 7.6 Hz, 2H), 1.62-1.58 (m, 2H), 1.38-1.31 (m, 2H), 0.94 (t, J = 7.4 3H); ^{31}P NMR ($CDCl_3$) δ 33.32; ^{13}C NMR ($CDCl_3$) δ 166.9, 151.2, 137.9, 137.5, 136.7, 135.0,134.2, 133.0, 131.8, 131.5, 130.4, 129.6, 128.7, 128.0, 127.1, 125.9, 121.8, 115.1, 67.2, 35.5, 34.6, 22.7, 14.0. HRMS-MALDI: calcd for $C_{36}H_{34}NO_2P$ ($M + H^+$): 544.240, measured: 544.235

N-(4-Butyl-phenyl)-2-(diphenyl-phosphinoyl)-naphthalene-1-carboximidic acid benzyl ester. (**1.33b**, 60%) ^{1}H NMR ($CDCl_3$) δ 9.20 (s, 1H), 8.30 (d, J = 8.0 Hz, 1H), 7.87-783 (m, 2H), 7.75-7.70 (m, 4H), 7.63-7.22 (m, 15H), 7.04 (d, J = 8.8 Hz, 2H), 4.65 (s, 2H), 2.57 (t, J = 7.6 Hz, 2H), 1.60-1.55 (m, 2H), 1.40-1.32 (m, 2H), 0.94 (t, J = 7.4 3H); ^{31}P NMR ($CDCl_3$) δ 33.22; ^{13}C NMR ($CDCl_3$) δ 166.2, 150.4, 140.6, 137.9, 136.6, 135.1, 134.2, 132.9, 131.5, 130.4, 129.6, 128.7, 128.6, 128.0, 127.3, 127.1, 125.9, 121.8, 67.9, 34.6, 33.5, 21.8, 13.8. HRMS-MALDI: calcd for $C_{40}H_{36}NO_2P$ (M + H^+): 594.256, measured: 594.251

N-(4-Butyl-phenyl)-3-(diphenyl-phosphinoyl)-naphthalene-2-carboximidic acid isopropyl ester. (**1.33c**, 55%) ^{1}H NMR ($CDCl_3$) δ 9.20 (s, 1H), 8.29 (d, J = 8.0 Hz, 1H), 7.86-784 (m, 2H), 7.75-7.71 (m, 4H), 7.64-7.33 (m, 6H), 7.30 (d, J= 8.4 Hz, 2H), 7.25 (dd, J = 12.0, 8.0 Hz, 2H), 7.05 (d, J= 8.4 Hz, 2H), 5.05 (sept, J= 6.4 Hz, 1H), 2.55 (t, J = 7.6 Hz, 2H), 1.62-1.58 (m, 2H), 1.38-1.31 (m, 2H), 1.16 (d, J= 6.4 Hz, 6H), 0.94 (t, J = 7.4 3H); ^{31}P NMR ($CDCl_3$) δ 33.26; ^{13}C NMR ($CDCl_3$) δ 166.7, 150.2, 137.9, 136.7, 136.0, 135.2, 133.0, 131.8, 129.7, 128.5, 127.9, 127.1, 126.0, 122.0, 66.9, 35.5, 34.6, 22.7, 21.5, 14.0. HRMS-MALDI: calcd for $C_{36}H_{36}NO_2P$ (M + H^+): 546.256, measured: 546.249.

N-(4-Butyl-phenyl)-3-(diphenyl-phosphinoyl)-naphthalene-2-carboximidic acid 2,2-dimethyl-propyl ester. (**1.33d**, 40%) ^{1}H NMR ($CDCl_3$) δ 9.21 (s, 1H), 8.30 (d, J = 8.0 Hz, 1H), 7.86-784 (m, 2H), 7.76-7.70 (m, 4H), 7.64-7.32 (m, 6H), 7.31 (d, J = 8.4 Hz, 2H), 7.24 (dd, J = 12.0, 8.0 Hz, 2H), 7.05 (d, J = 8.4 Hz, 2H), 3.60 (s, 2H), 2.55 (t, J = 7.6 Hz, 2H), 1.62-1.58 (m, 2H), 1.38-1.31 (m, 2H), 0.94 (t, J = 7.4 3H), 0.79 (s, 9H); ^{31}P NMR ($CDCl_3$) δ 33.18; ^{13}C NMR ($CDCl_3$) δ 166.5, 150.3, 137.9, 136.7, 136.0, 135.0, 132.9,

131.5, 129.6, 128.6, 128.0, 125.6, 121.8, 75.0, 35.5, 31.5, 34.6, 26.5, 22.7, 14.0. HRMS-MALDI: calcd for $C_{38}H_{40}NO_2P$ ($M + H^+$): 574.287, measured: 574.265.

N-(4-Butyl-phenyl)-3-(diphenyl-phosphinoyl)-naphthalene-2-carboximidic acid 8-(ter-butyl-diphenyl-silanyloxy)-octyl ester. (**1.33e**, 58%) ^1H NMR ($CDCl_3$) δ 9.20 (s, 1H), 8.30 (d, J = 8.0 Hz, 1H), 7.86-784 (m, 2H), 7.76-7.70 (m, 4H), 7.64-7.32 (m, 16H), 7.31 (d, J = 8.4 Hz, 2H), 7.24 (dd, J = 12.0, 8.0 Hz, 2H), 7.05 (d, J = 8.4 Hz, 2H), 3.80 (t, J = 6.8 Hz, 2H), 3.62 (t, J = 6.8 Hz, 2H), 2.55 (t, J = 7.6 Hz, 2H), 1.62-1.28 (m, 10H),1.17-1.09 (m, 6H), 1.02 (s, 9H), 0.94 (t, J = 7.4, 3H); ^{31}P NMR ($CDCl_3$) δ 33.23; ^{13}C NMR ($CDCl_3$) δ 166.5, 150.3, 137.9, 136.7, 136.0, 135.0, 132.9, 131.5, 129.6, 128.6, 128.0, 125.6, 121.8, 75.0, 35.5, 31.5, 34.6, 26.5, 22.7, 14.0. HRMS-MALDI: calcd for $C_{57}H_{64}NO_3PSi$ ($M + H^+$): 870.447, measured: 870.443.

N-(4-butylphenyl)-2-(diphenylphosphoryl)benzamide. (**1.34**, 37% for allyl and 67% from benzyl) ^1H NMR ($CDCl_3$) δ 10.54 (s, 1H), 8.09-8.06 (m, 1H), 7.70-7.63 (m, 5H), 7.53-7.49 (m, 2H), 7.44-7.39 (m, 5H), 7.32-7.30 (m, 2H), 7.15-7.09 (m, 1H), 7.01 (d, J = 8.4 Hz, 2H), 2.54 (t, J = 7.6 Hz, 2H), 1.59-1.52 (m, 2H),1.37-1.28 (m, 2H), 0.92 (t, J= 7.4, 3H); ^{31}P NMR ($CDCl_3$) δ 36.4; ^{13}C NMR ($CDCl_3$) δ 165.4, 141.7, 141.6, 139.0, 135.7, 133.4, 133.1, 132.9, 132.6, 132.5, 132.4, 131.8, 131.7, 131.3, 131.2, 130.3, 130.2, 129.3, 129.0, 128.8, 128.6, 120.3, 35.3, 33.9, 22.4, 14.2. HRMS-MALDI: calcd for $C_{29}H_{28}NO_2P$ ($M + H^+$): 454.190, measured: 454.181.

5.2 Chapter 3 Compounds

5.2.1 General Synthetic Procedures

All reactions were carried out under an atmosphere of argon using flame-dried glassware. A Büchi rotary evaporator equipped with a water condenser, and a water aspirator was used to concentrate *in vacuo*. Samples were further dried under reduced pressure on a high vacuum line.

Tetrahydrofuran (THF) was distilled from sodium metal and benzophenone. Dichloromethane (CH_2Cl_2), and toluene were distilled from calcium hydride. Diisopropylamine was dried over CaH_2 and subsequently distilled under argon and stored in a septum sealed serum bottle over solid KOH. All other solvents were purchased from Aldrich Chemical Company and used without further purification. All amino acids were purchased from Chem-Impex. All commercial reagents were purchased from Aldrich Chemical Co., or Acros Organics. Reactions were cooled to -78 °C *via* dry ice-acetone baths and to -15 °C *via* dry ice-methanol bath.

Flash column chromatography was performed using Merck grade 60 silica gel (230-400 mesh) and TLC analysis was carried out using Merck 60F-254 pre-coated silica sheets. Visualization of TLC plates was achieved using ultraviolet light, polyphosphomolybdic acid and cerium sulfate in EtOH with H_2SO_4, ninhydrin in EtOH with H_2SO_4 or iodine.

^1H NMR spectra were taken on a Varian Unity Inova 400, or a Varian Unity Inova 500 spectrometer in $CDCl_3$ at ambient temperature unless otherwise noted. ^1H chemical shifts in $CDCl_3$ were reported in ppm (δ units) downfield from tetramethylsilane. The solvent peak at 2.49 was used as an internal reference in DMSO-d_6, the solvent peak at

3.30 was used as an internal reference in MeOH-d_4. Solvent peaks were used as internal references for all ^{13}C NMR.

Mass spectroscopy was obtained at the University of Wisconsin-Madison School of Pharmacy. Electrospray ionization time of flight mass spectra (ESI-MS) was performed on a Micromass LCT Mass Spectrometer (Beverly, MA). Electron impact mass spectra (EI-MS) and fast atom bombardment spectra (FAB-MS) were performed on a Micromass AutoSpec Mass Spectrometer-magnetic sector (Beverly, MA).

5.2.2 Synthetic Procedures for Disulfide Formation

6-(tert-butyldimethylsilyloxy) hexanoic acid (**3.4**). 20.0 g (175.2 mmol) of ε-caprolactone were dissolved in a 1:1 MeOH:THF solvent mixture and stirred at room temperature for a few minutes. To this solution, 175 mL (525.6 mmol) of an aqueous 3N LiOH solution were added and reaction stirred at ambient temperature for 6 h. After such time, the reaction was quenched by lowering the pH to 2.0 via 1N HCl. The reaction was extracted with ether several times and organic layers dried over Na_2SO_4 followed by solvent removal. The resulting residue was dissolved in dry DMF, 29.8 g (438 mmol) of imidazole were added and the reaction stirred at 0 °C for a few minutes. To this mixture, 58.1 g (385.4 mmol) of TBSCl were added and reaction stirred for 16 h at room temperature before MeOH and ether were added. Ethereal layer was washed with a saturated solution of NH_4Cl, H_2O and brine. Organic layer was dried over Na_2SO_4, filtered and solvent removed. Resulting residue was column chromatographed (7:3 pet. ether:ether) to afford 33.5 g of a colorless oil (78% yield). ^1H NMR δ ($CDCl_3$) 3.56 (t, J = 6.8 Hz, 2H), 2.28 (t, J = 7.6 Hz, 2H), 1.63-1.29 (m, 6H), 0.85 (s, 9H), 0.08 (s, 6H). ^{13}C NMR δ ($CDCl_3$) 177.3,

64.3, 36.1, 33.0, 25.8, 25.1, 24.8, -5.3. LRMS (APCI) calcd for $[M-H]^+$ *m/z* 245.2, measured 245.2.

(R)-methyl 3-(benzylthio)-2-(6-(tert-butyldimethylsilyoxy) hexanamido) propanoate (**3.2**). 5.5 g (22.4 mmol) of **3.4** were dissolved in 4 mL of THF, solution cooled to 0 °C and stirred for a few minutes. In a separate flask, 4.5 g (17.3 mmol) of S-benzyl cysteine methylester (**3.3**) were dissolved in 65 mL of anhydrous CH_2Cl_2, solution cooled to 0 °C and stirred for a few minutes. To this solution, 2.2 mL (20.8 mmol) of freshly distilled N-mehtyl morpholine were added followed by 4.2 g (20.8 mmol) of DCC and reaction stirred at 0 °C for 15 minutes. After such time, the solution containing **3.4** was added drop-wise to the reaction mixture. After addition, ice bath was removed and reaction stirred for 4 h. Solvent was removed *in vacuo* and the resulting residue was dissolved in CH_2Cl_2 and washed with NH_4Cl, $NaHCO_3$, water and brine. Organic phase dried over Na_2SO_4, filtered and solvent removed. Resulting residue was subjected to silica gel chromatography (3:2 Hexane:EtOAc) to afford 7.0 g of **3.2** as an oil (89% yield). ^1H NMR δ ($CDCl_3$) 7.29-7.19 (m, 5H), 6.20 (d, J = 7.5 Hz, 1H), 4.79-4.75 (m, 1H), 3.67 (s, 3H), 3.66 (s, 2H), 3.56 (t, J = 6.0 Hz, 2H), 2.87 ABX (J_{AB} = 13.5, J_{AX} = 5.5), 2.80 ABX (J_{AB} = 13.5, J_{BX} = 5.0), 2.16 (t, J = 7.5 Hz, 2H), 1.72-1.13 (m, 6H), 0.85 (s, 9H), 0.01 (s, 6H). ^{13}C NMR δ ($CDCl_3$) 172.7, 171.6, 137.0, 128.8, 128.7, 127.2, 64.3, 52.9, 51.2, 38.9, 36.5, 33.2, 33.0, 25.8, 25.1, 24.8, -5.3. HRMS (MALDI) calcd for $[M + Na]^+$ *m/z* 476.2261, measured 476.2212.

N-(3-(benzylthio)-1-(tert-butyldiphenylsilyloxy)propan-2-yl)-6-hydroxyhexanamide (**3.6**). 12.9 g (28.4 mmol) of the **3.2** were dissolved in 400 mL of dry THF and stirred at -15 °C for 30 minutes. After such time, 1.1 g (21.9 mmol) of $LiBH_4$ were added and reaction

stirred at room temperature for 6 h. At this time, reaction was quenched by slow addition of cold MeOH and H_2O. Reaction then partitioned between H_2O and EtOAc and extracted (3 x 50 mL) with EtOAc. Organic phase dried over Na_2SO_4, filtered and solvent removed. Resulting residue was dissolved in anhydrous DMF, cooled to 0 °C and 7.7 g (113.6 mmol) of Imidazole added. Next, 10.1 g (36.9 mmol) of TBDPSCl were added to the mixture and reaction stirred at 0 °C for 1 h followed by 1 h of stirring at room temperature. Reaction quenched by addition of MeOH and partitioned between H_2O and EtOAc. Reaction mixture extracted several times with EtOAc. Organic layers washed with H_2O, NH_4Cl and brine. Organic phase then dried over Na_2SO_4, filtered and solvent removed. Resulting residue was then dissolved in THF and cooled to -15 °C. To this solution, 12 mL of a 1:1 H_2O:TFA solution were added and reaction stirred for 30 minutes at -15 °C. At this point, reaction warmed to 0 °C and stirred for an additional 45 minutes. Reaction quenched by slow addition of cold NH_4Cl then partitioned between H_2O:EtOAc and aqueous layer extracted with EtOAc (3 x 150 mL). Organic layers combined and washed with $NaHCO_3$, H_2O and brine. Organic phase dried over Na_2SO_4, filtered and solvent removed. Resulting residue was column chromatographed (7:2:1:1 Hexane:EtOAc:CH_2Cl_2:MeOH) to afford 12.5 g of **3.6** as an oil (80% yield). ^1H NMR δ ($CDCl_3$) 7.81-7.28 (m, 15H), 5.88 (d, J = 8.5 Hz, 1H), 4.26-4.20 (m, 1H), 3.94-3.92 (m, 2H), 3.77 (s, 2H), 3.68 (t, J = 6.5 Hz, 2H), 2.75-2.73 (m, 2H), 2.17-2.14 (m, 2H), 1.72-1.40 (m, 6H), 1.13 (s, 9H). ^{13}C NMR δ ($CDCl_3$) 172.4, 137.0, 132.6, 130.1, 128.8, 128.7, 128.4, 127.2, 67.3, 62.9, 54.2, 39.2, 36.8, 34.4, 31.6, 25.7, 25.6, 25.5, 24.7, 19.2. HRMS (MALDI) calcd for $[M + Na]^+$ *m/z* 572.2625, measured 572.2609.

S-6-(3-(benzylthio)-1-(tert-butyldiphenylsilyloxy)propan-2-ylamino)-6-oxohexyl ethanethioate (**3.1**). 1.3 g of PPh_3 (6.9 mmol) were dissolved in 35 mL of dry THF and stirred at 0 °C for a few minutes. To this solution, 1.3 mL (6.9 mmol) of DIAD were added and the reaction stirred for 30 minutes. To this mixture, 1.9 g (3.5 mmol) of **3.6** previously dissolved in THF were slowly added along with 0.5 mL of thioacitec acid. Reaction stirred at 0 °C for 30 minutes. Solvent removed and resulting residue column chromatographed (7:2:2 Hexane:CH_2Cl_2:EtOAc) to yield 1.4 g of **3.1** as an oil (95% yield). ^{1}H NMR δ ($CDCl_3$) 7.62-7.22 (m, 15H), 5.66 (d, J = 8.5 Hz, 1H), 4.18-4.11 (m, 1H), 3.87 ABX (J_{AB} = 10.5, J_{AX} = 3.5), 3.71 (s, 2H), 3.68 ABX (J_{AB} = 10.5, J_{BX} = 3.0), 2.85 (t, J = 7.5 Hz, 2H), 2.67 (d, J = 6.5 Hz, 2H), 2.31 (s, 3H), 2.09-2.05 (m, 2H), 1.66-1.34 (m, 6H), 0.85 (s, 9H). ^{13}C NMR δ ($CDCl_3$) 195.0, 172.4, 137.0, 134.0, 132.6, 130.1, 128.8, 128.7, 128.4, 127.2, 67.3, 54.2, 39.2, 36.8, 34.4, 33.0, 30.5, 27.8, 27.6, 25.6, 19.2. HRMS (MALDI) calcd for $[M + Na]^+$ *m/z* 630.2502, measured 630.2510.

N-(3-(benzythio)-1-(tert-butyldiphenylsilyloxy)propan-2-yl)-6-mercaptohexanamide (**3.8**). 326.5 mg of **3.1** (0.54 mmol) were dissolved in 5 mL of HPLC grade MeOH and stirred at room temperature for a few minutes. To this solution, 2 mL (1.0 mmol) of 0.5 M NaOMe solution were added and reaction stirred at room temperature for 1 h. After such time, solvent was removed and resulting residue dissolved in EtOAc and washed with cold dilute citric acid solution (4 x 30 mL) followed by H_2O (2 x 50 mL) and finally brine. Organic layer dried over Na_2SO_4, filtered and solvent removed. Resulting residue was column chromatographed (11:1:1:0.5 Hexane:EtOAc:CH_2Cl_2:MeOH) to afford 303.9 mg of **3.7** (87% yield).

(R)-N-(3-(benzylthio)-1-(1,8-naphthalimide)-2-yl)-6-hydroxyhexanamide (**3.10**). 5.6 g (12.5 mmol) of **3.2** were dissolved in THF and stirred at 0 °C for 30 minutes. After such time, 10.9 mL of a 2M solution of $LiBH_4$ in THF were added and the reaction mixture stirred at 0 °C for 1 h. Reaction allowed to reach ambient temperature and stirred for an extra 3 h. Reaction quenched by adding cold MeOH:H_2O followed by partition between H_2O and EtOAc. Aqueous phase extracted with EtOAc (3 x 50 mL), organic layers combined, washed with brine and dried over Na_2SO_4. Solution was filtered and solvent removed. The resulting residue was dissolved in 75 mL of anhydrous THF along with 4.7 g (17.9 mmol) of PPh_3. Solution stirred at ambient temperature for 5 minutes followed by addintion of 2.8 (14.3 mmol) of 1,8-naphthalimide. Finally, 2.8 mL (17.9 mmol) of DEAD were added dropwise over 10 minutes and the reaction mixture stirred at room temperature for 4 h. After such time, solvent was removed and resulting residue dissolved in EtOAc and partitioned between H_2O and EtOAc. Aqueous phase extracted several times with CH_2Cl_2. Organic layers dried over Na_2SO_4, filtered and solvent removed. Resulting residue was column chromatographed (7:2:1:0.3 Hexane:EtOAc:CH_2Cl_2:MeOH) to afford 3.7 g of a residue that was dissolved in THF, cooled at 0 °C and stirred for 10 minutes. At this point, 1 mL of a 1:1 TFA:H_2O solution was added and the reaction allowed to reach room temperature. Reaction mixture cooled again to 0 °C and quenched by addition of saturated $NaHCO_3$. Aqueous phase extracted with EtOAc (3 x 20 ml), organic layers combined, washed with brine and dried over Na_2SO_4. Solvent filtered and removed and resulting residue PTLC purified (7:3:2:1 Hexane:EtOAc:CH_2Cl_2:MeOH) to afford 2.1 g of **3.10** (36% overall yield). ^1H NMR δ ($CDCl_3$) 8.58 (dd, J = 7.2, 1.2 Hz, 2H), 8.21 (dd, J = 8.4, 0.8 Hz, 2H), 7.48 (t, J = 8.0 Hz, 2H), 7.39-7.20 (m, 5H), 6.20 (d, J = 8.0 Hz, 1H), 4.70-4.62 (m, 1H), 4.43-4.30 (m, 2H),

3.84 (t, J = 6.4 Hz, 2H), 2.77 ABX (J_{AB} = 14.0 , J_{AX} = 5.2), 2.67 ABX (J_{AB} = 14.0, J_{BX} = 6.8), 2.09-1.95 (m, 2H),1.49-1.09 (m, 6H). ^{13}C NMR δ ($CDCl_3$) 173.3,165.0, 138.3, 134.5, 131.8, 129.3, 128.8, 128.4, 127.3, 127.2, 122.5, 62.6, 48.4, 42.9, 36.8, 36.8, 34.5, 32.4, 25.4, 25.3

(R)-S-6-(3-(benzylthio)-1-(1,8-naphthalimide)-2-ylamino)-6-oxohexylethanethioate (**3.11**). 366 mg (1.40 mmol) of PPh_3 were dissolved in 7 mL of anhydrous THF, cooled to 0 °C and stirred for a few minutes. To this solution, 275 μL (1.40 mmol) of DIAD were added and the mixture stirred for 1 h at 0 °C. At such time, 100 μL (1.40 mmol) of thioacetic acid followed by 343 mg (0.7 mmol) of **3.10** previously dissolved in THF were added and reaction stirred for 2 h at 0 °C. At this point, the solvent was removed and residue PTLC purified (7:3:2:1 Hexane:EtOAc:CH_2Cl_2:MeOH) to afford 115 mg of **3.11** (30% yield). ^1H NMR δ ($CDCl_3$) 8.58 (d, J = 7.2, 2H), 8.21 (d, J = 8.4, 2H), 7.48 (t, J = 8.0 Hz, 2H), 7.39-7.21 (m, 5H), 6.214(d, J = 8.0 Hz, 1H), 4.70-4.61 (m, 1H), 4.44-4.33 (m, 2H), 3.84 (d, J = 3.2 Hz, 2H), 2.77 ABX (J_{AB} = 13.7 , J_{AX} = 5.1), 2.67 ABX (J_{AB} = 13.7, J_{BX} = 6.6), 2.58 (t, J = 7.1 Hz, 2H), 2.28 (s, 3H), 2.07-1.92 (m, 2H), 1.44-1.25 (m, 4H), 1.15-1.07 (m, 2H). ^{13}C NMR δ ($CDCl_3$) 196.0, 173.0, 165.0, 138.3, 134.6, 131.8, 131.8, 129.4, 128.8, 128.4, 127.3, 127.2, 122.5, 48.5, 42.8, 36.8, 36.7, 34.5, 30.8, 29.3, 28.9, 28.4, 25.2.

(R)-N-(3-(benzylthio)-1-(1,8-naphthalimide)-2-yl)-6-mercaptohexanamide (**3.12**). 50 mg (0.08 mmol) of **3.11** were dissolved in a 2:1 mixture of HPLC grade MeOH:anhydrous THF, solution cooled to 0 °C and stirred for 10 minutes. After such time, of 1 mL of 0.5N NaOMe in MeOH were added and reaction mixture stirred for 15 minutes at ambient temperature. Reaction quenched by addition of cold dilute citric acid solution and

partitioned between EtOAc and H_2O. Aqueous phase extracted several times with EtOAc, organic layers combined, whased with brine and dried over Na_2SO_4. Solution was filtered, solvent removed and residue column purified (7:3:2:1 Hexane:EtOAc:CH_2Cl_2:MeOH) to afford 25 mg of **3.12** (55% yield). ^{1}H NMR δ ($CDCl_3$) 8.58 (d, J = 7.2, 2H), 8.21 (d, J = 8.4, 2H), 7.48 (t, J = 8.0 Hz, 2H), 7.39-7.21 (m, 5H), 6.214(d, J = 8.0 Hz, 1H), 4.70-4.61 (m, 1H), 4.44-4.33 (m, 2H), 3.84 (d, J = 3.2 Hz, 2H), 2.77 ABX (J_{AB} = 13.7 , J_{AX} = 5.1), 2.67 ABX (J_{AB} = 13.7, J_{BX} = 6.6), 2.58 (t, J = 7.1 Hz, 2H), 2.07-1.92 (m, 2H), 1.44-1.25 (m, 4H), 1.15-1.07 (m, 2H). ^{13}C NMR δ ($CDCl_3$) 173.0, 165.0, 138.3, 134.6, 131.8, 131.8, 129.4, 128.8, 128.4, 127.3, 127.2, 122.5, 48.5, 42.8, 36.8, 36.7, 34.5, 29.3, 28.9, 28.4, 25.2.

6-(tritylthio)hexanoic acid (**3.16**) 0.215 g of Tritylmercaptan (0.778 mmol) were dissolved in HPLC grade acetonitrile and cooled to 0 °C. After a few minutes, 3.42 mL of NaOMe (0.5 M in MeOH, 1.74 mmol) were added and the reaction stirred for 15 minutes. To this solution, 0.167 g (0.856 mmol) of 6-bromohexanoic acid (**3.17**), previously dissolved in THF, were added drop-wise to the reaction mixture. After addition, the ice bath was removed and reaction stirred overnight at ambient temperature. Reaction quenched by addition of water and pH lowered to 3 with cold 1.2 M HCl. Reaction extracted with CH_2Cl_2, washed with brine and dried over Na_2SO_4. Reaction filtered, solvent removed and residue column purified (3:2 Hexane:EtOAc) to afford 0.191 g of **3.16** as an off white solid (95.3% yield). ^{1}H NMR δ ($CDCl_3$) 7.45-7.16 (m, 15H), 2.27-2.13 (m, 4H), 1.52-1.23 (m, 6H). ^{13}C NMR δ ($CDCl_3$) 180.2, 145.3, 130.4, 129.9, 129.8, 128.3, 128.2, 128.1, 127.5, 127.2, 126.8, 66.8, 34.1, 32.0, 28.6, 28.6, 24.5. LRMS (ESI) calcd for $[M + Na]^+$ *m/z* 413.2, measured 413.0.

O-methyl-S-trityl-L-cysteine hydrochloride (**3.15**). 10.00 g (0.028 mol) of *S*-trityl-L-cysteine were dissolved in 1.0 L of HPLC grade MeOH and cooled to 0 °C. After a few minutes, 16 mL (0.22 mol) of thionyl chloride were slowly added to the solution and stirred at 0 °C for 1 h. After such time, the reaction was allowed to reach ambient temperature (3 hrs.) before refluxed overnight under argon. Reaction was allowed to reach ambient temperature and residual MeOH and thionyl chloride were removed under high vacuum. After the solvent was removed, residue washed several times with dry THF (5 x 500 mL) to afford 11.23 g of **3.15** as a fine off white solid (98.6% yield). ^{1}H NMR δ (DMSO-d_6) 8.90 (bs, 3H), 7.38-7.25 (m, 15H), 3.80-3.75 (m, 1H), 3.64 (s, 3H), 2.72 (dd, J= 12.8, 6.4 Hz, 1H), 2.58 (dd, J = 12.8, 5.6 Hz, 1H). ^{13}C NMR δ (DMSO-d_6) 168.8, 144.3, 129.7, 128.9, 128.7, 128.6, 128.5, 128.2, 127.7, 127.3, 67.3, 53.6, 51.7, 32.0. LRMS (ESI) calcd for $[M\text{-}Cl]^+$ *m/z* 378.2, measured 378.0.

Methyl 3-(tritylthio)-2-(6-(tritylthio)hexanamido)propanoate (**3.14**) To 2.80 g (6.78 mmol) of methyl ester **3.15**, 40 mL dry THF were added, solution cooled to 0 °C and stirred for a few minutes. To this solution, 1.48 mL (8.46 mmol) of DIEA were added. The solution took on a deep violet color after each addition of DIEA. In a separate flask, 2.65 g (6.78 mmol) of **3.16** were dissolved in 60 mL of dry THF and cooled to 0 °C. To this solution, 1.48 mL (8.46 mmol) of DIEA were added followed by 1.43 g (8.81 mmol) of CDI and reaction stirred at 0 °C for 15 minutes. After such time, the solution containing **3.15** was added drop-wise to the reaction mixture. After addition, ice bath was removed and reaction stirred overnight. Solvent was removed *in vacuo* and the resulting residue was dissolved in CH_2Cl_2 and washed with NH_4Cl, $NaHCO_3$, water and brine. Organic phase dried over Na_2SO_4, filtered and solvent removed. Resulting gummy residue was

subjected to silica gel chromatography (3:2 Hexane:EtOAc) to afford 3.30 g of **3.14** as a white powder (65% yield). ^{1}H NMR δ ($CDCl_3$) 7.25-7.06 (m, 30H), 6.80 (bs, 1H), 4.72-4.68 (m, 1H), 3.68 (s, 3H), 3.17-3.16 (m, 1H), 2.92-2.90 (m, 1H), 2.43-2.26 (m, 2H), 2.12-2.08 (m, 2H), 1.62-1.38 (m, 6H). ^{13}C NMR δ ($CDCl_3$) 172.6, 171.5, 144.0, 129.3, 128.2, 126.3, 67.4, 53.2, 52.7, 39.4, 36.6, 26.5, 26.2, 23.5. HRMS (MALDI) calcd for $[M + Na]^+$ *m/z* 772.290, measured 772.290.

Methyl 6-oxo-1,2-dithia-5-azacyclodecane-4-carboxylate (**3.13a**) Methyl ester **3.13a** was obtained in 82% yield as a white solid.: mp 157 – 159 °C; ^{1}H NMR ($CDCl_3$) δ 6.58 (bd, *J* = 7.3 Hz, 1H), 4.95 (ddd, *J* = 7.9, 7.9, 3.7 Hz, 1H), 3.78 (s, 3H), 3.43 (dd, *J* = 15.0, 3.7 Hz, 1H), 3.15-3.03 (m, 2H), 2.89-2.80 (m, 1H), 2.46 (m, 1H), 2.36 (m, 1H), 1.97-1.87 (m, 2H), 1.85-1.77 (m, 2H). ^{13}C NMR ($CDCl_3$) δ 172.9, 170.9, 54.5, 53.1, 41.4, 40.3, 36.5, 27.0, 21.8. LRMS (ESI) calcd for $[M + H]^+$ *m/z* 250.1, found 249.9.

Methyl 6-oxo-1,2-dithia-5-azacycloundecane-4-carboxylate (**3.13b**) 0.170 g (0.67 mmol) of I_2 were dissolved in 400 mL of dry MeOH and stirred for a few minutes. To this solution, 0.500 g (0.67 mmol) of di-trityl **3.14**, previously dissolved in 100 mL of 9:1 MeOH:THF solution, were added drop-wise to the center of the reaction and stirred at ambient temperature over night. The reaction was quenched by addition of 4 mL of a 0.2 M solution of citrate/abscorbic acid. After addition, solution was partitioned between brine and CH_2Cl_2. The aqueous phase was washed several times (6 x 25 mL) with CH_2Cl_2 and organic phases combined, dried over Na_2SO_4 followed by filtration and solvent removal. The resulting residue was column purified over silica gel (4:2:1 Hexane:EtOAc:CH_2Cl_2) to afford 0.155 g of **3.13b** as a white solid (90% yield): mp 140 - 143 0 °C ^{1}H NMR δ ($CDCl_3$)

6.77 (d, J = 6.4 Hz, 1H), 5.36-5.28 (m, 1H), 3.80 (s, 3H), 2.95-2.75 (m, 1H), 2.74-2.58 (m, 1H), 2.44-2.26 (m, 2H), 2.05-1.83 (m, 3H), 1.82-1.40 (m, 5H). ^{13}C NMR δ ($CDCl_3$) 173.3, 170.7, 53.2, 52.7, 39.4, 36.6, 26.5, 26.2, 23.5. HRMS (MALDI) calcd for $[M + H]^+$ *m/z* 264.072, measured 264.072

Methyl 6-oxo-1,2-dithia-5-azacyclododecane-4-carboxylate (**3.13c**) Methyl ester 13c was obtained in 77.3% yield as a white solid: mp 132 - 135 °C; ^1H NMR ($CDCl_3$) δ 6.91 (bd, *J* = 5.7 Hz, 1H), 5.09 (bs, 1H), 3.78 (s, 3H), 3.27 (dd, *J* = 14.4, 2.6 Hz, 1H), 2.96 (m, 1H), 2.86 (m, 1H), 2.76 (m, 1H), 2.32 (m, 2H), 1.91 (m, 1H), 1.75 (m, 1H), 1.62 (m, 3H), 1.40 (m, 3H). ^{13}C NMR ($CDCl_3$) δ 172.6, 170.5, 53.6, 52.8, 36.0, 31.7, 25.6, 24.3, 23.7, 23.6, 22.8. LRMS (ESI) calcd for $[M + H]^+$ *m/z* 278.1, found 278.0.

6-oxo-1,2-dithia-5-azacycloundecane-4-carboxilic acid (**3.18b**). 0. 200 g (0.76 mmol) of **3.13b** were dissolved in 150 mL of a 1:1 THF:H_2O solution and stirred at ambient temperature for a few minutes. To this solution, 250 μL (0.80 mmol) of a 3 N LiOH solution were added and the reaction then stirred for 1h. At this point, disappearance of starting material was evident and reaction was quenched by addition of saturated solution of NH_4Cl. The pH of the solution was adjusted to 1 by addition of 1.2 M HCl. Solution partitioned between brine and CH_2Cl_2 and aqueous phase extracted several times (6 x 25 mL) with CH_2Cl_2. Organic layers dried over Na_2SO_4, filtered and solvent removed to yield a white solid that was used without further purification.

5.2.3 General Synthetic Procedures for Cap Group Installation

20 mg (0.080 mmol) of the acid were dissolved in 1 mL of dry THF and solution stirred at ambient temperature for a few minutes. To this solution, 16 mg (1.3 eq.) of CDI followed by 17.4 μL (1.3 eq) of DIEA were added and the reaction was stirred at ambient temperature for 30 min. After such time, the amine-bearing capped group was added drop-wise to the reaction mixture and stirred at ambient temperature overnight. Solvent was removed and the resulting residue was dissolved in CH_2Cl_2 and washed with NH_4Cl, $NaHCO_3$, water, and brine. The organic phase was dried over $NaSO_4$, filtered, and the solvent removed *in vacuo*. The resulting residue was purified by either column chromatography or preparatory TLC to yield the desired amide.

(R)-N-benzyl-6-oxo-1,2,5-dithiazecane-4-carboxamide (**3.20a**) Preparatory TLC (5:1 EtOAc:Hex), extraction (5:1 CH_2Cl_2:MeOH), and concentration afforded **3.20a** as an off-white solid (15.3 mg, 29%): mp 189 - 190 °C. ^{1}H NMR ($CDCl_3$) δ 7.36-7.21 (m, 5H), 7.0 (bt, *J* = 6.7 Hz, 1H), 6.71 (bd, *J* = 6.7 Hz, 1H), 4.73 (ddd, *J* = 10.2, 7.0, 3.3 Hz, 1H), 4.43 (dd, *J* = 15.2, 6.2 Hz, 1H), 4.39 (dd, *J* = 15.2, 5.8 Hz, 1H), 3.28 (dd, *J* = 15.7, 3.2 Hz, 1H), 3.20 (m, 1H), 3.16 (dd, *J* = 15.5, 10.8 Hz, 1H), 2.54 (m, 2H), 2.31 (m, 1H), 1.97 (m, 2H), 1.80 (m, 3H). ^{13}C NMR ($CDCl_3$) δ 174.3, 169.8, 137.9, 128.9, 127.7, 77.4, 43.6, 39.9, 36.5, 29.8, 26.6. LRMS (ESI) calcd for $[M + H]^+$ *m/z* 325.104; found 325.1.

(R)-N-benzyl-6-oxo-1,2-dithia-5-azacycloundecane-4-carboxamide. Preparatory TLC (5:1 EtOAc:Hexane) afforded **3.20b** as an off-white solid (14.1 mg, 26%): mp 192 - 193 0 °C. ^{1}H NMR δ ($CDCl_3$) 7.35-7.21 (m, 5H), 7.00 (bs, 1H), 6.75 (d, J = 6.4 Hz, 1H), 4.76-4.70 (m, 1H), 4.46-4.36 (m, 2H), 3.31-3.13 (m, 2H), 2.58-2.51 (m, 2H), 2.34-2.28 (m, 1H), 2.00-

1.60 (m, 7H). ^{13}C NMR δ ($CDCl_3$) 174.7, 172.1, 141.8, 128.7, 127.0, 126.8, 52.1, 44.1, 36.9, 35.2, 33.9, 26.7, 22.3. LRMS (ESI) calcd for $[M + H]^+$ *m/z* 339.1; measured 339.1.

(R)-N-(2-hydroxy-2-phenylethyl)-6-oxo-1,2,5-dithiazecane-4-carboxamide **(3.21a)**

Preparatory TLC (5:1 EtOAc:Hex), extraction (5:1 CH_2Cl_2:MeOH), and concentration afforded **3.21a** as a yellow oil (23.6 mg, 76%). ^1H NMR ($CDCl_3$) δ 7.35 (m, 4H), 7.29 (m, 1H), 7.19 (m, 1H), 6.88 (m, 1H), 4.82 (m, 1H), 4.74 (m, 1H), 3.64 (m, 1H), 3.33 (m, 1H), 3.22 (m, 1H), 3.16 (bs, 1H), 3.09 (m, 1H), 2.53 (m, 2H), 2.28 (m, 1H), 1.96 (m, 1H), 1.79 (m, 4H). ^{13}C NMR ($CDCl_3$) δ 174.5, 170.9, 141.7, 128.8, 128.2, 126.0, 73.5, 47.5, 46.0, 40.4, 36.5, 29.9, 26.6, 21.3. LRMS (ESI) calcd for $[M + H]^+$ *m/z* 355.1, found 355.0.

(R)-N-(2-hydroxy-2-phenylethyl)-6-oxo-1,2-dithia-5-azacycloundecane-4-carboxamide.

Preparatory TLC (5:1 EtOAc:Hexane) afforded **3.21b** as a yellow oil (24.2 mg, 75%): dec. ~110 0 °C. ^1H NMR δ ($CDCl_3$) 7.37-7.16 (m, 6H), 6.90-6.87 (m, 1H), 4.85-4.81 (m, 1H), 4.77-4.71 (m, 1H), 3.70-3.60 (m, 2H), 3.37-3.05 (m, 4H), 2.57-2.49 (m, 2H), 2.33-2.24 (m, 1H), 2.04-1.70 (m, 5H). ^{13}C NMR δ ($CDCl_3$) 174.7, 171.9, 140.7, 129.2, 128.0, 127.7, 72.6, 52.2, 44.2, 36.9, 35.2, 33.9, 26.7, 22.2. LRMS (ESI) calcd for $[M + H]^+$ *m/z* 369.1; measured 369.0.

(R)-N-(2-hydroxy-2-phenylethyl)-6-oxo-1,2-dithia-5-azacyclododecane-4-carboxamide

(3.21c) Preparatory TLC (5:1 EtOAc:Hex), extraction (5:1 CH_2Cl_2:MeOH), and concentration afforded **3.21c** as an oily yellow solid (36.3 mg, 98%). ^1H NMR ($CDCl_3$) δ 7.41-7.28 (m, 5H), 6.79 (m, 2H), 4.89 (m, 1H), 4.76 (m, 1H), 3.74 (dddd, *J* = 25.1, 13.9, 7.1, 3.2 Hz, 1H), 3.35 (m, 1H), 3.19 (ddd, *J* = 14.4, 12.2, 3.7 Hz, 1H), 3.11 (ddd, *J* = 14.4, 7.1, 1.6 Hz, 1H), 2.68 (m, 1H), 2.63 (m, 1H), 2.42 (m, 1H), 2.28 (m, 1H), 1.98-1.81 (m,

1H), 1.74-1.20 (m, 8H). ^{13}C NMR ($CDCl_3$) δ 174.2, 170.7, 170.4, 141.5, 141.5, 128.7, 128.1, 128.0, 126.0, 125.9, 73.2, 73.1, 47.7, 47.5, 36.0, 34.7, 25.4, 25.3, 24.3, 23.7, 23.5. LRMS (ESI) calcd for $[M + H]^+$ *m/z* 383.1, found 383.2.

(R)-N-(naphthalen-1-ylmethyl)-6-oxo-1,2,5-dithiazecane-4-carboxamide (**3.22a**)

Preparatory TLC (5:1 EtOAc:Hex), extraction (5:1 CH_2Cl_2:MeOH), and concentration afforded **3.22a** as a light-yellow solid (26.2 mg, 59%): mp 207 - 208 °C. ^1H NMR ($CDCl_3$) δ 7.93 (m, 1H), 7.87 (m, 1H), 7.81 (dd, *J* = 6.7, 2.9 Hz, 1H), 7.52 (m, 2H), 7.41 (m, 2H), 6.91 (bt, *J* = 5.5 Hz, 1H), 6.66 (bd, *J* = 6.7 Hz, 1H), 4.86 (d, *J* = 5.7 Hz, 2H), 4.72 (ddd, *J* = 10.4, 7.1, 3.3 Hz, 1H), 3.28 (dd, *J* = 15.5, 3.1 Hz, 1H), 3.15 (m, 1H), 3.15 (dd, *J* = 15.5, 10.6 Hz, 1H), 2.49 (m, 2H), 2.24 (m, 1H), 1.91 (m, 1H), 1.77 (m, 3H). ^{13}C NMR ($CDCl_3$) δ 174.2, 169.6, 134.0, 133.1, 131.4, 129.0, 128.8, 126.7, 126.6, 126.1, 125.5, 123.4, 41.8, 40.0, 36.4, 29.8, 26.6, 21.2. LRMS (ESI) calcd for $[M + H]^+$ *m/z* 375.1, found 375.1.

(R)-N-(naphthalen-1-ylmethyl)-6-oxo-1,2-dithia-5-azacycloundecane-4-carboxamide.

Preparatory TLC (5:1 EtOAc:Hexane) afforded **3.22b** as a light-yellow solid (28.2 mg, 63%): mp 215 - 218 0 °C. ^1H NMR δ ($CDCl_3$) 7.94-7.80 (m, 2H), 7.56- 7.40 (m, 3H), 6.91 (bs, 1H), 6.74 (d, J = 7.2 Hz, 1H), 4.85 (d, J = 5.6 Hz, 2H), 4.74-4.69 (m, 1H), 3.28 (dd, J = 15.6, 3.6 Hz, 1H), 3.18 (dd, J = 15.6, 10.8 Hz, 1H), 2.56-2.44 (m, 2H), 2.28-2.17 (m, 1H), 2.03-1.28 (m, 9H). ^{13}C NMR δ ($CDCl_3$) 174.8, 172.1, 133.9, 133.5, 132.7, 128.7, 126.9, 126.5, 125.9, 125.3, 52.2, 42.5, 36.9, 35.2, 33.9, 26.7, 22.2. LRMS (ESI) calcd for $[M + H]^+$ *m/z* 389.1; measured 389.0.

(R)-N-(2,3-dimethoxybenzyl)-6-oxo-1,2,5-dithiazecane-4-carboxamide **(3.23a)**

Preparatory TLC (5:1 EtOAc:Hex), extraction (5:1 CH_2Cl_2:MeOH), and concentration afforded **3.23a** as an oily yellow solid (31.6 mg, 94%): mp 203 - 205 °C. ^1H NMR ($CDCl_3$) δ 7.01 (bt, *J* = 8.0 Hz, 1H), 6.91 (bt, *J* = 4.8 Hz, 1H), 6.85 (dd, *J* = 10.3, 8.0 Hz, 2H), 6.63 (bd, *J* = 7.0 Hz, 1H), 4.71 (ddd, *J* = 10.5, 7.2, 3.1 Hz, 1H), 4.43 (d, *J* = 6.0 Hz, 2H), 3.86 (bs, 6H), 3.28 (dd, *J* = 15.4, 3.1 Hz, 1H), 3.18 (m, 1H), 3.11 (dd, *J* = 15.6, 10.6 Hz, 1H), 2.56 (m, 2H), 2.32 (m, 1H), 1.96 (m, 1H), 1.81 (m, 3H). ^{13}C NMR ($CDCl_3$) δ 174.0, 169.6, 152.8, 147.3, 131.4, 124.3, 121.3, 112.2, 77.3, 60.8, 55.9, 40.4, 39.1, 36.5, 29.8, 26.6. LRMS (ESI) calcd for $[M + H]^+$ *m/z* 385.1, found 385.2.

(R)-N-(2,3-dimethoxybenzyl)-6-oxo-1,2-diathia-5-azacycloundecane-4-carboxamide.

Preparatory TLC (5:1 EtOAc:Hexane) afforded **3.23b** as an off-white solid (36.0 mg, 73%): mp 206 - 208 0 °C. ^1H NMR δ ($CDCl_3$) 6.96-6.94 (m, 1H), 6.71 (d, J = 6.4 Hz, 1H), 6.52-6.46 (m, 2H), 4.74-4.69 (m, 1H), 4.46-4.27 (m, 2H), 3.85 (s, 6H), 3.82 (s, 3H), 3.35-3.13 (m, 2H), 2.58-2.52 (m, 2H), 2.35-2.29 (m, 1H), 2.04-1.65 (m, 7H). ^{13}C NMR δ ($CDCl_3$) 174.7, 172.1, 149.7, 148.5, 128.4, 122.0, 120.3, 113.4, 56.2, 52.2, 36.9, 35.2, 33.9, 26.7, 22.2. LRMS (ESI) calcd for $[M + H]^+$ *m/z* 399.1; measured 399.0.

(R)-N-(2,4,6-trimethoxybenzyl)-6-oxo-1,2,5-dithiazecane-4-carboxamide **(3.24a)**

Preparatory TLC (5:1 EtOAc:Hex), extraction (5:1 CH_2Cl_2:MeOH), and concentration afforded **3.24a** as an off-white solid (34.2 mg, 74%): mp 177 - 180 °C. ^1H NMR ($CDCl_3$) δ 6.95 (bt, *J* = 5.5 Hz, 1H), 6.71 (bd, *J* = 6.7 Hz, 1H), 6.46 (s, 2H), 4.71 (ddd, *J* = 10.3, 6.7, 3.2 Hz, 1H), 4.40 (dd, *J* = 14.7, 6.0 Hz, 1H), 4.30 (dd, *J* = 14.8, 5.6 Hz, 1H), 3.85 (s, 6H), 3.82 (s, 3H), 3.30 (dd, *J* = 15.5, 3.3 Hz, 1H), 3.20 (m, 1H), 3.16 (dd, *J* = 15.5, 10.7 Hz,

1H), 2.55 (m, 2H), 2.33 (m, 1H), 1.97 (m, 1H), 1.81 (m, 3H). ^{13}C NMR ($CDCl_3$) δ 174.3, 169.7,153.6, 133.5, 112.3, 104.7, 61.0, 56.3, 43.8, 39.6, 36.4, 26.5. LRMS (ESI) calcd for $[M + H]^+$ *m/z* 415.1, found 415.0.

(R)-N-(2,4,6-trimethoxybenzyl)-6-oxo-1,2-dithia-5-azacycloundecane-4-carboxamide. Preparatory TLC (5:1 EtOAc:Hexane) afforded **3.24b** as an off-white solid (28.5 mg, 75%): mp 180 - 183 0 °C. ^1H NMR δ ($CDCl_3$) 6.96-6.94 (m, 1H), 6.71 (d, J = 6.4 Hz, 1H), 6.52-6.46 (m, 2H), 4.74-4.69 (m, 1H), 4.46-4.27 (m, 2H), 3.85 (s, 6H), 3.82 (s, 3H), 3.35-3.13 (m, 2H), 2.58-2.52 (m, 2H), 2.35-2.29 (m, 1H), 2.04-1.65 (m, 7H). ^{13}C NMR δ ($CDCl_3$) 174.7, 172.2, 160.7, 158.7, 105.0, 92.7, 56.3, 52.2, 36.9, 35.2, 33.9, 26.7, 24.3, 22.2. LRMS (ESI) calcd for $[M + H]^+$ *m/z* 429.2; measured 429.0.

(R)-N-(4-phenyl)benzyl-6-oxo-1,2,5-dithiazecane-4-carboxamide (**3.25a**) Preparatory TLC (5:1 EtOAc:Hex), extraction (5:1 CH_2Cl_2:MeOH), and concentration afforded **3.25a** as an off-white solid (18.5 mg, 29%): mp 161 - 164 °C. ^1H NMR ($CDCl_3$) δ 7.56 (m, 4H), 7.44 (m, 2H), 7.33 (m, 3H), 7.04 (bt, *J* = 4.9 Hz, 1H), 6.71 (bd, *J* = 6.9 Hz, 1H), 4.75 (ddd, *J* = 9.9, 6.8, 3.2 Hz, 1H), 4.47 (dd, *J* = 15.0, 6.1 Hz, 1H), 4.43 (dd, *J* = 15.0, 5.7 Hz, 1H), 3.30 (dd, *J* = 15.7, 3.4 Hz, 1H), 3.20 (m, 1H), 3.18 (dd, *J* = 15.7, 10.8 Hz, 1H), 2.55 (m, 2H), 2.32 (m, 1H), 1.98 (m, 2H), 1.80 (m, 3H). ^{13}C NMR ($CDCl_3$) δ 174.4, 169.9, 140.8, 140.7, 136.9, 128.9, 128.1, 127.6, 127.5, 127.2, 77.3, 43.3, 39.8, 36.5, 32.1, 29.5, 26.6. LRMS (ESI) calcd for $[M + H]^+$ *m/z* 401.1, found 401.1.

(R)-N-(4-phenyl)benzyl-6-oxo-1,2,-dithia-5-azacycloundecane-4-carboxamide (**3.25b**) Preparatory TLC (5:1 EtOAc:Hexane) afforded **3.25b** as an off-white solid (19.0 mg, 31%):

mp 165 - 167 0 °C. ^{1}H NMR δ ($CDCl_3$) 7.48-7.12 (m, 9H), 7.03-6.99 (m, 1H), 6.80 (d, J = 7.2 Hz, 1H), 4.83-4.78 (m, 1H), 4.48-4.39 (m, 2H), 3.28-3.10 (m, 2H), 2.55-2.50 (m, 2H), 2.33-2.25 (m, 1H), 1.98-1.55 (m, 7H). ^{13}C NMR δ ($CDCl_3$) 174.9, 172.0, 140.1, 136.4, 134.6, 129.4, 128.3, 128.2, 127.7, 127.5, 52.2, 44.2, 36.9, 35.2, 33.9, 26.7, 22.2. LRMS (ESI) calcd for $[M + H]^+$ *m/z* 415.2; measured 415.0

(R)-4-(4-benzylpiperidine-1-carbonyl)-1,2,5-dithiazecan-6-one (**3.26a**) Preparatory TLC (5:1 EtOAc:Hex), extraction (5:1 CH_2Cl_2:MeOH), and concentration afforded **3.26a** as a light-yellow solid (37.3 mg, 97%): mp 163 - 164 °C. ^{1}H NMR ($CDCl_3$) δ 7.28 (m, 2H), 7.20 (m, 1H), 7.12 (m, 2H), 6.79 (t, *J* = 6.6 Hz, 1H), 5.25 (m, 1H), 4.25 (m, 1H), 3.94 (m, 1H), 3.15-2.93 (m, 4H), 2.78 (m, 1H), 2.55 (m, 3H), 2.38 (m, 2H), 1.95-1.64 (m, 9H). ^{13}C NMR ($CDCl_3$) δ 172.5, 168.1, 168.0, 139.8, 129.7, 129.2, 128.5, 126.3, 77.3, 50.2, 46.2, 45.9, 44.0, 43.5, 43.0, 42.9, 42.9, 42.7, 39.0, 38.8, 38.3, 38.2, 36.4, 36.3, 32.7, 31.7, 29.8, 26.7, 26.6, 22.1. LRMS (ESI) calcd for $[M + H]^+$ *m/z* 393.2, found 393.2.

(R)-4-(4-benzylpiperidine-1-carbonyl)-1,2-dithia-5-azacycloundecan-6-one. Preparatoty TLC (5:1 EtOAc:Hexane) afforded **3.26b** as a light-yellow solid (35.0 mg, 95%): mp 166 - 167 0 °C. ^{1}H NMR δ ($CDCl_3$) 7.31-7.11 (m, 5H), 6.79 (bs, 1H), 5.23-5.21 (m, 1H), 4.55-4.50 (m, 1H), 3.99-3.84 (m, 1H), 3.12-2.95 (m, 4H), 2.80-2.74 (m, 1H), 2.59-2.54 (m, 3H), 2.43-2.28 (m, 2H), 1.90-1.68 (m, 8H), 1.26-1.08 (m, 3H). ^{13}C NMR δ ($CDCl_3$) 172.6, 168.5, 140.1, 129.3, 129.27, 128.6, 128.6, 126.4, 126.3, 50.3, 46.3, 46.0, 44.2, 43.7, 43.1, 43.1, 43.0, 42.9, 39.0, 38.9, 38.5, 38.3, 36.5, 36.4, 32.9, 31.9, 26.7, 22.2. LRMS (ESI) calcd for $[M + H]^+$ *m/z* 407.2; measured 407.1

(R)-4-(1-benzhydrylpiperazine-4-carbonyl)-1,2,5-dithiazecan-6-one (**3.27a**) Preparatory TLC (5:1 EtOAc:Hex), extraction (5:1 CH_2Cl_2:MeOH), and concentration afforded **3.27a** as an off-white solid (32.6 mg, 79%): mp 222 - 224 °C. ^{1}H NMR ($CDCl_3$) δ 7.39 (m, 4H), 7.28 (m, 4H), 7.20 (m, 2H), 6.73 (bm, 1H), 5.20 (m, 1H), 4.23 (s, 1H), 3.69-3.43 (m, 4H), 3.10 (m, 2H), 3.03 (m, 1H), , 2.76 (m, 1H), 2.39 (m, 5H), 2.32 (m, 1H), 1.96-1.73 (m, 4H). ^{13}C NMR ($CDCl_3$) δ 172.6, 168.3, 142.1, 128.9, 128.0, 127.5, 76.0, 52.2, 51.6, 43.8, 42.7, 39.0, 36.4, 26.7, 22.2. LRMS (ESI) calcd for $[M + H]^+$ *m/z* 470.2, found 470.0.

(R)-4-(1-benzhydrylpiperazine-4-carbonyl)-1,2-dithia-5azacycloundecan-6-one.

Preparatory TLC (5:1 EtOAc:Hexane) afforded **3.27b** as an off-white solid (28.6 mg, 80%): mp 225 - 226 0 °C. ^{1}H NMR δ ($CDCl_3$) 7.40-7.18 (m, 10H), 6.77 (d, J = 8.8 Hz, 1H), 5.23-5.17 (m, 1H), 4.25 (s, 1H), 3.67-3.48 (m, 4H), 3.10-3.03 (m, 3H), 2.78-2.71 (m, 1H), 2.43-2.27 (m, 7H), 1.94-1.77 (m, 5H). ^{13}C NMR δ ($CDCl_3$) 172.6, 168.4, 142.1, 128.9, 128.0, 128.0, 127.5, 76.1, 52.2, 51.7, 46.1, 43.8, 42.7, 38.9, 36.4, 26.7, 22.2. LRMS (ESI) calcd for $[M + H]^+$ *m/z* 484.2; measured 484.0

(R)-N-(2,2-diphenylethyl)-6-oxo-1,2,5-dithiazecane-4-carboxamide (**3.28a**) Preparatory TLC (5:1 EtOAc:Hex), extraction (5:1 CH_2Cl_2:MeOH), and concentration afforded **3.28a** as a white solid (41.1 mg, 98%): mp 171 - 173 °C. ^{1}H NMR ($CDCl_3$) δ 7.33-7.19 (m, 10H), 6.56 (t, *J* = 5.7 Hz, 1H), 6.50 (bd, *J* = 7.1 Hz, 1H), 4.56 (ddd, *J* = 10.5, 7.2, 3.3 Hz, 1H), 4.17 (t, *J* = 8.1 Hz, 1H), 3.86 (m, 2H), 3.16 (m, 1H), 3.11 (dd, *J* = 15.6, 3.3 Hz, 1H), 3.00 (dd, *J* = 15.5, 10.6 Hz, 1H), 2.48 (m, 1H), 2.32 (m, 1H), 2.18 (m, 1H), 1.87 (m, 1H), 1.81-1.61 (m, 3H). ^{13}C NMR ($CDCl_3$) δ 173.9, 170.0, 141.8, 128.9, 128.3, 128.2, 127.1, 112.5, 50.7, 43.9, 40.1, 36.3, 26.7, 21.2. LRMS (ESI) calcd for $[M + H]^+$ *m/z* 415.2, found 415.0.

(R)-N-(2,2-diphenylethyl)-6-oxo-1,2-dithia-5-azacycloundecane-4-carboxamide (**3.28b**) Preparatory TLC (5:1 EtOAc:Hexane) afforded **3.28b** as a white solid (40.5 mg, 97%): mp 178 - 180 0 °C. ^{1}H NMR δ ($CDCl_3$) 7.32-7.21 (m, 10H), 6.58-6.55 (m, 1H), 6.50 (d, J = 7.2 Hz, 1H), 4.58-4.53 (m, 1H), 4.20-4.17 (m, 1H), 3.91-3.80 (m, 2H), 3.21-2.98 (m, 2H), 2.52-2.48 (m, 1H), 2.34-2.26 (m, 1H), 2.21-2.16 (m, 1H), 1.93-1.69 (m, 7H). ^{13}C NMR δ ($CDCl_3$) 173.9, 170.0, 141.8, 128.9, 128.3, 128.3, 127.1, 50.7, 44.0, 40.1, 36.3, 31.9, 26.7, 21.2. LRMS (ESI) calcd for $[M + H]^+$ *m/z* 429.2; measured 429.0.

(R)-N-(2,2-diphenylethyl)-6-oxo-1,2-ditha-5-azacyclododecane-4-carboxamide (**28c**) Preparatory TLC (5:1 EtOAc:Hex), extraction (5:1 CH_2Cl_2:MeOH), and concentration afforded **28c** as an off-white solid (37.6 mg, 93%): mp 185 - 186 °C. ^{1}H NMR ($CDCl_3$) δ 7.31 (m, 4H), 7.24 (m, 6H), 6.66 (bs, 1H), 6.31 (bt, *J* = 5.2 Hz, 1H), 4.66 (bm, 1H), 4.20 (t, *J* = 8.0 Hz, 2H), 3.95 (ddd, *J* =13.9, 8.0, 6.1 Hz, 1H), 3.85 (ddd, *J* = 13.7, 8.1, 5.5 Hz, 1H), 3.02 (m, 2H), 2.63 (m, 1H), 2.57 (bs, 1H), 2.17 (m, 2H), 1.89 (bm, 1H), 1.76 (bm, 1H), 1.70-1.50 (m, 4H), 1.50-1.29 (m, 3H). ^{13}C NMR ($CDCl_3$) δ 173.7, 169.6, 141.8, 128.9, 128.9, 128.3, 127.1, 50.7, 44.0, 35.9, 34.7, 29.9, 25.4, 24.5, 23.7. LRMS (ESI) calcd for $[M + H]^+$ *m/z* 443.2, found 443.2.

(R)-N-(2-bromobenzyl)-6-oxo-1,2,5-dithiazecane-4-carboxamide (**3.29a**) Preparatory TLC (5:1 EtOAc:Hex), extraction (5:1 CH_2Cl_2:MeOH), and concentration afforded **3.29a** as a yellow-white solid (21.2 mg, 41%): mp 207 - 214 °C. ^{1}H NMR ($CDCl_3$) δ 7.54 (dd, 7.9, *J* = 0.9 Hz, 1H), 7.32 (dd, *J* = 7.7, 1.9 Hz, 1H), 7.28 (dd, *J* = 7.3, 0.9 Hz, 1H), 7.15 (m, 2H), 6.70 (bd, *J* = 6.8 Hz, 1H), 4.74 (ddd, *J* = 10.8, 6.9, 3.2 Hz, 1H), 4.47 (d, *J* = 6.0 Hz, 2H),

3.27 (dd, J = 15.7, 3.4 Hz, 1H), 3.21 (m, 1H), 3.14 (dd, J = 15.6, 10.8 Hz, 1H), 2.55 (m, 2H), 2.33 (m, 1H), 1.98 (m, 1H), 1.81 (m, 3H). ^{13}C NMR ($CDCl_3$) δ 174.3, 169.9, 136.9, 133.0, 130.2, 129.4, 127.8, 123.8, 44.0, 39.7, 36.5, 29.8, 26.6, 21.2. LRMS (ESI) calcd for $[M + H]^+$ *m/z* 403.0, found 403.0

(R)-N-(4-bromobenzyl)-6-oxo-1,2,5-dithiazecane-4-carboxamide (**3.30a**) Preparatory TLC (5:1 EtOAc:Hex), extraction (5:1 CH_2Cl_2:MeOH), and concentration afforded **3.30a** as an off-white solid (21.5 mg, 44%): mp 196 - 198 °C. ^{1}H NMR ($CDCl_3$) δ 7.44 (d, J = 8.3 Hz, 2H), 7.12 (d, J = 8.3 Hz, 2H), 7.06 (m, 1H), 6.69 (bd, J = 6.6 Hz, 1H), 4.70 (ddd, J = 10.4, 6.7, 3.3 Hz, 1H), 4.35 (d, J = 6.2 Hz, 2H), 3.28 (dd, J = 15.7, 3.4 Hz, 1H), 3.20 (m, 1H), 3.16 (dd, J = 15.6, 10.8 Hz, 1H), 2.54 (m, 2H), 2.32 (m, 1H), 1.97 (m, 1H), 1.80 (m, 3H). ^{13}C NMR ($CDCl_3$) δ 174.5, 170.0, 134.7, 131.9, 129.4, 112.4, 43.0, 39.4, 36.5, 29.8, 26.5, 21.1. LRMS (ESI) calcd for $[M + H]^+$ *m/z* 403.0, found 402.9.

(R)-N-(benzo[d][1,3]dioxol-5-ylmethyl)-6-oxo-1,2,5-dithiazecane-4-carboxamide (**3.31a**) Preparatory TLC (5:1 EtOAc:Hex), extraction (5:1 CH_2Cl_2:MeOH), and concentration afforded **3.31a** as an off-white solid (22.9 mg, 51%): mp 168 - 169 °C. ^{1}H NMR ($CDCl_3$) δ 6.92 (bt, J = 5.3 Hz, 1H), 6.76-6.66 (m, 4H), 5.94 (s, 2H), 4.70 (ddd, J = 10.5, 6.8, 3.3 Hz, 1H), 4.30 (d, J = 5.9 Hz, 2H), 3.28 (dd, J = 15.5, 3.4 Hz, 1H), 3.20 (m, 1H), 3.16 (dd, J = 15.6, 10.8 Hz, 1H), 2.54 (m, 2H), 2.32 (m, 1H), 1.97 (m, 1H), 1.81 (m, 3H). ^{13}C NMR ($CDCl_3$) δ 174.3, 169.8, 148.1, 147.1, 131.7, 121.1, 108.5, 108.3, 101.2, 43.5, 39.8, 36.5, 29.8, 26.6, 21.2. LRMS (ESI) calcd for $[M + H]^+$ *m/z* 369.1, found 369.1.

5.3 Biological Experiments

5.3.1 General Procedure for SDS-PAGE and Western Blot Analysis

All incubations carried out at ambient temperature for 48 hours using S2 *Drosophila* cells. Following incubation, cell were lysed and nuclei dissolved in a 2:1 Laemelli buffer:1X PBS solution. A 15% SDS-PAGE analysis was performed on the samples and gel content transferred to a PVDF membrane. After transfer, the membrane was washed for 10 minutes with 0.4% Tween 20 in 1X PBS (T-PBS), 0.3% T-PBS and finally with 0.2% T-PBS. The membrane was the "blocked" for 1 hour using a 5% non-fat milk solution (2.5 g of non-fat dry milk dissolved in 50 mL of 0.2%T-PBS) followed by washes with 0.2% T-PBS (x 3) for 10 minutes. The membrane was then transferred to a bag and 4 mL of the blocking solution were added along with 4 mL of anti-H2B antibody. The bag was sealed and kept at room temperature for 5 minutes followed by membrane removal, brief wash with 0.2% T-PBS and re-bagging with 4 mL of blocking solution along with 4 mL of anti-hyper Ac-H4 antibody. Treatment with anti-hyper Ac-H4 antibody proceeded for 2 hours at room temperature at which time the membrane was washed with 0.2% T-PBS for 10 minutes (x 3). After that, membrane washed with secondary antibody (20 mL of blocking solution along with 4 mL of anti-rabbit antibody) for 1 hour. Membrane washed with 0.2% T-PBS for 10 minutes (x 3) before detection. Detection was performed using ECL system (GE Health Care). The membrane was washed with a mix of solution A and B (2 mL and 50 mL respectively) at room temperature for 5 minutes and transferred to a bag and exposed to film.

5.3.2 General Procedure for Flour de Lys Assays

HDAC inhibition assays were performed using the HDAC Fluorimetric Assay/Drug Discovery Kit (BioMol, Inc). Compounds were incubated in 0.5 mL per reaction of HeLa extract for 4 hours at room temperature in black 96-well plates (Corning Costar, Inc.), in 24 mL HDAC assay buffer (50 mM Tris-HCL pH 8.0, 137 mM NaCl, 2.7 mM KCl, 1 mM $MgCl_2$). Compound stocks were prepared at 25X final test concentration (20 mM) in 50% 1, 4 Dioxane, 50% ddH_20. 1 μL of compound was added to each reaction and incubated in the presence and absence of 50 mM DTT. Following incubation, 25 mL of substrate solution was added to a final concentration of 100 μM and incubated for 30 minutes at room temperature. Developer solution was prepared by diluting the 20X stock to 1X in HDAC assay buffer. 50 mL of developer solution was added to each reaction and incubated at room temperature for 15 minutes. The reactions were read on a Victor^3-V fluorescence plate reader using 360 nm excitation and 460 nm emission filters. The percent inhibitions were determined by calculating the percent loss of signal with test compounds from control reactions treated with solvent only (50% 1, 4 Dioxane, 50% ddH_20).

5.3.2 General Procedure for Cytotoxicity Assays

All cell lines except NmuMG were maintained in RPMI medium 1640 supplemented with 10% (wt / vol) FBS and penicillin-streptomycin (PS) (100 units / mL and 100 μg / mL). NmuMG cells were maintained in DMEM supplemented with 10% wt / vol FBS (FBS), 10 μg / mL insulin, and penicillin / streptomycin (PS) (100 units / mL and 100 μg / mL, respectively). Cells were harvested by trypsinization using 0.25% trypsin and 0.1% EDTA and then counted in a hemocytometer in duplicate with better than 10%

agreement in field counts. Cells were plated at a density of 10,000–15,000 cells per well of each 96-well black tissue culture treated microtiter plate. Cells were grown for 1 h at 37 °C, with 5% CO_2 / 95% air in a humidified incubator to allow cell attachment to occur before compound addition. Library members were stored at -20 °C under desiccating conditions before the assay. Library member stocks (100X) were prepared in 96-well V-bottom polypropylene microtiter plates. Five serial 1:2 dilutions were made with anhydrous DMSO at 100X the final concentration used in the assay. The library member-containing plates were diluted 1:10 with complete cell culture medium. The 10X stocks (10 μL) were added to the attached cells by using a Biomek FX liquid handler (Beckman Coulter). Library member stocks (10 μL) were added to 90 μL of cells in each plate to ensure full mixing of stocks with culture media by using a Biomek FX liquid handler with 96-well head. Cells were incubated with the library members for 72 h before fluorescence reading. Test plates were removed from the incubator and washed once in sterile PBS to remove serum containing calcium esterases. Calcein AM (acetoxymethyl ester) reagent (30 μL, 1 M) was added and the cells were incubated for 30 min at 37 °C. Plates were read for emission by using a fluorescein filter (λex 485 nm, λem 535 nm). An equal volume (30 μL) of cell titer-glow reagent (Promega Corporation, Inc.) was added and incubated for 10 min at room temperature with gentle agitation to lyse the cells. Each plate was re-read for luminescence to confirm the inhibition observed in the fluorescent Calcein AM assay. IC50 calculation for library members were done by plotting percent inhibitions as a function of log[concentration] and then fit to a four parameter logistic model which allowed for a variable Hill slope utilizing XL*fit* 4.2 software as previously reported. [1]

5.3.3 General Procedure for Cytoblot Assays

The compounds were supplied to the Small Molecule Screening Facility (SMSF) at a concentration of 5 mM in DMSO. Library member stocks were prepared (100X) in anhydrous DMSO in 96-well V-bottom polypropylene microtiter plates. The library member-containing plates were diluted 1:10 with complete cell culture medium to generate 10X stocks. Library member stocks were added (10 μL) to the attached cells by using a Biomek FX liquid handler (Beckman Coulter). The human lung adenocarcinoma cell line (A549) was maintained in RPMI medium 1640 supplemented with 10% (wt/vol) FBS and penicillin-streptomycin (PS) (100 units/mL and 100 μg/mL). Cells were incubated with library members for 24 hours prior to fixation. Cell supernatants were removed and treated adherent cells were washed 1 time in phosphate buffered saline (PBS) pH 7.4. Cells were fixed by addition of 100 uL of 3.7% formaldehyde and incubated for 20 minutes at 4 °C. Fixed cells were washed 5 times in PBS with 0.1% Triton-X 100 to permeabilize cell membranes. Cytoblots were performed after cells were permeabilized. Fixed cells were incubated with 150 μL Odyssey Blocking Buffer (Licor, inc.) for 1 hour with gentle shaking at room temperature. All primary antibody solutions were made by diluting the antibodies 1:100 with Odyssey blocking Buffer except for anti-nrf2, which was prepared by 1:50 dilution in Odyssey Blocking Buffer. Each treated plate of cells were incubated with 50 uL of one primary antibody solution: mouse anti-p21 (BD Pharmingen, 556430), rabbit anti-nrf2 (Santa Cruz Biotechnology, inc, H-300), goat anti-keap1 (Santa Cruz Biotechnology, E-20), rabbit anti-AKT (Cell Signaling Technology, inc.), rabbit anti AKT phospho-specific serine 473 (Cell Signaling Technology, inc.), rabbit anti-AKT phospho-specific tyrosine 308 (Rockland immunochemicals, inc.), mouse anti-p53 (Calbiochem, OP43L), rabbit anti Acetyl-histone H3 (Upstate Biotechnology, 06-598),

or rabbit anti-acetyl-histone H4 (Upstate Biotechnology,06-599), for 2 hours at room temperature with gentle shaking. Each plate was washed 5 times with PBS pH 7.4. Cells were incubated with either IR dye 680 congjugate

5.4 References

(1) Langenhan, J. M.; Peters, N. R.; Guzei, I. A.; Hoffman, M.; Thorson, J. S. Enhancing the Anticancer Properties of Cardiac Glycosides by Neoglycorandomizaion. *Prod. Natl. Acad. Sci. U.S.A.* **2005**, *102*, 12305-12310.

Appendix

Listed in order of appearance are the ^{1}H NMR spectra of:

1.30b, 1.32a, 1.32b, 1.33a, 1.32c, 1.33b, 3.1, 3.2, 3.4, 3.6, 3.13b, 3.14, 3.16, 3.20b, 3.21b, 3.22b, 3.23b, 3.24b, 3.25b, 3.26b, 3.27b, 3.28b.

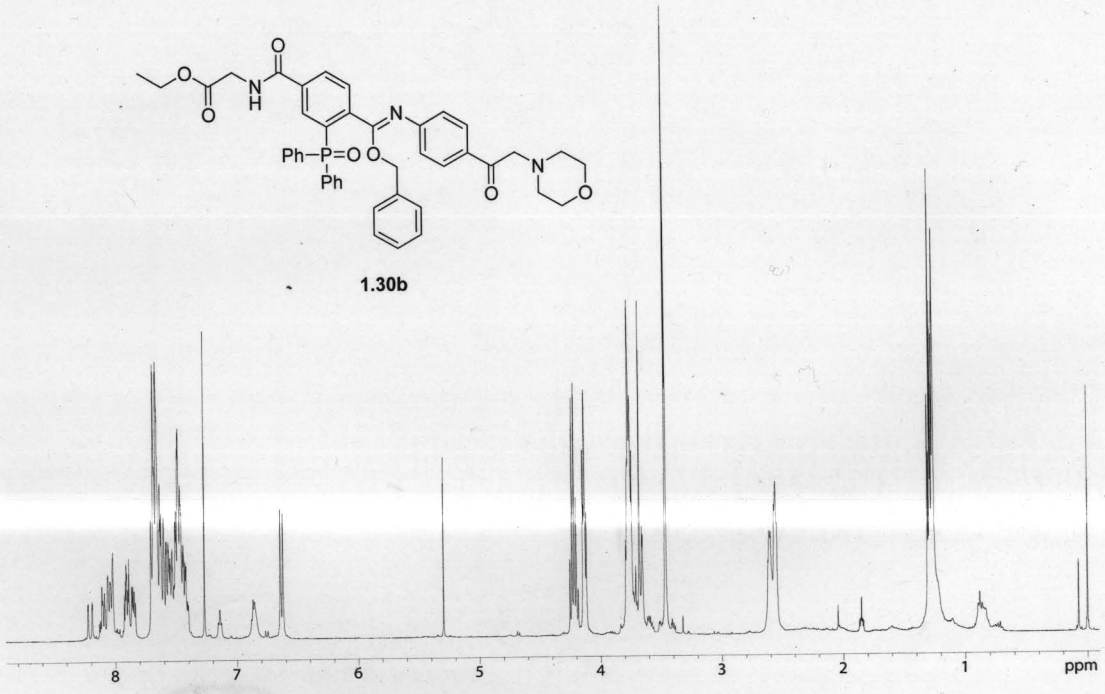

1.30b

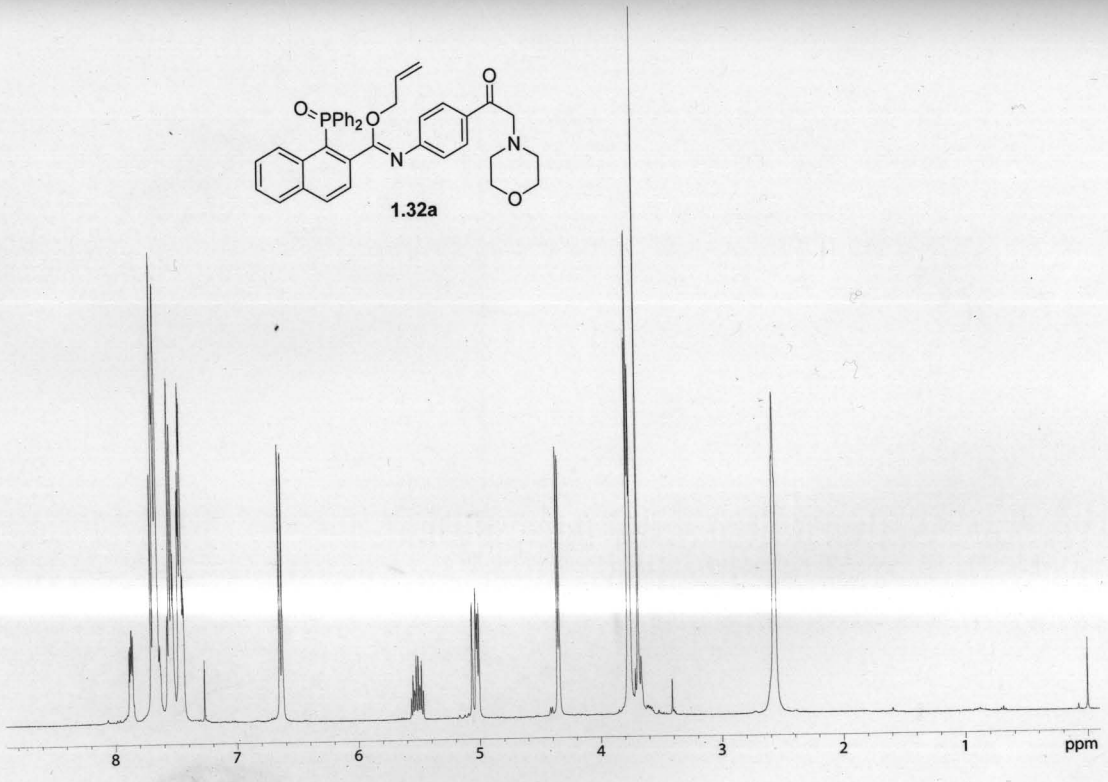

1.32a

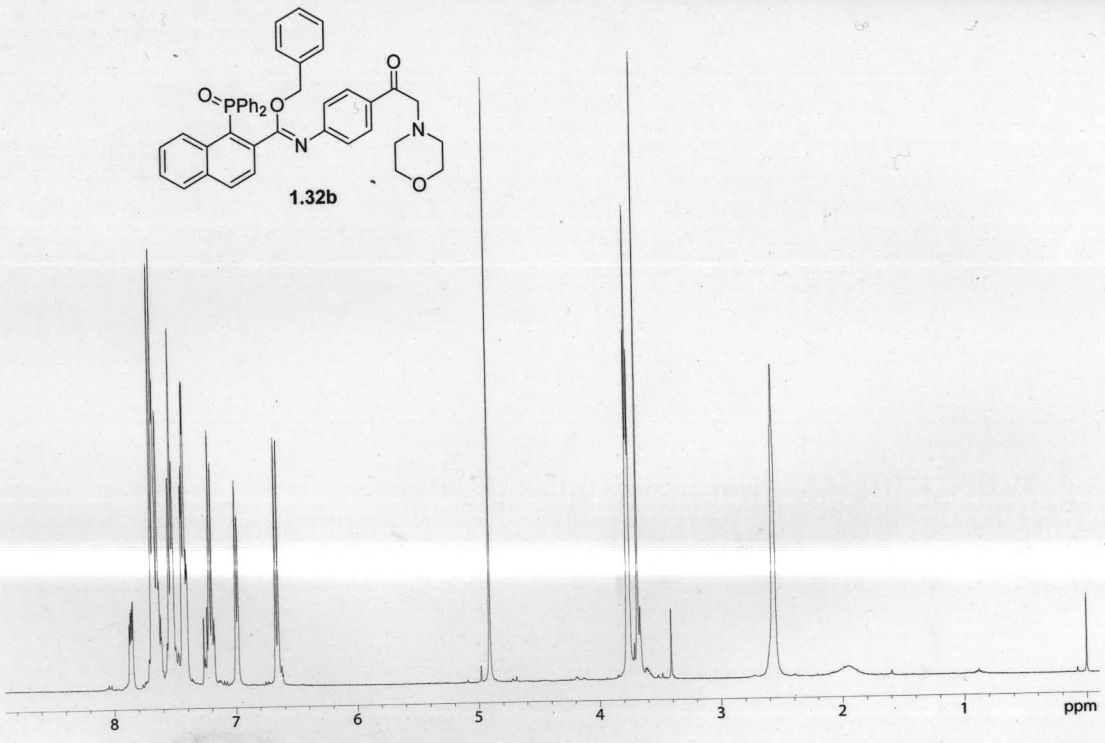
O
O=PPh2
O
N
N
O
1.32b
8
7
6
5
4
3
2
1
ppm

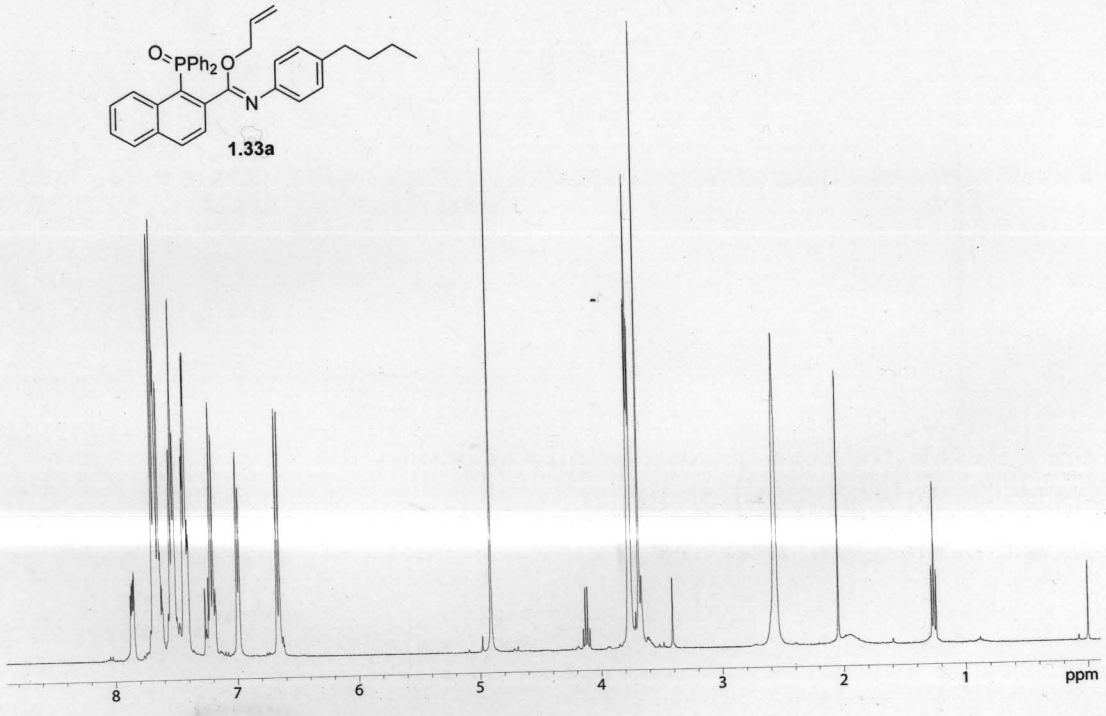
O=PPh2
O
N
1.33a
8
7
6
5
4
3
2
1
ppm

1.32c

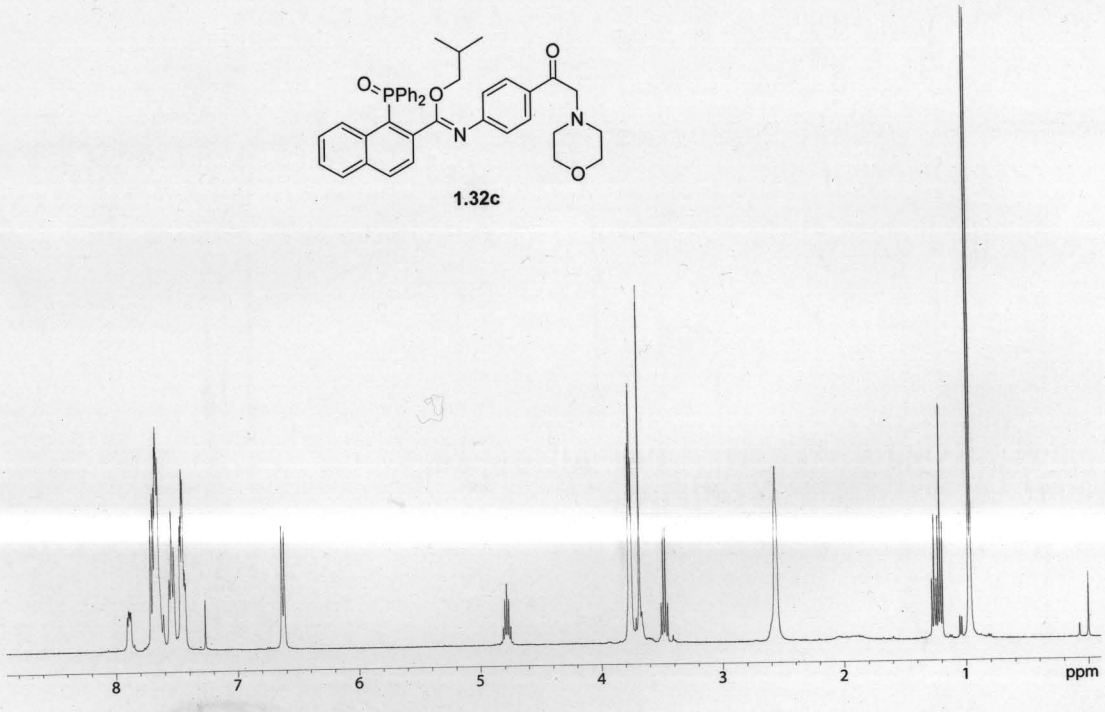

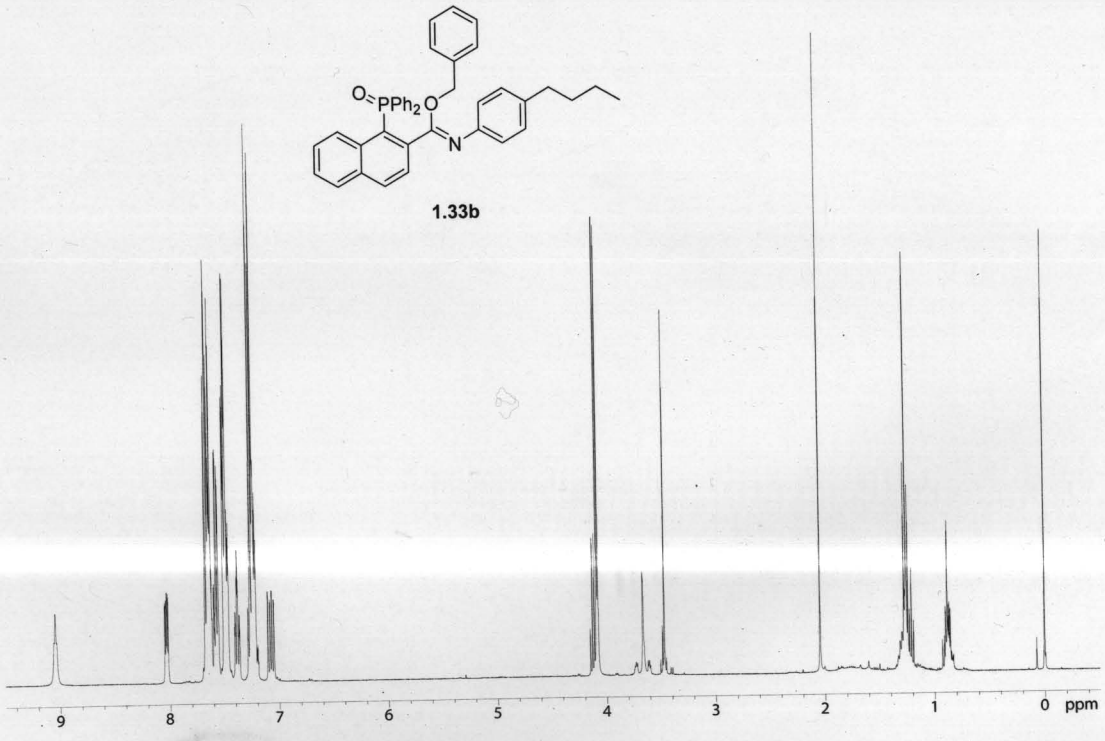

1.33b

3.1

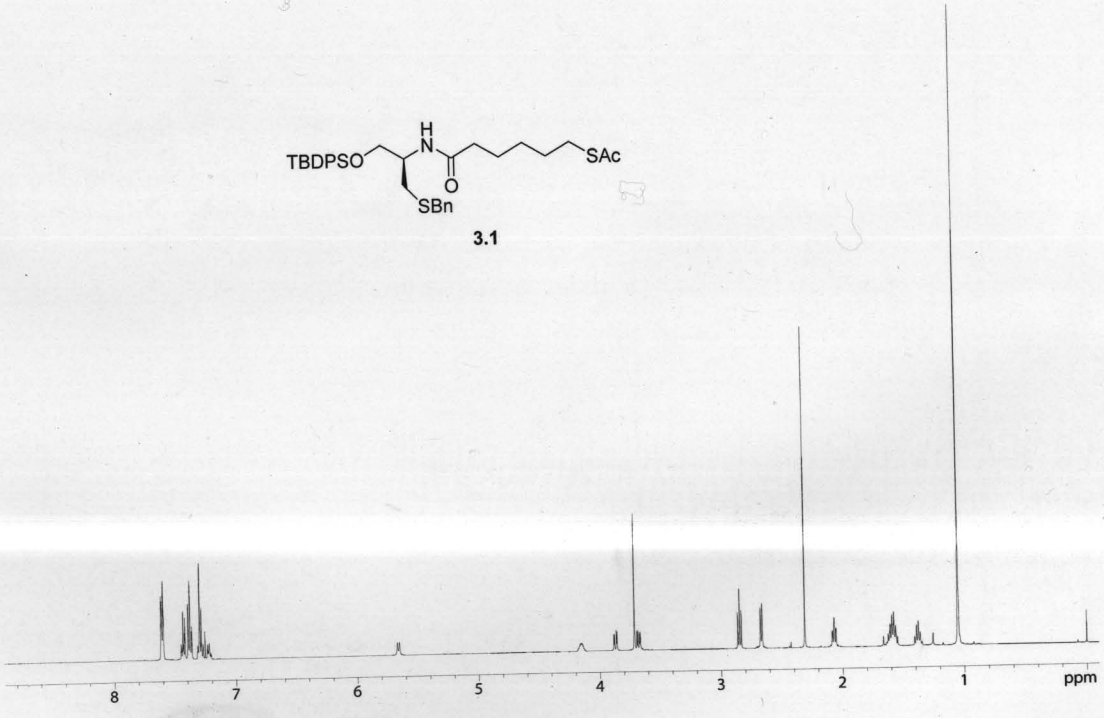

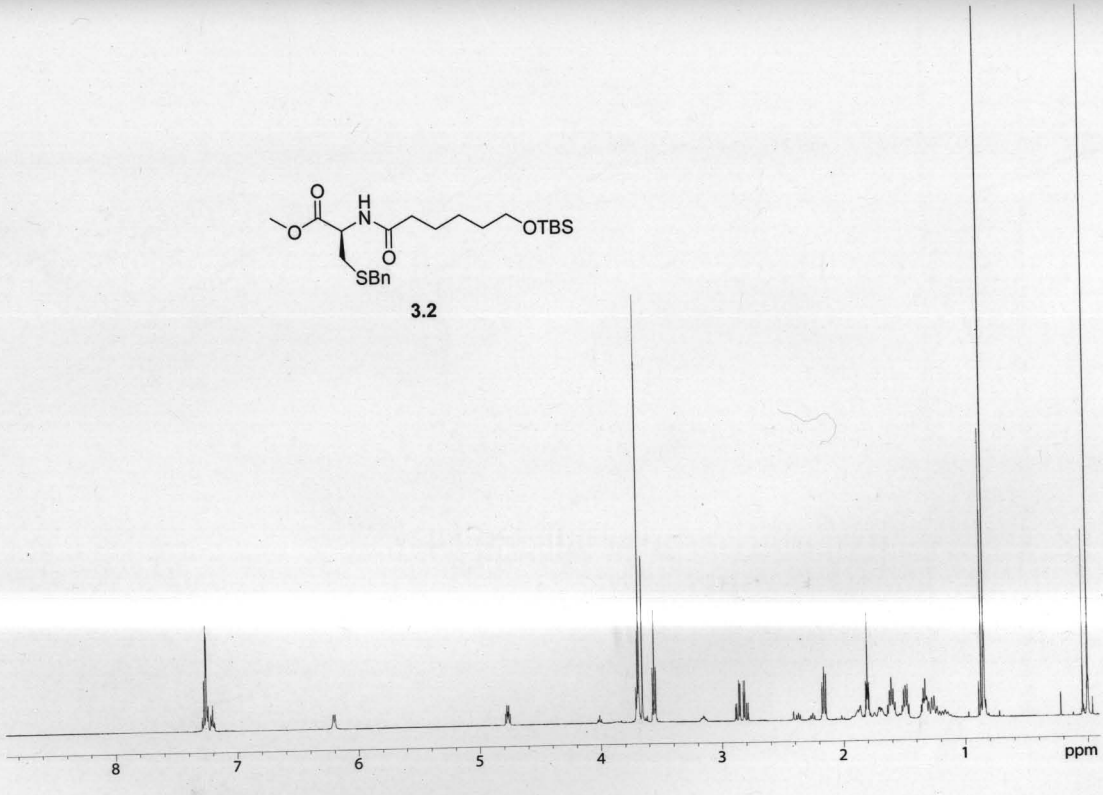

3.2

3.4

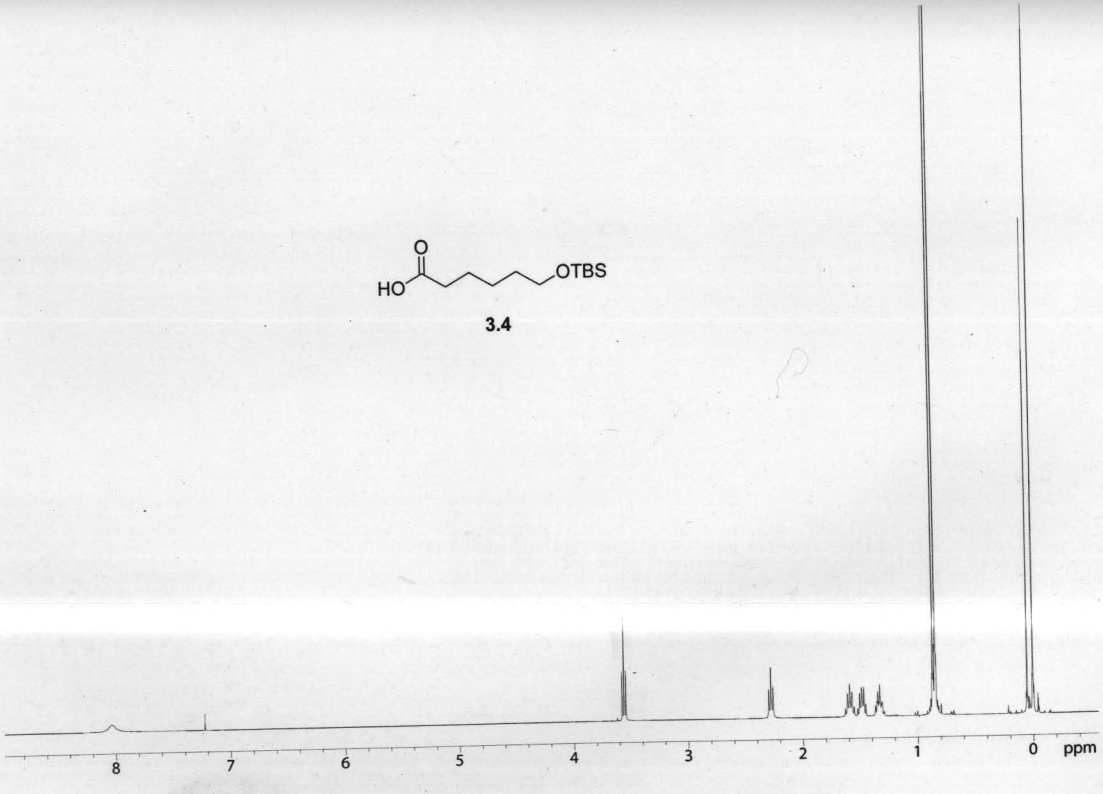

3.6

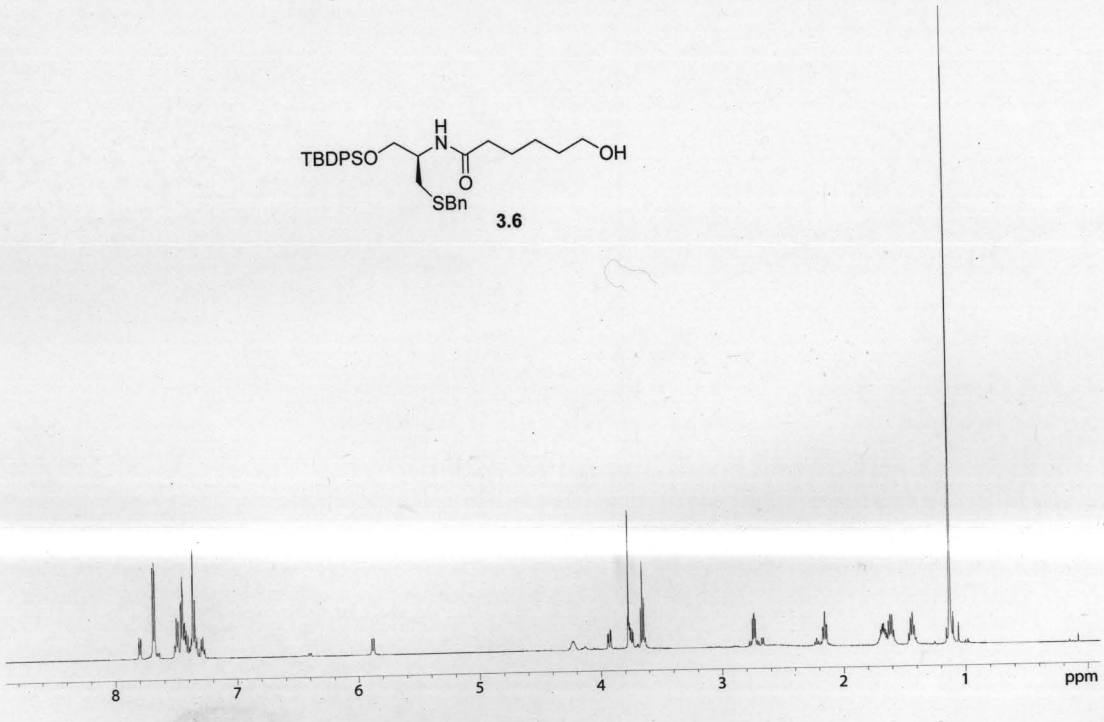

3.13b

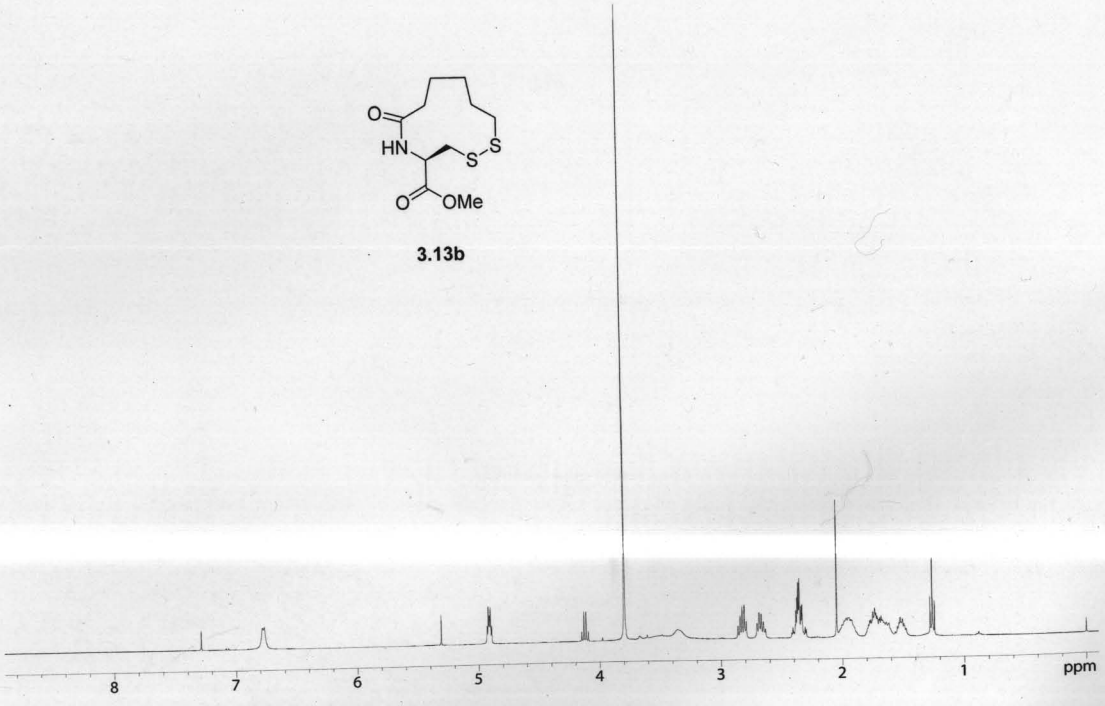

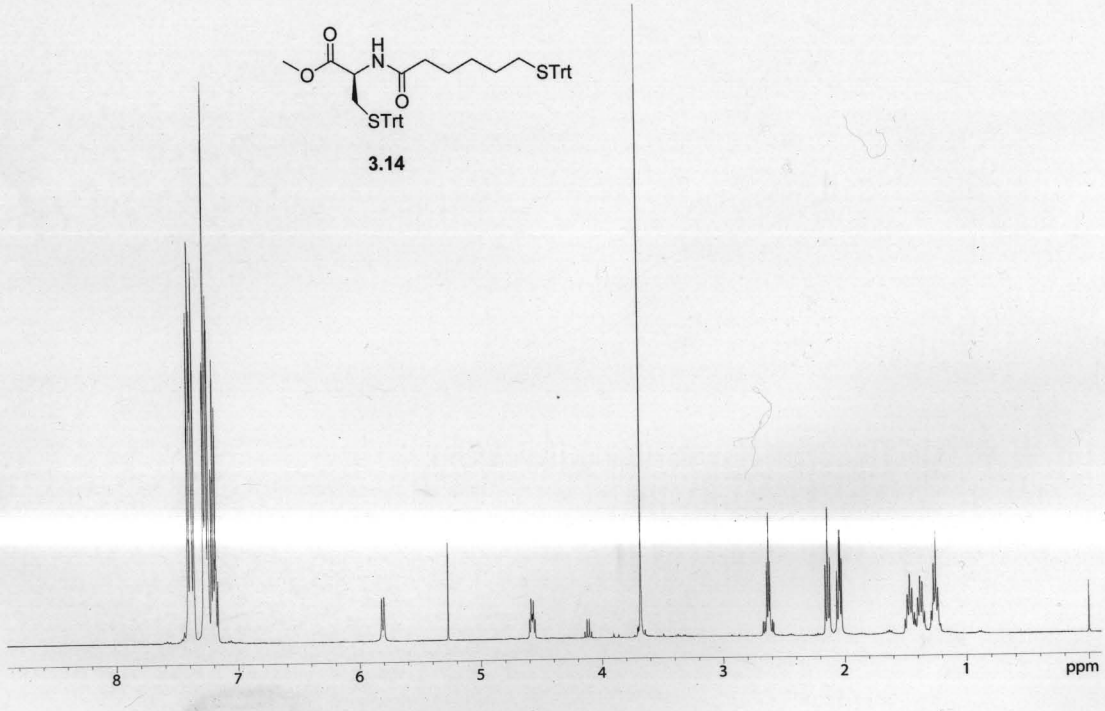

3.14

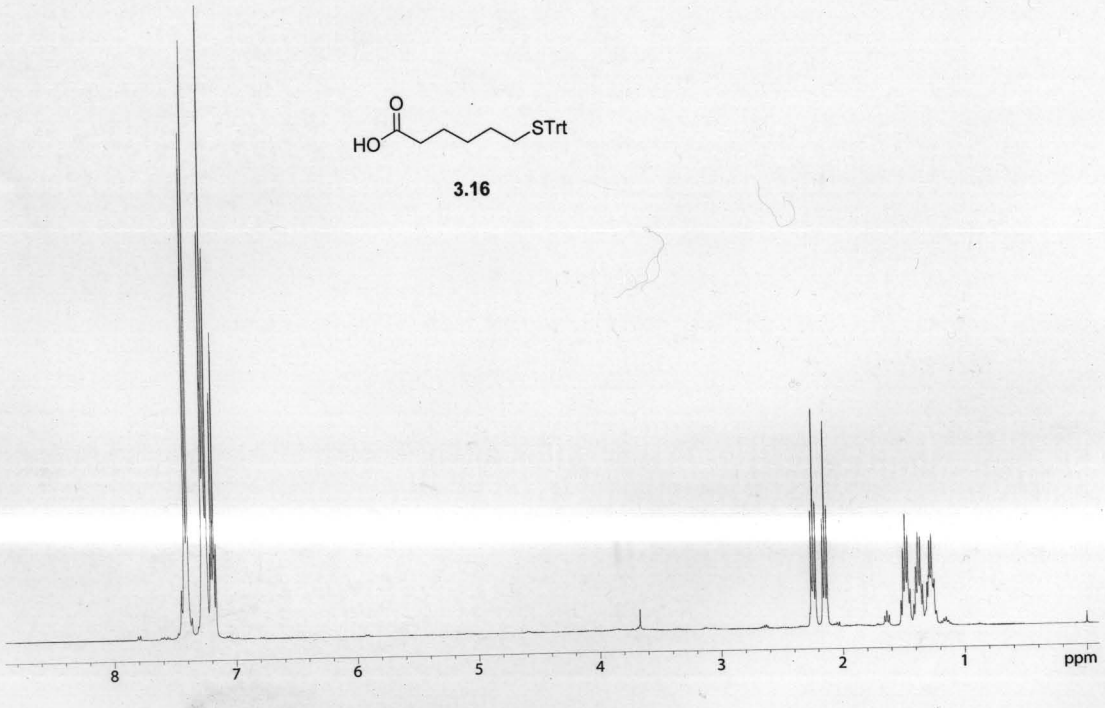

3.16

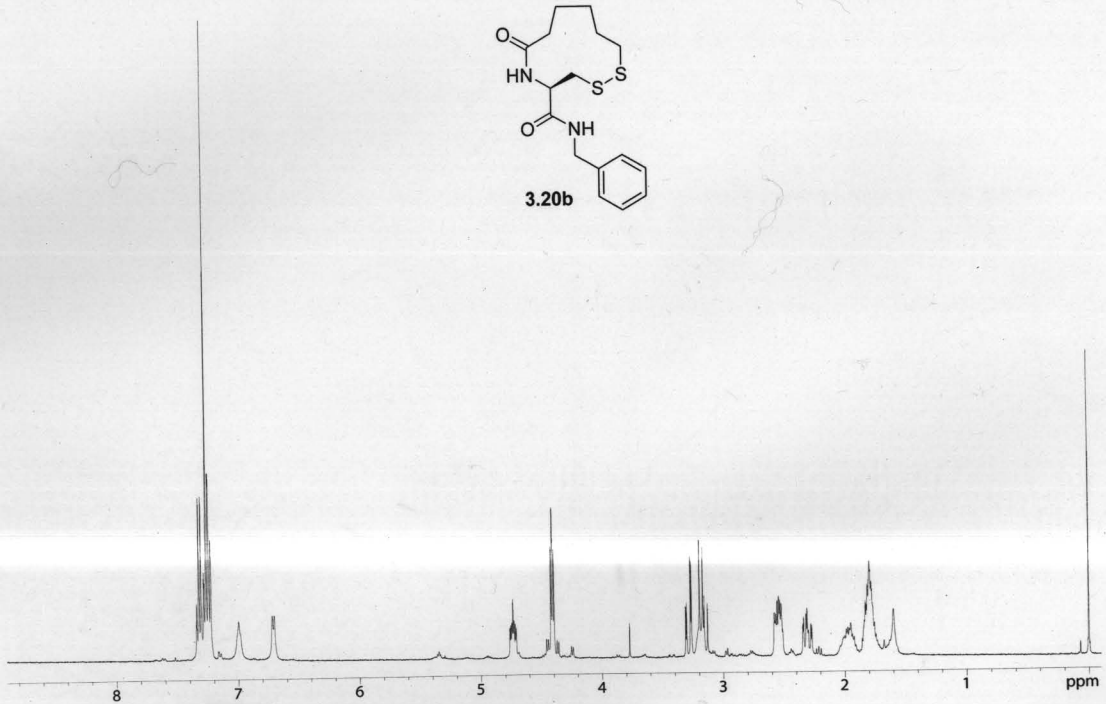

3.20b

3.21b

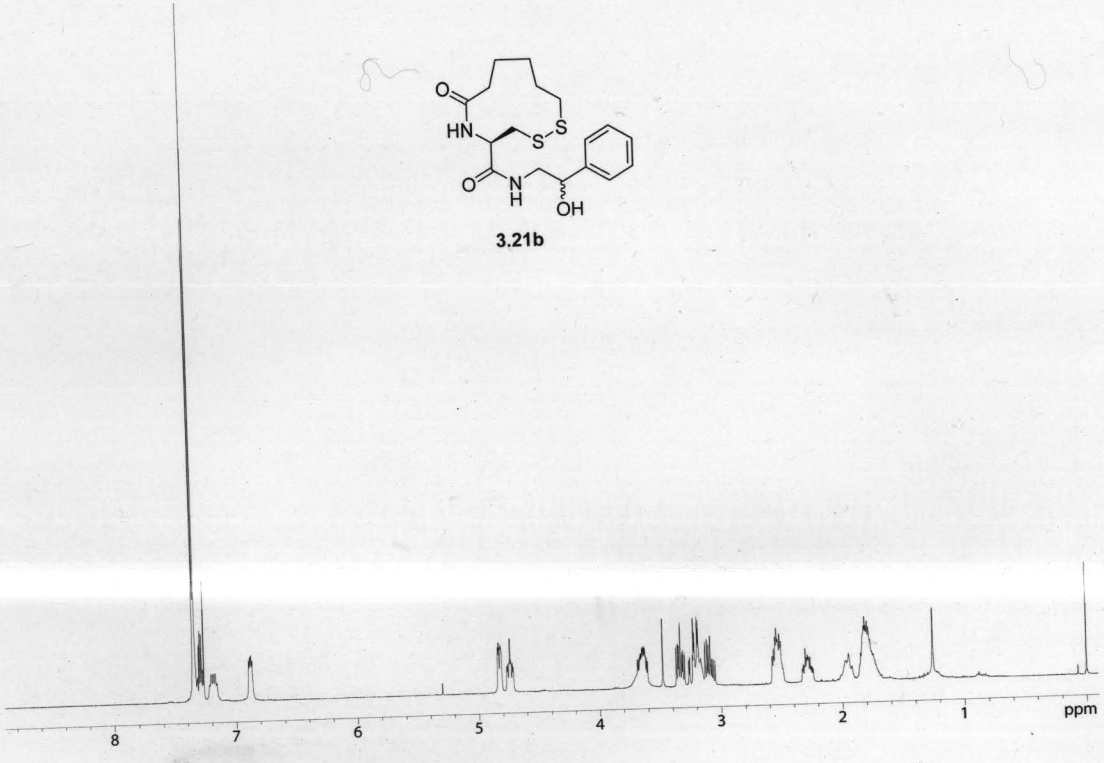

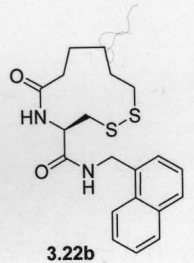

3.22b

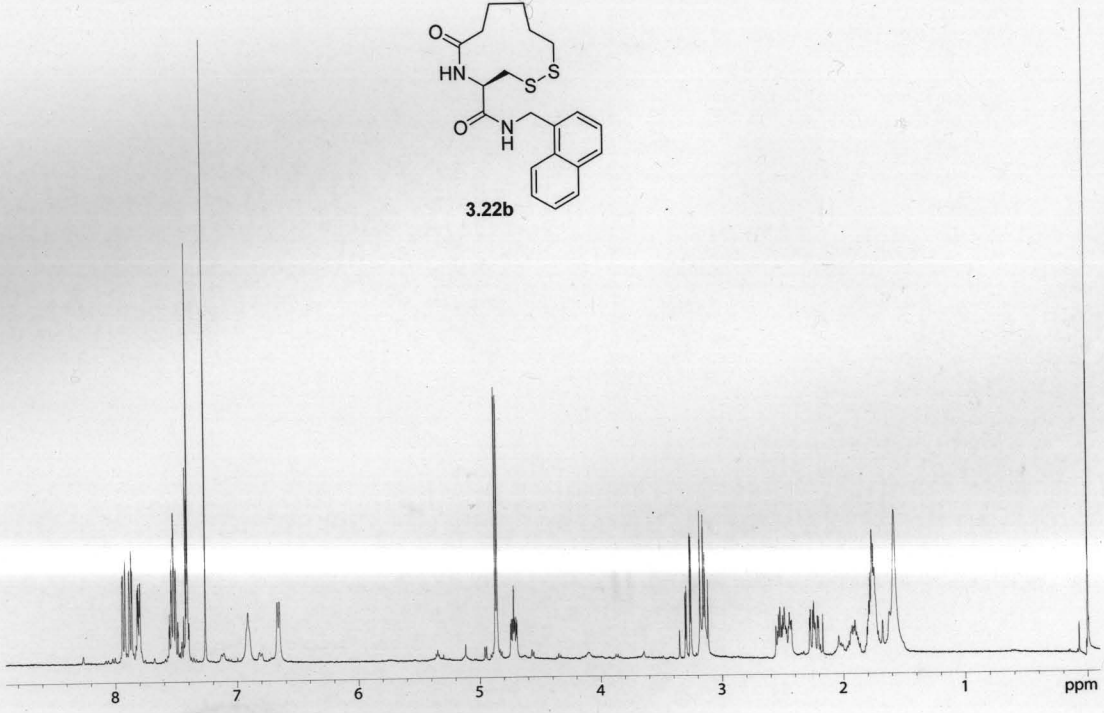

3.23b

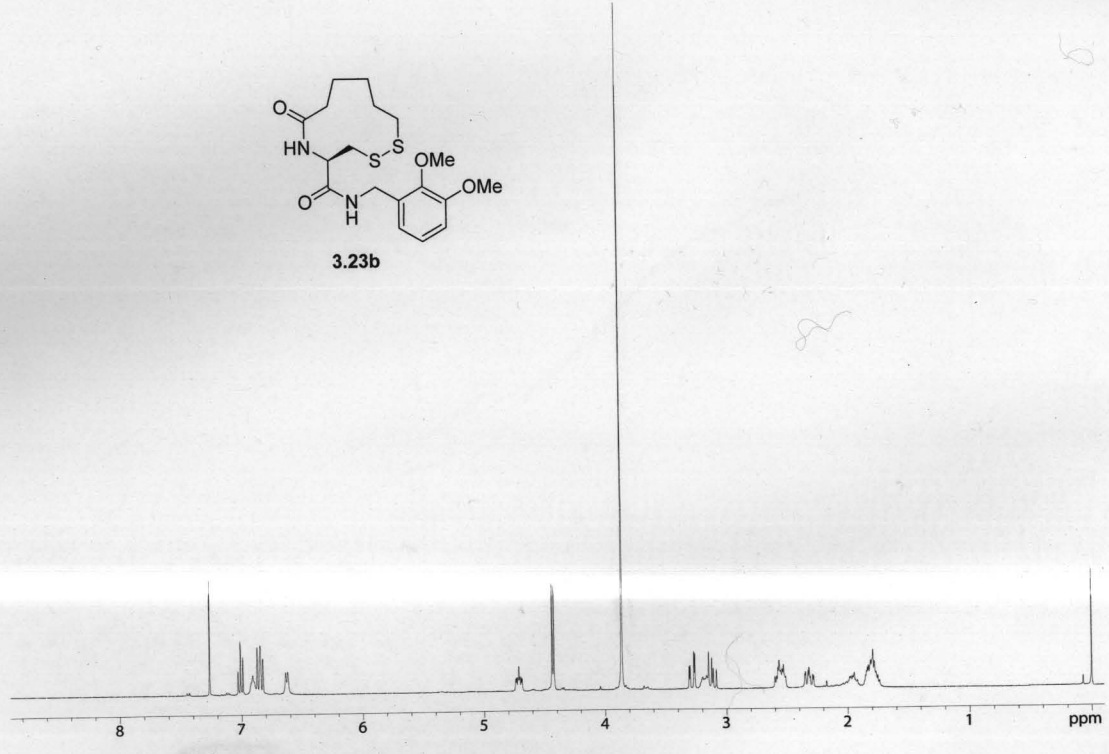

3.24b

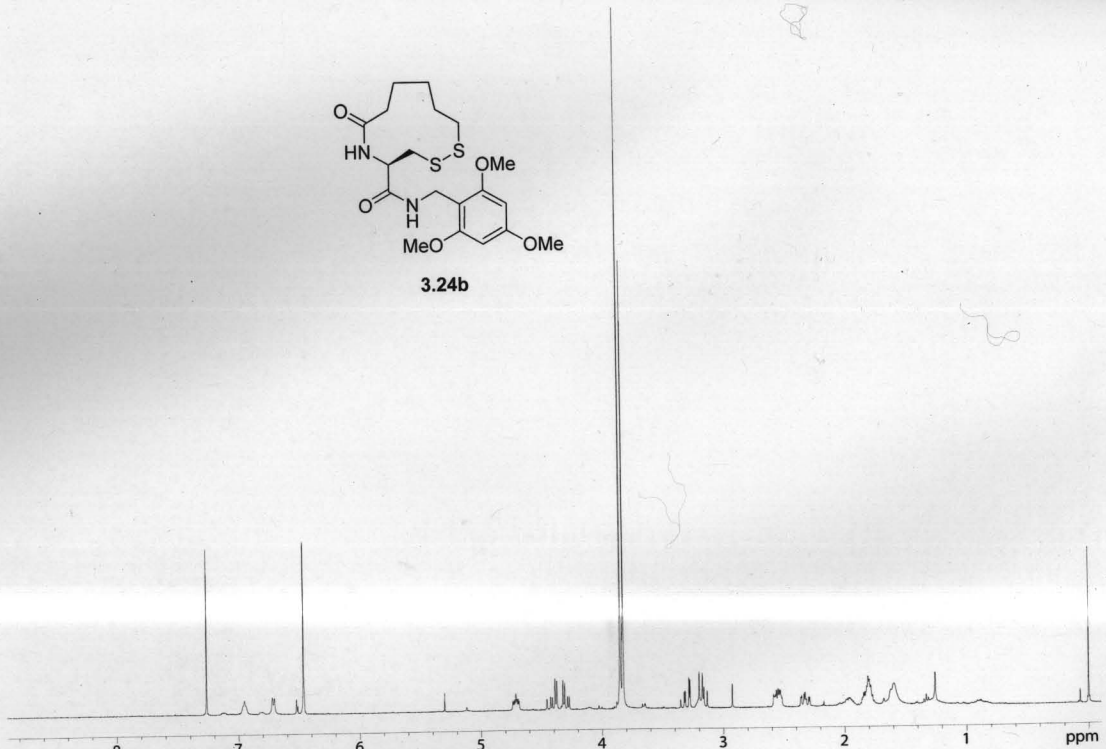

3.25b

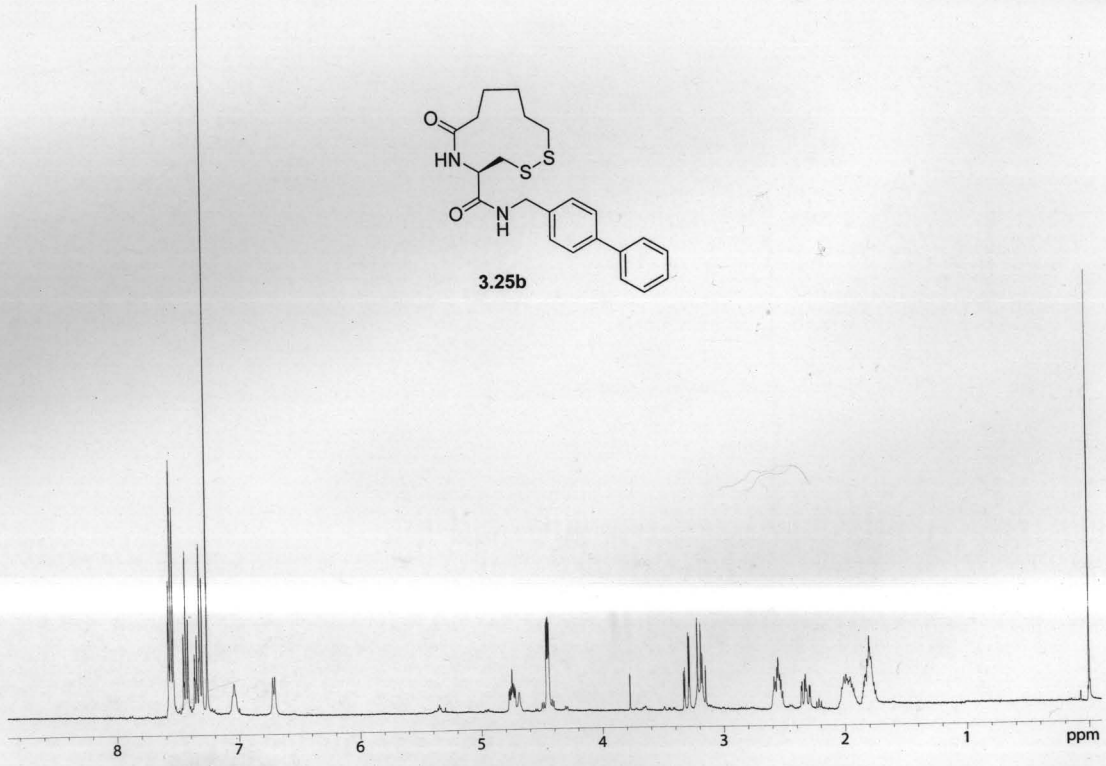

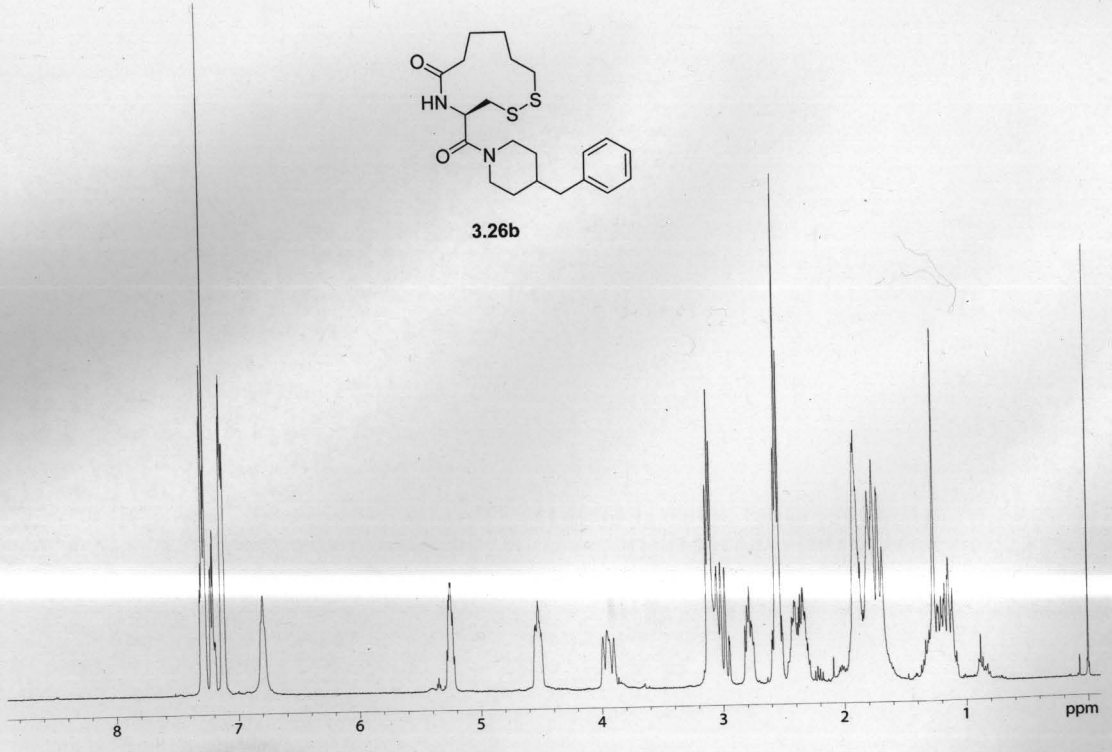

3.26b

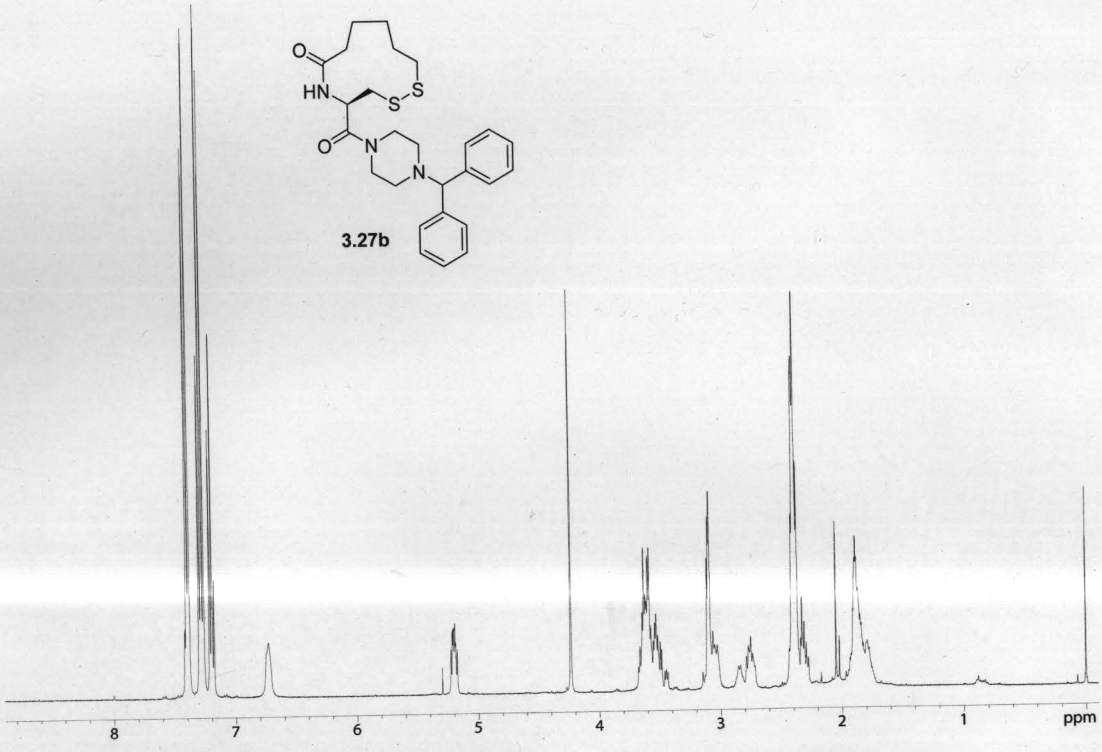
O
HN
S
S
O
N
N
3.27b
8
7
6
5
4
3
2
1
ppm

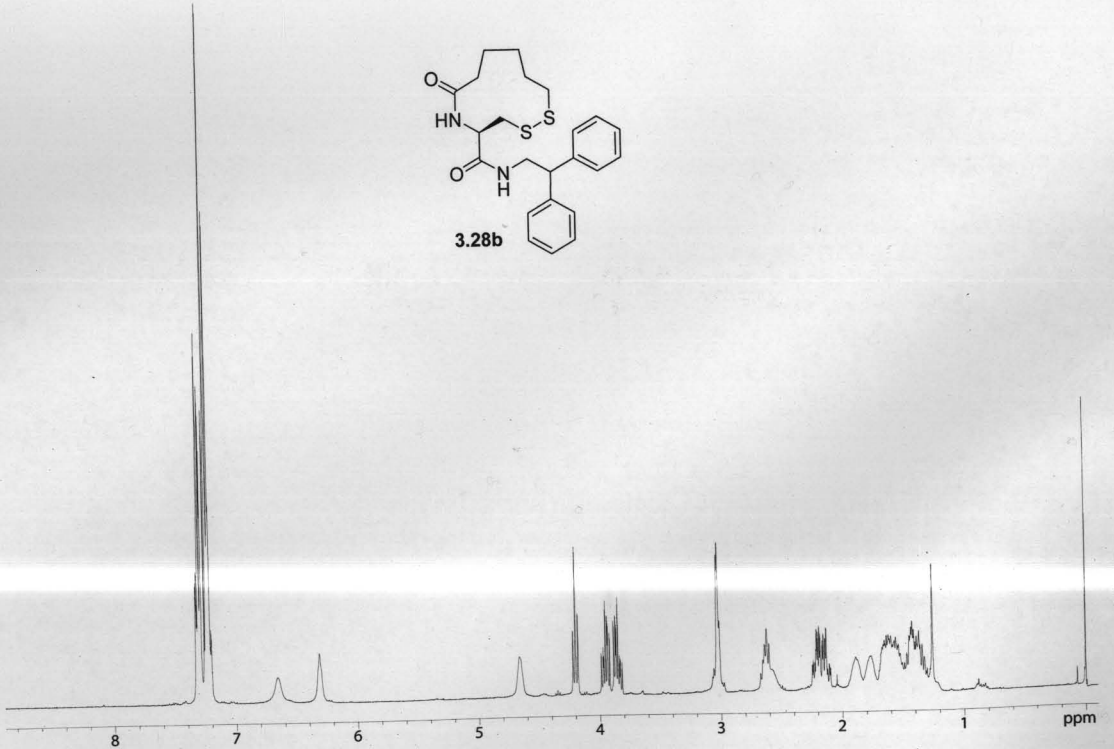
O
HN
S
S
O
N
H
3.28b
8
7
6
5
4
3
2
1
ppm